Managed by Platinum Foundation
GANDHINAGAR INSTITUTE OF TECHNOLOGY
AICTE Approved | Affiliated with Gujarat Technological University

'GIT-Journal of Engineering and Technology'

ISSN 2249–6157
(Print & Online)

Published By,

Gandhinagar Institute of Technology
Khatraj - Kalol Road, Moti Bhoyan,
Tal. Kalol, Dist. Gandhinagar-382721
Phone: 9904405900, 02764-281860/61
Fax: 02764-281862
E-mail: director@git.org.in, jet@git.org.in
Website: www.git.org.in

About Gandhinagar Institute of Technology

Gandhinagar Institute of Technology is established by Platinum Foundation in 2006. It offers under graduate programs in Mechanical Engineering, Information Technology, Computer Engineering, Electronics and Communication Engineering, Electrical Engineering and Civil Engineering and Post graduate program in MBA (Finance, Human Resource Development, and Marketing), M.E. in Mechanical Engineering with specialization in Thermal Engineering and Computer Aided Design & Computer Aided Manufacturing and M.E. in Computer Engineering with specialization in Software Engineering.

All these programs are approved by AICTE, New Delhi and affiliated to Gujarat Technological University. We have elaborate laboratory facilities and highly motivated and qualified faculty members. We are also arranging technical seminars, conferences, industry-institute interaction programs, workshops and expert lectures of eminent dignitaries from different industries and various reputed educational institutes.

Our students are innovative and have excellent acceptability to latest trends and technologies of present time. Our students have also participated in various technical activities as well as sports activities and have achieved various prices at state level. We have two annual publications, a National level research journal 'GIT-Journal of Engineering and Technology (ISSN 2249–6157)' and 'GIT-a Song of Technocrat' (college magazine).

Trustees and Governing Body Members

Shri Hareshbhai B. Rohera

Shri Ghanshyambhai V. Thakkar

Shri Deepakbhai N. Ravani

Shri Pravinbhai A. Shah

Smt Varshaben M. Pandhi

Shri Mahendrabhai R. Pandhi

Message from the Director

It gives me immense pleasure that the ninth issue of our National journal 'GIT-Journal of Engineering and Technology' is being published with ISSN 2249 – 6157 for ninth successive year. The annual journal contains peer reviewed technical papers submitted by the researcher of all domains of engineering and technology. The issue is a result of imaginative and expressive skill and talent of GIT family. Research papers were invited from the researcher of all domains of engineering and technology. More than 30 research papers were received. After peer review about 21 papers are selected and are being published in this issue of the journal.

GIT was established in 2006 and during a short span of ten years; it has accomplished the mission effectively for which it was established. Institute has been constantly achieving the glory of excellence in the field of curricular and co-curricular activities. For the eighth consecutive year an annual technical symposium TechXtreme 2016 was successfully organized by the institute. More than 2000 students of various technical institutions across the Gujarat participated in the Techfest. Prizes worth Rs 2 lacs and trophies were given to the winners. Annual cultural event Jazba 2015 was organized with participation of more than 1000 students of the institute in various cultural events of Debate, Quiz, Essay writing, Rangoli, Music, Dance, Drama etc.

The institute is Resource Center of IIT Bombay for conduction of Spoken Tutorials on various open source software like Linux, Latex, Scilab, Python, Java, Netbeans, C, C++, Liber Office, Php MySQL, etc. Institute organize various technical seminar, expert lectures, debate competition, rangoli competition, kite flying competition, Ratri B4 Navaratri, and sports activities to nurture multifaceted talent of its students. Institute has also arranged blood donation drives and thalassemia testing program. Students have also participated and won prizes in various sports, technical and cultural events organized by other Institutions including that of GTU.

The Institute is also emphasis on academic development of its faculty members. During the year, many International and National papers has been published and presented by the faculty members. The faculty members have also been deputed to attend large number of seminars/workshops/training programs/symposiums.

Publication of the journal of national level is not possible without whole hearted support of committed and experienced Trustees of Platinum Foundation and I take an opportunity to express my deep feelings of gratitude to all of them for their constant support and motivation.
It's my privileged to compliment the staff members and the students for showing high level of liveliness throughout the year. I also congratulate the team of the 'GIT-Journal of Engineering and Technology' for their untiring effort to bring out this eighth issue of the journal.

Dr N M Bhatt
Director & Chief Editor

Index

Wardriving – An Innovation to Wi-Fi Network

Mr. Nirav K. Shah[a], Mr. Parag B. Makwana[b]

Asst. Prof , Shree Swaminarayan College of Computer Science, Sardarnagar, Bhavnagar – 364001 India, M. K. Bhavnagar University
Asst. Prof., Shree Swaminarayan College of Computer Science, Sardarnagar, Bhavnagar – 364001 India, M. K. Bhavnagar University

Abstract
Wardriving is searching for Wi-Fi wireless networks by moving vehicle. It involves using a car or truck and a Wi-Fi-equipped computer, such as a laptop or a PDA, to detect the networks. It was also known as 'WiLDing' (Wireless Lan Driving).Many wardrivers use GPS devices to measure the location of the network find and log it on a website. For better range, antennas are built or bought, and vary from omnidirectional to highly directional. Software for wardriving is freely available on the Internet. Wardriving was named after wardialing because it also involves searching for computer systems with software that would use a phone modem to dial numbers sequentially and see which ones were connected to a fax machine or computer, or similar device.

Keywords: wifi, wardriving, wardialing, nuclear war, warcart.

INTRODUCTION

WarDriving is an activity that is misunderstood by many people.This applies to both the general public, and to the news media that has reported on WarDriving. Because the name "WarDriving'* has an ominous sound to it, many people associate WarDriving with a criminal activity WarDriving originated from wardialing, a technique popularized by a character played by Matthew Broderick in the film WarGames, and named after that film. Wardialing in this context refers to the practice of using a computer to dial many phone numbers in the hopes of finding an active modem.

A WarDriver drives around an area, often after mapping a route out first, to determine all of the wireless access points in that area. Once these access points are discovered, a WarDriver uses a software program or Web site to map the results of his efforts. The concept of driving around discovering wireless networks probably began the day after the first wireless access point was deployed. However, WarDriving became more well-known when the process was automated by Peter Shipley, a computer security consultant in Berkeley, California.

WHY WAR?

This is kind of an unfortunate prefix, in these rather twitchy times. Wardriving has nothing whatsoever to do with war. The term is the offspring of the term wardialing, which was the (now mostly extinct) practice of dialing random phone numbers via computer to see if you could find an answer modem. Wardialing, in turn, came out of the 1983 cult movie War Games, in which a teenager got himself (and the rest of the world) into serious trouble by creating an autodialer that eventually found its way into a DOD computer programmed to wage nuclear war. The kid was looking for computers supporting online games and had no strong intent to "break into" anything—the problems that developed lay with an essentially undefended military computer.

TERMINOLOGY OF WARDRIVING

The term WarDriving comes from WarDialing, a term you may be familiar with being that it was introduced to the general public by Matthew Broderick's character,David Lightman, in the 1983 movie, WarGames. WarDriving employs the same concept, although it is updated to a more current technology: wireless networks. A WarDriver drives around an area, often after mapping a route out first, to determine all of the wireless access points in that area. Once these access points are discovered, a WarDriver uses a software program or Web site to map the results of his efforts. Based on these results, a statistical analysis is performed. This statistical analysis can be of one drive, one area, or a general overview of all wireless networks. The concept of driving around discovering wireless networks probably began the day after the first wireless access point was deployed. However, WarDriving became more well-known when the process was automated by Peter Shipley, a computer security consultant in Berkeley, California.

HOW IT WORKS?

The idea behind wardriving is to detect IEEE 802.11 (Wi-Fi) traffic using a wireless network card that accepts all network traffic in the area, regardless of the signal's intended target. Wireless access points (WAPs) broadcast frames containing their service set identifier (SSID) and a few other items. This is done so that computers can automatically detect networks.

With wardriving, one analyzes these signals to create a map of WAPs and their coverage areas. The word driving in wardriving derives from the fact that one typically uses a car to traverse roads while analyzing wireless network information.

To perform wardriving, one typically requires the following:

1. A computer – this can be a desktop, laptop or even PDA
2. A wireless networking software utility (for more information, see Software for Wardriving - notably, NetStumbler

for Windows, Kismet for Linux, and KisMac for Macintosh.)

3. A Wi-fi client adapter
4. An external antenna for your Wi-fi adapter – since most adapters have weak antennas and most likely the car will shield many signals, the antenna will aid in finding signals (optional)

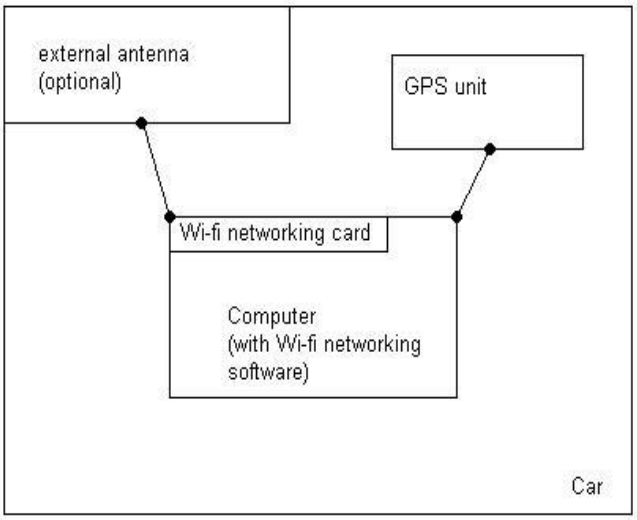

Fig.1 Overview of Wardriving design

5. A GPS receiver – not absolutely necessary but it allows one to easily map the WPAs to geographical maps (optional)

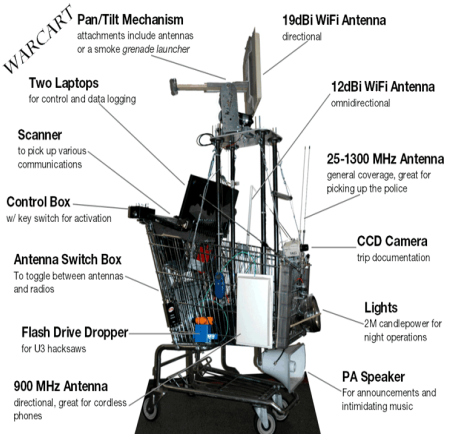

Fig. 2 Actual image of Wardrivring

WARDRIVE HARDWARE

There are several different configurations that can be effectively used for WarDriving, including:

- Getting the hardware
- Choosing a wireless network card
- Deciding on an external antenna
- Connecting your antenna to your wireless NIC

The most commonly used WarDriving setup utilizes a laptop computer.To WarDrive with a laptop, you need several pieces of hardware and at least one WarDriving software program. A successful laptop WarDriving setup includes:

- A laptop computer
- A wireless NIC Card
- An external antenna
- A pigtail to connect the external antenna to the wireless NIC
- A handheld global positioning system (GPS) unit
- A GPS data cable
- A WarDriving software program
- A cigarette lighter or AC adapter power inverter

Because most of the commonly used WarDriving software is not resource intensive, the laptop can be an older model. If you decide to use a laptop computer to WarDrive, you need to determine the WarDriving software you plan to use as well. For instance, if you do not feel comfortable with the Linux operating system, you will have to rely on tools that are

supported in a Microsoft Windows environment. Because NetStumbler only works in Windows environments, your choice of software is limited. A typical laptop WarDriving setup is shown in Figure I.

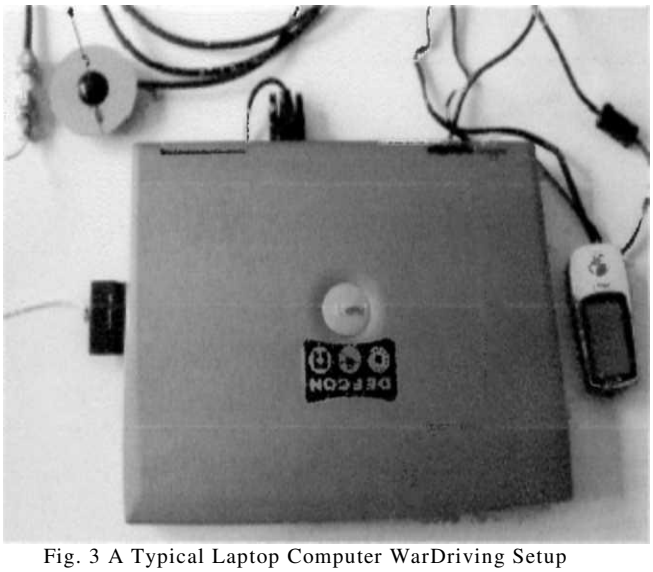

Fig. 3 A Typical Laptop Computer WarDriving Setup

The Personal Digital Assistant (PDA) Setup

PDAs are the perfect accessory for the WarDriver because they are highly portable. The Compaq iPAQ or any number of other PDAs that utilize the ARM, MIPS, or SH3 processor can be utilized with common WarDriving software packages.

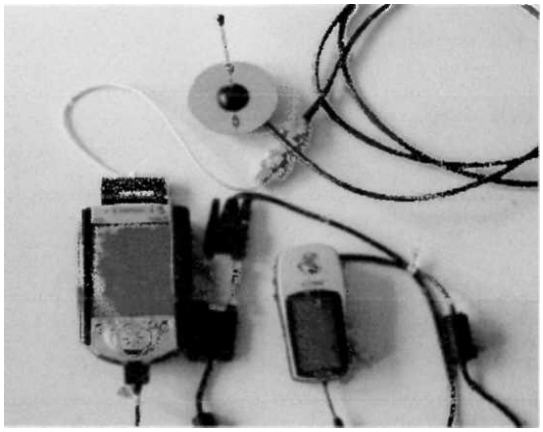

Fig. 4: A Typical PDA WarDriving Setup

As with the laptop setup, the PDA setup requires additional equipment in order to be successful:

- A PDA with a data cable
- A wireless NIC Card
- An external antenna
- A pigtail to connect the external antenna to the wireless NIC
- A handheld global positioning system (GPS) unit
- A GPS data cable
- A null modem connector
- A WarDriving software program

MAPPING SITES AND SOTWARE

There are several different ways to plot stumbled stations on a map. To use WiGLE, WiFiMaps and Stumbverter. For any of these systems, you must have used a GPS receiver to add geographical coordinate data to your stumbling log files. The coordinates provided by GPS are what locate the stations on a map. The caution, of course, is that your GPS receiver reports your position as you received a station's beacon, not the position of the station itself! (This should be obvious but it's easy to forget.) Multiple readings on the same station allow some utilities to triangulate an approximation of the station's

position and range, but how accurate such approximations are is a little unclear. WiGLE seems to do the best job on that score, but even then, if you only sense stations from one direction, the triangulated position will be skewed in one direction.

WIGLE (WIRELESS GEOGRAPHIC LOGGING ENGINE)

WiGLE (Wireless Geographic Logging Engine) is a complete system for mapping stumbled APs, and includes a Web database and several mapping clients. As best I know, it's the oldest such system in existence, and has been in operation since September 2001. Here's how it works, from a height: Users upload log files containing records of stumbled APs, which are processed and added to a database. "Map pack" data files may be downloaded by county (US only) and plotted on-screen using one of the WiGLE clients.

WiGLE performs triangulation calculations on multiple readings of each stumbled station, in order to more precisely determine the actual physical location of the station. (Remember that the GPS coordinates recorded for a station during a wardriving run are your location when your Wi-Fi client adapter hears the station, not the coordinates of the station itself!) Each station is plotted as a point on a map, and you can pan and zoom to get the full picture of any given county.

The WiGLE system includes several different clients:

- JiGLE is the oldest, and is written in Java. It should run anywhere Java will run.
- DiGGLER is a native-code Windows client written in Delphi. It does basically what JiGLE does, but does not require the Java VM. It's small, fast, and doesn't mess with your registry. (Can you tell I'm a Delphi fan?) It is, however, limited to running under 32-bit Windows.
- PRInGLE is a client for Palm OS, which is not yet released but should be soon.

The clients come with sample maps, but in actual use, you must request a WiGLE map pack for download. These are free, and are available for any county in the US. (You must register with the WiGLE system to download map packs.) On the backend, WiGLE map packs are generated by RiGLE, the using public domain TIGER geographic databases distributed by the Federal Government. The generated maps are thus not encumbered by anyone else's copyrights.

Wardrivers may upload log files in any of several formats, including NetStumbler and MiniStumbler (export as text); DStumbler text, and the Kismet CWGD, CSV, XML, and GPS formats. Uploads are handled through a page on the WiGLE Web site. Uploaded stations are immediately available for downloading in a map pack. You can upload the results of a wardriving run, and then immediately download an updated map pack reflecting the results of that run.

FUTURE SCOPE

The rapid rise and evolution of networking technologies continues to have a profound impact on the assumptions underlying many aspects of law. Like the war-driving challenge legislators and courts to find solutions that protect a property owner's rights while encouraging the free flow of information. By prohibiting use of a Wi-Fi network only when the network operator has implemented security measures, courts and legislators will encourage the development and use of this valuable technology. Simultaneously, this approach will promote sensible security practices, and protect network operators who have indicated their access preferences.

CONCLUSION

The sudden popularity of wireless networks, combined with a popular misperception that no additional steps to secure those networks are necessary, has caused a marked increase in the number of insecure computer networks that can be accessed without authorization. This in turn has given rise to the sport of wardriving detecting and reporting the existence of insecure wireless networks, ostensibly without actually accessing the network. Wardriving may also involve illegally accessing and monitoring the networks once so discovered. The sport of discovering connections to wireless computer networks can be done while driving in a car or while strolling on foot with a PDA When a network is identified, the Hotspot access point(AP) can be marked with a coded symbol in chalk on a wall or sidewalk, or war chalked. This will alert others to the presence of an open or insecure wireless network in a given location which they might choose to access themselves. Other variations include war stumbling (accidental discovery of an open access point).

Most hackers or wardriving hobbyists use freeware tools such as NetStumbler, or Kismet.These software programs can be used for the wholly legitimate purpose of helping network administrators make their systems more secure. They work by detecting the service set identifier (SSID) number that wireless networks continuously broadcast to identify themselves to their authorized users. Unfortunately, unless steps are taken by the wireless network operator to restrict what and to whom the network broadcasts as part of this process of signaling to users, then unauthorized users can also discover the existence of the network. In that event, drive-by snoopers and casual passersby alike will not only be able to detect the network, but will be able to access network resources unless some system is in place to restrict network access, such as requiring a user ID and password to log on to the system.

Information gathered in this manner can be correlated with geographical information provided by the Global Positioning System (GPS) and uploaded to maps posted on the Internet showing the location of access points (AP) for Wi-Fi networks. Commercial services such as Wi-Finder provide maps of wireless networks that provide free or paid public Internet access.

References

[1] Heim, Kristi "Seattle packed with Wi-Fi spot", 2005.
[2]Rose Frank "Wired War Driving" 2007.
[3]Marwick, Alice "Seattle Wifi Map Project", 2005.
[4] http://www.wigle.net/
[5] http://www.wardrive.net

Distributed Database Systems

Mr.Parag Makwana[a] , Mr.Nirav Shah[b]

[a]*Asst. Prof , Shree Swaminarayan College of Computer Science, Sardarnagar, Bhavnagar – 364001 India, M. K. Bhavnagar University*
[b]*Asst. Prof., Shree Swaminarayan College of Computer Science, Sardarnagar, Bhavnagar – 364001 India, M. K. Bhavnagar University*

Abstract
A distributed database appears to a user as a single database but it is a set of databases stored on multiple computers. Data on several computers can be simultaneously accessed and modified using a network. Each database server in the distributed database is controlled by its local DBMS, and each cooperates to maintain the consistency of the global database..

Keywords: Distributed data storage, distributed transaction , sharing, query processing, schema object .

1. Concept of Distributed Database

In a distributed database system, the database is stored on several computers. The computers in a distributed system communicate with each other through various communication media, such as high–speed buses or telephone lines.They do not share main memory, nor do they share a clock. The processors in a distributed system may vary in size and function. They may include small microcomputers, work stations, minicomputers, and large general– purpose computer systems. A distributed database system consists of a collection of sites, each of which may participate in the execution of transactions which access data of one site, or several sites. The main difference between centralized and distributed database systems is that, in the Centralized, the data resides in one single location, while in the Distributed database, the data resides in several locations.

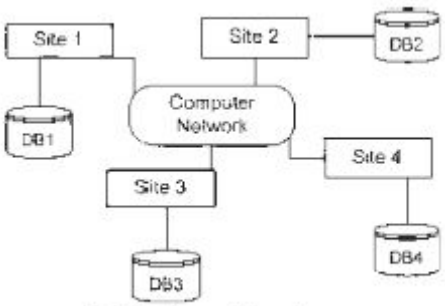

A Distributed Database

1.1. Distributed Database

Logically interrelated collection of shared data and a description of this data, physically distributed over a computer network. Distributed databases are useful now days as many branches of the organizations are geographically separated. Thus, accessing a centralized database at one location may cause many issues such as slow accessibility, session's time out, inefficiency, no load sharing etc. Thus, to have more efficient system, concept of distributed databases provides proves to be more lucrative.

1.2.Client Server and Nodes

A database server is the software managing a database, and a client is an application that requests information from a server. Each computer in a system is a node. A node in a distributed database system can be a client, a server, or both. For example, in Figure , the computer that manages the HQ database is acting as a database server when a second statement statement is issued against against the local DEPT table and is acting as a client when it issues a First and
third statement against remote EMP in the SALES database.

1.3.Direct & indirect connections

A client can connect directly or indirectly to a database server. A direct connection occurs when a client connects to a server and accesses information from a database contained on that server. In contrast, an indirect connection occurs when a client connects to a server and then accesses information contained in a database on a different server. In above Figure, when the client application issues the first and third statements for each transaction, the client is connected directly to the intermediate HQ database and indirectly to the SALES database that contains the remote data.

2.Distributed DBMS Architecture

A distributed database system allows applications to access data from local and remote databases. In a homogenous distributed database system, each database is an Oracle Database. In a heterogeneous distributed database system, at least

one of the databases is not an Oracle Database. Distributed databases use client/server architecture to process information requests. Three types of database systems.

2.1. *Homogenous Distributed Database Systems*

In a homogeneous distributed database system, all sites have identical database management system software, are aware of one another, and agree to cooperate in processing user's requests. A homogenous distributed database system is a network of two or more Oracle Databases that reside on one or more machines. Below Figure illustrates a distributed system that connects three databases: hq, mfg, and sales.

An application can simultaneously access or modify the data in several databases in a single distributed environment. For example, a single query from a Manufacturing client on local database mfg can retrieve joined data from the products table on the local database and the dept table on the remote hq database. For a client application, the location and platform of the databases are transparent. You can also create synonyms for remote objects in the distributed system so that users can access them with the same syntax as local objects. For example, if you are connected to database mfg but want to access data on database hq, creating a synonym on mfg for the remote dept table enables you to issue this query.

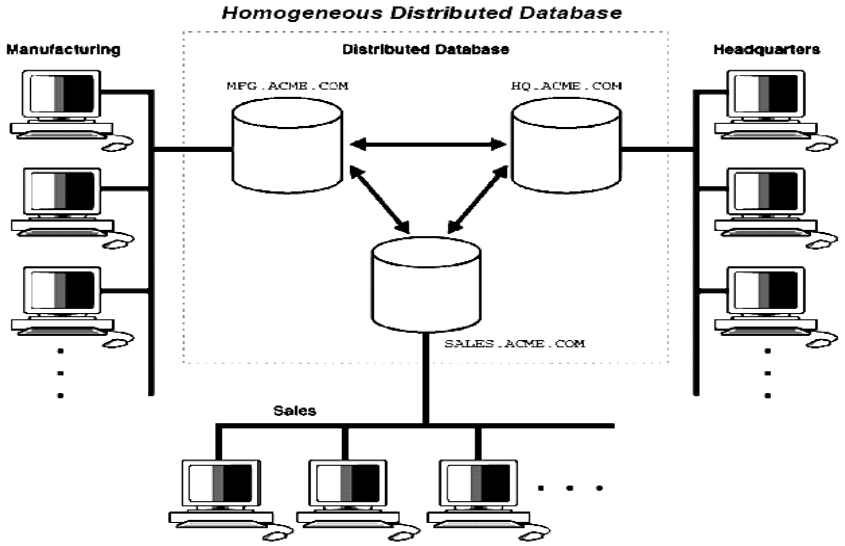

2.2Heterogeneous Distributed Database Systems

In a heterogeneous distributed database, Different sites may use different schemas, and different database-management system software. The sites may not be aware of one another, and they may provide only limited facilities for cooperation in transaction processing. In a heterogeneous distributed database system, at least one of the databases is a non-Oracle Database system. To the application, the heterogeneous distributed database system appears as a single, local, Oracle Database .local Oracle Database server hides the distribution and heterogeneity of the data. The Oracle Database server accesses the non-Oracle Database system using Oracle Heterogeneous Services in conjunction with an agent. If you access the non-Oracle Database data store using an Oracle Transparent Gateway, then the agent is a system-specific application. For example, if you include a Sybase database in an Oracle Database distributed system, then you need to obtain a Sybase-specific transparent gateway so that the Oracle Database in the system can communicate with it. Generic connectivity can be use to access non-Oracle Database data stores so long as the non-Oracle Database system supports the ODBC or OLE DB protocols. c architectures as below.

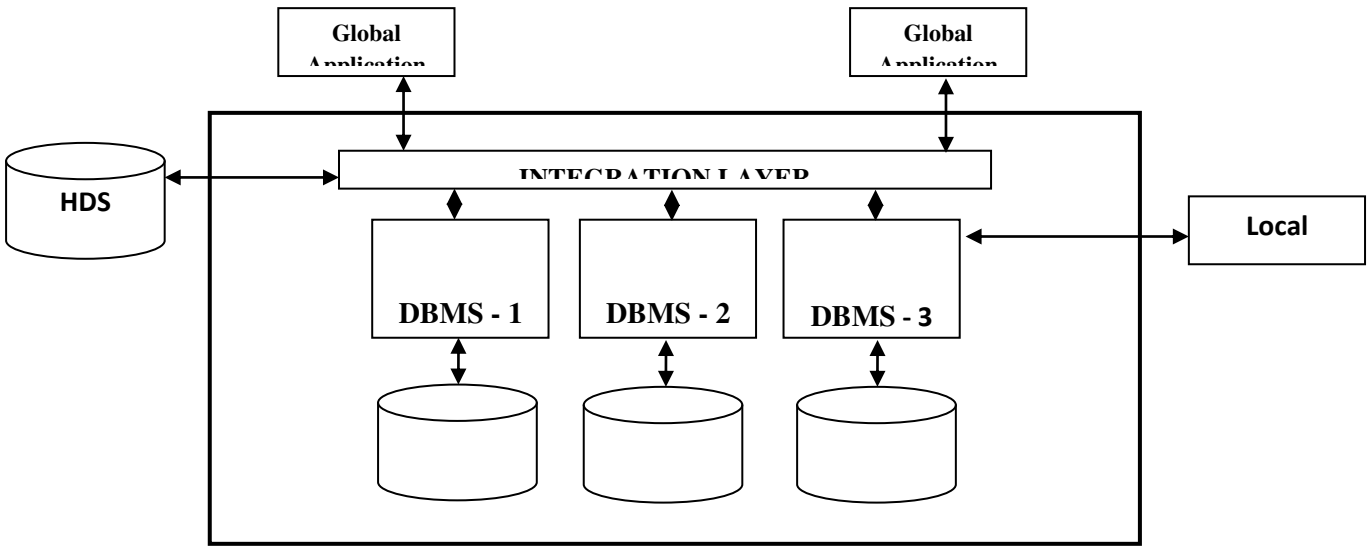

Industries are a heterogeneous system consist of different subsystem. Subsystem are interconnected to each other to communicate with each module. The subsystem must be interconnected to reach the complexity needed for an optional performance. Various heterogeneous distributed database systems are cyber physical systems, IOT (internet of things) are industries revolution.

2.2.1 Generic Connectivity

Generic connectivity allows to connect non-Oracle data stores by using either a Heterogeneous Services ODBC agent or a Heterogeneous Services OLE DB agent, both are included with the Oracle product as a standard feature. Any data source compatible with the ODBC or OLE DB standards can be accessed using a generic connectivity agent. Generic connectivity is implemented as one of the following types of Heterogeneous Service agents: ODBC agent for accessing ODBC data providers. OLE DB agent for accessing OLE DB data providers that support SQL. processing--sometimes referred to as OLE DB (SQL) OLE DB agent for accessing OLE DB data providers without SQL processing support. Each user session receives its own dedicated agent process resulted by the first use in that user session of the database link to the non-Oracle system. The agent process ends when the user session ends. The advantage to generic connectivity is that it does not require one to purchase and configure a separate system-specific agent. user simply need an ODBC or OLE DB driver that can interface with the agent.

2.2.2 Transparent Gateway Agents

For each non-Oracle Database system that you access, Heterogeneous Services can use a transparent gateway agent to interface with the specified non-Oracle Database system. The agent is specific to the non-Oracle Database system, so each type of system requires a different agent. The transparent gateway agent facilitates communication between Oracle Database and non-Oracle Database systems and uses the Heterogeneous.Services component in the Oracle Database server. The agent executes SQL and transactional requests at the non-Oracle Database system on behalf of the Oracle Database server. A transparent gateway agent is a system-specific source and behaves as if you had an Oracle database. Gatway enables integration with data stores such as : DB2, SQL Server. Heterogeneous Services extend the Oracle SQL engine to recognize the SQL and procedural capabilities of the remote non-Oracle system and the mappings required to obtain necessary data dictionary information. Heterogeneous Services provides two types of translations: the ability to translate Oracle SQL into the proper dialect of the non-Oracle system as well as data dictionary translations which displays the metadata of the non-Oracle system in the local format. For situations where no translations are available, native SQL can be issued to the non-Oracle system using the pass-through feature of Heterogeneous Services. The capabilities, SQL mappings, data type conversions, and interface to the remote non-Oracle system are contained in the gateway. The gateway interacts with Heterogeneous Services to provide the transparent connectivity between Oracle and non-Oracle system. The gateway doesn't have to be installed on the machine running Microsoft SQL Server. The gateway doesn't use SQL Server client, but uses MS-ODBC driver for SQL server that comes with all windows installations

2.3. Client/Server Database Architecture

A database server is the Oracle software that manages a database, and a client is an application that requests information from a server. Each computer in a network is a node that can host one or more databases. Each node in a distributed database system can act as a client, a server, or both, depending on the situation. For example, in Figure , the computer that manages the HQ database is acting as a database server when a second statement statement is issued against against the local DEPT table and is acting as a client when it issues a First and third statement against remote EMP in the SALES database.

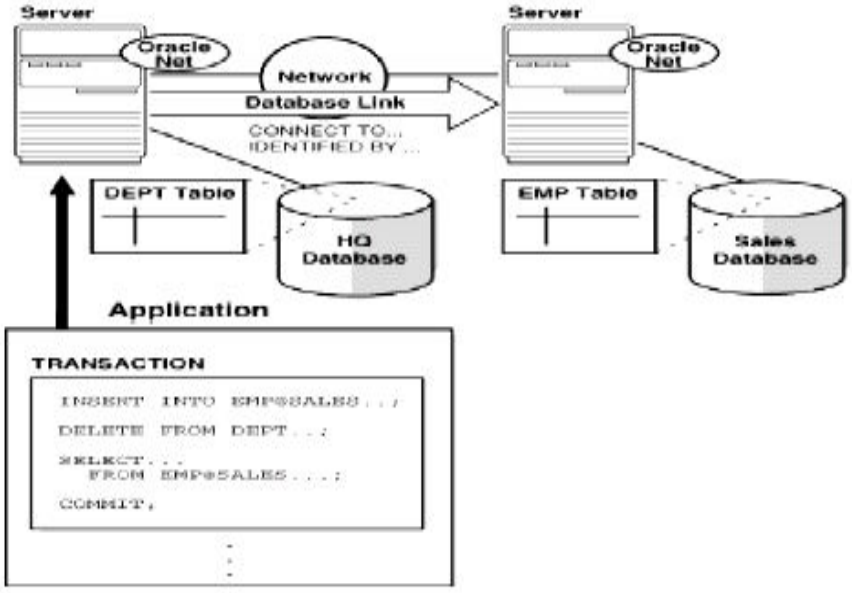

A client can connect directly or indirectly to a database server. A direct connection occurs when a client connects to a server and accesses information from a database contained on that server. For example, if you connect to the hq database and access the dept table on this database as in above Figure, you can issue the following: SELECT * FROM dept; This query is direct because you are not accessing an object on a remote database. In contrast, an indirect connection occurs when a client connects to a server and then accesses information contained in a database on a different server. For example, if you connect to the hq database but access the emp table on the remote sales database as in above Figure you can issue the following: SELECT * FROM emp@sales;

References

[1] M Tamer Ozsu & Patrick volduriez . Principals of Distributed database systems.
[2] Chhanda Ray.,2009. Distributed database systems.

A study on Data mining classification and functionalities

Mr. Arpit Parekh[a], Mr. Nirav Shah[b]

[a]*Asst. Professor, Shree Swaminarayan College Of Computer Science, Sardarnagar, Bhavnagar – 364001, Gujarat, India*
[b]*Asst. Professor, Shree Swaminarayan College Of Computer Science, Sardarnagar, Bhavnagar – 364001, Gujarat, India*

Abstract
Data mining is the semi-automatic extraction of patterns, changes, associations, anomalies, and other statistically significant structures from large data sets. Data mining means the non-trivial extraction of implicit, previously unknown, and potentially useful information from data. In data mining process various patterns are extracted and this is why it is also known as pattern discover. There are a number of data mining classification and functionalities including Concept/Class Description: Characterization and Discrimination, Mining Frequent Patterns, Associations, and Correlations, Classification and Prediction, Cluster Analysis, Outlier Analysis & Evolution Analysis. In this paper a number of classification techniques and functionalities are included which are used in various areas for data mining principle and proved to be very helpful in the decision making process in their business and other areas. This paper is very helpful to select a data mining classification technique and functionalities for a particular application.

Keywords: Kinds of databases, knowledge mined, techniques utilized, application adapted, Association, classification, Clustering, Prediction.

1. Introduction

Data mining is the task of discovering interesting patterns from large amounts of data where the data can be stored in databases, data warehouses or other information repositories. Data mining is an interdisciplinary field, the confluence of a set of disciplines, including database systems, statistics, machine learning, visualization, and information science.

Data mining is the practice of automatically searching large stores of data to discover patterns and trends that go beyond simple analysis. Data mining uses sophisticated mathematical algorithms to segment the data and evaluate the probability of future events. Data mining is also known as Knowledge Discovery in Data (KDD).

Techniques from other disciplines may be applied, such as neural networks, fuzzy set theory, knowledge representation, inductive logic programming, or high-performance computing. Because of the diversity of disciplines contributing to data mining, data mining research is expected to generate a large variety of data mining systems.

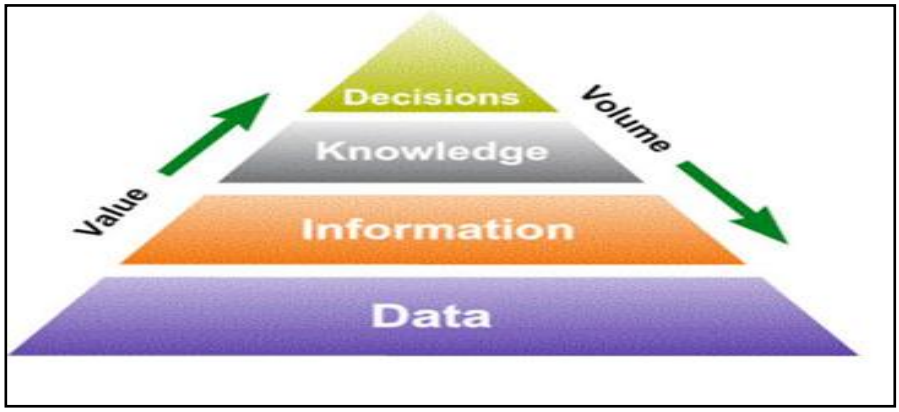

Fig.1 Data Mining works with Warehouse Data

It is necessary to provide a clear classification of data mining systems, which may help potential users distinguish between such systems and identify those that best match their needs.

Data mining tasks can be classified into two categories: Descriptive and Predictive. Descriptive mining tasks characterize the general properties of the data in the database. Predictive mining tasks perform inference on the current data in order to make predictions. It is important to have a data mining system that can mine multiple kinds of patterns to accommodate different user expectations or applications. Furthermore, data mining systems should be able to discover patterns at various granularities. Because some patterns may not hold for all of the data in the database, a measure of certainty or "trustworthiness" is usually associated with each discovered pattern.

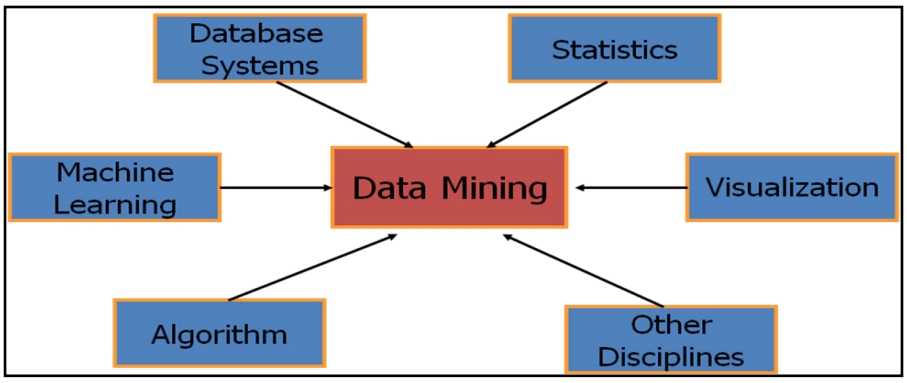

Fig.2 Data Mining: Confluence of Multiple Disciplines

2. Classification of Data Mining Systems:

Data mining systems can be classified categorized according to various criteria, as follows:

a) Classification according to the kinds of databases mined:

Database systems can be classified according to different criteria (such as data models, or the types of data or applications involved).We may have a relational, transactional, object-relational, or data warehouse mining system. If classifying according to the special types of data handled, we may have a spatial, time-series, text, stream data, multimedia data mining system, or a Worldwide Web mining system.

b) Classification according to the kinds of knowledge mined:

Data mining systems can be categorized according to the kinds of knowledge they mine, that is, based on data mining functionalities, such as characterization, discrimination, association and correlation analysis, classification, prediction, clustering, outlier analysis, and evolution analysis.
Data mining systems can be distinguished based on the granularity or levels of abstraction of the knowledge mined, including generalized knowledge (at a high level of abstraction), primitive-level knowledge (at a raw data level), or knowledge at multiple levels.
Data mining systems can also be categorized as those that mine data regularities (commonly occurring patterns) versus those that mine data irregularities (such as exceptions, or outliers).

c) Classification according to the kinds of techniques utilized:

Data mining systems can be categorized according to the underlying data mining techniques employed.
These techniques can be described according to the degree of user interaction involved (e.g., autonomous systems, interactive exploratory systems, query-driven systems) or the methods of data analysis employed (e.g., database-oriented or data warehouse– oriented techniques, machine learning, statistics, visualization, pattern recognition, neural networks, and so on).

d) Classification according to the applications adapted:

Data mining systems can also be categorized according to the applications they adapt. Data mining systems may be tailored specifically for finance, telecommunications, DNA, stock markets, e-mail, and so on.
A database is any organized collection of data. Database creates with proper planning of Data mining classification. Here we define the concept of classification with example of Co-Workers and Patient Information.

Fig. 3 classification can be represented with examples of Co-Workers

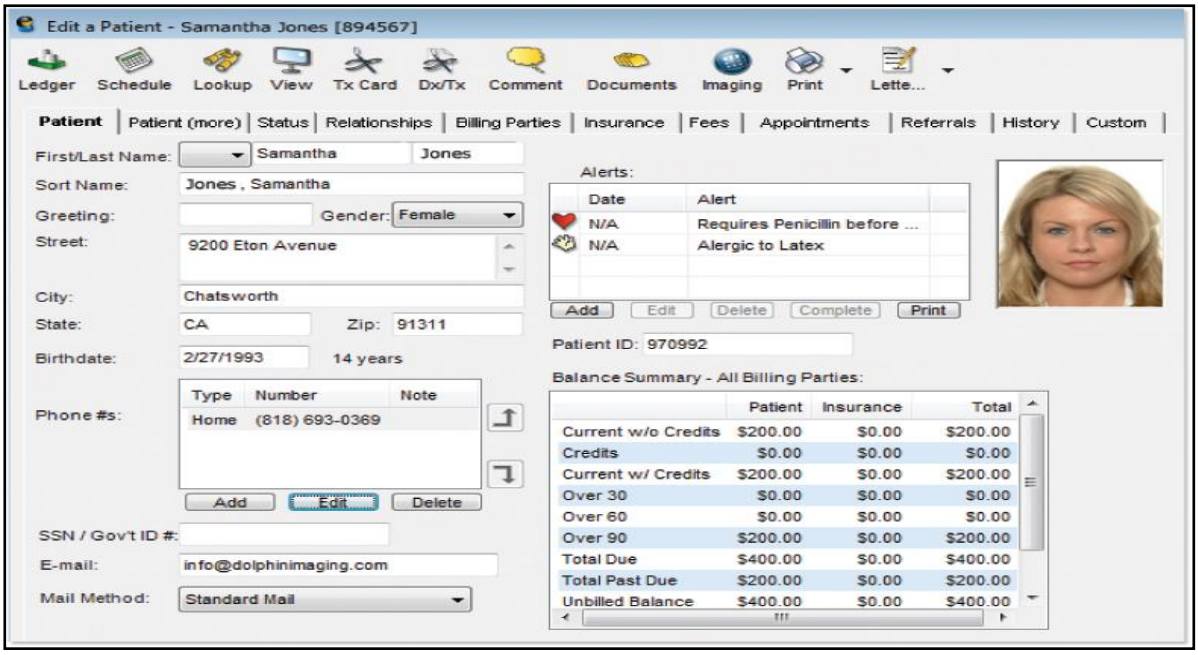

Fig. 4 classification can be represented with examples of Patient Information

WHO USES DATAMINING CLASSIFICATION?

[1] **Banking:** Future prediction
[2] **Amazon.com (Online Stores):** Recommendation
[3] **Facebook:** Prediction how active a user will be after 3 months?

3. Data mining functionalities:

A) Concept/Class Description: Characterization and Discrimination

Data can be associated with classes or concepts. It can be useful to describe individual classes and concepts in summarized, concise, and yet precise terms. Such descriptions of a class or a concept are called class/concept descriptions.

These descriptions can be derived via

(1) Data characterization, by summarizing the data of the class under study the target class) in general terms, or

(2) Data discrimination, by comparison of the target class with one or a set of comparative classes (often called the contrasting classes), or

(3) Both data characterization and discrimination.

Data characterization is a summarization of the general characteristics or features of a target class of data.

The output of data characterization can be presented in various forms. Examples include pie charts, bar charts, multidimensional data cubes, and multidimensional tables.

Data discrimination is a comparison of the general features of target class data objects with the general features of objects from one or a set of contrasting classes.

The target and contrasting classes can be specified by the user, and the corresponding data objects retrieved through database queries.

The methods used for data discrimination are similar to those used for data characterization.

The forms of output presentation are similar to those for characteristic descriptions, although discrimination descriptions should include comparative measures that help distinguish between the target and contrasting classes. Discrimination descriptions expressed in rule form are referred to as discriminate rules.

B) Mining Frequent Patterns, Associations, and Correlations

Frequent patterns, are patterns that occur frequently in data. There are many kinds of frequent patterns, including item sets, subsequence, and substructures.

A frequent item set typically refers to a set of items that frequently appear together in a transactional data set, such as milk and bread.

A frequently occurring subsequence, such as the pattern that customers tend to purchase first a PC, followed by a digital camera, and then a memory card, is a (frequent) sequential pattern.

A substructure can refer to different structural forms, such as graphs, trees, or lattices, which may be combined with item sets or subsequence.

If a substructure occurs frequently, it is called a (frequent) structured pattern. Mining frequent patterns leads to the discovery of interesting associations and Correlations within data.

Association rules are discarded as uninteresting if they do not satisfy both a Minimum support threshold (Large) and a minimum confidence threshold (high).

Additional analysis can be performed to uncover interesting statistical Correlations between associated attribute-value pairs.

Frequent item set mining is the simplest form of frequent pattern mining. Single-dimensional association rules Multidimensional association rules.

C) Classification and Prediction

Classification is the process of finding a model (or function) that describes and distinguishes data classes or concepts, for the purpose of being able to use the model to predict the class of objects whose class label is unknown.

The derived model is based on the analysis of a set of training data. The derived model may be represented in various forms, such as classification (IF-THEN) rules, decision trees, mathematical formulae, or neural networks.

A decision tree is a flow-chart-like tree structure, where each node denotes a test on an attribute value, each branch represents an outcome of the test, and tree leaves represent classes or class distributions. Decision trees can easily be converted to classification rules.

A neural network, when used for classification, is typically a collection of neuron-like processing units with weighted connections between the units.

Whereas classification predicts categorical (discrete, unordered) labels, prediction models continuous-valued functions.

It is used to predict missing or unavailable numerical data values rather than class labels.

Regression analysis is a statistical methodology that is most often used for numeric prediction.

Prediction also encompasses the identification of distribution trends based on the available data.

Classification and prediction may need to be preceded by relevance analysis, which attempts to identify attributes that do not contribute to the classification or prediction process.

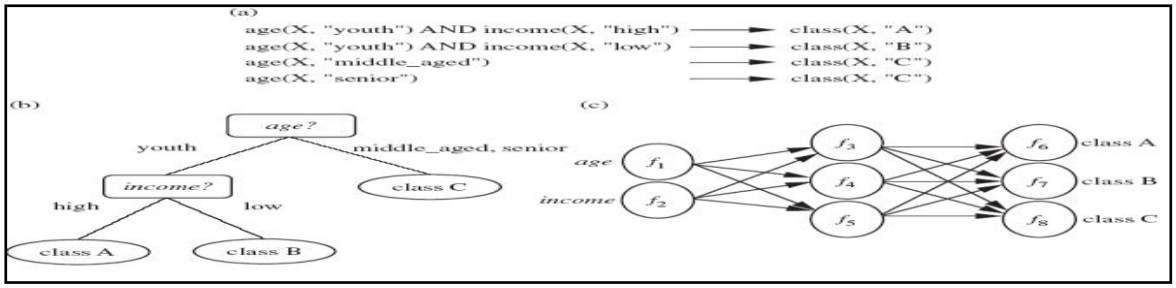

Fig. 5 classification model can be represented in various forms, such as (a) IF-THEN rules (b) A decision tree, or (c) Neural network.

D) Cluster Analysis

Clustering analyses data objects without consulting a known class label. The class labels are not present in the training data simply because they are not known to begin with.

The objects are clustered or grouped based on the principle of maximizing the intra class similarity and minimizing the interclass similarity.

Each cluster that is formed can be viewed as a class of objects, from which rules can be derived.

Clustering can also facilitate taxonomy formation, that is, the organization of observations into a hierarchy of classes that group similar events together.

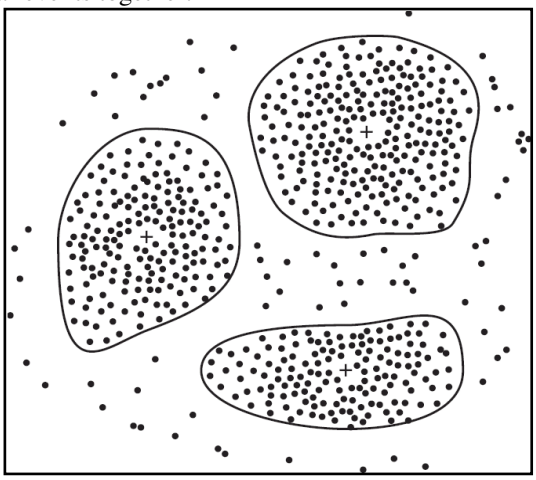

Fig. 6 cluster Analysis

E) Outlier Analysis & Evolution Analysis

A database may contain data objects that do not comply with the general behaviour or model of the data. These data objects are outliers.

In some applications such as fraud detection, the rare events can be more interesting than the more regularly occurring ones.

The analysis of outlier data is referred to as outlier mining.

Data evolution analysis describes and models regularities or trends for objects whose behaviour changes over time.

Although this may include characterization, discrimination, association and correlation analysis, classification, prediction, or clustering of time related data, distinct features of such an analysis include time-series data analysis, sequence or periodicity pattern matching, and similarity-based data analysis.

Data mining is

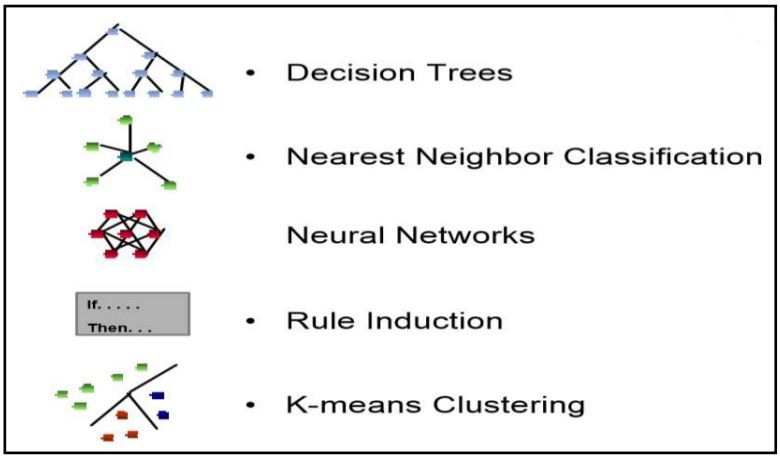

Fig. 7 Data mining functionalities

Acknowledgements

In Database management system multiple requirements are available and include new business techniques. In above discussion we see that the Business Database management and Data mining depended on the performance of various classification types and functionalities performance.

In the data mining move toward, information is requested, processed, and merged continuously, so the information

is with good grace mining for difference mining classification and functionalities.
Quantifiable business benefits have been proven through the integration of data mining with current information systems, and new products are on the horizon that will bring this integration to an even wider audience of users.
Use data to build a model of the real world (domain of interest) describing patterns and relationships.

References

[1] Data Warehousing, Data Mining and OLTP; Alex Berson, Stephen J. Smith 1997, McGraw Hill
[2] Data Mining – Concepts & Techniques; Jiawei Han & Micheline Kamber, Jain Pei, Morgan Kaufmann publication; Third Edition
[3] R. E. Sorace, V. S. Reinhardt, and S. A. Vaughn, "High-speed digital-to-RF converter," U.S. Patent 5 668 842, Sept. 16, 1997.
[4] http://www.tutorialspoint.com/data_mining/dm_classification_prediction.htm
[5] http://en.wikipedia.org.
[6] https://webdocs.cs.ualberta.ca/~zaiane/courses/cmput690/notes/Chapter1/
[7] Google Scholar. http://scholar.google.com/scholar
[8] My blog: www.aparekh5888.blogspot.com
[9] Witten I. H., Frank E., "Data mining: Practical machine learning tools and techniques with Java implementations", Morgan Kau fmann, San Francisco, CA. USA, 2000.
[10] Jain N., Srivastava V., "DATA MINING TECHNIQUES: A SURVEY PAPER". IJRET: International Journal of Research in Engineering and Technology, Vol. 02 Issue 11, 2013.
[11] http://www.slideshare.net

Content Based Video Retrieval and Indexing

Mr.Anshuman S. Patel[a]

[a]Asst. prof, Information Technology Department, Government Polytechnic, Sector-26, Gandhinagar-382026,anshu_info@yahoo.co.in

Abstract- The advances in computing technologies, high speed communication networks, mass Storage devices and consumer electronics have resulted in large amounts of multimedia data being generated in digital form throughout the world. Search for desire information in such bulky data is still very difficult and time consuming. One of the solution of this problem is content based video retrieval. This paper surveys the generalized architecture of content based video retrieval.

Keywords- Content-based Image Retrieval systems (CBIRS), Content-based Image Retrieval (CBVRS), Optical Characters Recognition (OCR), QBIC, graphical user interface (GUI)

I. INTRODUCTION

We are in an era where the technologies that enable people to easily capture and share digitized video data are rapidly developing and becoming universally available. Personal computers are continually getting faster, smaller, and cheaper, while high-speed and reliable networking has shifted towards mobile and wireless access. To date, handheld devices and the Internet have become a common method to create and transport video documents. As a result, there has been a huge increase in the utilization of video as one of the most preferred types of media due to its content richness for many significant applications. In order to support and maintain video growth, further enhancement on the current solutions for Content-Based Video Retrieval (CBVR) is underway from last few years[1,2].

A. CBIRS vs. CBVRS

CBIRS start flourishing on the Web. Their performances are continuously improving and their base principles span a wide range of diversity. Such as QBIC [3], Virage [4], Visualseek [5]. CBVR systems appear like a natural extension (or merge) of CBIR. However, number of factors that are ignored when dealing with images which should be dealt with when using videos Such as temporal information. These factors may complicate the querying system. The temporal information in video brings the concept of motion for the objects present in the document. In CBIRS image are stationary so object are match according to color, shape but motion doesn't play any role. In CBVR two video documents may contain the same objects but little relevance may be found between the two. Since they may have different direction of motion. It is therefore essential to encode within the indexing of a video document the behavior of all objects throughout the document.

Another aspect that does not exist in CBIRS and that should be consider in CBVRS is the structural organization of the document. A video document can be organized into a hierarchical structure (see section 2 video structure).

Another issue in CBVR is the complexity of the querying systems. A very elaborated retrieval systems would allow flexibility for the user to specify its query parameters. Query-by-example systems used in CBIRS require the user to show the system one or more documents similar to what he is looking for. Although this method is easy for images since image can be scan easily. But in context of video scanning of video document is far more complicated.

The rest of the paper is organized as follows. In section-II, a generalized video structure is discussed In section-III, component of general video retrieval system is discuss. Finally in section-IV, we conclude the topic.

II. VIDEO STRUCTURE

The temporal structure of a video is an important aspect for video retrieval as it provides a logical hierarchy that allows the user to drill down to find the target object. The temporal structure of a video as shown in figure-1.
knowledge base or annotation of the content for the levels to be appropriately constructed. An act or episode for example has little to do with the physical characteristics of the video and requires semantic knowledge of film scripts. Syntactic levels may also require some domain knowledge but it is generally small.

2.1 Frames

All videos consist of frames and are designed to be played back at a preset number of frames per second (fps). Extracting individual frames is not a challenge for video retrieval research as video decoders are designed to be able to present each frame. Since time difference between frames are small content between frames are similar. So, video retrieval system doesn't need to represent all frames individually. Instead frames can be sampled with a larger time period or alternatively higher level structural.

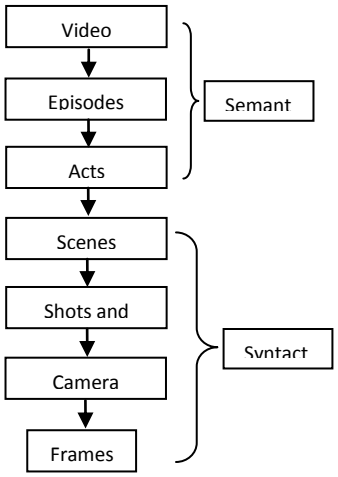

Figure 1: Temporal structure of a video sequence.

2.2 Camera Operations

Camera operations include panning, tilting, dollying, and zooming. One shot may consist of a number of camera operations following one after the other. Camera operations result in global optical flow that can be detected using optical flow analysis. Different motion vector patterns are generated by different camera operations. Determining the type of camera operation from the motion vectors is relatively simple however its performance can be affected by motion within the scene.

2.3 Shots and Cuts

A shot is a single continuous camera recording. A shot may consist of multiple camera operations. Shots are separated by cuts between two shots. There are two types of cuts, abrupt and gradual. An abrupt cut simply has a frame from the previous shot followed by a frame from the next shot. Gradual cuts involve a transition from one shot to the next over a number of frames. Example like effect of dissolve, wipe etc. Abrupt cuts are relatively easy to detect by observe change in pixel value between two frame. Gradual cuts are more difficult to detect as they occur over a number of frames.

2.4 Scenes

A scene is a physical or virtual location. A scene may consist of many camera shots but from different locations and orientations. That's why change between two scenes cannot detect by analyzing individual pixels value because it may be a cut between two shots of the same scene. Scene change detection requires features from frames that will change less between shots and more between scenes. So, rather than looking for changes between scenes try to group shots that have similar characteristics.

III. COMPONENTS OF VIDEO RETRIEVAL SYSTEMS
IV.

A good CBVR system must provide interface so that a naive user able to interact by provide his query and computer would give the exact result. The success of retrieval depends on the completeness and effectiveness of the indexes. Indexing techniques are determined by the extractable information through automatic or semi-automatic content extraction. the content extraction process aims to automatically identify and classify the event(s) that is contained within each playback segment. Since video contains rich and multidimensional information, it needs to be modelled and summarized to get the most compact and effective representation of video data.

3.1 Video Segmentation

Indexing could be performed on the whole video stream but it would be too coarse. On the other hand, if the indexing is based on each frame, it would be too dense as a frame often does not contain any important information. Usually indexing is done on a group of sequential frames with similar characteristics.

A. Shot Boundaries Detection

Shot is a sequence of video frames which have similar characteristics. Shots extraction requires the computation of an appropriate metric (algorithm) to characterize the change of video content between two frames and a threshold to determine whether the change is important enough to be defined as a shot boundary. Three main methods which can be used for shot boundaries detection are described below: pixel-wise frame difference, histogram comparison, audio assisted. Pixel-wise frame difference technique detects shot boundaries by measuring a qualitative change

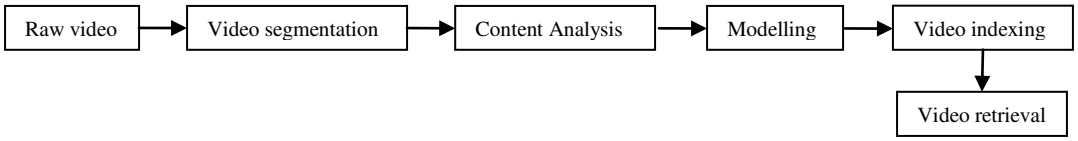

Figure 2: Components of Content-based Video Retrieval Architecture

between two frames by simply comparing the spatial corresponding pixels in the two frames and determining the amount of the pixels that have changed. Thus it is also called pair-wise pixel comparison algorithm.
Colour histogram can be used due to its effectiveness in characterizing the global distribution of an image without knowing the component objects that make up the image. Colour histogram comparison should also be less sensitive to object motion than pixel difference technique. Histogram technique based on fact that two frames which have unchanging backgrounds and objects will show little difference in the histograms. Unfortunately, histogram is still sensitive to global camera operations and it may fail when the histograms within a shot are different due to changes in lighting conditions, such as flashes and flickering objects.
To increase the accuracy of shot detection, the audio content which is synchronized with a shot and related to the visual content can be used. Thus, certain audio characteristics can be used to help determining shot boundaries.

B. Scene Detection

Shot-based indexing can be fully automated, but they are lack in semantic information. To overcome this limitation, scenes need to be extracted as a sequence of shots which represent and can be described by a semantic content description. Scene are difficult to detect due to need for understanding the video contents. One approach is by measuring the semantic correlation of consecutive shots based on dominant colour grouping and tracking. Similarly, scene can be detected via continuous coherence in which related shots are grouped into scenes which defines a single dramatic event. Or a scene can be formed by grouping a sequence of shots which depict a particular object activity or event.

3.2 Content Analysis

A video document is composed of image-sequence, audio tracks, and textual content video content analysis should utilize the techniques use for audio and image analysis.

A. Audio analysis

Audio track in a video document is synchronized with the content presented in the video sequences. Therefore techniques from audio analysis for video content can be used for video content analysis. Audio features can be extracted in two levels frame and clip. In frame level it is a group of neighbouring samples which last for short time. Audio signal is stationary in it; therefore, short term features can be extracted. In Clip level it consists of a sequence of frames last over a clip. To understand the semantic contents of a signal clip level features are important as human often needs a longer audio analysis.

B. Image Analysis

Image include colour, texture, and shape. This image features can be used for video content analysis, like colour feature, shape feature and texture feature. Colour features can be use for measuring the similarity between visual documents. Color feature is used content management due to its robustness to complex background, scaling, orientation, and perspective. Methods like color histogram and moment can be use for it.Shape features is another important image feature since good shape representation technique are unique, robust against translation, scaling and rotation. Shape representations can be categorized into boundary- (outer shape) and region- (entire shape) based. Texture is an important image feature as it describes visual patterns which are homogeneous and not produced from single colour or intensity. Texture can be described by six features: coarseness, contrast, directionality, regularity, likeliness, and roughness.

C. Video Optical Character Recognition

Different Optical Characters Recognition (OCR) method are available which can be used to analyse the contain. Especially content like news video having text. Video OCR techniques contain three steps, Text detection and localization i.e. text occurrences in multiple video frames are detected. Text segmentation and extraction*:* text

regions are segmented from the complex background and the quality of the texts is enhanced. Text recognition text regions are fed to OCR to convert them into texts.

3.3 Modelling Video Data

A data model in a DBMS (Database Management System) provides a framework to express the properties of the data items to be stored and retrieved from the system. The main aim of video modelling is to hide video's complexities by representing them with formal language or schema based on its unique characteristics, the content, and the application it is intended for. There are some specific requirements for video data models: a) Support for multi-level video structure abstraction. b) Support for spatial and temporal relationship. c) Support for gradual annotation of a video stream: it is required since the first round of annotation is often incomplete because video annotation still relies heavily on human intervention which is very much subjective. d) Support video data independence: it means that the video model should be easily shared and re-used by not depending on the way video data is stored physically and how it is perceived by the viewers within the specific application context.

Relational model has limitations that make it unsuitable for video data modelling as given below: a)The process of normalization will fragment a 'real world' entity into many relations with a physical structure to reflect the entity's structure, leading to expensive joins during query processing. b) Relational model assumes horizontal and vertical homogeneity of data structure. Horizontal homogeneity means each tuple of a relation must be composed of the same attributes and vertical means that the values of a column must be derived from the same domain. But in case on video scene from different domains exits. c) different video have different characteristic so universal database structure cannot be use for all.d)Relational database cannot handle complicated characteristics of time dependent multimedia such as audio and video

Another type data model is Object Oriented models introduce the concept of Abstract Data Types (ADT or encapsulation) which hides internal data structure and shows only the external operations that can be applied on the object .The major strength of OO is its capability to support complex data definitions. The important difference between OO and relational model lies in the way relationships are implemented. However, the main disadvantage of OO is OODBMS suffers from poor performance when supporting large-scale system such as video database; because query optimization is highly complex

Object Relational (OR) modelling is becoming popular to deal with media data such as video as it can combine the strength of OO with relational modelling and address its limitations. Basically, OR contains relational model and uses SQL as the query language. OR modelling scheme modifies the relational model to support OO features by introducing new features that include base data type extension, complex objects support, inheritance, and rule systems.

3.4 Video Indexing

Indexing of the video content is needed for time efficient retrieval of video. Video indexing approaches can be categorized based on the two main levels of video content: low-level (perceptual) features and high-level (semantic) annotation. The main benefits of low-level feature-based indexing techniques are: They can be fully automated using feature extraction techniques, such as Image and sound analysis and Users can use similarity search using certain feature characteristics such as the shape and colour of the objects on a frame or the volume of the sound track.

In the following subsections, three major indexing techniques are discussed: A) Segment-based video indexing techniques(indexes low level features), including shot-based, object-based, and event-based indexing, B) Annotation-based video indexing, and C) Indexing approaches which aim to bridge semantic gap.

A. Segment-Based Video Indexing

During the process of indexing texts, a document is divided into smaller components such as sections, paragraphs, sentences, phrases, words, letters and numerals, and thereby indices can be built on these components. Using a similar approach, video can also be decomposed into a hierarchy similar to the storyboards in filmmaking in this approach we can do indexing on the basis of key frames, object and event as shown in figure 3. In key frame indexing we find key frame of shots and do indexing on basis of that. Object-based video indexing aims to distinguish particular objects throughout video Sequence to capture content changes and do indexing on the basis of object characteristics. Event based video indexing aims to index frames where a new event occur from raw video track. Example frame where goal happen in a football match.

Table 3.1 summarizes segment-based, object-based, and event- based video indexing techniques in terms of their benefits and weaknesses.

Feature-based Indexing Technique	Benefits	Limitations
Segments-based (indexed by key frames)	Can be easily automated. Segments reveal temporal structure well (e.g. in hierarchy). Supports queries by image Similarity. Enable intuitive browsing through visual key frames that represent the whole shot.	Hard to determine the best key frame. Both manually and automatically especially, for application/user specific contexts. Motion and temporal information is not represented.
Object-based	By identifying objects throughout. scene, and tracking the motion, content changes can be identified from a video sequence. Easier when video is compressed Using MPEG-4 object based coding standard.	Object detection becomes difficult. In certain situations, such as complex background, mall sized objects and large number of overlapping objects such as soccer ball.
Event-based	Event is often how viewers remember video content easily Event is a feature and can be considered to be close to semantic.	Event detection is generally Difficult. Often has to be named using domain specific terms to make more sense to users.

Table 3.1 summarizes segment-based, object-based, and event- based video indexing techniques in terms of their benefits and weaknesses.

B) Annotation-Based Video Indexing

Text data management, such as Information Retrieval (IR) techniques have matured and

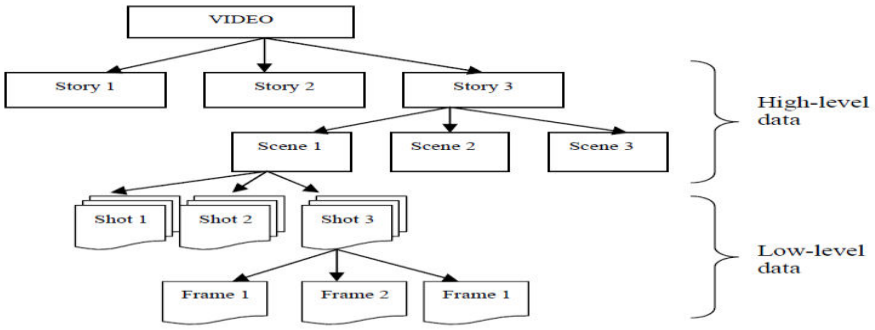

Figure 3 Segment-Based Indexing

in successfully supported by traditional DBMSs. Thus, another alternative for Managing video is to annotate the semantics of video segments using key words or free texts. Thus, user queries can be managed using standard query language, such as SQL and browsing can be based on hierarchical topic (or subject) classification [. However, the major limitation of this approach is the fact that it would be extremely tedious and ineffective to manually annotate every segments of video. On the other hand, the process of mapping low-level video features into high-level semantic concepts is not straight forward.

C) Indexing by Bridging Semantic Gap

some indexing methods is require that bridge the Semantic gap between high-level concepts and low-level features. Methods like Query by Example with Relevance Feedback and Browsing with compact representation helps in bridging that gap. Query by Example with Relevance Feedback method based on the fact that audio-visual feature extraction is easier than semantic understanding and possible to fully automated the system. For example, given a sample video shot, the system should find the indexed segments which have the closest characteristics such as similar speaker pitch and similar face. Browsing with compact representation method based on fact that Video documents are long due to its spatial and temporal Dimensions. Users should benefit from more compact representations of video Document. Like key frames and video snapshot in Image-based representations. Some of compact representation is summarization and skimming i.e. intelligent fast-forward

3.5 Video Retrieval

Queries can be used to retrieve the video from indexes. Queries can be classified according to the following categories. Query by content, Query using matching, Query functions or query behaviour, Query temporal unit.

A. Query by content

This classification is based on the nature of video content that is required to satisfy the query. Like Semantic (information) query, Audiovisual (AV) query and Meta (information) query. Semantic query requires an understanding of the high-level semantic content of the video data, which usually can be partially satisfied using the information from the semantic video annotations. Thus it is the most complex type of query in video database. For example: finding scenes with Actor = "A" AND Emotion ="Crying". Audiovisual query depends on the AV features of the video and usually does not need the semantic understanding of the video data (thus only need a minimal degree of interpretation of the AV features). In most cases, this query can be satisfied automatically or semi-automatically by the analysis or computation. For example: finding shots where camera is stationary AND lens action is zoom-in. Meta query attempts to extract the information about the video data, such as the producer, date of production, and length. Thus it can be answered in most cases using an automatic conventional text based searching while the meta-annotations may need to be manually. For example: finding out a video directed by Stephen Spielberg and titled "Jurassic Park".

B. Query using matching

This type query requires extracting matching objects(sample) from the database. Therefore, some processing is applied to the AV features such as sound and image analysis to match the query sample and the video data. It can be classify into two parts . Exact-match query that Requires exact match between the query and the video data. For example: finding scenes with object = "Actor X". and Similarity-match query (Often known as Query by Example): this query type does not allow exact matching. Because of the complex nature of video data, this query type is more required. For example: finding all the shots, in which object that is similar to a given image appears.

C. Query functions or query behaviour

This query type depends on the functions that queries perform. It can be divided into two categaroies Location-deterministic query, Browsing query, Iterative query and Tracking queries. Location-deterministic query try to specifically locate certain video information within the database; therefore users must have a clear idea on the video contents. For example: finding the location of all scenes with actor X. The result would be the pointers to the beginning of such the scenes. Browsing query may be used when users are not sure about what they can retrieve or they are unfamiliar with the structures and types of the available information in the video database. Thus system should allow formulation of fuzzy queries to browse through the database. While browsing, no specific entities are required, therefore the system must provide some data sets to represent each of the video data in the system such as iconic descriptions (or key-frames) combined with some textual metadata annotations. For example: browsing contents of video which genre="Sport".

Iterative query is an extended browsing query as the system needs to provide a graphical user interface (GUI) that allows users to incrementally refine their queries until the most satisfying results are obtained. Tracking queries deals with the tracking of visual quantities in the video. For example: tracking the ball throughout this scene. The result shows the location of the ball in each of the frames in shot.

D. Query based on temporal unit

These queries classify the granularity of video data required to satisfy query. It can be divide into Unit query and Sub-unit query. Unit query deals with the complete units of video. For example: finding a sport video, which has player A in it. While Sub-unit query deals with parts of video data, such as frames, clips and scenes. For example: finding the scenes where actor X appears, finding the shots in which a player with 'this type of face' appears.

V. CONCLUSION

This paper survey the generalized architecture of CBVR and the methods can be used to implement each step. Existing CBIR and CBVR systems have matured to the point of being commercially deployable [6.7]. But still challenges are to index millions of objects rather than thousand of object. Therefore increased complexity is due to indexing this million of object rather than increased complexity of feature extraction representation or used interaction technique. Another problem is to handle 3-D object if objects are in million because representing them and Comparing two 3D structures are very more complex .

REFERENCES

[1]. Ichiro Ide, Koji Yamamoto*?*, and Hidehiko Tanaka," Automatic Video Indexing Based on Shot Classi_cation", AMCP'98, LNCS 1554, pp. 87-102, 1999.
[2]. Hong Lu1, Xiangyang Xue1, and Yap-Peng Tan2,"Content-Based Image and Video Indexing and Retrieval".
[3]. M. Flickner, H. Flickner, W. Niblack, J. Ashley, Q. Huang, B. Dorn, M. Gorkani, J. Hafner, D. Lee, D. Steel and D. Yanker, "Query by image and video content: the QBIC system," IEEE Computer, Sept. 1995, vol. 28 (9), pp. 23-32.
[4]. J. Bach, C. Fuller, A. Gupta, A. Hampapar, B. Harawitz, R. Humpherey, F. Jain, and C. Shu, "The Virage image search engine: An open frame work for image management," in *Proc. SPIE: Storage and Retrieval for Image Video Databases*. Feb. 1996, Vol. 2670, pp. 76-87.
[5]. John R. Smith and Shih-Fu Chang, "VisualSeek: a fully automated content-based image query system," *ACM Multimedia*, 1996, pp. 87-95.
[6]. J. Bach, C. Fuller, A. Gupta, A. Hampapur, B. Gorowitz, R. Humphrey, R. Jain, and C. Shu,"Virage image search engine: an open framework for image management," in Proceedings of
the SPIE, Storage and Retrieval for Image and Video Databases IV, (San Jose, CA), pp. 76–87, SPIE, February 1996.
[7]. M. Flickner, H. Sawhney, W. Niblack, J. Ashley, Q. Huang, B. Dom, M. Gorkani, J. Hafner,
D. Lee, D. Petkovic, D. Steele, and P. Yanker, "Query by image and video content: The QBIC system," IEEE Computer, pp. 23–32, September 1995.
[8]. M. Irani, H. Sawhney, R. Kumar, and P. Anandan, "Interactive content-based video indexing and browsing," in First IEEE Workshop on Multimedia Signal Processing, 1997.
[9] F. Arman, R. Depommier, A. Hsu, and M.-Y. Chiu, "Content-based browsing of video se quences," in ACM Multimedia '94, pp. 97–103, 1994.
[10] H. Ueda, T. Miyatake, and S. Yoshizawa, "IMPACT: An interactive natural-motion-picture dedicated multimedia authoring system," in ACM CHI'91, pp. 343–350, 1991.
[11] M. Mills, J. Cohen, and Y. Y. Wong, "A magnifier tool for video data," in Proceedings of CHI '92, pp. 93–98, 1992.
[12] M. G. Christel, M. A. Smith, and D. B. Winkler, "Evolving video skims into useful multimedia abstractions," in ACM CHI'98, pp. 171–178, April 1998.
[13]. E. Elliott and G. Davenport, "Video streamer," in ACM CHI '94 Conference Companion, pp. 65–66, 1994.
[14]. R. C. Veltkamp and M. Tanase, Content-Based Image and Video Retrieval, ch. A Survey of
Content-Based Image Retrieval Systems, pp. 47–101. Kluwer, 2002.
[15]. H. Tamura, S. Mori, and T. Yamawaki, "Textural features corresponding to visual perception," IEEE Transactions on Systems, Man, and Cybernetics, vol. 8, pp. 460–473, June 1978.
[16] J. R. Smith and S.-F. Chang, "VisualSEEk: A fully automated content-based image query system," in ACM Multimedia, pp. 87–98, 1996.

Dead Code Elimination Techniques in Eclipse Compiler for Java

Hiral Karer[a],Rachana Baldania[b], Kinjal Mori[c]
[a]Dharmsinh Desai University,Nadiad and 38701, India
[b]Dharmsinh Desai University,Nadiad and 38701, India
[c]Dharmsinh Desai University,Nadiad and 38701, India

Abstract

Eclipse compiler for Java (ECJ) is open source incremented compiler. We reform features of ECJ, related to optimization technique called as dead code detection and elimination. ECJ identifies the dead code. We are extending this compiler to eliminate the dead code. In this paper we are describing the structure of ECJ. For dead code elimination approach we have used Single Static Assignment (SSA) strategy. After applying definition- use (DU) chain on SSA, we detect dead code and eliminate it. In this paper we are describing two algorithms: 1) To convert Java source code into SSA. 2) To eliminate dead code. Hence by implementing dead code elimination in ECJ, we are utilizing space and execution time of program which leads to improve efficiency of compiler.

Keywords: efficiency; optimization; directory structure;Nomenclature

1. Introduction

Eclipse compiler for Java (ECJ) used in Eclipse IDE to compile a Java source code. We are elaborating the directory structure of ECJ with its functionality.

To eliminate dead code we take approach of Single Static Assignment (SSA). The source code is transferred into SSA form. For this transformation we introduce an algorithm. In SSA form, each variable is assigned exactly once statically.

To eliminate dead code, first we have to identify variable which are never used in program. Through an example we describe how dead code is identified in Eclipse.

Poor choice of data structure and variable lead to slow compilation, data structure like processor and memory allocation for unused variable. To overcome this problem we have to choose better advanced optimization technique named as dead code elimination. We describe algorithm with example of it.

This paper is structured as follows: In section 2, we are describing the directory structure of ECJ compiler. In section 3, we are describing procedure for SSA strategy in ECJ compiler for dead code elimination technique. In section 4, we are describing dead code detection in ECJ compiler. In section 5, we are describing dead code elimination and its algorithm. In section 6, we are describing Experimental analysis. In section 7, we are describing Conclusion. In section 8, we are describing Future extension.

2. Director structure of ECJ

ECJ -Eclipse Compiler for **Java**. It is open source incremental model. The batch compiler class is located in the **JDT Core** plug-in. The name of the class is org.eclipse.**jdt**.compiler.batch.BatchCompiler. It is packaged into plugging/org.eclipse.**jdt**.core_3.5.2.v_981_R35x.jar ECJ can also be used as pure Batch compiler outside of Eclipse.

Now we describe a directory structure of ECJ. It is a jar file in eclipse. Many packages are created in ECJ. Functions of ECJ are distributed package wise [1]. The structure of package is shown in figure 1.

There are two main packages 1.core and 2.internal. In core package, there is one package, named as compiler and another is a java file which is adapter file of apache ant. Inside compiler package there are further one package and some java files. All files are used for different purposes like to report program during compilation or to report cancellation of the compilation .Batch package contains class which has public API invoking ECJ. This API gives reasons for failing of compilation. Batch package has one html file which contains the Batch compiler API.

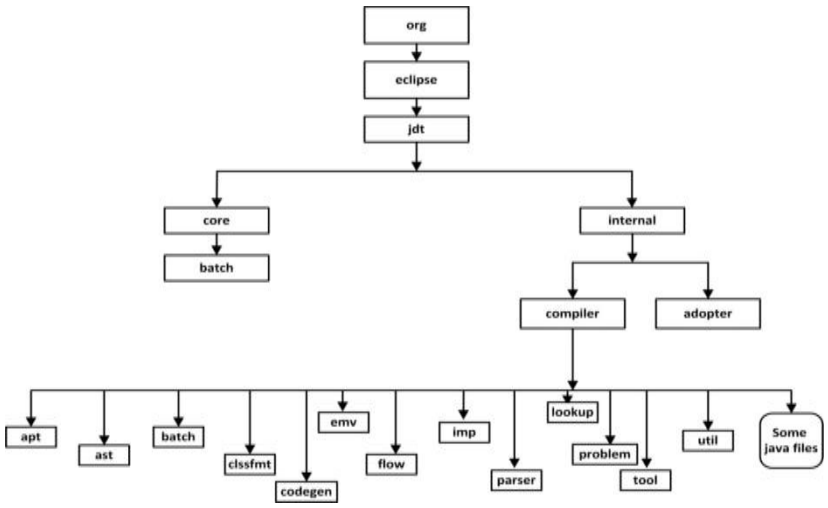

*Fig **1.** Directory structure of ECJ*

We are describing a structure of another package named as internal, which has two sub packages named as adapter and compiler. Adapter sub package has initial API with implementation and file which contain message property. Compiler is most important sub package which contain all the important java files which are useful for compiling a program. To fulfill our goal of elimination, we modify the Java files which are placed inside this package. This sub package contains various sub packages and Java files. Function of these classes to store all class-path into array. Compiler.java contains all declared methods. We get a result of different methods through CompilationResult.java. Description of sub package is given below.

apt: It contains files related to process, classes for various type of type checking methods which have methods to check different type of type checking. Also has a class which handles operation in eclipsemanager and eclipsecompiler.

ast: This sub package has classes to handle variable declaration, various type of expression declaration. These classes contain methods related to array, branch and break statement.

batch: Contains a classes related to classpath as location, source, directory etc. This sub package contains Main.java which is main file of ECJ.

classfmt: It has classes which have information about methods, innerclasses, classpaths, files etc.

env: It contains interfaces to represents target files of to denote compilation units. Using this interface we get starting and ending point of source file.

flow: Java files of this package contain logic related to flow of the program Each class contains logic for branch statement, conditional and unconditional flow respectively.

impl: CompilerStatus.java and CompilerOption.java are important classes. We declare a variable according to feature of compiler inside CompilerOption.java these variables are type of Boolean to enable and disable the feature. Methods of CompilerStatus.java class are used to observe the efficiency of compiler.

lookup: Files related to binding.

parser: Various techniques of parser are implemented.

problem: Logic related to problems like type ,property and handles of problems are implemented.

tool: files related to Eclipse are store here eg. EclipseCompier.java and EclipseCompilerImp.java. Role of these files to register methods which are used in compiler. Methods are implemented which are used in ECJ.

util: It has files which are shared by all packages. General purpose files are stored into this subpackage.

3. Procedure for SSA strategy

In compiler design, static single assignment form is a property of an intermediate representation (IR), which requires that each variable is assigned exactly once, and every variable is defined before it is used [8]. Static single-assignment form arranges for every value computed by a program to have a unique assignment. SSA form simplifies several important optimizations, for example copy propagation, dead code elimination and common sub expression elimination etc.[6].

We use SSA approach for dead code elimination. We describe procedure to convert from Java code to SSA in

section 3.1. Example based on SSA is also given into the section 3.2.

3.1 Procedure to convert into SSA form

Remark;- Phi function is used when different definition of same variable occur into join node at that time to assign a new variable to these variables.eg. y1=phi(y,y); Here y and y are the different definition of same variable. Y1 is new variable.
Input:- Java code.
Output:- Code in SSA form
Variables:-Counter and variable_namei (where i is postfix number of variable).
Step 1:- Scan whole program and find the variables. Take a individual counter for each variable. Initially counter value is 0.
Step 2:- If the node is join node then
Put phi function for a variable due to which node become a join node.
Find predecessor of the node. In the predecessor, check whether definition of that variable has given any postfix number.
If it has then copy postfix number into the phi function and increment the counter value of that variable and assign this incremented value as the postfix to the variable which is placed at the left side of '=' sign.
Join node:- A node which has more than one predecessor
Go to step 3.
Step 3:- If there is arithmetic operation in the block then
Assign counter value as the postfix to the variable which placed at right side of '=' sign and increment the counter value.
Assign a counter value as postfix to the variable placed at left side of '=' sign.
Step 4:- If line has arithmetic operation but not contain assignment operation then
Assign counter value of that variable as postfix.
Step 5:- Go to step 2 until all variable in the program has assigned single vale.

3.2 Tracing a procedure with example

A ECJ -Eclipse Compiler for **Java**. It is open source incremental model. The batch compiler class is located in the **JDT Core** plug-in. The name of the class is org.eclipse.**jdt**.compiler.batch.BatchCompiler. It is packaged into plugging/org.eclipse.**jdt**.core_3.5.2.v_981_R35x.jar ECJ can also be used as pure Batch compiler outside of Eclipse.

Now we describe a directory structure of ECJ. It is a jar file in eclipse. Many packages are created in ECJ. Functions of ECJ are distributed package wise [1]. The structure of package is shown in figure 1.

There are two main packages 1.core and 2.internal. In core package, there is one package, named as compiler and another is a java file which is adapter file of apache ant. Inside compiler package there are further one package and some java files. All files are used for different purposes like to report program during compilation or to report cancellation of the compilation .Batch package contains class which has public API invoking ECJ. This API gives reasons for failing of compilation. Batch package has one html file which contains the Batch compiler API.

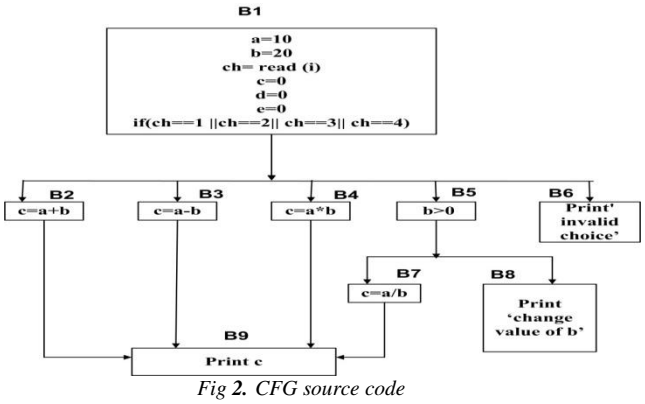

Fig 2. CFG source code

We give name to each basic block as B1, B2, etc.
Join node;- B9.
Predecessor of B9:- B2, B3, B4 and B7.

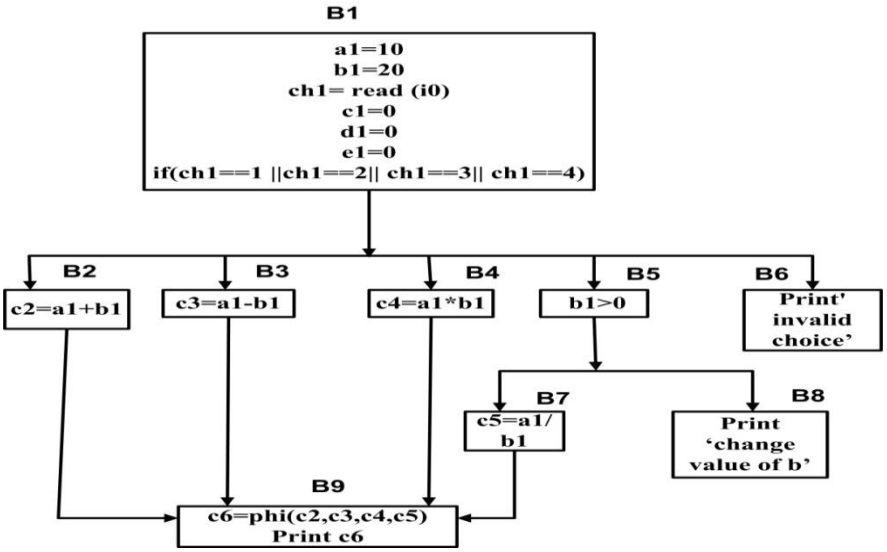

Fig 3. CFG after applying SSA

B9 become join node due to the 'c' variable. So we place phi function inside B9 for 'c' variable.

4. Dead code detection in ECJ

We write a source code on Eclipse IDE and can see the yellow line under a dead code into the figure 4. Cursor is moved onto this yellow line and popup is opened as warning as it is a dead code.

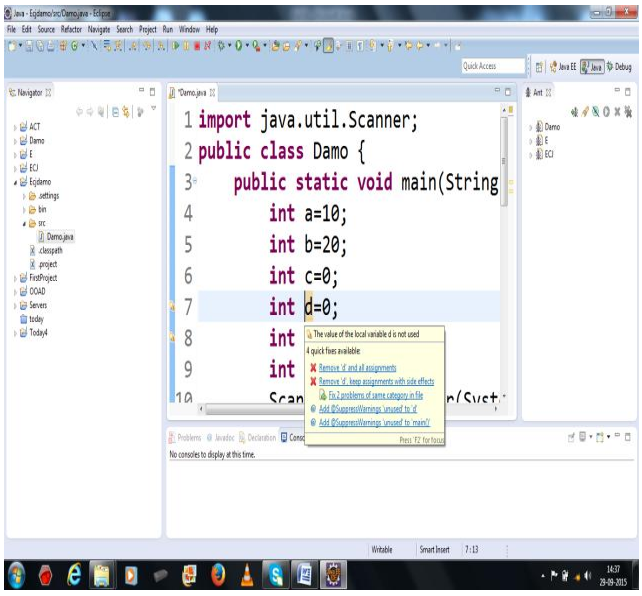

Fig 4. Dead code detection

5. Dead code elimination

In compiler theory, **dead code elimination** is a compiler optimization to remove **code** which does not affect the program results. Dead code is either not executed or executed but its result never be used by the program. This type of code will be eliminated.

After converting into SSA, we apply DU chain on SSA [5] i.e. find a variable which definition is given into the program but it does not use during the execution of the program. Result of this strategy will be dead code. The

variable which has its definition but it has not any use, this type of variable called as dead code [6].

Algorithm to eliminate dead code is written in the section 5.1. Example on dead code elimination is give in the section 5.2.

5.1Algorithm to eliminate dead code

Input:- program in form of SSA
Output:- program with dead code elimination
Arrays:- temp, define, check.
Remark:- Size of temp array is depend upon length of each line of program, Size of define array is equal to number of variables are declare into the program, Size of check array depend on length of each line of program.
Variable:- define.

```
Begin
Do for each line of program
        If line contain phi function, then
                Remove line
        End if
         If line contain any datatype, then
                Split a line when space or '='is come and save into 'temp' array.
                Choose second element of 'temp' array.
                If it contain ',' , then
                        Split it when ',' is come and save it into 'define' array.
                Else
                        Save it into 'define' variable.
                End if
        End if
        Do for each element of 'define' array.
                Copy element of 'define' arrays into 'define' variable.
                Compare the contain of 'define' variable with all line of program.
                        If match is found, then
                        Split a line when either any
                        1. Assignment operator or
                        2. Conditional operator is come.
                        And save it into 'check' array..
                        If index for contain of 'define' variable into 'check' array is less then 0, then
                                Print as variable has no use.
                        End if
                        End if
                End loop.
`       End loop
End loop
End.
```

Example

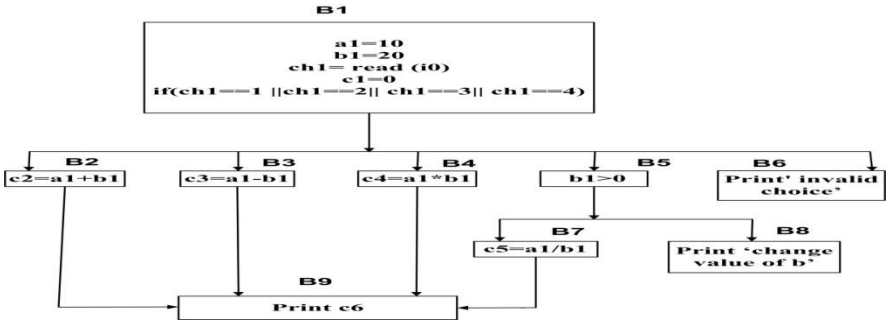

Fig 5. CFG after eliminating dead code and phi function.

6. Experimental analysis

In figure 6 we can see layout of eclipse IDE. Text.java file contains some dead code. We compiled this file using apache ant. This file does not contain our derived algorithm. Without eliminating the dead variable, building time is 975 milliseconds.

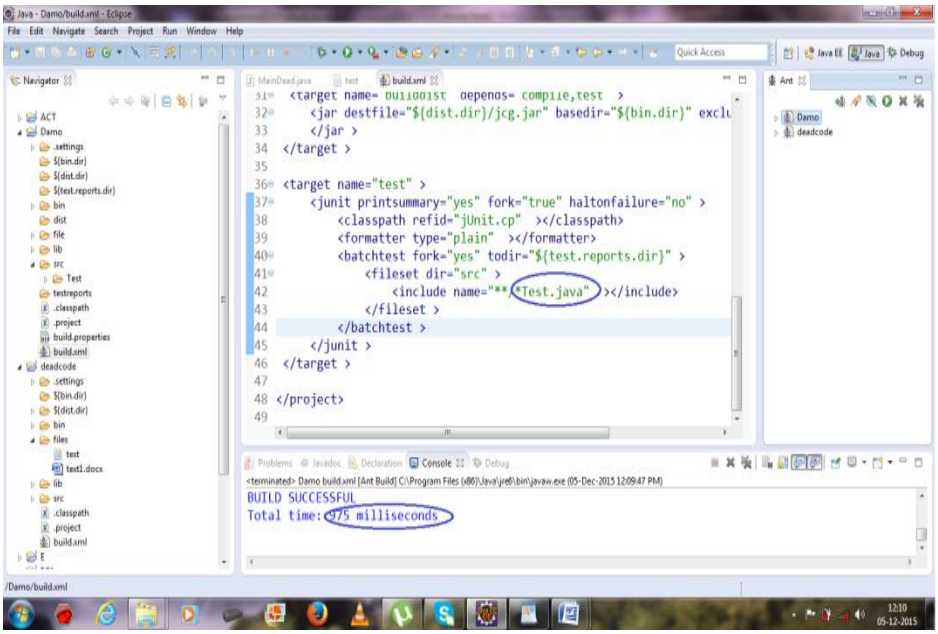

Fig 6. Before applying derived algorithm.

MainDead.java contains our derived algorithm. In figure 7 we can see that after applying derive algorithm on dead code, the building time is 942 milliseconds. Its means time is reduced as compare with 975 milliseconds.

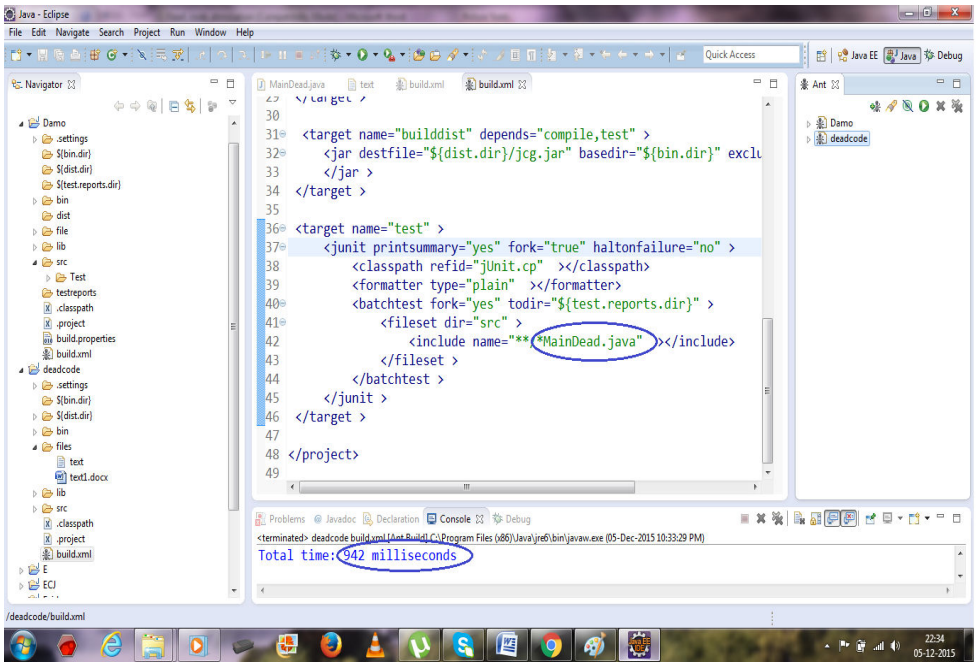

Fig 7.After applying derived algorithm.

7. Conclusion

The elimination of dead code is achieved by using our derived algorithm. From our experimental analysis, we can see that the building time of program is reduced after applying our algorithm. Due to dead code elimination, memory register for dead code becomes free. So we can utilize space and execution time of program which improves efficiency of ecj.

8. Future extension

For future work we can introduce another optimization technique in ECJ. For that we will have to focus on recalculation of expression done by the compiler. To eliminate this recalculation we need to work on common sub expression elimination. By this approach we could utilize the execution time of program. So more efficiently compiler can work

Acknowledgements

I have opportunity to thank them all who have helped me directly or indirectly to make the project successful. I would like to thank my guide Prof. Purvi Soni who have guided and supported me throughout the project because of which the project has seen the light of accomplishment. His constant inspiration and encouragement along with his valuable guidance has been instrumental in the project.

References

[1]www.eclipse.org

[2]Jagdish Bhatta- Effectness of Inlining, Common Subexpression and Deacode Elimination in Optimining Compiler in IJCSN International Journal of Computer Science and Network, Volume 3, Issue 1, February 2014

[3]Coen J. Burki, Dr. Harald H. Vogt- How to save on software maintance cost 2014 Omnext BV.

[4]Matthias Braun, Sebastian Buchwald, Sebastian Hack, Roland LeiBa, Christoph Mallon, Andess Zwinkau – Simple and efficicent onstuction of static singe assignment form in spinger-verlag Berlin, Heidelberg @2013.

[5]Ki-Tae Kim, Je-Min Kim, and Weon-Hee Yoo- Dead Code Elimination in CTOC@2007 IEEE J. Clerk Maxwell, A Treatise on Electricity and Magnetism, 3rd ed., vol. 2. Oxford: Clarendon, 1892, pp.68-73.

[6]Jan Olaf Blech Lars Gesellensetter Sabine Glesner-Formal Verification of Dead Code Elimination in Isabelle/HOL @ 2005 IEEE K. Elissa, "Title of paper if known," unpublished.

[7]Masataka Sassa , Toshiharu Nakaya , Masaki Kohama, Takeaki Fukuoka, Masahito Takahashi and Ikuo Nakata-Static Single Assignment Form in the COINS Compiler Infrastructure– Current Status and Background – SPA 2003.

[8]Vugranam C. Sreedhar1, Roy Dz-Ching Ju2, David M. Gillies3, and Vatsa Santhanam4- Translating Out of Static Single Assignment Form,at Springer-Verlag Berlin Heidelberg 1999.

Anonymizing Sensitive Based Attributes using Hadoop MapReduce

Shivaprakash Ranga[a], Lochan[a], Brinda[b]

[a]*Assistant Professor,Computer Science & Engineering, Sri Venkateshwara College of Engineering, Bengaluru – 562157, India*

[b]*Assistant Professor, Department of Computer Engineering,Anjuman-I-Islam's Kalsekar Technical Campus,Navi Mumbai – 410206, India*

Abstract

Storing big set of private records at local database results in internal attacks with local storage problems and storing records in cloud without anonymization results in external attacks, which both results in privacy breach. To offer privacy, previously proposed Personal Anonymization technique uses two attributes: Sensitive Disclosure Flag (SDF) and Sensitive Weight (SW) which are set on the basis of required privacy. Frequency Distribution Block (FDB) and Quasi-Identifier Distribution Block (QIDB) are used for anonymization. Our proposed approach is the extension of previous work, first each patient IDs in the medical record is changed using Permute method and then the records are generalized to provide anonymity and finally original and anonymized records are saved in cloud which removes the big data storage problem at local system. This work is implemented on Hadoop Map-Reduce Framework. Only data owner can view the records by fetching from cloud using Inverse Permute method and the anonymized records are made available for the researchers to understand the patterns for a particular disease.

Keywords: Personal Anonymization, Map-Reduce, BigData.

1. Introduction

Big data[1] is different from past data warehousing efforts because it performs analytics on almost any type of data file or format, including images, videos, and data gathered from social media. The privacy of data is a huge concern which increases in the context of Big Data. Cloud computing has become a viable, mainstream solution for big data processing, storage and distribution, but moving large amounts of data in and out of the cloud presents a privacy challenge for organizations. There is great public fear regarding the inappropriate use of personal data on cloud, particularly through linking of data from multiple sources but, Personal information present in different organizations will research for understanding patterns there by achieving betterment of the community, for example personal health details of different patients are present in different hospitals and this information can be used by researchers to understand the patterns for a particular disease and hence improve the identification of the diagnosis.

Table 1. Patient Published Data

ID	Age	Zipcode	Disease
1	26	586171	Gastric Ulcer
2	28	586176	Stomach Cancer
3	32	586362	Flu
4	36	586175	Heart Disease
5	42	586178	Heart Disease
6	46	586177	Stomach Cancer

Nowadays with the trend of Big data usually all hospitals go with public cloud for storing the huge health data records. However, numerous hospitals are still hesitant to take advantage of cloud due to privacy and security concerns. Medical privacy or health privacy is the practice of keeping information about a patient confidential. This involves both conversational discretion on the part of health care providers, and the security of medical records. The medical data records present in hospital contains detailed information regarding the patient like name, address, DOB, zip code, symptoms and disease. Usually to preserve the individual privacy the hospital admin removes the details including name and address which
are considered personal from the huge personal health records before it is given to cloud, however this raw health records contain details like zip, DOB that can be linked with other external publicly available data bases for re-identification of sensitive value. For example consider the details of the Patient Published by the hospital in Table 1, which does not contain details regarding name, address and other personal information. The attacker can use the publicly available external data base shown in Table 2 and join these details with Table 1 thereby revealing personal details.

The entire details regarding sensitive information i.e. disease and the identity of the individual are of great

concern because the individuals are not ready to share their sensitive information. The join operation on both Table 1 and Table 2 gives the value Rahul from zip code 589171 and age 26 is having Gastric ulcer. This type of discloser is called Record Level Disclosure. Attributes present in Published Patient Data that can be linked to external publicly available data bases like ZIP, DOB are called Quasi-Identifier (Q) attributes.

Table 2. External Voters Data Base

Name	Age	Zipcode
Rahul	26	586171
Shiva	28	586176
Sita	32	586362
Jeet	36	586175
Sachin	42	586178
Mani	46	586177

However, Data owners of personal health records have to publish the data for significant human benefits as the records are analyzed and mined by research centers. But in storing the data on cloud, the data privacy is at the high risk of disclosure because of the failure of some traditional privacy protection measures on cloud which results in severe social reputation impairment to data owners. Hence, data privacy issues need to be addressed before the data sets are analyzed or shared on cloud. Most widely adopted method for data privacy preservation is Data anonymization which refers hiding identity which preserves privacy of an individual while certain aggregate information is exposed to data users for diverse analysis and mining. Under this modification of data is done in such a way that the resultant table has duplicated records there by restricting the disclosure and this process is called generalization [3,4]. Once the Table is generalized various methods were used to check the property of duplication and distribution. To measure this Samarati and Sweeney [5,6] introduced k-anonymity. A Table satisfies k-anonymity if every record in the table is indistinguishable from at least k-1 other records with respect to every set of quasi-identifier attributes.

Table 3. 2-Anonymus Table

Zipcode	Age	Disease
586***	[20-30]	Gastric ulcer
586***	[20-30]	Stomach Cancer
586***	[30-40]	Flu
586***	[30-40]	Flu
589***	[40-50]	Flu
586***	[40-50]	Heart Disease

Table 3 shows a 2-anonymous generalization for Table 1. Let us assume that the attacker uses the publicly available data base and finds that Rahul's zip code is 586171 and his age is 26 and wants to know the disease of Rahul, the attacker observes the anonymized Table 3 from which attacker understands that 586171 and 26 has been generalized to 586*** and age [20-30] which cannot be linked with voters database record and hence the disease cannot be inferred. But still there is drawback with k-anonymity. Consider, if the attacker tries to infer Sita's disease who is related to group 3 but since the entire group contains the same sensitive attribute the attacker infers that her disease is Flu. This leakage of sensitive value leads to Attribute Level Disclosure. This happens if all the diseases indicated in a group are related to the same disease.

Major disclosures of health records take place at record level and attribute level. To avoid this various anonymity techniques have been proposed, but each of them have several drawbacks. Author[2] uses SW-SDF Based Personal Privacy with QIDB-Anonymization on Medical Data which overcomes the disadvantages of various anonymization techniques. The core of this scheme is two additional flags with the original table. Sensitive Disclosure Flag (SDF) determines whether record owner sensitive information is to be disclosed or not. The second flag is Sensitive Weigh

(SW) which indicates how much sensitive the attribute is. SDF is dependent on SW. Frequency Distribution Block (FDB) and Quasi Identifier Distribution Block(QIDB) which is used in anonymization.

The rest of the paper is organized as follows. In section 2, the prior works on privacy preserving techniques are illustrated. The proposed scheme is defined in Section 3 . Section 4 presents results and analysis. Section 5 concludes the paper.

2. Related Work

Author in [2] proposes a novel privacy preserving technique that over comes the Personalized privacy preservation [9] and other anonymization techniques. Initial anonymization algorithm was called k-anonymity technique [5,6] but the drawback of this approach is that it is prone to record level disclosure. To overcome this disadvantage l-diversity [7] was proposed i.e. Privacy beyond k-anonymity, disadvantage is that it is prone to Skewness and Back ground Knowledge Attack. t-closeness [8] is used to overcome the disadvantages of l-diversity but it has larger information loss.

In [9] the record owner can indicate his privacy by indicating in terms of a guarding node. The drawback of this method is that it may require several iterations based on the guarding node, sensitive attribute is also generalized which has larger information loss. The most important drawback is that distribution of sensitive attribute has not been taken in to account while anonymization.

The disadvantage of SW-SDF based anonymization proposed in [2] is that, it doesn't provide data security on database in local system from external attacks and also local database doesn't support processing a large set of health records. Further storing the original records as well as anonoymized records in local database increases the local storage. The proposed work overcomes these disadvantages, once the original data records are sent for processing, local system contains only IDs and name of the patients which removes the burden of data storage in local database. Along with the remaining fields of health records, permutated values of each IDs are saved in cloud. These permuted IDs secures the health records from the external linking attacks. For processing the large set of health records proposed work is implemented on hadoop framework. Then the records anonymized data and partial-anonymized data (those who want to reveal) are stored in cloud and made available to researchers.

3. Proposed Work

The main motivation of the proposed approach is to make personalized anonymization of the large scale health records depending on the fact that, few patients are ready to reveal their sensitive data and some patients are not ready to reveal. For processing large scale of data, Hadoop MapReduce framework is considered for implementing. Basically, MapReduce on cloud has two levels of parallelization i.e., job level and task level. Job level parallelization means that multiple MapReduce jobs can be executed simultaneously to make full use of cloud infrastructure resources. Combined with cloud, MapReduce becomes more powerful and elastic as cloud can over infrastructure resources on demand, e.g., Amazon Elastic MapReduce service [10]. Task level parallelization refers to that multiple mapper or reducer tasks in a MapReduce job are executed simultaneously over data split. The proposed SW-SDF scheme provides personal privacy anonymization by separating anonymized data and partial-anonymized data. Both datasets are stored in public cloud and made available to researchers.

The proposed work of SW-SDF Based Personal Privacy with QIDB Anonymization using Hadoop framework is divided mainly into four modules as shown in figure 1. They are Admin Module, Mapper and Anonymizer Module, MapBased Reducer Module and Cloud Database Module

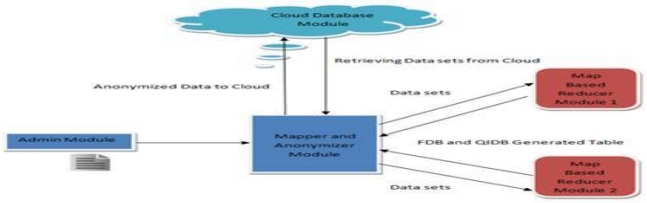

3.1. Admin Module

In this module hospital admin, adds two flags with the original dataset. Sensitive Disclosure Flag SDF which is obtained from the individual patient when they are providing their data. The flag SDF=0 means that the patient is not ready to disclose his sensitive at-tribute whereas SDF=1 doesn't mind revealing his sensitivity. SW is set by the admin based on the prior knowledge of sensitive attribute. The value of SW=0 is used when the sensitive attribute is a common disease like Flu and SW=1 for sensitive attribute like Cancer which is not common. The SDF and SW are taken from [2]. In proposed scheme each IDs in the health record is changed using permute method as shown in Table 5 so that hackers cannot link the patient details. The modified dataset shown in Table 4 is sent to next Mapper and Anonymizer Module and these records are saved in cloud without SW and SDF column. Admin keeps only original IDs and Name in hospital local database. To obtain a original records admin uses a inverse Permute method as shown in Table 6 to retrive a original record. This removes the burden of storing the large dataset at local system.

Table 4. Modified Dataset Table with SW and SDF values

ID	Age	Zipcode	Disease	SW	SDF
1	24	584170	Flu	0	1
3	34	584171	Flu	0	1
8	39	560017	Stomach Cancer	1	1
27	35	584173	Heart Disease	1	0
124	36	584171	Flu	0	1
725	36	584175	Stomach Cancer	1	0
5046	25	560018	Stomach Cancer	1	0

3.2. Mapper and Anonymizer Module

Authors of [2] have not considered large set of health records, as a result the local sys-tem becomes slow when it processes large datasets.

Table 5. pseudocode: Genarating Permute ID
pseudocode: Genarating Inverse Permute ID

```
For each, n
Do
permute id,x = n!+n-1
end
```

Table 6.

```
Original ID, n
for (i=1,i++) until x= 1
do
Flour(x/i)=x
When x=1 corresponding i=n
End
```

The proposed scheme is implemented on Hadoop framework. Mapper and Anonymizer module is master of Hadoop framework, the Mapper partitions the dataset among the number of Reducers and sends to the Map-Based Reducer Module. The result from the different MapBased Reducer Module is FDB generated Table 8 and QIDB generated Table 9. These two tables are combined and final anonymization is done by running SW-SDF anonymization algorithm, taken from [2]. SDF-SW provides personal privacy anonymization by separating anonymized and partial anonymized data. There are totally four threshold attributes to be considered for SW-SDF anonymization algorithm.

i) Th_n minimum number of records in T.
ii) Th_{ittr} maximum number of iterations that must be performed. ittr it indicates the amount of generalization.
iii) Th_{supp} minimum number of sensitive values for suppression.
iv) Th_{acc} minimum number of sensitive values for disclosure.

If SW is greater than Th_n then calculate the difference between QIDB and FDB Probability. The value (QIDB +/- Thacc) should be approximately equal to the difference value. If value is less then FDB probability, disclose the data

else suppress data. The detailed SW-SDF anonymization algorithm is described in Table 7. In paper [2] disclosing the data meant providing no generalization hence even if the data is sensitive there is no personal privacy provided. But in proposed scheme disclosed data is generalized with basic Anonymity and it is called partial anonymized data and the suppressed data is the anonymized data which is generalized with higher Anonymity, shown in Table 11 and 12 respectively. The anonymized and partial anonymized set of data with permuted IDs is given to Cloud Database module where they are stored in cloud server.

3.3. MapBased Reducer Module

This module is the slave of Hadoop framework. The partitioned datasets from Mapper and Anonymizer module is processed at each MapBased Reducer modules to generate Frequency Distribution Block (FDB) and QuasiIdentifier Distribution Block (QIDB). FDB and QIDB are taken from [2]. FDB contains distribution of every disease with respect to original private data. For every record with SW=1 and SDF=0 QIDB is created. This module first counts the total number of rows in the datasets table and selects the unique Disease example like Gastric Ulcer, Stomach Cancer, flu, Heart Diseases etc. At each MapBased Reducers FDB probability is calculated and all the resultant probability is added into the FDB table. After generating FDB table, QIDB table is generated only for sensitive diseases with SW=1.

$$\text{FDBprobability} = \frac{\text{NumberofCountOnEachDisease}}{\text{TotalNumbero fCount}} \qquad (1)$$

The result from the different MapBased Reducer Module is FDB generated table QIDB generated table are shown in Table 8 and Table 9 which is given to the Mapper and Anonymizer Module for further processing.

Table 8. FDB Generated Table

Disease	FDB Probability
Flu	0.4
Stomach Caner	0.4
Heart Disease	0.2

Table 9. QIDB Generated Table

Disease	QIDB Probability
Flu	0
Stomach Caner	0.5
Heart Disease	0.5

$$QIDBprobability = \frac{NumberofCountSatisfyingSW = 1, SDF = 0}{TotalNumberofCountofSensitiveDisease} \qquad (2)$$

3.4. Cloud Database Module

In paper [2] all storage was in local system which increases the chances of privacy loss if any attacks happens at local system and further any crash of local system might result in complete data loss. So, in the proposed scheme Cloud Database module is added which is implemented on Amazon S3 public cloud. This module stores the original health record with permuted IDs as shown in Table 10 which is only available to the Admin and also stores the anonymized and partial anonymized records as shown in Table 11 and Table 12 respectively which are available for the researchers. Admin's local database has only original IDs and patient names. Whenever Admin wants to retrieve the entire health record he uses the inverse permute algorithm to link the original IDs from the local database with the permuted IDs from the cloud.

Table 10. Modified Dataset Table with permuted ID's

ID	Age	Zipcode	Disease
1	24	584170	Flu
3	34	584171	Flu
8	39	560017	Stomach Cancer
27	35	584173	Heart Disease
124	36	584171	Flu
725	36	584175	Stomach Cancer
5046	25	560018	Stomach Cancer

4. Result and Analysis

Our proposed scheme achieves the complete privacy for each individual patient by implementing personal data anonymization. The data records which are needed to be sup-pressed are generalized with more anonymity i.e two columns are generalized as shown in Table 12 and data records which needed to be disclosed are generalized with less anonymity i.e. one column is generalized as shown in Table 11 These two tables are made available for researchers and as only anonymized data are present in cloud and published in public, there is no possible way of external linkage attack. Patient original IDs and name are only present in local database. The permuted IDs with all other details are stored in cloud as shown in Table 10. The admin can inverse-permute the IDs using the original IDs to get the complete records when needed. So, the local database is free from large storage of data as well as internal attack.

Table 11. Partial Anonymized data

Age	Zipcode	Disease	Records
24	584***	Flu	1
34	584***	Flu	1
36	584***	Flu	2
39	560***	Stomach Cancer	2
28	584***	HeartDisease	1

Table 12. Anonymized data

Age	Zipcode	Disease	Records
[30-40]	584***	Heart Disease	1
[20-30]	560***	Stomach Cancer	1
[30-40]	584***	Stomach Cancer	1

5. Conclusions

In working with cloud and Big data, Personalized privacy is an important research direction and SW-SDF is a better option for personalized Privacy. SW indicates the sensitivity of records which has to be given privacy and SDF gives the individual view of revealing or suppressing data. Even though when the disease is common but patient wants privacy, the records are generalized with basic anonymity. For the sensitive diseases, the records are generalized with more anonymity. As the private database contains only patient IDs and name it removes the burden of storage and IDs in cloud are stored in permuted form which overcomes record linkage and attribute linkage, in turn giving complete individual privacy. The anonymized records are made available for the researchers to understand the patterns for a particular disease.

References

[1] Patel, A.B., Birla, M., Nair, U.: Addressing big data problem using Hadoop and Map Reduce, In 2012 Nirma University International Conference on Digital Object Identifier, pp. 1–5, (2012).
[2] Kiran P., Dr Kavya N P.: SW-SDF Based Personal Privacy with QIDB-Anonymization Method In: (IJACSA) International Journal of Advanced Computer Science and Applications.) 3(8), pp. 60–66, (2012).
[3] Lefevre K., Dewitt D. J. and Ramakrishnan R.: Incognito: Efficient full-domain k-anonymity, In Proceed-ings of ACM SIGMOD. ACM, New York, pp. 49–60, (2005).
[4] Fung B. C. M., Wang K. and Yu P. S.: Anonymizing classification data for privacy preservation, In IEEE Trans. Knowl. Data Engin,pp. 711–725, (2007).
[5] P. Samarati.: Protecting Respondents Privacy in Microdata Release, IEEE Trans. on Knowledge and Data Engineering (TKDE), 13(6), pp. 1010–1027, (2001).
[6] L. Sweeney.: k-Anonymity: A Model for Protecting Privacy, International J.Uncertain. Fuzz., 10(5), pp. 557–570, (2002).
[7] Machanavajjhala A, Gehrke J, Kifer D and Venkitasubramaniam M.: l-diversity: Privacy beyond k-anonymity, In ICDE Conference, (2007).
[8] Ninghui Li , Tiancheng Li , Suresh Venkatasubramanian.: t-Closeness: Privacy Beyond k-Anonymity and lDiversity, In Proceedings of the 22nd IEEE International Conference on Data Engineering(ICDE), (2006).
[9] Xiao X. and Tao Y.: Personalized privacy preservation, In Proceedings of the ACM SIGMOD Confer-ence.ACM, New York, (2006).
[10] Amazon Elastic MapReduce http ://aws:amazon:com/elasticmapreduce:

Object or its feature identification from Mobile Reviews in Gujarati Language

Himadri Patel[a], Rudri Mehta[b], Anish Shaikh[b], Ravija Mehta[b], Namrata Patel[b], Devangshi Patel[b]

[a]*Assistant Professor, SRIMCA, Uka Tarsadia University, Bardoli394601, India*
[b]*Student, , SRIMCA, Uka Tarsadia University, Bardoli394601, India*

Abstract

Sentiment Analysis or Opinion Mining is a field of Natural Language Processing aims at determining what other people think, comment and gives their opinion. Each comment given by user contains object or feature of an object for which opinion is given, either explicitly or implicitly. Extracting an object or feature of an object can be considered as a sub-task of opinion mining process. Gujarati is a popular Indian language which is not having any work done in the field of opinion mining. In our work we are giving start-up by implementing methodology to identify object or its feature from a review in Gujarati language. We are using review of mobile devices and extracting object or feature of an object from those reviews.

Keywords: Opinion mining; Feature extraction; Object identification; Mobile reviews; Gujarati, Supervised learning.

1. Introduction

Opinion mining is becoming very popular after evolution of web 2.0. This field uses content posted by user on web in the form of blog, post, comment, article or small message etc. Researchers use this content to identify and analyze the opinion written by the user. Commonly, the task is to identify whether the opinion is positive, negative or neutral. However, some researchers may also focus of the degree of opinion. The general process of opinion mining contains several sub tasks. One of them is to identify object or feature of an object for which opinion is written. In this work, reviews of mobile devices in Gujarati language are used as dataset.

Feature is also known as aspect. Aspect based opinion mining deals with the extraction of opinion aspects by applying various techniques. Aspect can be an implicit or explicit.

E.g. "The display is clear."

"The phone is small enough to put in my pocket."

The feature "display" appears in the first sentence explicitly. However, in the second sentence, the feature "size" is not directly mentioned but only implied by the word "small".

1.1 Basic Terminologies:

This section defines the primary terminologies used in feature identification. Following are the primary definition.

- Feature (Bing, 2012): Features refer to all the components, qualities or physical characteristics of a product such as size, color, weight, speed, etc.
- Opinion Sentence (Bing, 2012): An opinion sentence is a sentence that consists of at least one product feature and its corresponding opinion word.
- Explicit and Implicit feature (Bing, 2012): An explicit feature is a feature of a product which is directly talked about in review sentence. An implicit feature is a feature that is not explicitly mentioned in the sentence and it can be implied.
- Frequent and Infrequent feature (Bing, 2012): A feature f is frequent if it appears in majority of the review sentences f is called infrequent if it is only appeared in a few numbers of reviews.

2. Methodology

Methodology used in this work can be divided into two parts: pre-processing phase and processing phase. These phases are discussed below in details:

2.1 Pre-processing phase:

The main task done in this phase is to collect and clean the data as per the requirement of processing phase. Gujarati language is resource poor language and not having enough review data or data related to opinion given by

users. So, the data are collected from different review websites in English language and translated into Gujarati language using a translation tool.

The translated sentences were having few translation errors and other noise in it. For example, words like 'awesome, performance, Samsung, android' are un-translated. So, next task done in the pre-processing phase is to clean those data. This process is done manually. In this step, all wrong translations and un-translated words are correctly translated and then noise like repetition of punctuation mark and spelling mistakes are also corrected manually.

The next task is to apply POS tagging on those translated and noise free sentences. Gujarati POS tagger implemented in (Patel, 2008) is used for tagging the sentences. The translated sentences looks like shown in below given example.

E.g. કેમેરા N_NN શ્રેષ્ઠ JJ છે V_VAUX .RD_PUNC

For implementing POS tagger to our data, we transformed the word file into feature file; the document file should contain only word in each line with an additional space. So, we have to write document such that it contains single word along with a space in one line. The tagger uses crfsuit for adding POS tags in the sentences. This tagger is already trained and having training model. Due to lack of data and time, the same training model is used instead of training the same with data of our domain.

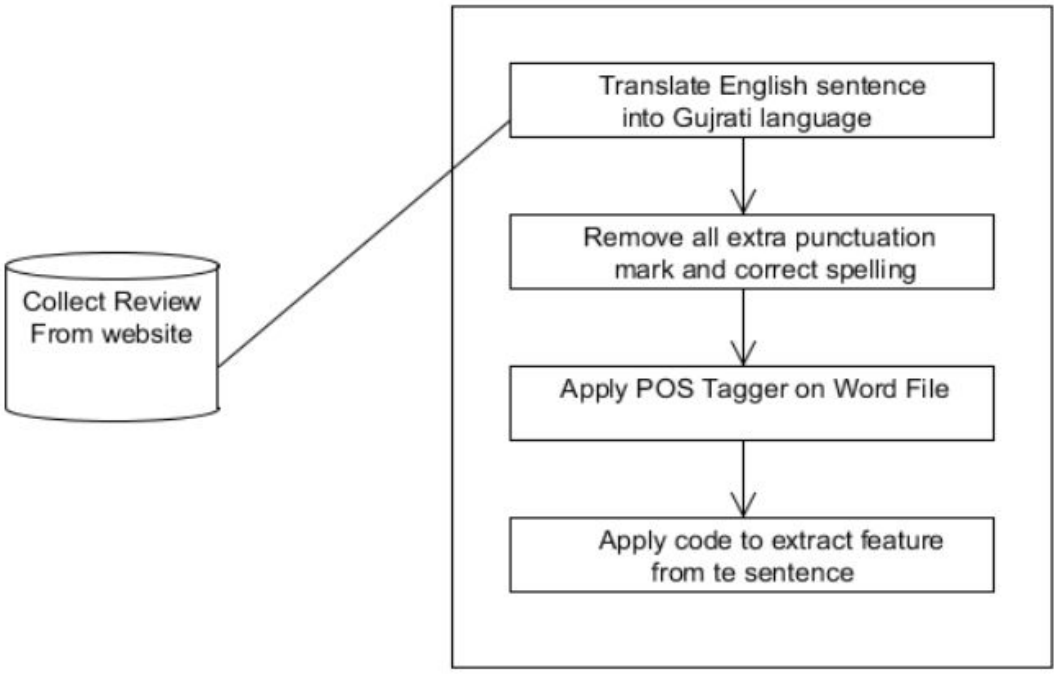

Fig. 1. System Architecture

2.2Processing phase:

In the processing phase, the task of extracting object or feature of an object is done from the tagged dataset of mobile reviews in Gujarati language prepared using POS tagger. The main idea is based on the concept from (Kumar, 2012), (Dalal, 2013) that in a sentence noun or noun phrase can be considered as an object or feature of an object and adjective in a sentence can be treated as opinion given by user.

The code is written in Java for fetching nouns and adjectives. The steps are as follows for the algorithm implemented in Java:

Step 1. Read the file having words with its tags.

Step 2. Start a loop to traverse each line from the file:

Step 3. Search for tags for noun and adjective in the line of current iteration and mark the corresponding words as noun or adjective respectively.

Step 4. Add it in an array along with its actual sentence.
Step 5. End a loop.
Step 6.

The sentences we have collected are categorized into positive and negative sentences. The output of these code is ready to be used for further processing which we are going to implement to identify polarity of the sentence: positive

or negative. As we are already having labeled data with positive and negative label, we are planning to implement supervised learning method for further enhancement.

3. Experiments and Analysis

1. Table 1. Statistical analysis of dataset

Total line (239)	Total lines	Translated	Correctly lines	Translated
Positive Lines	167		130	
Negative lines	72		52	

In preprocessing step mobile reviews of English language are translated into Gujarati language. Few of the translated lines are having errors. The statistics for the same is given in Table 1.

In this statistical analysis of dataset total 239 lines are translated and then positive and negative reviews are identified from that total line. In which there are 167 positive lines and 72 negative lines from that line 130 line from the positive lines and 50 lines from negative lines are correctly translated. The remaining incorrectly translated lines are manually corrected and few of the lines are discarded from those lines and finally 216 lines are considered for evaluation of processing phase.

2. Table 2. Output of code

Review	Noun	Adjective
સેમસંગ ફોન ખૂબ જ ખરાબ છે .	સેમસંગ, ફોન	ખરાબ

Following is discussion about result of processing phase. Table 2 shows sample output of the processing phase. 93.51 % features are extracted using that code. Some features are not extracted and it gives wrong output. Table 3 shows few examples of incorrect output.

3. Table 3. Result of feature extraction

Sr. No	Sentence	Incorrect output	Correct output
1.	હું તે ખરીદી કરવા માટે આગળ જોઉં છુ.	ખરીદી	તે
2.	તે હાથમાં સરસ લાગે .	હાથમાં	તે
3.	હું આ સૂચવુ નહિ .	સૂચવુ	આ
4.	એક મહાન ડિસપ્લે પરંતુ સરેરાશ કેમેરા.	પરંતુ,સરેરાશ,કેમેરા	ડિસપ્લે, કેમેરા

The reason for wrong output is errors in output of POS tagger but few errors are of the processing phase developed here. Following Table 4 discussed about statistical analysis of processing phase result.

4. Table 4: Statistical Result of output

Total Extracting line	Total Correct line	Total Incorrect line
216	202	12

According to the analysis total 202 lines give correct output out of 216 lines which is 93.51%.

4. Conclusion and future work

In this research paper we implemented module for extracting object or feature of an object from the review sentences in Guajarati language. The code is implemented in Java and accuracy achieved is 93.51%. Here, the implemented work may not be applicable in some cases for the sentences in Gujarati language. So, some other technique can be used for improvement of accuracy. Also, POS tagger can be trained using the data of the same

domain used for this work to improve accuracy in POS tagger. Another point of improvement can be to generate dataset directly in Gujarati language instead of translating from English language.

References

[1] Bing Liu. (2012). Sentiment Analysis and Opinion Mining, Morgan & Claypool Publishers.
[2] A. Kumar, T. M. Sebastian. (2012). Sentiment Analysis on Twitter. IJCSI International Journal of Computer Science Issues. 9(4). 372-378.
[3] Mita Dalal, Mukesh Zaveri. (2013). Semisupervised Learning Based Opinion Summarization and Classification for Online Product Reviews. Retrieved from http://www.hindawi.com/journals/acisc/2013/910706/ (accessed December 3, 2015)
[4] Ion Smeureanu, Cristian Bucur. (2012). Applying Supervised Opinion Mining Techniques on Online User Reviews. Informatica Economică 16(2). 81-92.
[5] C. Patel, K. Gali. (2008, January). Part-Of-Speech Tagging for Gujarati Using Conditional Random Fields. Paper presented at IJCNLP-08 Workshop on NLP for Less Privileged Languages, Hyderabad, India.
[6] Rudri Mehta & et. al.(2015). A Comparative Study of Methods for Feature Extraction in Opinion Mining. National Journal of System and Information Technology.7(1). 31-36.

A Survey of Video Object Tracking Methods

Mukesh Parmar

PG Student Of ComputerEngineering ,Swaminarayan College Of Engineering & Technology,Kalol,382721,India

Abstract

Object tracking finds its application in several computer vision applications, such as video compression, surveillance, robotics etc. Object tracking is a process of segmenting a region of interest from a video scene and keeping track of its motion, position and occlusion. The tracking is performed by monitoring objects' spatial and temporal changes during a video sequence, including its presence, position, size, shape Difficulties in tracking objects can arise due to abrupt object motion, changing appearance patterns of both the object and the scene, nonrigid object structures, object-to-object and object-to-scene occlusions, and camera motion. tracking of an object mainly involves two preceding steps object detection and object representation. Object detection is performed to check existence of objects in video and to precisely locate that object. In this survey, we categorize the tracking methods on the basis of the object and motion representations used, provide detailed descriptions of representative methods in each category, and examine their pros and cons.

Keywords: object detection ,object representation, object tracking, point tracking, shape tracking.

1.Introduction

Object tracking is an important task within the field of computer vision. The proliferation of high-powered computers, the availability of high quality and in expensive video cameras, and the increasing need for automated video analysis has generated a great deal of interest in object tracking algorithms.[1] There are three key steps in video analysis: detection of interesting moving objects, tracking of such objects from frame to frame, and analysis of object tracks to recognize their behaviour. Therefore, the use of motion-based recognition, that is, human identification based on gait, automatic object detection, automated surveillance, that is, monitoring a scene to detect suspicious activities or unlikely events video indexing, that is, automatic annotation and retrieval of the videos in multimedia databases ,human-computer interaction, that is, gesture recognition, eye gaze tracking for data input to computers ,traffic monitoring, that is, real-time gathering of traffic statistics to direct traffic flow ,vehicle navigation, that is, video-based path planning and obstacle avoidance capabilities.[2]

In its simplest form, tracking can be defined as the problem of estimating the trajectory of an object in the image plane as it moves around a scene. In other words, a tracker assigns consistent labels to the tracked objects in different frames of a video. Additionally, depending on the tracking domain, a tracker can also provide object-centric information, such as orientation, area, or shape of an object. Tracking objects can be complex due to loss of information caused by projection of the 3D world on a 2D image, noise in images, complex object motion, nonrigid or articulated nature of objects, partial and full object occlusions, complex object shapes, scene illumination changes, and real-time processing requirements.[2]

There are three key steps in video analysis: detection of interesting moving objects, tracking of such objects from frame to frame, and analysis of object tracks to recognize their behaviour [3].Actually videos are sequences of images, each of which called a frame, displayed in fast enough frequency so that human eyes can percept the continuity of its content. It is obvious that all image processing techniques can be applied to individual frames. Besides, the contents of two consecutive frames are usually closely related [3].An image, usually from a video sequence, is divided into two complimentary sets of pixels. The first set contains the pixels which correspond to foreground objects while the second complimentary set contains the background pixels. This result is often represented as a binary image or as a mask. It is difficult to specify an absolute standard with respect to what should be identified as foreground and what should be marked as background because this definition is somewhat application specific . Generally, foreground objects are moving objects like people, boats and cars and everything else is background. Many a times shadow is represented as foreground object which gives improper output. The basic steps for tracking an object are described below:

a) Object Detection
Object Detection is a process to identify objects of interest in the video sequence and to cluster pixels of these objects. Object detection can be done by various techniques such as temporal differencing , frame differencing , Optical flow and Background subtraction [1].

b) Object Representation
Object representation involves various methods such as Shape-based representation, Motion-based representation, Color based representation and texture based representation where object can be represented as vehicles, birds, floating clouds, swaying tree and other moving objects.[4]

c) Object Tracking
Tracking can be defined as the problem of estimating the trajectory of an object in the image plane as it moves around a scene. Point tracking, kernel tracking and silhouette tracking are the approaches to track the object.[1]

2.Object Tracking Methods

2.1 Point Tracking

Objects detected in consecutive frames are represented by points,and the association of the points is based on the previous object state which can include object position and motion. This approach requires an external mechanism to detect the objects in every frame. An example of object correspondence is shown in figure

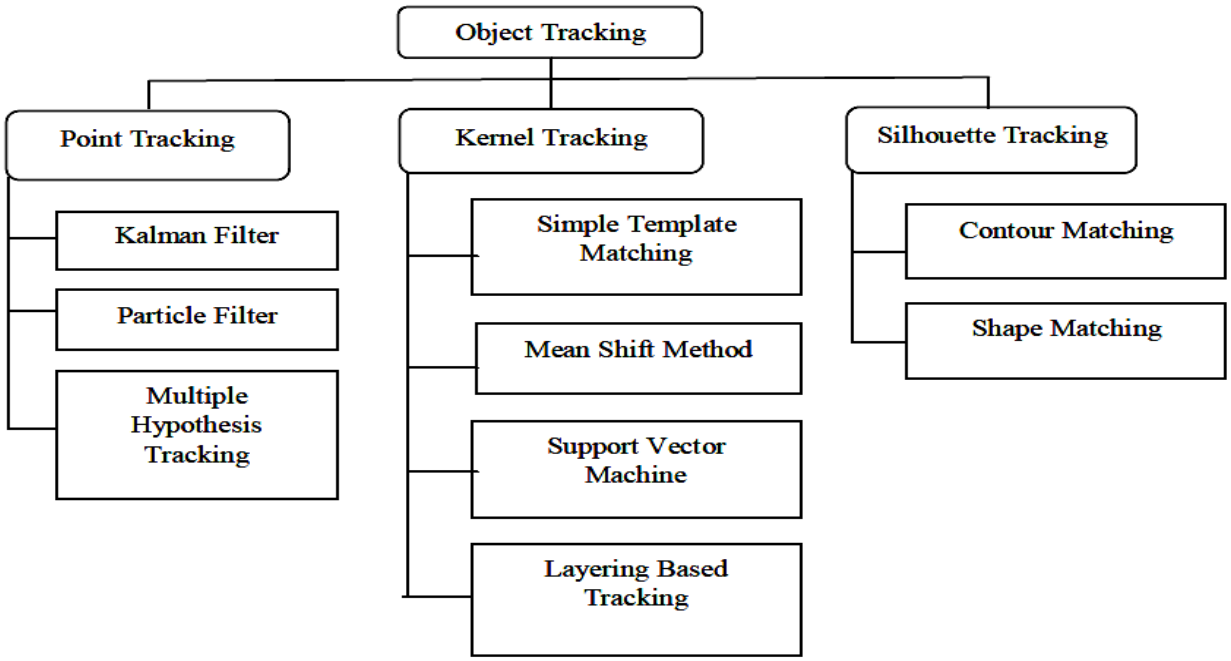

Fig 1.Types of Object Tracking [1]

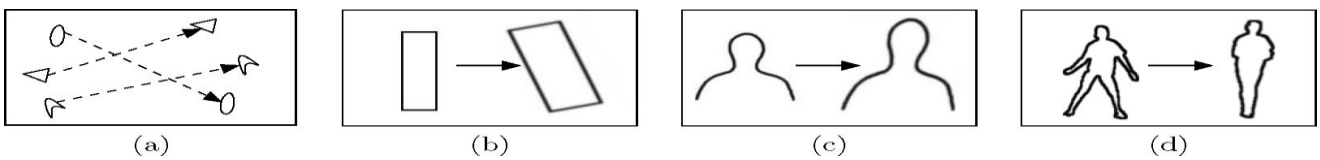

Fig 2. (a) Different tracking approaches. Multipoint correspondence, (b) parametric transformation of a rectangular patch, (c, d) Two examples of contour evolution.[2]

2.1.1 Kalman Filter

A Kalman filter[10] is used to estimate the state of a linear system where the state isassumed to the distributed by a Gaussian. The Kalman filter is a recursive predictive filter that is based on the use of state space techniques and recursive algorithms. It is estimated the state of a dynamic system. This dynamic system can be disturbed by some noise, mostly assumed as white noise. To improve the estimated state the Kalman filter uses measurements that are related to the state but disturbed as well. Kalman filtering is composed of two steps. Thus the Kalman filter consists of two steps:[4]

1.The prediction

2.The correction

In the first step the state is predicted with the dynamic model. The prediction step uses the state model to predict the new state of the variables.

$$X^t = D\,X^{t-1} + W \quad (1)$$

$$\sum{}^t = D \sum{}^{t-1} D^t + Q^t \quad (2)$$

Where X^t and Σ^t are the state and covariance predictions at time t. D is the state transition matrix which defines the relation between the state variables at time t and t-1. Q is the covariance of the noise W. Similarly the correction step uses the current observation Z^t to update the object state.

$$K^t = \sum{}^t M^t [\, M \sum{}^t M^t + R^t]^{-1} \quad (3)$$

$$X^t = X^t + K^t [Z^t - M\,X^t] \quad (4)$$

where M is the measurement matrix, K is the Kalman gain which is called as the Riccati equation used for propagation of the state models. The updated state *Xt* is distributed by Gaussian. Similarly Kalman filter and extended Kalman filter assumes that the state is distributed by a Gaussian. In the second step it is corrected with the observation model, so that the error covariance of the estimator is minimized. In this sense it is an optimal estimator. Kalman filter has been extensively used in the vision community for tracking .[4] The Kalman filter estimates a process by using a form of feedback control. The filter estimates the process state at some time and then obtains feedback in the form of noisy measurements. The equations for Kalman filters [3] fall in two groups: time update equations and measurement update equations. The time update equations are responsible for projecting forward (in time) the current state and error covariance estimates to obtain the priori estimate for the next time step. The measurement update equations are responsible for the feedback. Kalman filters always give optimal solutions.

2.1.2 Particle Filter

Particle filter is a filtering method based on Monte Carlo and recursive Bayesian estimation. The particle filter, also known as condensation filter and they are suboptimal filters. The core idea is that density distribution is present using random sampling particles. There is no restriction to the state vector to deal with nonlinear and non-Gaussian problem, and it is the most general Bayesian approach.[5] The working mechanism of particle filters is given as follows. The state space is partitioned as many parts, in which the particles are filled according to some probability measure. The higher probability, the denser the particles are concentrated. The particle system evolves along the time according to the state equation, with evolving pdf determined by the FPK equation. Since the pdf can be approximated by the point-mass histogram, by random sampling of the state space, we get a number of particles representing the evolving pdf.

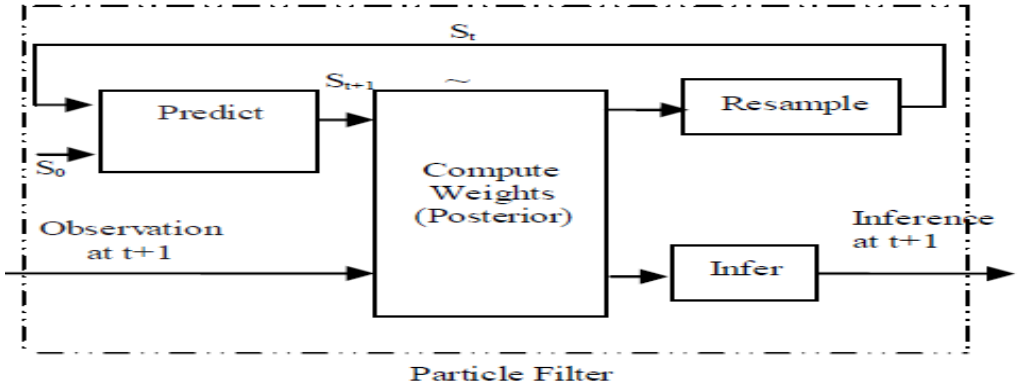

Fig3 Particle Filter

The basic steps block diagram in particle filtering is shown above[6]
The above Fig. 3 represents the particle filtering (PF) scheme. Consider a system whose state is changing in time $S_t = f(S_{t-1}, W_t)$ where S_t is the system state at time t. The function f is called the state transition model and says that the system is Markovian. That is, S_t depends on the previous state S_{t-1} and the system (process) dynamics W_t, which enable the system to change in time. Also, assume the system is being partially observed using a set of noisy sensors $Z_t = h(S_t, V_t)$. Here h is called the observation model and captures the relationship between the current system state S_t, the sensor observation Z_t, and sensor noise V_t. The randomness associated with W_t and V_t is assumed to be known and captured through pdfs [6].

2.1.3. Multiple Hypothesis Tracking

A key strategy in MHT is to delay data association decisions by keeping multiple hypotheses active until data association ambiguities are resolved. MHT maintains multiple track trees, and each tree represents all of the hypotheses that originate from a single observation . At each frame, the track trees are updated from observations and each track in the tree is scored. The best set of non-conflicting tracks (the best global hypothesis) can then be found by solving a maximum weighted independent set problem . Afterwards, branches that deviate too much from the global hypothesis are pruned from the trees, and the algorithm proceeds to the next frame.[7]
If motion correspondence is recognized using only two frames, there is always a limited chance of an incorrect correspondence. Better tracking outcomes can be acquired if the correspondence choice is overdue until several frames have been observed. The MHT[11] algorithm upholds several correspondences suggestions for each object at each time frame The final track of the object is the most likely set of correspondences over the time period of its observation.[1] MHT is an iterative algorithm. Iteration begins with a set of existing track hypotheses. Each hypothesis is a crew of disconnect tracks. For each hypothesis, a prediction of object's position in the succeeding frame is made. The predictions are then compared by calculating a distance measure. MHT is capable of dealing with: Tracking multiple object, Ability to tracks for objects entering , exit of Field Of View (FOV). It also handles occlusions, Calculating of Optimal solutions [7].

2.2. Kernel Tracking

Kernel tracking [1] is usually performed by computing the moving object, which is represented by a embryonic object region, from one frame to the next. The object motion is usually in the form of parametric motion such as translation, conformal, affine, etc.These algorithms diverge in terms of the presence representation used, the number of objects tracked, and the method used for approximation the object motion. In real-time, illustration of object using geometric shape is common. But one of the restrictions is that parts of the objects may be left outside of the defined shape while portions of the background may exist inside. This can be detected in rigid and non-rigid objects .They are large tracking techniques based on representation of object, object features ,appearance and shape of the object.

2.2.1. Simple Template Matching

Template matching [1] is a brute force method of examining the Region of Interest in the video. In template matching, a reference image is verified with the frame that is separated from the video. Tracking can be done for single object in the video and overlapping of object is done partially. Template Matching is a technique for processing digital images to find small parts of an image that matches, or equivalent model with an image (template) in each frame. The matching procedure contains the image template for all possible positions in the source image and calculates a numerical index that specifies how well the model fits the picture that position. It can capable of dealing with tracking single image and partial occlusion of object.
Template matching [7]is a brute force method of examining the ROI in the ongoing video a simple way of tracking ithreference image. Here in template matching, a reference image is verified with the frame that is separated from the video. It can track only single object in the video. Translation of motion only can be done in template matching. Capable of dealing with: Tracking single image, Partial occlusion of object, Necessity of a physical initialization.

2.2.2 Mean Shift Method

Mean-shift tracking [1]tries to find the area of a video frame that is locally most similar to a previously initialized model. The image region to be tracked is represented by a histogram. A gradient ascent procedure is used to move the tracker to the location that maximizes a similarity score between the model and the current image region. In object tracking algorithms target representation is mainly rectangular or elliptical region. It contain target model and target candidate. To characterize the target color histogram is chosen. Target model is generally represented by its probability density function (pdf). Target model is regularized by spatial masking with an asymmetric kernel.
The task is to first define an Region of Interest (ROI) from moving Object by segmentation and then tracking the object from one frame to next. Region of interest is defined by the rectangular window in an initial frame. Tracked object is separated from background by this algorithm. The accuracy y of target representation and localization will be improved by Chamfer distance transform. Minimizing the distance amongst two color distributions using the Bhattacharya coefficient is also done by Chamfer distance transform. In tracking an object, we can characterize it by a discrete distribution of samples
and kernel is localized . Steps for kernel tracking: Probabilistic distribution of target in firs frame is obtained using color feature. Compare the distribution of first frame with consecutive frame. Bhattacharya coefficient is used to find the degree of similarity between the frames. Loop will continue till the last frame [8].Capable of dealing with: Tracking only single object, Object motion by translation and scaling. Necessity of a physical initialization. Object is partial occlusion [7].

2.2.3. Support Vector Machine (SVM)

SVM [1] is a broad classification method which gives a set of positive and negative training values. For SVM,the positive samples contain tracked image object, and the negative samples consist of all remaining things that are not tracked. It can handle single image, partial occlusion of object but necessity of a physical initialization and necessity of training. SVM is a broad classification method which gives a set of positive and negative trainingvalues. For SVM, the positive samples contain tracked image object, and the negative samples consist of all remaining things that are not tracked. During the analysis of SVM, score of test data to the positive class Capable of dealing with:[7] Tracking single image. Partial occlusion of object. Necessity of a physical initialization . Necessity of training. Object motion by translation.

2.2.*4. Layering based tracking*

This is another method of kernel based tracking[1] where multiple objects are tracked. Each layer consists of shape representation (ellipse), motion such as translation and rotation, and layer appearance, based on intensity. Layering is achieved by first compensating the background motion such that the object's motion can be estimated from the rewarded image by means of 2D parametric motion. Every pixel's probability of calculated based on the object's foregoing motion and shape features [8]. It can capable of tracking multiple images and fully occlusion of object.[7] Capable of dealing with: Tracking multiple images. Fully occlusion of object. Object motion by translation, scaling and rotation.

2.3 Silhouette Tracking

Some object will have complex shape such as hand, fingers, shoulders that cannot be well defined by simple geometric shapes. Silhouette based methods [9] afford an accurate shape description for the objects. The aim of a silhouette-based object tracking is to find the object region in every frame by means of an object model generated bythe previous frames. Capable of dealing with variety of object shapes, Occlusion and object split and merge.[1]

2.3.1 Contour Tracking

Contour tracking methods [9], iteratively progress a primary contour in the previous frame to its new position in the current frame. This contour progress requires that certain amount of the object in the current frame overlay with the object region in the previous frame. Contour Tracking can be performed using two different approaches. The first approach uses state space models to model the contour shape and motion. The second approach directly evolves the contour by minimizing the contour energy using direct minimization techniques such as gradient descent. The most significant

advantage of silhouettes tracking is their flexibility to handle a large variety of object shapes. Contour tracking methods[8], in divergence to shape matching methods, iteratively develop an original contour in the foregoing frame to its new position in the present frame, overlapping of object between the current and next frame. Contour tracking is in form of State Space Models. State Space Models: State of the object is named by the parameters of shape and the motion of the contour. The state is updated for each time according to the maximum of probability. In Contour Tracking, explicitly or implicitly are used for the representation on silhouette tracking. Representation based on explicitly will defines the boundaries of silhouette whereas in case of implicitly, function defined by grid.

2.3.2 Shape Matching

These approaches examine for the object model in the existing frame. Shape matching performance is similar to the template based tracking in kernel approach.Another approach to Shape matching [9] is to find matching silhouettes detected in two successive frames. Silhouette matching, can be considered similar to point matching. Detection based on Silhouette is carried out by background subtraction. Models object are in the form of density functions, silhouette boundary, object edges. Capable of dealing with single object and Occlusion handling will be performed in with Hough transform techniques. These approaches examine for the object model in the existing frame. Shape matching performance is similar to the template based tracking in kernel approach. Another approach to Shape matching is to find matching silhouettes detected in two successive frames. Silhouette matching, can be considered similar to point matching which is described . Detection based on Silhouette is carried out by background subtraction. Models object are in the form of density functions, silhouette boundary, object edges.[8] Capable of dealing with: Edge based template, Silhouette tracking feature of shape matching are able to track only single object. Occlusion handling will be performed in with Hough transform techniques .

Table:1 Qualitative Comparison for Tracking methodologies.(#:no of objects tracking, S:single,M:multiple,P:partial,F:full, Symbols √ and × denote whether the tracker can or cannot handle occlusions, and requires or does not require training).

Sr.no.	Method	Category	#	Entry	Exit	Occlusion	Optimal	Training Rule
1	Kalman filter	Point tracking	S	√	√	×	√	-
2	MHT	Point tracking	M	√	√	√	√	-
3	Particle Filter	Point tracking	M	×	×	√	√	-
4	Template matching	Kernel Tracking	S	-	-	P	-	×
5	Mean shift	Kernel Tracking	S	×	×	P	-	×
6	SVM	Kernel Tracking	S	-	-	P	-	√
7	Layering based tracking	Kernel Tracking	M	-	-	F	-	×
8	Shape matching	Silhouette tracking	S	-	-	×	-	×
9	Contour matching	Silhouette tracking	M	-	-	F	√	√

Acknowledgements

I am very grateful and would like to thank my guide and teacher Prof.N R Patel, Prof. Darshana Mistry for their advice and continued support without them it would not have been possible for me to complete this report. I would like to thank all my friends, colleague and classmates for all the thoughtful and mind stimulating discussions.

References

[1] Himani S. Parekh, Darshak G. Thakore, Udesang K. Jaliya 2014. A Survey on Object Detection and Tracking Methods, International Journal of Innovative Research in Computer and Communication Engineering 2, p.2970

[2] Alper Yilmaz,Omar Javed,Mubarak Shah 2006. Object Tracking: A Survey, *ACM Comput . Surv. 38*, 4, Article 13 p.45.

[3] Gandham Sindhuja, DR.Renuka Devi S M 2015. A Survey on Detection and Tracking of Objects in Video Sequence, International Journal of Engineering Research and General Science 3,p.418 ISSN 2091-2730

[4] Barga Deori, Dalton Meitei Thounaojam 2014. A survey on moving object tracking in video, International Journal on Information Theory (IJIT), 3 p.31

[5] Md. Zahidul Islam, Chi-Min Oh and Chil-Woo Lee 2009. Video Based Moving Object Tracking by Particle Filter, International Journal of Signal Processing, Image Processing and Pattern . 2, p.119

[6] G.Mallikarjuna Rao 2013. Visual Object Target Tracking Using Particle Filter: A Survey, I.J. Image, Graphics and Signal Processing, 6,p. 57

[7] J.Joshan Athanesious, P.Suresh 2012. Systematic Survey on Object Tracking Methods in Video, International Journal of Advanced Research in Computer Engineering & Technology (IJARCET)Volume 1, Issue 8, October 2012

[8] Rahul Mishra, Mahesh K. Chouhan, Dr. Dhiiraj Nitnawwre 2012 .Multiple Object Tracking by Kernel Based Centroid Method for Improve Localization, International Journal of Advanced Research in Computer Science and Software Engineering, p 137.

[9] Mr. Joshan Athanesious J; Mr. Suresh P, March 2013.Implementation and Comparison of Kernel and Silhouette Based Object Tracking, International Journal of Advanced Research in Computer Engineering & Technology, p. 1298

[10] Rupesh Kumar Rout: A Survey on Object Detectionand Tracking Algorithms, Department of Computer Science and EngineeringNational Institute of Technology Rourkela,June 2013

[11] Chanho Kim , Fuxin Li, Arridhana Ciptadi , James M. Rehg : Multiple Hypothesis Tracking Revisited,

Two Wheeler Vehicle Model Development for Driving Simulator Application

Dankan v gowda[a], kishore d v[b], ramachandra a c[c],pandurangappa c[d]

[a]Asst .Professor with the Electronics and Communication Engineering Department , Sri Venkateshwara college of Engineering, Bengaluru, 562157, Karnataka, India

[b]Asst .Professor with the Electronics and Communication Engineering Department, Sri Venkateshwara college of Engineering, Bengaluru, 562157, Karnataka, India

[c] HOD & Professor with the Electronics and Communication Engineering Department, Alpha College of Engineering, Bangalore, Karnataka, India

[d]Professor with the Mathematics Department , University B.D.T. College of Engineering, Davanagere, Karnataka, India

Abstract: Driving Simulators play an important role in research concerning mainly human factors and the development of new advanced driver assistance and safety systems. Driving simulator experiences must be as close as possible to reality, in order to conduct simulator experiments that generate accurate results, so they can be extrapolated to real driving situations. One part of the driving simulator that influences the driver perception is the vehicle dynamics model. This is the part of the simulator software that calculates the physics and motion of a real vehicle according to the driver inputs and environmental conditions. The most important issue in designing a driving Simulator is how to implement a modeling dynamics of the real vehicle systems effectively and further requires that all events in the simulator occur in real time. Therefore, this project aims at developing one such vehicle model for a simulator which allows a cost effective and efficient way to check the reliability and efficiency of the developed ABS (antilock braking system) algorithm and also to demonstrate the functionality of ABS. This paper presents modeling of ABS controller for longitudinal dynamics has been done for a motorcycle. A library of Engine model has been developed whose capacity is tunable. Suspension system is modeled in order to simulate different road conditions.

Keywords: Simulator, Anti-Lock Braking system, Safety System, Suspension System, Engine model.

I.INTRODUCTION

Vehicle Safety is the study and practice of design, construction, equipment and regulation to minimize the occurrence and consequences of automobile accidents. Today's modern human being spends major part of his life traveling from one place to another. With growing population the vehicular traffic on city cross roads have also increased. To avoid accidents several steps were taken as to prepare certain standard drive guidelines. To go for a certain road safety rules and regulations, But none of the methods were able to completely isolate the accidents from the roads [1]. So it came to engineers as a duty to design the vehicle in such way that almost importance is given to safety of occupant under the most severe most collision conditions. Modern vehicles are equipped with a number of devices that are designed to prevent accidents, and to keep the driver and occupant's safe if an accident does occur. These devices generally fall under two categories: active driving safety and passive driving safety.

1. **Active driving safety:** Refers to devices and systems that help keep a vehicle under control and prevent an accident. These devices are usually automated to help compensate for human error For example: Anti-lock brakes prevent the wheels from locking up when the driver brakes, enabling the driver to steer while braking. Traction control systems prevent the wheels from slipping while the car is accelerating. Electronic stability control keeps the car under control and on the road.

2. Passive Driving safety: refers to systems in the car that protect the driver and passengers from injury if an accident does occur. Air bags provide a cushion to protect the driver and passengers during a crash. Seat belts hold passengers in place so that they aren't thrown forward or ejected from the car. Rollover bars protect the car's occupants from injury if the vehicle rolls over during an accident. The objective of this project is to enable various loop simulations in order to analyze the performance of different safety functions. A vehicle model is used to represent a real vehicle in a model based environment [2]. Vehicle model is a sophisticated component which makes use of two wheeler dynamics concepts to achieve a real vehicle behavior.

In this project, an ABS controller is embedded into the vehicle model and the performance of the vehicle with and without ABS is analyzed. The simulations are performed in real time with dynamic driver inputs. This enables an improved way of optimizing the controller algorithm, tuning the parameters, and testing the functionalities at lower costs.

II.MOTIVATION AND SCOPE OF THE PROJECT

The motivation of the project is to make a Vehicle Motion Simulator which enables the users to feel the importance of various vehicle safety functions. It offers a virtual reality environment which helps in realizing the importance of vehicle safety systems when a hazardous driving condition is encountered. The current existing simulator can be further extended in various domains like rider training, gaming simulator and software in the loop testing of newly developed safety functions. Since all the tests do not require a real vehicle, track testing cost could be saved. It consumes less time and offers good accuracy levels.

III. METHODOLOGY

A commonly adopted approach for handling a new problem is: first build simplified model, linear as far as possible, by ignoring certain nonlinearities and other physical properties which may be present in the system and thereby get an approximate idea of the dynamic response of a system; a more complete model is then built for more complete analysis. A physical system is a collection of physical objects connected together to serve an objective. No physical system can be represented in its full physical intricacies and therefore idealizing assumptions are always made for the purpose of analysis and synthesis of systems. An idealized physical system is called a physical model. A physical system can be modeled in a number of ways depending upon the specific problem to be dealt with and the desired accuracy. Once a physical model of a physical system is obtained, the next step is to obtain a mathematical model which is the mathematical representation of the physical model through use of appropriate physical laws. Depending upon the choice of variables and the coordinate system, a given physical model may lead to different mathematical models. When the mathematical of a physical system is solved for various input conditions, the result represents the dynamic response of the system.

Thus the following approach is made:

1. Knowing vehicle dynamics concepts.
2. Understanding the underlying physical principles.
3. Mathematical modelling of the system using the physical equations.
4. Developing the simulink model for functionalverifaction.

IV.VEHICLE MODEL ARCHITECTURE

Motor cycles are composed of are composed of a great variety of mechanical parts, including some complex ones, from a strictly kinematic point of view, by considering the suspensions o be rigid, a motorcycle can be defined as simply a spatial mechanism composed of four rigid bodies:

- The rear assembly (frame, saddle, tank and motor-transmission drivetrain group),
- The front assembly (the fork, the steering head and the handlebars),
- The front wheel,
- The rear sheel.

These rigid bodies are connected by three revolute joints (the steering axis and the two wheels) and are in contact with the ground at two wheel/ground contact point as show in figure 4.1.

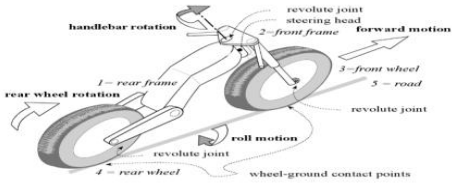

Figure 4.1 Kinematic Structure of a Motorcycle [2].

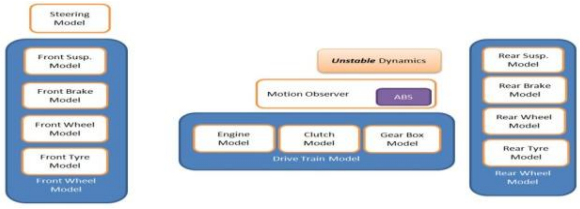

Figure 4.2 Vehicle Model Architecture

The major subsystems in the Vehicle model architecture are front and rear wheel assembly, drive train system, steering system and ABS controller. the functions of these subsystems are explained as follows.

Front/Rear wheel assembly: The front/rear wheel assemblies consist of tire model, wheel model, brake model and the suspension system.

Brake system: A **vehicle brake** is a brake used to slow down a vehicle by converting its kinetic energy into heat. The basic hydraulic system, most commonly used, usually has six main stages: the brake pedal, the brake boost (vacuum servo), the master cylinder, the apportioning valves, and finally the road wheel brakes themselves.

There are two types of braking system

- Friction brake
- Electromagnetic brake

Friction brake:

A friction brake is a type of automotive brake that slows or stops a vehicle by converting kinetic energy into heat energy, via friction. The heat energy is then dissipated into the atmosphere. In most systems, the brake acts on the vehicle's road wheel hubs, but some vehicles use brakes which act on the axles or transmission. Friction brakes may be of either drum or disc type.

A **drum brake** is a vehicle brake in which the friction is caused by a set of brake shoes that press against the inner surface of a rotating drum [3]. The drum is connected to the rotating road wheel hub.

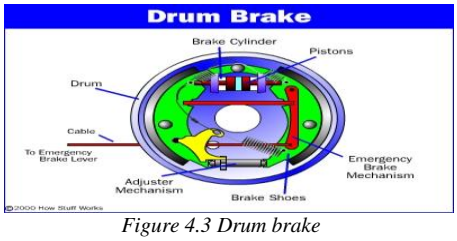

Figure 4.3 Drum brake

Figure 4.4 Disk brake

The **disc brake** is a device for slowing or stopping the rotation of a road wheel. A brake disc (or rotor in U.S. English), usually made of cast iron or ceramic, is connected to the wheel or the axle. To stop the wheel, friction material in the form of brake pads (mounted in a device called a brake caliper) is forced mechanically, hydraulically, pneumatically or electromagnetically against both sides of the disc. Friction causes the disc and attached wheel to slow or stop.

Suspension system: This component defineds the suspension system of the vehicle. The main target of the suspension in the model is to calculate the load transfers generated when driving.

Suspension is the term given to the system of springs, shock absorbers and linkages that connects a vehicle to its wheels and allows relative motion between the two. Suspension systems serve a dual purpose — contributing to the vehicle's road holding/handling and braking for good active safety and driving pleasure, and keeping vehicle occupants comfortable and reasonably well isolated from road noise, bumps, and vibrations, etc. These goals are generally at odds, so the tuning of suspensions involves finding the right compromise. It is important for the suspension to keep the road wheel in contact with the road surface as much as possible, because all the road or ground forces acting on the vehicle do so through the contact patches of the tires. The suspension also protects the vehicle itself and any cargo or luggage from damage and wears [4].

Tire model: The tire model is one of the motorcycle's most important components. Its fundamental characteristic is its deformability, which allows contact between the wheel and the road to be maintained even when small obstacles are encountered. In addition to improving the comfort of the ride, the tire improves adherence, an important characteristic both for the transfer of large driving and braking forces to the ground, and for the generation of lateral forces. The performance of a motorcycle is largely influenced by the characteristics of its tires.

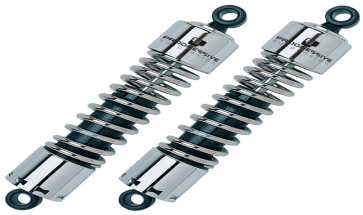

Figure 4.5 Suspension sytem

Figure 4.6 motor cycle tire

Steering system: The steering system model has main goal calculating of the steer angle of the wheels as a function of the driver's input through the steering wheel and driving conditions. The basic aim of steering is to ensure that the wheels are pointing in the desired directions. This is typically achieved by a series of linkages, rods, pivots and gears. One of the fundamental concepts is that of caster angle – each wheel is steered with a pivot point ahead of the wheel; this makes the steering tend to be self-centering towards the direction of travel. The steering linkages connecting the steering box and the wheels usually conforms to a variation of Ackermann steering geometry, to account for the fact that in a turn, the inner wheel is actually travelling a path of smaller radius than the outer wheel, so that the degree of toe suitable for driving in a straight path is not suitable for turns [5]. The angle the wheels make with the vertical plane also influences steering dynamics as do the tires.

Drive train / power train system: In a motor vehicle, the term **power train** or **power plant** describes the main components that generate power and deliver it to the road surface. This includes the engine, transmission, drive shafts, differentials, and the final drive. Sometimes "power train" is used to refer to simply the engine and transmission, including the other components only if they are integral to the transmission [6].

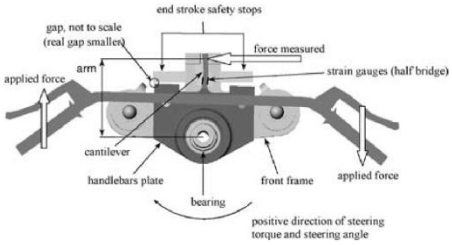

Figure 4.6Motorcycle steering system

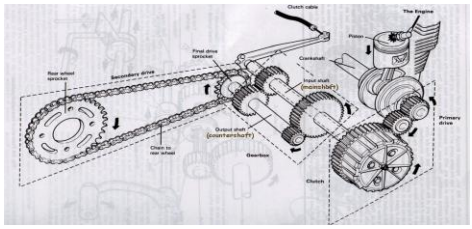

Figure 4.7Motorcycle drive train systems

V. APPLICATIONS OF VEHICLE MODEL

1. Riding simulators: A riding simulator is a virtual reality tool which gives a driver on board a feeling that he drives an actual vehicle whose motion is caused by the driver input and corresponding visual, motion, and audio signals are generated. Vehicle simulation can be defined as the representation of vehicle and system dynamics characteristics with varying degrees of realism for research, design, training or entertainment purpose. It requires simulation of the environment to an extent appropriate for the purposes of the simulation, and it further requires that all events in the simulator occur in real time. Real term is a term, which is used to denote that all time relationships in the simulator consists of a software application for simulating vehicle dynamics and presenting the results in virtual 3D environment, and a haptic interface. The system makes it possible to simulate wheeled vehicles of various configurations on arbitrary terrains.

2. Vehicle Software Valiadation :

The key aspect of any automotive embedded systems technology is able to develop and produce new functions in car/bike within short development cycles, our vehicle model can be used for one such application. Real-time simulation of Vehicle Safety Functions based on the driver inputs (e.g.: Motorcycle ABS, TCS etc.)

VI. CONCLUSION

In this paper, an attempt was made to understand the applications of vehicle motion simulators and that they can be used to simulate various vehicle safety functionalities. This paper focused on design, development and testing of a two wheeler vehicle model. A model was successfully developed which involved modeling of a drive train, suspension system, road model (bump/pothole), ABS controller and development of test tool. Various kinds of simulations were understood and implemented. This thesis deals with software in the loop and driver in the loop simulations. The vehicle model behavior was studied carefully and the results obtained were compared against real vehicle measurement data. Thus, the model was tuned so as to achieve as realistic as possible simulations.

REFERENCES

[1] H. Mirzaeinedjad, M. Mirzaei,*"A novel method for non-linear control of wheel slip in anti-lock braking systems"*, Control Engineering Practice vol. 18, pp. 918-926, 2010.

[2] S. C. baslamisli, I. E. Kose and G Anlas, *"Robust control of antilock brake system"*, Vehicle System Dynamics, vol.45, no. 3, pp. 217-232, March 2007.

[3] S. B. Choi, *"Antilock Brake System with a Continuous Wheel Slip Control to Maximize the Braking Performance and the Ride Quality"*, IEEE Transaction on Control Systems Technology, vol. 16, no. 5, September 2008.

[4] K.Z. Rangelov, *"SIMULINK Model of a Quarter-Vehicle with an Antilock Braking System"*, Master's Thesis-Eindhoven: Stan Ackermans Institute, 2004.- Eindverslagen Stan Ackermans Institute, 2004102

[5] A.B. Sharkawy, *"Genetic fuzzy self-tuning PID controllers for antilock braking system"*, Engineering Applications of Artificial Intelligence, vol.23, pp. 1041-1052, 2010.

[6] A. Poursamad, *"Adaptive feedback linearization control of antilock braking system using neural network"*, Mechatronics, vol. 19, pp. 767-773, 2009.

Resource allocation and appropriate selection of D2D pair as a trade-off between throughput and power

Godkhindi Shrutkirthi[a],Mehul Shah[b]
[a] PG Student, GCET, Gujarat Technological University, Anand, India
[b] Associate professor, Gujarat Technological University, Anand, India

Abstract
Device to Device (D2D) has gained a lot of attention due to its feature of controlled communication, in the absence of base station. D2D communication has given significant improvement in throughput for local services and thereby leading to the feature of spectrum efficiency. Among different D2D techniques underlay technique has been majorly opted, due to facility of parallel sharing of licensed spectrum albeit interference creation is a major issue. As the same spectrum is accessed, it becomes necessary to decide when D2D has to be used and when cellular so that the overall system throughput increases.
The demand for higher data rates and new connection are increasing at large speed now days. So it becomes important to decide which D2D connection has to be given priority for establishing connection. Here two methods for the appropriate selection of D2D pair which should be allowed in order to increase overall system throughput are proposed. The first method depends on the distance of D2D pair from the base station, and then resource allocation depending upon the trade-off between throughput and transmission power of D2D device, is presented

Keywords: Device to device communication (D2D), Signal to noise interference ratio (SINR)

Nomenclature

D2D	Device to device
P	Transmission Power
G	Channel Gain
N_o	Noise Power Density
I	Interferance
Greek symbols	
γ_C	Signal to Interference Noise Ratio for Cellular user
γ_d	Signal to Interference Noise Ratio for D2D user
y	No. of users

1. Introduction

In the last few decades there is a very rapid evolution in communication systems. Communication systems have changed from wired system to wireless system to 1G-2G-3G-4G and so on. There is also a very wide emergence of new technical gadgets such as smart phones, tablets, smart watches etc. Due to this a major increase in their numbers has occurred along with the different kind of services. Albeit the total spectrum capacity remains the same. This entails to best efficient utilization of the spectrum in terms of congestion, power control and frequency utilization.

Taking under consideration of the demand for high bandwidth consuming applications and services the development of 3GPP (Third Generation Partnership Project), LTE (Long Term Evolution), UMTS (Universal Mobile Telecommunications System), EUTRA (Evolved Universal Mobile terrestrial radio access), EUTRAN (EUTRAN network) technology were evolved [1]. There has been many methods such as cognitive radio, Bluetooth and ZigBee are invented to increase spectrum efficiency. Cognitive Radio systems makes use of white spaces to increase spectrum efficiency. Enhanced Bluetooth is advanced use of Bluetooth technology which provides faster communication and data transfer than the traditional Bluetooth speed. Device to device communication is one of such techniques.

In simple words, device to device communication can be defined as direct connection between two users without intermediate base station connection. In traditional cellular communication, the connection between two users is through one or more base stations. Every call between two cellular users is through the base stations. D2D is a non-transparent communication to the base station and network, as there is no involvement of base station during the communication. This leads to the advantage of offloading of cellular traffic at the base station. The involvement of the base station is only till the communication establishment. D2D is also possible without the use of base station, but such D2D occur only in the unlicensed spectrum.

The classification of D2D is done on basis of use of the spectrum. If communication of D2D occurs in licensed spectrum then it is known as In-band D2D, while if D2D communication occurs in unlicensed spectrum then it is

known as out-band D2D communication. Feature of accessing both licensed and unlicensed spectrum is the major advantage of D2D. Depending upon the network, either can be selected. The working and connection establishment for both in-band and out-band is different. Due to this reason both methods cannot be accessed at the same time. Out-band allows the D2D communication in unlicensed band which does not affect the spectral use of licensed version. It also offloads the spectrum. But it is not reliable as base station cannot access it, so it is less preferred.

In-band D2D gives the facility of reliable communication between two devices in near vicinity with higher data rate and also reduces overloading effect. But as it allows the use of licensed spectrum, the issues such as interference management, resource allocation and energy consumption have to be solved. If in-band licensed spectrum is divided into separate parts for use of D2D and cellular, then it is called as overlay D2D. In overlay D2D, interference is not much affected as the spectrum is divided [2]. In underlay D2D, direct communication occurs between cellular users in the same spectrum and the spectrum is shared by both cellular and D2D at same time. This parallel sharing leads to major problem of interference. The same spectrum resources are now used for both. So it becomes more crucial to decide which one communication is more beneficial than the other.

There are many works done in underlay D2D communication in which there are different method suggested in order to reduce interference[3][4]. There are techniques presented to reduce transmission power so that the interference can be reduced. Power optimization approach considering a MINLP (Mixed integer nonlinear programming) based algorithm are presented in [5][6]. There can be many ways to improve spectrum efficiency considering sharing of spectrum i.e. orthogonally or non-orthogonally between D2D and cellular. There are concepts of different modes of D2D such as forced D2D, path loss D2D and opted D2D. Selection of one of these mode enable higher throughput and spectral efficiency [7].

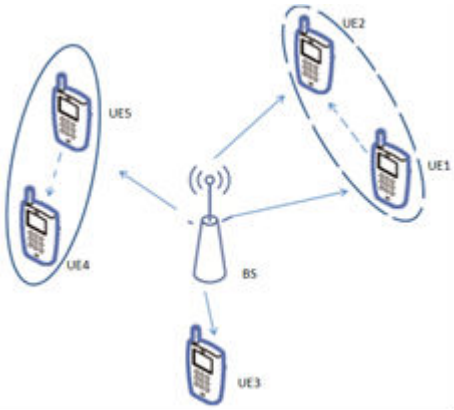

Figure1: A simple example of D2D and cellular network

The increasing demand of spectrum and high data rates has demanded more and more use of D2D communication. One of the important problem is to identification and selection of such D2D pair which increases the overall system throughput. When many D2D pair are in demand then due to limited resources for D2D communication some of the links need to be prioritize and some of the links should continue as cellular.

In this paper the effect of in-band interference on cellular and D2D communication is shown. Interference reduction concept is used to achieve better throughput. Two concepts are also presented for deciding priority of resource allocation for D2D communication.

2. System Model

A single cell network with full load is considered. Base Station decides the resources and power assigned for D2D transmission so that the interference to the primary cellular networks can be controlled. An OFDM based system is considered in which uplink is a SC-FDMA and downlink is through OFDM scheme. D2D connection establishment for uplink band is considered. A cellular network with 100 users and one base station at the centre are considered. Users are distributed in the cellular coverage area as per uniform distribution. A PSK modulation scheme is used for uplink transmission. Near-far effect is considered with respect to base station. For evaluation of path loss a system with slow fading effect is considered. Interference is evaluated as directly dependent on the path loss occurred.

The required transmission power for D2D is comparatively lesser than that of regular cellular

communication as the distance between two devices is very less.
For the above scenario, effect of the varying value of interference range is examined first. As interference range increases throughput decreases. Algorithm for deciding prior D2D from given D2D pairs is presented next.

2.1 Effect of interference on D2D and cellular throughput

Underlay communication has many advantages over other types of D2D communication. As there is involvement of base station for establishing communication, the factor of reliability and spectrum efficiency also increases. As the underlay D2D communication occurs in the licensed band, it is certain that there will be increase in interference of the network. This interference occurs due to presence of both cellular and D2D communication. It becomes necessary to reduce this interference present in the system. It can be easily reduced by reducing the transmission power of the devices. But doing so may decrease the SINR of the signal.

Interference range is considered to reduce interference in D2D. The clusters of users present near the devices, which can create considerable interference to the D2D communication are evaluated first. It is observed that the total interference that affects the SINR of the communication, occurs due to this cluster of users only. Taking under consideration this interference created by users in cluster, the throughput of the D2D communication is evaluated. Then the cluster range is varied (interference range), and throughput is calculated for each D2D communication. Increasing interference range reduces the throughput of the system. The cancellation of the interference should be selected in such a way that required throughput is achieved. The cellular throughput in presence of D2D connection is evaluated next. The effect of varying interference range on D2D and cellular is shown in fig.2 in simulation result section.

3. Resource allocation for D2D

A. Distance based Resource allocation for D2D

The major problem in D2D underlay is to decide that, in which case the D2D communication is to be considered and when Cellular? Both D2D and cellular has parallel use of licensed spectrum. Considering the increasing demand of more and more connections, it is important to assign priorities among D2D connections.

Underlay is parallel sharing of licensed spectrum. There is use of same resources in both cellular and D2D. As the resources are limited and of constant number the same can be used for full cellular system with no D2D, but this will drop down the spectrum efficiency and system throughput. So combined use of cellular and D2D is selected. This leads to the decision of mode of selection. The resources for D2D or cellular must be selected in such a way that the resource utilization remains optimum along with overall higher system throughput.

When there are many pairs demanding for D2D connections, the base station has to decide which pair should be given first preference to form D2D connection. Even when there are limited D2D connections possible in the system and higher number demand for D2D connection, the base station must assign D2D resource to only such pairs, which would improve the overall system throughput.

We consider the case of D2D communication only in uplink spectrum. SINR for both cellular and D2D is shown respectively as per equation 1 and 2.

$$\gamma_c^{Ul} = \frac{G_{Bc} P_c}{N_0 + I + \sum_d y\ P_d G_{dB}} \quad \text{--------- (1)}$$

$$\gamma_d^{Ul} = \frac{\sum_c y\ P_d G_{dd}}{N_0 + I + \sum_c y\ P_c G_{dc}} \quad \text{---------- (2)}$$

A priority deciding method based on SINR.

Step-1: For the scenario considered in section II, several D2D pair in the cluster with similar properties (same amount of interference) are considered. Also the distance of D2D transmitter and receiver must be limited by certain range (in range of ±2 units).

Step–2: For simplicity SINR of cellular is referred as C_SINR and SINR of D2D is referred as D_SINR. Then C_SINR and D_SINR for the set of D2D pairs are calculated.

Step-3: The difference of C_SINR and D_SINR of each selected pair is evaluated next.

It is observed that as the distance of the D2D pair from the base station increases, the difference of C_SINR and D_SINR also increases. The SINR difference of cellular and D2D is much less when the pair is present near the base station. As the distance of D2D pair increases from the base station this difference of C_SINR and D_SINR also increases. This is reflected by the simulation result shown in fig.3 of simulation result section.

This is used to decide the priority for resource allocation for D2D connection. When one deals with the overall system throughput, the throughput of combine system i.e. cellular and D2D will be much larger than only cellular system if this result is considered in order to allot the priority for D2D connection.

All this calculation and priority decision is taken at the base station. It is work of base station to decide how many D2D pairs have to be established, how many D2D resources is to utilized and when D2D or when cellular connection is to be formed.

From the above results it become evident that selection of the D2D pair which is comparatively away from the base station is more preferable than pair nearer to base station, in case they have same interference conditions. This helps base station for allotting the resources, which would lead to significant increase in the system throughput.

B. Resource allocation for D2D as trade-off between throughput and transmission power

Direct communication has lead to significant increase in the SINR value of the communication link. Increase in throughput is very essential for high data rate communication. But many a times once required SINR is achieved, the excess of SINR is not utilized fully. In such cases when required SINR is achieved, then there is no further need to increase the SINR. This can be utilized in order to reduce the transmission power. This is application where one needs uninterrupted communication and not much high data rates. This trade-off between the transmission power and throughput is described in this section

.

D2D transmission power is less than cellular transmission power, as D2D is only for devices in near proximity. This value of D2D transmission is fixed value. This value of D2D transmission power is required in order to attain the required SINR for communication. In this section the total D2D range is divided into two parts, one lower range and other upper range. The upper range is the range which has $D2D_{tx} - D2D_{rx}$ distance larger than 18 units (here in the simulation condition D2D range as 25 units is considered). And D2D range less than 18 units fall in lower range. Here the D2D pairs falling in lower range are considered.

For resource allocation the trade-off between throughout and transmission power is considered. A scenario with priority for power saving scheme is considered. First a sufficient SINR value which would provide stability in transmission with clarity is deduced. As priority to power saving is considered one allows a throughput drop down up to desirable level.

Following steps are executed.

Firstly the required minimum SINR and channel gain are set. The D2D transmission power is 15dB less than cellular [2].

The simulation results shows a considerable high throughput as compared to cellular.

Next the D2D transmission power is reduced. On reducing the transmission power of D2D, gradually throughput drops.

The comparison of dropping ratio of throughput to the reduction of power is shown.

The result shows that % of power reduction is considerably higher than % drop of throughput.

Resource allocation scheme proposed here considers two conditions, in which, priority to have higher throughput or power reduction with sufficient throughput are selected. Here the throughput achieved by power reduction is also higher than that of cellular communication. If one wishes to have very high data rates then power control may not be

selected. In other cases where power saving has priority, then with slight reduction in throughput large power saving can be done. In majority cases for about 30% power reduction there is about less than 10% throughput drop down. All this prioritizing of power control or throughput is decided at the base station end.

Depending upon the situation either one is selected by the base station. In this way power control can be utilized. It has to be noted that % of power control is much higher than % of throughput drop down as shown in fig.2 in simulation result section.

4. Simulation methodology and parameters

Here as described above a D2D communication in uplink is established. Here interference considered is dependent on path loss factor. SINR is calculated on basis of above equation mentioned in system model section.

Following algorithm is followed

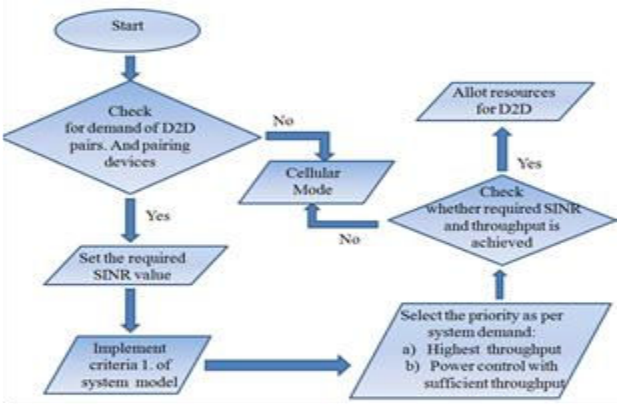

Figure2: Flowchart for algorithm

Here first a threshold for interference cancellation is considered, and then calculated the BER and throughput for both Cellular and D2D communication. By increasing the threshold, the BER also increases and by increasing the interference threshold value there is a decrease in system throughput. Comparison of both cellular communication between two device and D2D communication is evaluated.

Further comparison of the SINR of D2D and cellular, for D2D pairs at different distance from base station is considered. The evaluation is done by varying distance of D2D pair from base station. The results for the difference of their D2D and cellular SINR are evaluated and plotted in fig.3.

In the later part, the trade-off between throughput and transmission power is shown. As described in above section when power drop is considered for D2D pairs in lower range, the throughput drop is much less as compared to reduced power this is described by simulation results shown in fig.4.

Table 1. Parameter Table

Parameters	Values
Cell Area	500 × 500
No. of users	100
D2D Range	25 units
Interference Range	50 units
Transmission Power	40 dB
D2D Transmission Power	25 Db
Noise Power density	-174 dBm/ Hz
Noise Figure	5 Db
Resource Block Bandwidth	180 Khz

5. Simulation Results

5.1. Effect of interference on D2D and cellular throughput

The figure below gives the comparison of D2D and cellular communication for varying interference range described in the introduction.

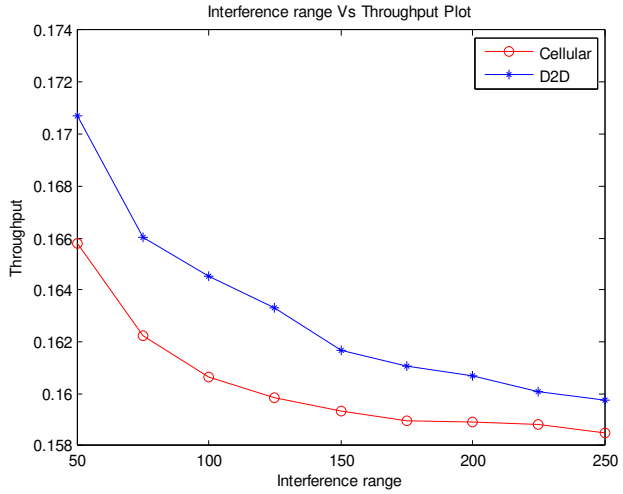

Figure3: Graph showing effect on Throughput by varying interference

Here the simulation results show the D2D throughput and cellular throughput between same end points, for a fully loaded system. It is seen that the increasing interference range there is decrease in throughput of both D2D and cellular. But at all times the D2D throughput is high than cellular throughput.

5.2 Varying distance of D2D pair from base station

Here the results describe one of the criteria for resource allocation, the distance based method. The graph showing the difference of C_SINR and D_SINR as the distance from the base station increases is plotted.

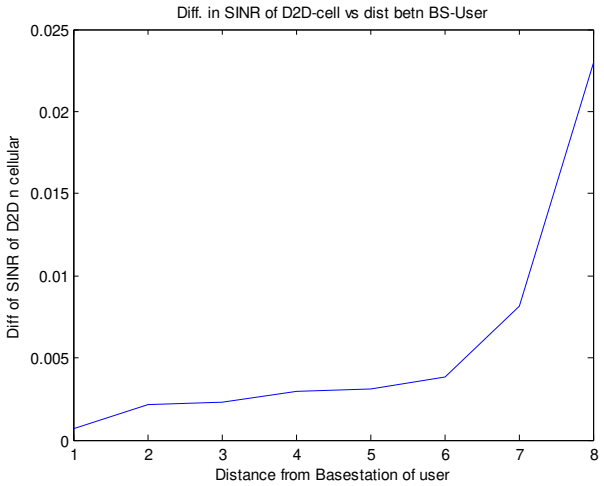

Figure4: SINR difference as distance from base station increases

From the graph it is observed that if the distance between D2D distance (distance between D2D transmitter and receiver) of two different D2D pairs falls in same range, then difference C_SINR and D_SINR is directly proportional to its distance from the base station. So when the two different D2D pair falling in same interference range are demanding for resources. Then the priority of resource allocation would be to the pair which is at the farther distance from the base station.

5.3 Trade-off between throughput and transmission power.

The power control method depends upon device mutual distance from each other. The throughput obtained by D2D is considerably higher than cellular. This is utilized for fast and smoother communication. The throughput obtained is sufficiently higher than required threshold value. But at times this excess SINR is not required, and this high value is not justified. This can be used for power control method. A method for efficient allocation of resources which provide required throughput with power control method. The % of throughput drop is comparatively than % of power drop. This is shown by the following graph.

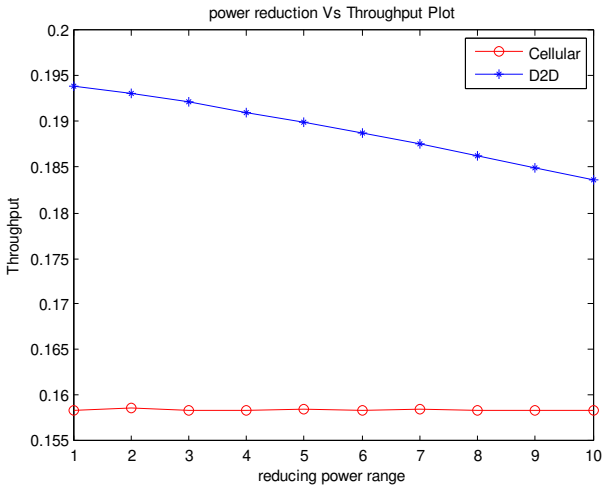

Figure5: Throughput vs. power reduction for D2D devices

The simulation model as described above is implemented and reduced the power up to 40% is considered. Then throughput is evaluated for this dropping power. The value of throughput is still higher than cellular in dense condition (high density of neighbouring users), by maintaining desired SINR.

6. Conclusion

Here comparison of D2D to Cellular communication is shown. Initially the effect on throughput by varying interference range is evaluated. It was seen that increasing the interference range the system throughput of the D2D reduces but this reduced throughput value is still higher than that of cellular. Later two different resource allocation methods which are executed at base station are presented. First, depending upon the analyses of the difference in SINR of D2D and cellular by varying the D2D pairs distance from the Base station is shown. And later the trade-off between throughput and transmission power is considered. It is observed that even by dropping power of D2D sufficient throughput can be obtained. One can therefore opt for required connection as per demand, whether higher throughputs are required or sufficient throughput with power reduction

References

[1] Pekka Janis, Chia-Hao Yu, Klaus Doppler, Cassio Ribeiro, Carl Wijting, Klaus Hugl, Olav Tirkkonen, Visa Koivunen, 'Device-to-Device Communication Underlaying Cellular Communications Systems.' Int. J. Communications, Network and System Sciences, 2009, 3, 169-247

[2] B. Kaufman and B. Aazhang, "Cellular networks with an overlaid device to device network," in Proceedings of Asilomar Conference on Signals, Systems and Computers, 2008.

[3] Arash Asadi, Qing Wang and Vincenzo Mancuso, "A Survey on Device-to-Device Communication in Cellular Networks" in arXiv:1310.0720v6[cs GT]. IEEE ,2014

[4] Shaoyi Xu, Haiming Wang, Tao Chen, Qing Huang, Tao Peng, 'Effective Interference Cancellation Scheme for Device-to-Device Communication Underlaying Cellular Networks', IEEE magazine 978-1-4244-3574-6/10, 2010

[5] Klaus Doppler, Mika Rinne, Carl Wijting, Cassio B. Ribeiro, and Klaus Hugl, 'Device-to-Device Communication as an Underlay to LTE-Advanced Networks' IEEE Communications Magazine , December 2009

[6] Chia-Hao Yu, Klaus Doppler, Cassio B. Ribeiro, and Olav Tirkkonen, 'Resource Sharing Optimization for Device-to-Device Communication Underlaying Cellular Networks.' IEEE transactions on wireless communications, vol. 10, no. 8, August 2011

[7] Sami Hakola, Tao Chen Janne Lehtom and Timo Koskela," Device-to-Device (D2D) Communication in Cellular Network -

Performance Analysis of Optimum and Practical Communication Mode Selection", in the WCNC , IEEE communication society, 2010.

[8] Daquan Feng, Lu Lu, Yi Yuan-Wu, Geoffrey Ye Li, Gang Feng, and Shaoqian Li, 'Device-to-Device Communications Underlaying Cellular Networks', IEEE transactions on communications, vol. 61, no. 8, August 2013

[9] Anurag Kumar, D. Manjunath, Joy Kuri, WIRELESS NETWORKING, Morgan kaufmann publishers

[10] Guanding Yu, Zhaoyang Zhangt, Yan Chen, Jing Shi, and Peiliang Qiu, 'A Novel Resource Allocation Algorithm for Real-time Services in Multiuser OFDM Systems' IEEE magazine, 0-7803-9392-9/06,2006

A Review on Fingerprint Classification for Brain Mapping

Simeen R Khan[a], Heena R Kher[b]

[a]A D Patel Institute of Technology,Electronics & Communication Engineering Department, Anand-388121, Gujarat, India,
[b]A D Patel Institute of Technology,Electronics & Communication Engineering Department, Anand-388121, Gujarat, India,

Abstract

Dermatoglyphics alludes to the branch of science in the investigation of the examples of skins (dermal) edges present on the fingers, toes and the soles of human. Deductively it has been demonstrated that no two individuals can have the same fingerprints in this world. Once a human is conceived, its fingerprints are formed and they stay unaltered up till the end of his life. Fingerprints begin creating when the foetus arrives in mother's womb from thirteenth week of gestation period. This is the same period when the cerebrum of the embryo likewise begins developing. In this way, the advancement in formation of fingerprints and the development of mind happens at the same time. This paper gives a brief summary about various features that can be obtained from fingerprints and the detailed procedure for the proposed algorithm to work and detect all the features so that they can be used for further classification, with the help of which brain mapping will be carried out.

Keywords: *Biometrics; Image Processing; Fingerprints; Minutiae; Ridge Ending; Thinning .*

1.INTRODUCTION

The study of skin patterns refers to the study of formation of naturally occurring ridges on certain body parts, namely palms, fingers, soles and toes. The finger prints of both hands are not the same. They do not change size or shape throughout a person's life, except in cases of serious injuries that scar the dermis. The uniqueness of a person's finger prints have been linked to a person's personality and preferences by analyzing mapping of brain through fingerprints. The study of fingerprints has become more common, therefore, some parents began to analyze their child's (or baby's) prints; with the intention to identify their potential early, and provide guidance accordingly to help expand their potential. The different regions of our brain are reflected by our ten fingerprints. The features extracted are crucial for the purpose of brain mapping.

Figure 1. Types of minutiae observed: (a) Ridge Ending (b) Bifurcation (c) Crossover (d) Isolated Point (e) Continuing Ridge

Uniqueness of fingerprints makes them a very attractive biometric identifier. Fingerprint recognition represents the oldest method of biometric identification. Its history is going back as far as at least 2200 BC [1]. A fingerprint consists of (as shown in Fig.1) ridges (lines across fingerprints), ridge endings, bifurcations (single point diverging on two sides), crossover (two ridges intersecting each other), dot (isolated point) and ridge continuing (does not terminate) and valleys (spaces between ridges). The pattern of the ridges and valleys is unique for each individual. The probability of finding two fingerprints similar is of 1.9x1015 [1]

2. PREVIOUS WORK

edicinal specialists and researchers have found that the measure of brain cells conveyed in various parts of the mind offers us some assistance with understanding a man's different intelligences and in addition his intrinsic potential capacities and identity. Our fingerprints uncover to us what we need and how we learn, changing our lives through an all-encompassing, instruction approaches. Brain mapping through unique finger impression is produced in the human by fingers, palms, toes, and feet toes on the lines. Brain mapping through fingerprint is generated in the human by fingers, palms, toes, and feet toes on the lines. In the genetic counselling related to science the person's skin texture in the 13th week of embryonic development to 19 weeks of the formation of the brain are synchronous growth lines and striae. After the formation of striae, it remains unchanged. Not much of the work is done on brain mapping but a significant amount of relative work is done on fingerprints. Hence all the essential details required for the process of classification of fingerprint can easily be retrieved from the previous work pursued in this field from relevant papers.

Byong Ho Cho et al.[2] presented a novel method on core analysis. For the classification purpose, till now the methods used were all based on singularity and minutiae but due to small size of image, the delta points are frequently excluded. Thus, using only core points, classification is done and is proved to be efficient for classification into four classes namely: arch, left, loop, right loop, and whorl using the characteristics of a

fingerprints of being unique and unchangeable, the large. In this paper, an input image is enhanced and segmented to discard the background. Now based on computed orientation and directional vectors, core points are selected using Poincare index and K means grouping method. Thus by obtaining core points classification is done and accuracy of 91.6% is achieved for the process of classification based on the location and number of core points present.

Xeujun Tan et al.[3] in his paper presented a new feature learning algorithm which unlike the conventional methods, uses combination of feature extraction and genetic programming thus learning composite features that have been adopted from amalgamation of the older primitive image processing operators. Their Genetic Programming explored many unconventional ways that are never used in fingerprint methods and still yield exceptionally good results. The parallel working of Genetic programming and agility of computers allow the space search to be extra ordinary. Their approach can find better composite features for the extraction of important and useful features. When using a Bayesian classifiers without any rejection of fingerprints from NIST-4 database, the correct rates for 4 and 5-class classification are 93.3% and 91.6% respectively. Hence it is favorable compared to other published results.

Dingri Wan and Jie Zhou [4] in this paper showed the importance of fingerprints in the form of biometrics and for the process of identification as well as the task of verification. He has also pointed regarding the necessity of database to be of a certain kind and how when the database present if it is small, reliable and accurate results are obtained. In this paper not only is the importance of minutiae for largescale fingerprint recognition been kept in mind but they have also proposed a polynomial model to approximate the mapping of fingerprint density and also making intensive use of model's parameter which can be regarded as a new kind for representation of various features of fingerprint. Consequently, using the novel features obtained from the density model, the whole matching system can be made less computationally complex and with negligible storage cost. By incorporating a decision level fusion scheme along with density map for the combination of density map matching with customary minutiae matching, the resultant obtained showed a much better and acceptable result that obtained on using the minutiae matching alone. In this paper they propose a model of density map compared to the convenient model when computed directly are more susceptible to noise and distortion. Hence using a polynomial map for its approximation i.e. intuitive shadow of ridges' parameters. The modeled density map being global and complementing the minutiae an exceptional result is obtained. Moreover the effect of sharp changes of ridge distance and not susceptible to noise. Due to little repetitions between the model and the map hence their compatibility is phenomenal. Along with combining a recognition model is also developed whose performance is seen to be enhanced.

Gualberto Agularetsal et al.[5] demonstrated the need for proper fingerprint identification. Moreover its importance in biometric system and the forensics is also illustrated. Based to the uniqueness of the features ridges and valley, two major methods used fingerprint matching are minutiae matching and global pattern matching. These techniques are cost effective and less complex. Images quality also plays an imperative role as the type of scanner used has an impact on false minutiae appearance. The proposed algorithm uses a combined of fast Fourier transform and Gabor fields on the input image acquired through biometric device 44000 of Digital persona Inc. This process is mainly used from procuring of minutiae (ridge end bifurcate) as well as to enhance the prominent features. Finally the extracted features are used to perform the task of identification of class to perform the task of identification of class. Because of regularity and continuity properties of fingerprint image, occluded and corrupted image can also be recovered .The main advantage is achieved by using Fast Fourier Transform and Gabor field together as result is very robust even in area of high curvature.

Arun Ross et al.[6] shows that from minutiae, three level of information about the parent fingerprint can be elicited v.i.z. orientation field information, the class or type information and friction ridge structure. Any fingerprint consists of 150 different minutiae types among which the ridge ending and ridge bifurcation are most stable points and are unique hence for classification only salient features are stored in a compact form. The past studies using neural network and orientation map was used for determining the shape but the error rate was high. Biometric template provided feature reconstruction which could fool a system, generic image having same resemblance or total image which will be identical. The advantage of such study helps to defend against various attacks and shows us importance of minutiae. Thus relying just on minutiae obviates the need of singular points. Firstly the author estimates the ridge orientation by using a set of three minutiae points to predict the orientation of component minutiae points so that they are in suitable range and avoided very small area. By estimating the orientation and validating it via histogram as well as the triplet method, correlation is obtained which proves the efficacy of the algorithm. The histogram of mean square error shows its efficiency as the ridge orientations are consistent. Following are the major steps of the proposed algorithms image registration is done by detecting registration points using Hough transfer. Next a feature vector is extracted from orientation of minutiae and its different cases. Using K- nearest neighbor, classification of finger prints take place. Based on the result obtained by analyzing classifier

performance fingerprint reconstruction is done using Gabor filter based technique. The fingerprint reconstruction process can be moderated using iterative hill climbing.

Sheng Li and Alex Kot [7] suggested an improved scheme for full fingerprint recognition. They sheds light on how different systems store minutiae based fingerprints as templates differently and as to how they are taken for granted due to their small size and are thought to be of containing no significant information at all. This paper proposes scheme through which a recovered image i.e. a replica of original image can be constructed only through a minutiae template. The technique is based on amplitude and frequency modulated (AM-PM) fingerprint model. It has been shown from previous work that through the template, a skeleton of original fingerprint can be constructed. Moreover taking advantage of amplitude and frequency model, the phase image can be divided into continuous model, the phase image can be divided into continuous or spiral phase and by mixing the both the reconstructed image with can be obtained but it doesn't match with its different impression. In this paper using amplitude modulation (AM) and Phase Modulation (PM), an estimation of continuous phase from ridge pattern was done. It was similar ridge flow to original fingerprint. After combining the continuous and spiral phase computed through the minutiae template, a phase image of refinement process was introduced to reduce the artifacts located at the line segments. Finally, a look alike fingerprint image was reconstructed according to thinned version estimated from the refined phase image. Thus in this paper, a new orientation unwrapping algorithm was proposed which causes fewer ridge displacements in the reconstructed fingerprint. Due to refinement process it reduced the artifacts due to discontinuity in the continuous phases as indicated by experimental results.

Jin Fei Lim et al [8] emphasized the importance of biometrics in research area and the ease at which fingerprint are widely used because of its universally accepted unique features. But the limitation being the inability of a system to process low quality fingerprints. The technique earlier used were of minutiae based and image based. The proposed algorithm took in the features from both the techniques and found a hybrid way to compensate the limitation of both the techniques. On analyzing, it can be observed that the results obtained are better compared to both the techniques. Since the identification is one to many matching whereas verification is one to one matching process out of the three techniques v.i.z. feature, pattern and principal component analysis. At the beginning of the algorithm, image acquisition was carried out after which the preprocessing steps of histogram computation took into effect. The process of core detection algorithm was carried out after which division of the image takes place at non overlapping regions, the region of interest is computed. Then the processing on Gabor field was carried out for any residual noise to be removed. Next in image segmentation, ridge flow estimation would be carried out using Sobel filter and Least Square Approximation. Morphological operation of opening and closing were carried out for proper extraction of minutiae. Image post processing was carried out for proper removal of noise and to avoid false minutiae. Minutiae matching took place using the percentage of similarity score. The highest was considered. When tested with low quality images image based technique performed better and achieved 92.5% success rate. Proposed hybrid method made correct matches to all the fingerprints to correct individuals.

Leandra Webb et al.[9] have emphasized upon the recent increase of biometrics, challenge was the time taken for the huge database to be checked. Hence to make the classification easy they were divided into different bins. Now considering the case of flat fingerprint which usually had missing singular points specifically delta of the left or right loop or is not captive, this algorithm comes handy. Tested on 833 flat fingerprint images from FVC2000 Database 1 the accuracy is 91.1%. Based on Henry Galton's classification the fingerprints were grouped into whorl (W), right loop(R), left loop (L), tented arch and plain arch. Out of numerous approaches; Rules based is optimum as it is close to human experts and no training is required. However when some portion of the image is missing, more rules are employed which helps for classification. When a singular point like a single loop exists with no delta, they use the rule of searching the region below the loop for its orientation and its convergence gives an idea of its type. The drawback would be that these classification method do not account for all possible instances of flat fingerprints which as missing singular points.

Kai Cao et al. [10] showed that minutiae points are most distinctive features for fingerprint recognition. Contradicting the fact that minutiae cannot be used for reconstruct due to lack of information, this paper demonstrate the possibility. Among all the level 1 (Global feature), Level 2 (minutiae, local region and bifurcation) and Level 3 (fine scale detail e.g. pores) set of minutiae has been most distinctive features it is believed to have reasonably high accuracy. Existing reconstruction and ridge pattern reconstruction out of which the orientation field could be made for minutiae or from singular points, however all the previous approaches based on given minutiae don't utilize any prior knowledge of fingerprints orientation and thus may result in a non-fingerprint orientation and thus may result in a non-fingerprint like orientation. In the proposed reconstruction algorithm from an input set of minutiae denoting the local direction a dictionary based fingerprint. Reconstruction method is proposed which is composed of orientation patch dictionary and continuous phase patch dictionary. The first step is orientation patch dictionary

which displays the dominant orientation in a block. The continuous phase patch dictionary in which there is high quality fingerprints and are enhanced using Gabor filtering and then using orientation patch clustering along with fingerprint patch clustering, orientation and frequency field estimation is carried out. After orientation field reconstruction in which foreground is determined using convex hull for dilation. Fingerprint reconstruction is followed by fingerprint image refinement. Thus although the result obtained is quite near to the original image but still the human experts can know the difference as the original image without noise is ideal and further the use of singular features may enhance and improve the reconstruction process.

Xuanbin Si et al. [11] sheds some light on distortion of fingerprints. He gives an insight of the dilemma of low quality images being left unidentified by the fingerprint scanner as it is very sensitive. The extremity of low quality images can be known by type of recognition system. E.g. Positive recognition is a system in which the person is willingly wanting to get recognized as in case of attendance. Here the fault of low quality image would lead to false reject of legitimate users. Whereas in negative recognition, the user is uncooperative and doesn't intend on being recognized. Thieves and unlawful people want the system to fail to prevent finding the true identity. Hence for negative recognition, a robust system is a must. In this paper, the input image is a distorted finger print which then goes to distortion detection. If the fingerprint is undistorted then it goes in for normal detection else it goes for distortion rectification which is performed in order to get a undistorted version of it. Image to be rectified is registered using ridge orientation map and period map for feature vector. For training purpose SVM classifier is used for classification. Rectification is regression problem. Here the input is the output is the distortion field. In its database several reference distorted fingerprints are present with the corresponding distortion fields. When the input is fed, it compares the finger to its nearest neighbor and its corresponding distortion field is used to rectify the input. Main advantage is that no changes is existing sensors or acquisition method is not required. The result obtained of this experiment on three databases improved the recognition rate significantly .However the efficiency of system can be made more robust and speed also can be improved. Moreover rolled fingerprints are not its strongest point.

3. CONCLUSIONS

Recent innovations and findings for biometrics, especially fingerprint's framework has propelled numerous gatherings to lead to new approaches and results. All unique finger impression images need to be grouped and classified by pre-characterized criteria. This is of immense significance so as to defeat the precision and the identification speed issues. Various methodologies have been implemented for around quite a long that contrast in the features used to depict the singular points for grouping of fingerprint images. In any case, a potential approaches to enhance the calculations particularly on pre-processing steps still need to be improved. A minutiae-based fingerprint feature extraction is a crucial basic step, where the main problem in feature extraction section is quality of fingerprint image. Most important factor in detection of minutiae stage would be detection of features like bifurcation and ridge endings so that when processed, false features are not generated. As observed, it can be deduced that along with minutiae i.e. ridge ending and bifurcation, other significant features like the isolated point, crossing as well as continued ridges can also be extracted.

Acknowledgements

I am deeply indebted to my Guide, Dr. Heena Kher for providing me with supervision, motivation and encouragement throughout this work. Her insight, full of knowledge and enthusiasm has been invaluable. She led me to the correct direction at every stage to prepare this dissertation. Without her care and supervision, I would have not been able to complete this work. I am also grateful to my colleague graduate students, for providing a friendly and enjoyable environment during this work. I would like to express my appreciation to all who directly or indirectly involve in helping me at all stages of my work. Last but not the least I would like to thank my family members, who taught me the value of hard work by their own example. They provided me enormous support during this works directly and indirectly.

References

[1] K. Karu and A. Jain, "Fingerprint classification", *Pattern Recognition*, vol. 29, no. 3, pp. 389-404, 1996.

[2] Badler, W. (1991). Dermatoglyphics: Science transition,. pp. 95.

[3] B. Cho, J. Kim, J. Bae, I. Bae and K. Koo, "Fingerprint Image Classification by Core Analysis", In *Signal Processing Proceedings, 5th International Conference on*, *IEEE*, vol. 3, no. 5, pp. 1534-1537, 2000.

[4] X. Tan, B. Bhanu and Y. Lin, "Fingerprint Classification Based on Learned Features", *IEEE Transactions on Systems, Man, and Cybernetics-Part C: Applications and Reviews,* vol. 35, no. 3, pp. 287-300, August 2005.

[5] D. Wan and J. Zhou, "Fingerprint recognition using model-based density map", *IEEE Transactions on Image Processing*, vol. 15, no. 6, pp. 1690-1696, Jun 2006.

[6] G. Aguilar, G. Sánchez, To Scano, M. Salinas, M. Nakano and H. Perez, "Fingerprint Recognition", Second International Conference on Internet Monitoring and Protection(IEEE), vol. 2, pp. 32-38, 2007.

[7] A. Ross, J. Shah and A. Jain, "From Template to Image: Reconstructing Fingerprints from Minutiae Points", *IEEE Transactions on Pattern Analysis and Machine Intelligence*, vol. 29, no. 4, pp. 544-560, 2007.

[9] S. Li and A. C. Kot, "An Improved Scheme for Full Fingerprint Reconstruction", *IEEE Transactions on Information Forensics and Security*, vol. 7, no. 6, pp. 1906-1912, December, 2012.

[10] F. L. Jen and R. Y. Yin Chin, "Enhancing Fingerprint Recognition Using Minutiae-Based and Image-Based Matching Techniques", in *First International Conference on Artificial Intelligence, Modelling & Simulation (IEEE)*, Malaysia, 2013.

[11] Webb, L., & Mathekga, M., "Towards a Complete Rule-Based Classification Approach for Flat Fingerprints", In *Computing and Networking (CANDAR), 2014 Second International Symposium on (IEEE)*. pp. 549-555, 2014

[12] K. Cao and A. K. Jain, "Learning Fingerprint Reconstruction From Minutiae to Image", *IEEE Transactions on Information Forensics and Security,* vol. 10, no. 1, pp. 104-117, January 2015.

[13] Si, X., Feng, J., Zhou, J., & Luo, Y." Detection and Rectification of Distorted Fingerprints", *IEEE Transactions on Pattern Analysis and Machine Intelligence,* vol. 3, pp. 555-568, 2015.

[14] A. K. Jain, S. Prabhakar, L. Hong, and S. Pankanti, "Filterbank-based fingerprint matching", *IEEE Transactions on Image Processing*, vol. 9, no. 5, pp. 846–859, May 2000.

[15] R. Cappelli, D. Maio and D. Maltoni, "A Multi-Classifier Approach to Fingerprint Classification", *Pattern Analysis & Applications*, vol. 5, no. 2, pp. 136-144, 2002.

[16] S. Pankanti, S. Prabhakar, and A. K. Jain, "On the individuality of fingerprints", *IEEE Transactions on Pattern Analysis and Machine Intelligence.*, vol. 24, no. 8, pp. 1010–1025, Aug. 2002.

[17] F. Pernus, S. Kovacic, and L. Gyergyek, "Minutiae-based fingerprint recognition", in *Processing 5th Int. Conference on Pattern Recognition*, Miami Beach, 2003, pp. 1380–1382.

[18] N. Yager and A. Amin, "Fingerprint classification: a review", *Pattern Analysis & Applications*, vol. 7, no. 1, pp. 77-93, 2004.

[19] J. Zhou and J. Gu, "A model-based method for the computation of fingerprints' orientation field", *IEEE Transaction on Image Processing*, vol. 13, no. 6, pp. 821–835, Jun. 2004

[20] J. Feng, Z. Ouyang and A. Cai, "Fingerprint matching using ridges", *Pattern Recognition*, vol. 39, no. 11, pp. 2131-2140, 2006.

[21] E. Yun and S. Cho, "Adaptive fingerprint image enhancement with fingerprint image quality analysis", *Image and Vision Computing*, vol. 24, no. 1, pp. 101-110, 2006.

[22] G. Chao, S. Lee and H. Lai, "Fingerprint image enhancement and postprocessing based on the directional fields", *Pattern Recognition and Image Analysis*, vol. 17, no. 4, pp. 560-566, 2007.

[23] J. Feng, "Combining minutiae descriptors for fingerprint matching", *Pattern Recognition*, vol. 41, no. 1, pp. 342-352, 2008.

[24] J. Li, W. Yau and H. Wang, "Combining singular points and orientation image information for fingerprint classification", *Pattern Recognition*, vol. 41, no. 1, pp. 353-366, 2008

[25] D. Maltoni, D. Maio, A. K. Jain, and S. Prabhakar*, Handbook of Fingerprint Recognition*, 2nd edition Springer-Verlag, 2009.

[26] G. Nie, Q. Meng, L. Zhu, Z. Zhang, M. Guo, J. Wang and J. Yang, "Automated fingerprint classification based on directional image tracing and core axis", *Journal of Computer Applications*, vol. 31, no. 1, pp. 70-73, 2011.

[27] S. Sul, "Classification-based Automatic Fingerprint Identification System for Large Distributed Fingerprint Database", *Journal of Biometrics & Biostatistics*, vol. 2, no.2, 2011.

[28] M. Munir, M. Javed and S. Khan, "A hierarchical k-means clustering based fingerprint quality classification", *Neurocomputing*, vol. 85, pp. 62-67, 2012.

[29] X. Si, J. Feng, and J. Zhou, "Detecting fingerprint distortion from a single image", in *Proc. IEEE Int. Workshop Inf. Forensics Security*, pp. 1–6, 2012.

[30] S. Yoon, J. Feng, and A. K. Jain, "Altered fingerprints: Analysis and detection", *IEEE Trans. Pattern Anal. Mach. Intell.*, vol. 34, no. 3, pp. 451–464, Mar. 2012.

[31] S. Dass, "Fingerprint-Based Recognition", *International Statistical Review*, vol. 81, no. 2, pp. 175-187, 2013.

[32] J. Feng, J. Zhou, and A. K. Jain, "Orientation field estimation for latent fingerprint enhancement*", IEEE Trans. Pattern Anal. Mach. Intell.*, vol. 35, no. 4, pp. 925–940, Apr. 2013.

[33] H. Jung and J. Lee, "Noisy and incomplete fingerprint classification using local ridge distribution models", *Pattern Recognition*, vol. 48, no. 2, pp. 473-484, 2015.

[34] A. Akhil Anjikar, "Study of Ridge Based and Image Based Approach for Fingerprint Gender Classification", *The International Journal of Innovative Research in Computer and Communication Engineering*, vol. 03, no. 03, pp. 1599-1604, 2015.

[35] R. Cappelli, A. Lumini, D. Maio and D. Maltoni, "Fingerprint classification by directional image partitioning", *IEEE Transactions on Pattern Analysis and Machine Intelligence*, vol. 21, no. 5, pp. 402-421, 1999.

Reduction of Lower Order Harmonics in a Grid-Connected Single-Phase PV Inverter

Prakash Solanki[a],Ripan Patel[b]
[a]PG student, LCIT, Bhandu and 384120, India
[b]Assistant Prof., LCIT, Bhandu and 384120, India

Abstract
In this paper, a simple single-phase grid-connected photovoltaic (PV) inverter topology consisting of a boost section, a low voltage single-phase inverter with an inductive filter, and a step-up transformer interfacing the grid is considered. Ideally, this topology will not inject any lower order harmonics into the grid due to high-frequency pulse width modulation operation. However, the non-ideal factors in the system such as core saturation-induced distorted magnetizing current of the transformer and the dead time of the inverter, etc., contribute to a significant amount of lower order harmonics in the grid current. A novel design of inverter current control that mitigates lower order harmonics is presented in this paper. An adaptive harmonic compensation technique and its design are proposed for the lower order harmonic compensation. In addition, a proportional-resonant-integral (PRI) controller and its design are also proposed. This controller eliminates the dc component in the control system, which introduces even harmonics in the grid current in the topology considered. The complete design has been validated with Simulation results and good agreement with theoretical analysis of the overall system is observed.

Keywords: Adaptive filters, harmonic distortion, inverters, solar energy, PRI, THD.

Nomenclature	
L_{boost}	Inductor of boost stage
L_{filt}	AC side filter inductor
ΔV	Voltage ripple on dc bus
Va; Vb	Outputs of SOGI
Vg	Grid Voltage
Kp; PR; Kr	Gains of PR controller
Kv; Tv	Gains of PI controller

1. Introduction

Renewable sources of energy such as solar, wind, and geothermal have gained popularity due to the depletion of conventional energy sources. Hence, many distributed generation (DG) systems making use of the renewable energy sources are being designed and connected to a grid. The topology of the solar inverter system is simple. It consists of the following three power circuit stages:
1) A boost converter stage to perform maximum power point tracking (MPPT);
2) A low-voltage single-phase *H*-bridge inverter;
3) An inductive filter and a step-up transformer for interfacing with the grid.

The system will not have any lower order harmonics in the ideal case. However, the following factors result in lower order harmonics in the system: The distorted magnetizing current drawn by the transformer due to the nonlinearity in the *B–H* curve of the transformer core, the dead time introduced between switching of devices of the same leg [2] – [6], on-state voltage drops on the switches, and the distortion in the grid voltage itself. There can be a dc injection into the transformer primary due to a number of factors. These can be the varying power reference from a fast MPPT block from which the ac current reference is generated, the offsets in the sensors, and A/D conversion block in the digital controller. This dc injection would result in even harmonics being drawn from the grid, again contributing to a lower power quality. The advantage of the adaptive filter-based method is the inherent frequency adaptability which would result in same amount of harmonic compensation even when there are shifts in grid frequency. The implementation of adaptive filters is simple. Thus, in this paper, an adaptive filter-based method is proposed. This method estimates a particular harmonic in the grid current using a least-mean-square (LMS) adaptive filter and generates a harmonic voltage reference using a proportional controller. This voltage reference is added with appropriate polarity to the fundamental voltage reference to attenuate that particular harmonic.
This paper includes an analysis to design the value of the gain in the proportional controller to achieve an adequate level of harmonic compensation. The effect of this scheme on overall system dynamics is also analyzed. This method is simple for implementation and hence it can be implemented in a low-end digital controller.

2."Origin of Lower Order Harmonics and fundamental current control"

This section discusses the origin of the lower order harmonics in the system under consideration. The sources of these harmonics are not modeled as the method proposed to attenuate those works independent of the harmonic source.

2.1 Origin of Lower Order Harmonics

1) *Odd Harmonics:* The dominant causes for the lower order odd harmonics are the distorted magnetizing current drawn by the transformer, the inverter dead time, and the semiconductor device voltage drops. Other factors are the distortion in the grid voltage itself and the voltage ripple in the dc bus. The magnetizing current drawn by the transformer contains lower order harmonics due to the nonlinear characteristics of the *B–H* curve of the core.
2) *Even Harmonics:* The topology under consideration is very sensitive to the presence of dc offset in the inverter terminal voltage. The dc offset can enter from a number of factors such as varying power reference given by a fast MPPT block.

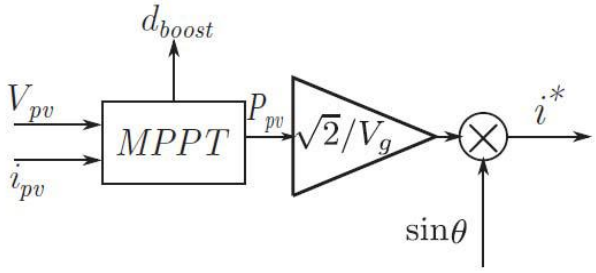

Figure 1: *Generation of an inverter ac current reference from an MPPT block.*

In Fig. 1, d_{boost} is the duty ratio command given to the boost converter switch; V_{pv} and i_{pv} are the panel voltage and current respectively.

B. Fundamental Current Control

1) Introduction to the PRI Controller: Conventional stationary reference frame control consists of a PR controller to generate the inverter voltage reference. a modification to the PR controller is proposed, by adding an integral block, *GI* as indicated in Fig. 2. The modified control structure is termed as a PRI controller.

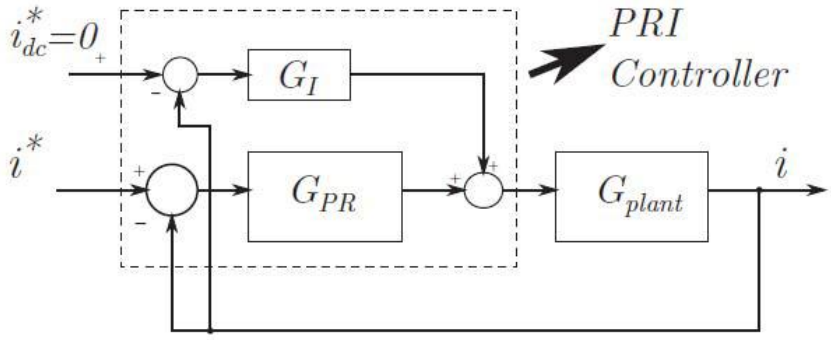

Figure 2*: Block diagram of the fundamental current control with the PRI controller.*

Here

$$G_I = K_I/s \quad (1)$$

$$G_{PR}(s) = K_p + (K_r s/(s^2 + \omega^2)) \quad (2)$$

The plant transfer function is modeled as

$$G_{plant}(s) = V_{dc}/(R_s + sL_s) \quad (3)$$

This is because the inverter will have a gain of to the voltage reference generated by the controller and the impedance offered is given by ($R_s + sL_s$) in s-domain. *Rs* and *Ls* are the net resistance and inductance referred to the primary side of the transformer respectively.

2) Design of PRI Controller Parameters: The fundamental current corresponds to the power injected into the grid. The control objective is to achieve UPF operation of the inverter. First, a PR controller is designed for the system assuming that the integral block is absent, i.e., KI = 0. Design of a PR controller is done by considering a PI controller in place of the PR controller.

Let

$$G\text{PI}(s) = Kp1\ ((1 + sT)/sT) \tag{4}$$

With the PI controller as the compensator block and without integral block, the forward transfer function will be

$$G\text{forw}(s) = Kp1\ ((1 + sT)/sT))(\ V\text{dc}/(Rs + sLs)) \tag{5}$$

If is the required bandwidth, then Kp1 can be chosen to be

$$Kp1 = \omega_{bw} R_s T\ /V\text{dc} \tag{6}$$

Now, if the PI controller in (5) is written as

$$G\text{PI}(s) = (Kp1 + Ki1)/s \tag{7}$$

The closed-loop transfer function is given as

$$Gcl,\text{PRI} = i(s)/i^*(s) = G\text{plant}\ G\text{PR}/(1 + G\text{plant}(G\text{PR} + GI\ )) \tag{8}$$

Without the integral block, the closed-loop transfer function would be

$$Gcl,\text{PR} = G_{\text{plant}}\ G_{\text{PR}}/(1 + G\text{plant}G_{\text{PR}}) \tag{9}$$

$$G\text{plant} = M/(1 + sT) \tag{10}$$

Where M=Vdc/Rs. The numerators in both (8) and (9) are the same. Thus, the difference in their response is only due to the
denominator terms in both. The denominator in (8) can be obtained as

$$\begin{aligned}\text{den}_{\text{PRI}} =&[(T_s^4 + (1 + MKp\ )s^3 + (\omega_0{}^2T + M(Kr + KI\ ))s2)/s(1 + sT\ )(s^2 + \omega_0{}^2)\ ] \\ &+ [\ (\omega_0{}^2\ (1 + MKp\ )s + MKI\omega_0{}^2)/s(1 + sT\ )(s^2 + \omega_0{}^2\ )\ ]\end{aligned} \tag{11}$$

Similarly, the denominator in (9) is given by

$$\begin{aligned}\text{den}_{\text{PR}} =&[T_s^3 + (1 + MKp\ )s^2 + (\omega_0{}^2T + MKr\ )/s(1 + sT\ )(s^2 + \omega_0{}^2\ )] \\ &+[\ (MKp + 1)\omega_0{}^2/(1 + sT\ )(s^2 + \omega_0{}^2\ )\ ]\end{aligned} \tag{12}$$

2.2 Comparison of Mitigation Techniques

Sr. No	Mitigation Technique	Features	Drawbacks
1.	Passive Harmonic Filtering	• Most commonly used and inexpensive	• Very bulky. • Cause resonance at selected frequency
2.	Active Harmonic Filtering	• Very efficient in suppression of harmonics. • Can eliminate more than one harmonic at a time. • Do not resonate with power system. • Can also provide PF correction and voltage regulation.	• More expensive than passive filters. • Large and complex.
3.	Selective Harmonic Elimination	• Selected harmonics of low order are eliminated completely. • Significant reduction in cost, size and weight of the filtering system	• Only a limited number harmonics are eliminated and unconsidered harmonics can reach very high amplitudes. • Maximum switching frequency is limited to a few hundreds of hertz.

4.	Voltage flicker tracking using algorithms	• Accurate, fast, and easy to implement. • Flexible. Eliminates use of APF and DSTATCOM. • Can also compensate for reactive power, harmonic and unbalance.	• Complex calculations increase computational burden on controller.
5.	Z-source inverter (ZSI) based DG system	• Provides the unique buck-boost feature to the inverter. • Optimizes the power output better than conventional VSI. • Low switching losses and improved reliability.	• Increases complexity of system.

3. Adaptive Harmonic Compensation

In this section, the concept of lower order harmonic compensation and the design of the adaptive harmonic compensation block using this adaptive filter are explained.

A. Review of the LMS Adaptive Filter

The adaptive harmonic compensation technique is based on the usage of an LMS adaptive filter to estimate a particular harmonic in the output current. This is then used to generate a counter voltage reference using a proportional controller to attenuate that particular harmonic.

B. Adaptive Harmonic Compensation

The LMS adaptive filter discussed previously can be used for selective harmonic compensation of any quantity, say grid current. To reduce a particular lower order harmonic (say i_k) of grid current:
1) i_k is estimated from the samples of grid current and phase locked loop (PLL) unit vectors at that frequency;
2) A voltage reference is generated from the estimated value of i_k ;
3) Generated voltage reference is subtracted from the main controller voltage reference.
The Fig.3 shows the power circuit topology considered. This topology has been chosen due to the following advantages: The switches are all rated for low voltage which reduces the cost and lesser component count in the system improves the overall reliability.

This topology will be a good choice for low-rated PV inverters of rating less than a kilowatt. The disadvantage would be the relatively larger size of the interface transformer compared to topologies with a high-frequency link transformer.

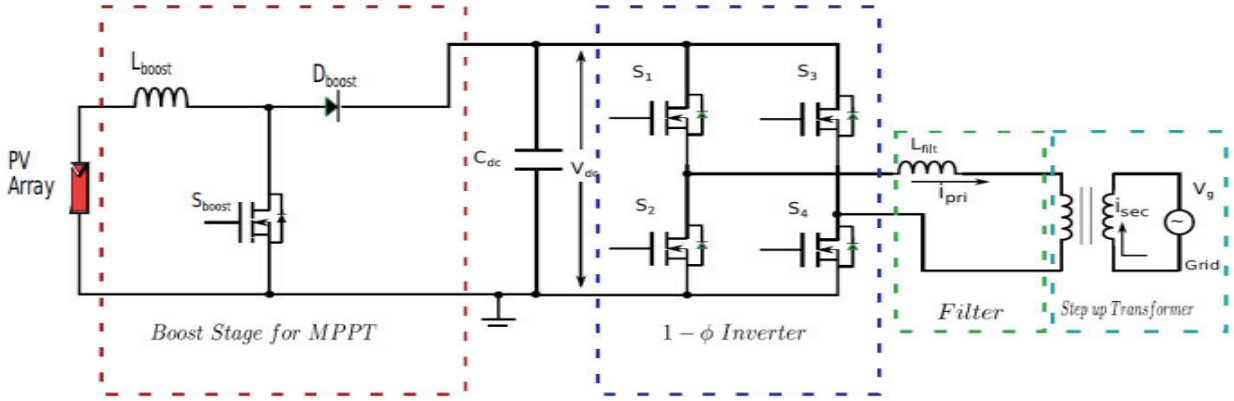

Figure 3: *Power circuit topology of the 1 − phase PV system for a low-voltage inverter with 40V dc bus connected to 230V grid using a step-up transformer*

4. Simulation Results

4.1 Grid connected single-phase PV inverter before compensation

The grid connected single-phase PV inverter before compensation is shown in fig.4.

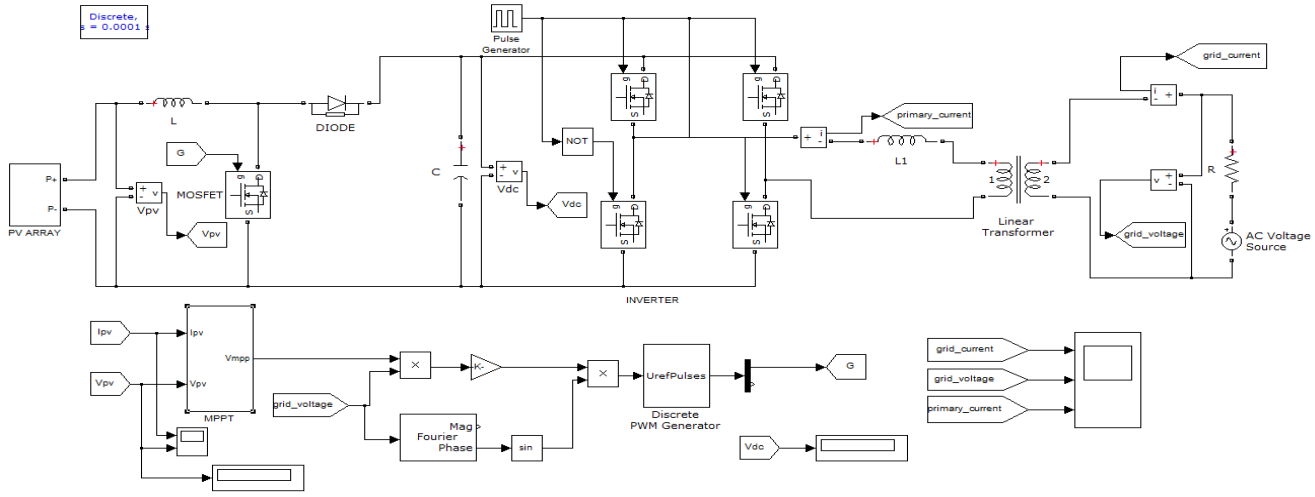

Figure 4: *Grid connected single-phase PV inverter before compensation*

The Fig.4. Consists of PV array, boost converter, single phase inverter, an inductive filter& a step-up transformer for interfacing with the grid. The PV array gives the values are V_{pv}=10.69v, I_{pv}=10.09A, V_{dc}=14.55 v. The boost converter boost up the voltage & current. The capacitor is used to the purpose of continuous current flowing. The inverter converts DC power to AC power. In the inverter each IGBT has resistance of 0.1Ω.the transformer having nominal power of 150VA; operating frequency is 50HZ, L=500_e^{-3}, C=6600_e^{-6} , R=0.1Ω, in ac voltage source, peak amplitude=230V.

4.2 Block Diagram OF PV Array

The block diagram of PV array is shown in fig.5

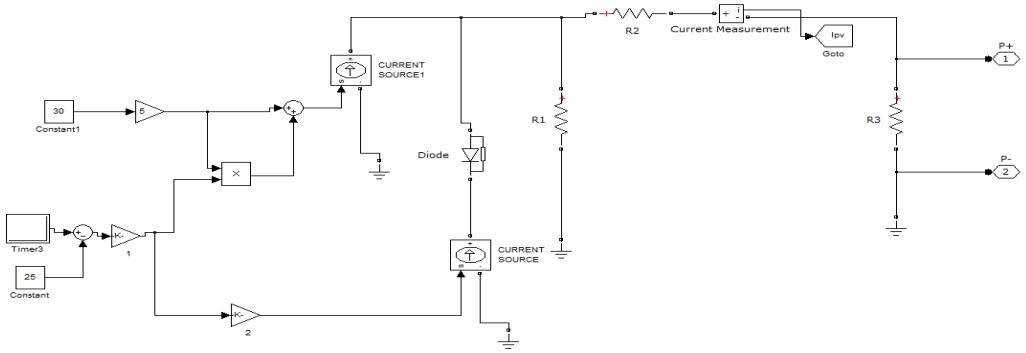

Figure 5: block diagram of PV array

In the PV array, R_1=1Ω, R_2=100Ω, R_3 =5Ω.For diode R=0.001Ω,V_f =0.8V, snubber resistance R_s =500Ω, snubber capacitance C_s = 250_e^{-6}.

4.3 Block Diagram of MPPT Algorithm

The block diagram of MPPT algorithm is shown in fig.6

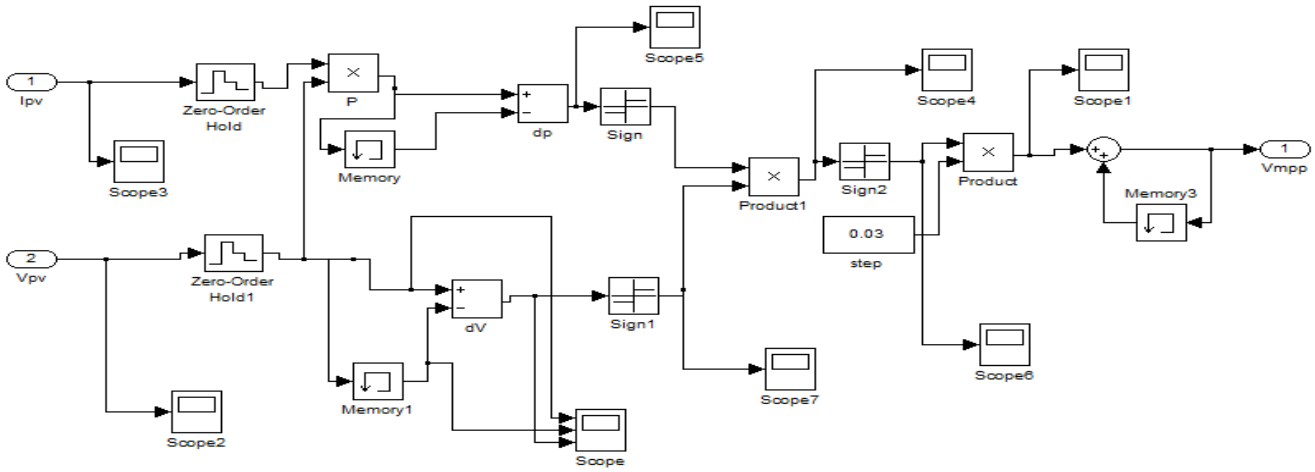

Figure 6: Block diagram of MPPT Algorithm

The Fig.6. Shows Block diagram of MPPT Algorithm. It gives the max. power to the circuit.

5. Grid Connected Single-Phase PV Inverter with PR Controller

The grid connected single-phase PV inverter with PR controller is shown in fig.7.

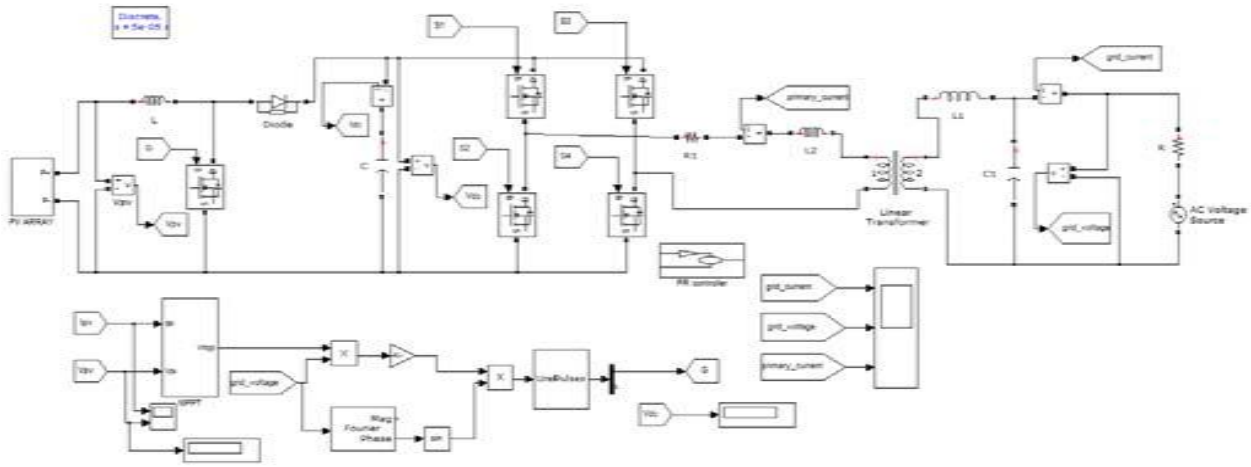

Figure 7: Grid connected single-phase PV inverter with PR controller

The Fig.7. Consists of PV array, boost converter, single phase inverter, an inductive filter& a step-up transformer for interfacing with the grid. The PV array gives the values are V_{pv}=29.62V,I_{pv} =9.90A, V_{dc}=41.7v. The boost converter boost up the voltage & current. The capacitor is used to the purpose of continuous current flowing. The inverter converts DC power to AC power. The transformer having nominal power of 150VA; operating frequency is 50HZ, $L=500_e^{-3}$,$L_1=1_e^{-3}$ $L_2=100_e^{-3}$, $C=6600_e^{-6}$,$C_1=100_e^{-6}$, R=0.1Ω, R_1=90Ω.In ac voltage source, peak amplitude=230V.it is also consists of PR controller.

5.1 Block diagram of PR Controller

The block diagram of PR controller is shown in fig.8.
PR controller means proposed resonant controller. It gives the values of K_p=3,K_r =594.

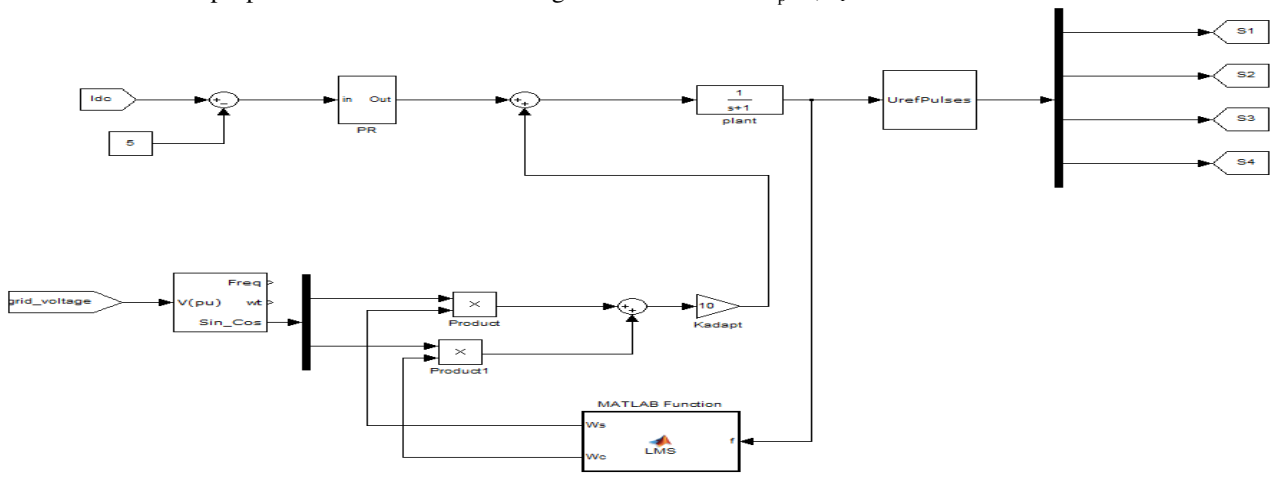

Figure 8: block diagram of PR controller

6. Grid Connected Single-Phase PV Inverter with PRI Controller

The grid connected single-phase PV inverter with PRI controller is shown in figure 9.

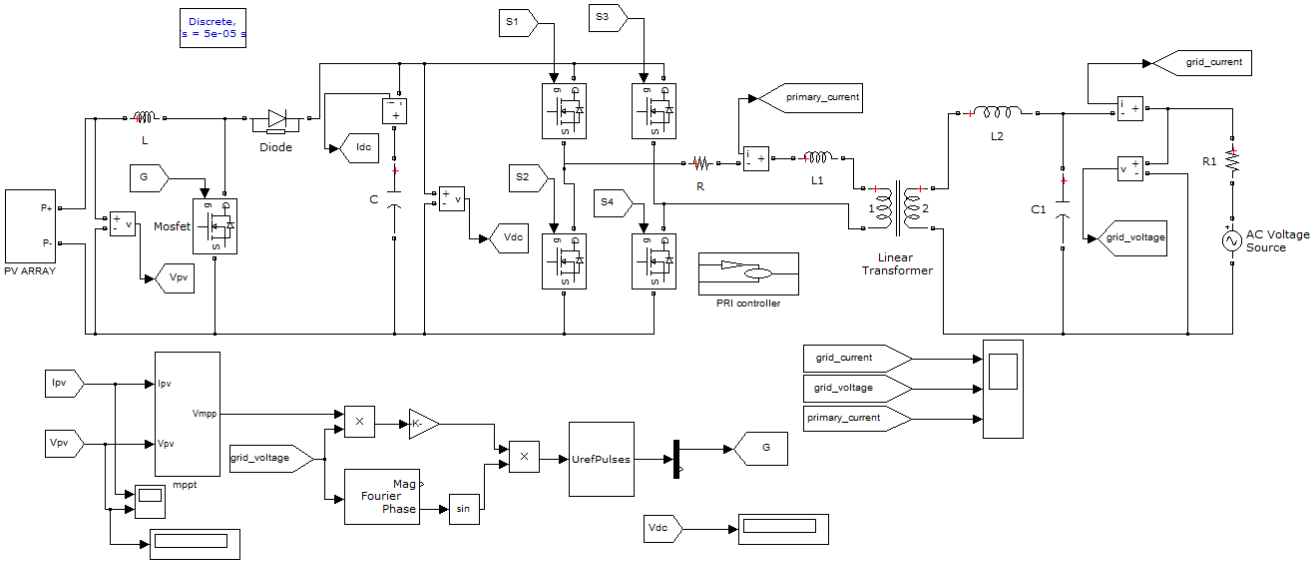

Figure 9: Grid connected single-phase PV inverter with PRI controller

The Fig.9, Consists of PV array, boost converter, single phase inverter, an inductive filter& a step-up transformer for interfacing with the grid. The PV array gives the values are V_{pv} =29.62V, I_{pv}=9.903A, V_{dc}=43.77v.The boost converter boost up the voltage & current. The capacitor is used to the purpose of continuous current flowing. The inverter converts DC power to AC power. In the inverter each IGBT has resistance of 0.1Ω. The transformer having nominal power of 150VA; operating frequency is 50HZ, $L=500_e^{-3}$, $L_1=100_e^{-3}$, $L_2=1_e^{-3}$, $C=6600_e^{-6}$, $C_1=200_e^{-6}$, R=200Ω, R_1=0.1Ω.In ac voltage source, peak amplitude=230V.it is also consists of PRI controller.

6.1 Block diagram of PRI controller

The block diagram of PRI controller is shown in fig.10.

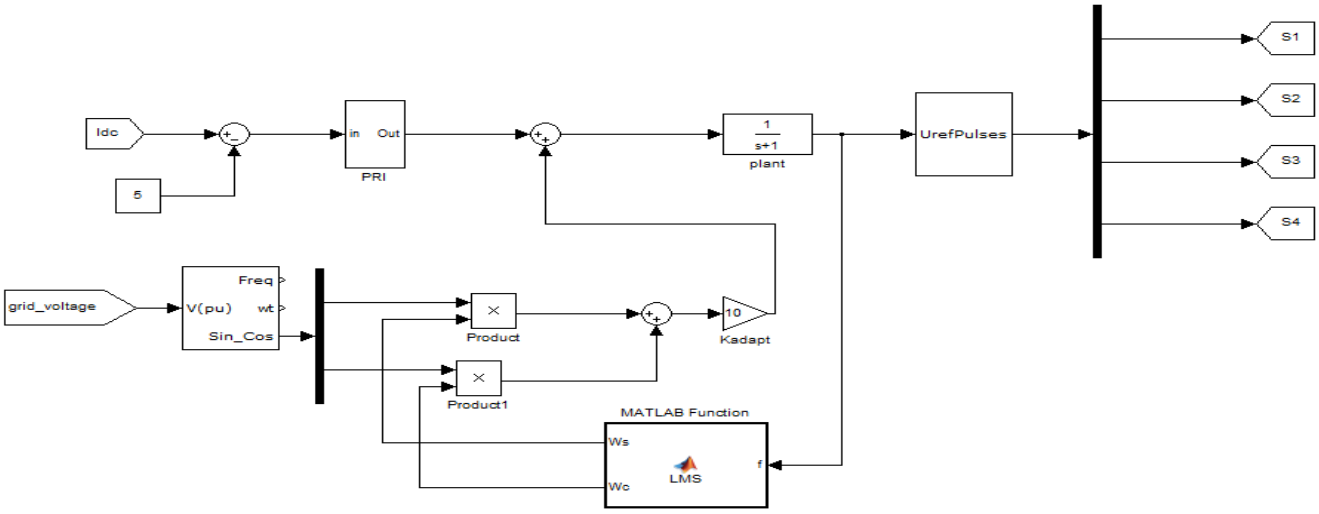

Figure 10: Block diagram of PRI controller

From the Fig.10 PRI controller means Proportional Resonant Integral controller. In this controller the values of K_p =3, K_r=594,K_I =100.

6.2 Simulink results of Grid connected single-phase PV inverter before compensation

The Simulink results of namely PV current, PV voltage, Grid current, Grid voltage, Primary current of Grid connected single-phase PV inverter before compensation are shown in the Fig.11.

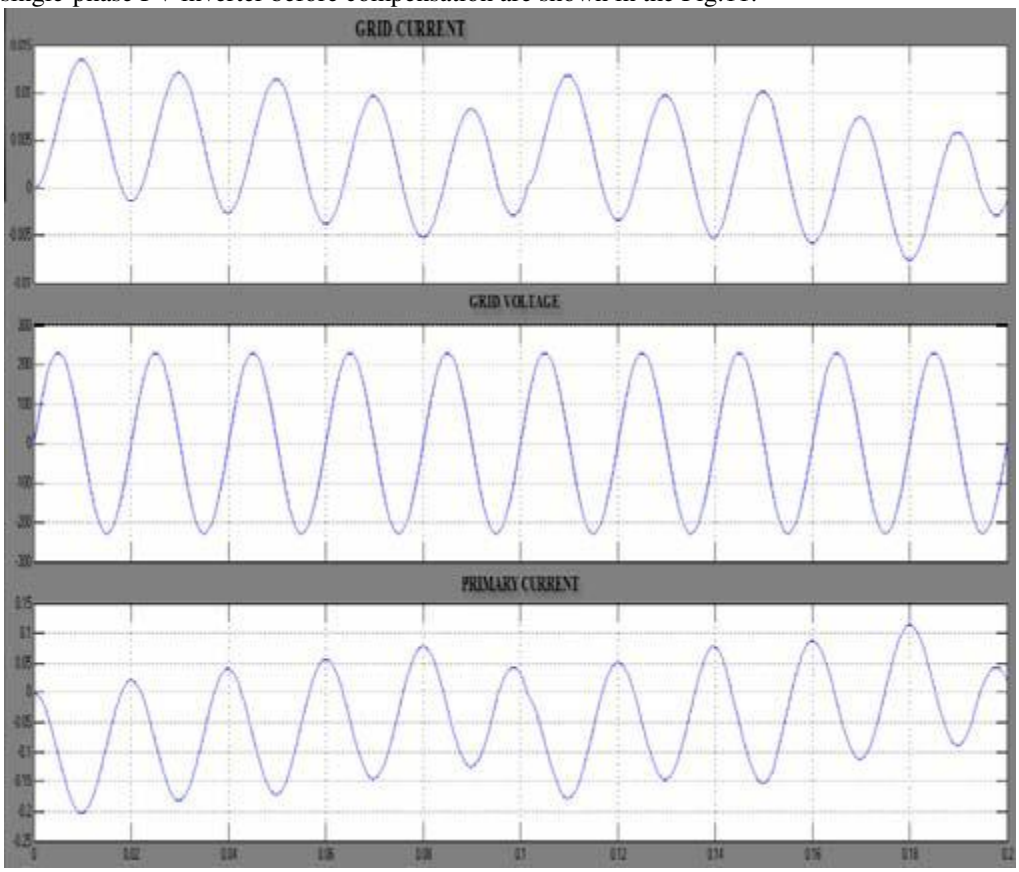

Figure 11: Output waveforms of PV inverter before compensation

From the output waveforms Shown in Fig.11. It is observed that the grid current, grid voltage & primary current are in sinusoidal form. Total harmonic distortion in Grid current of single-phase PV inverter before compensation. It is observed that the THD in Grid current is 9.14%.

6.4 Simulink results of Grid connected single-phase PV inverter with PR controller

The Output waveforms of Grid connected single-phase PV inverter with PR controller is shown in fig.12.

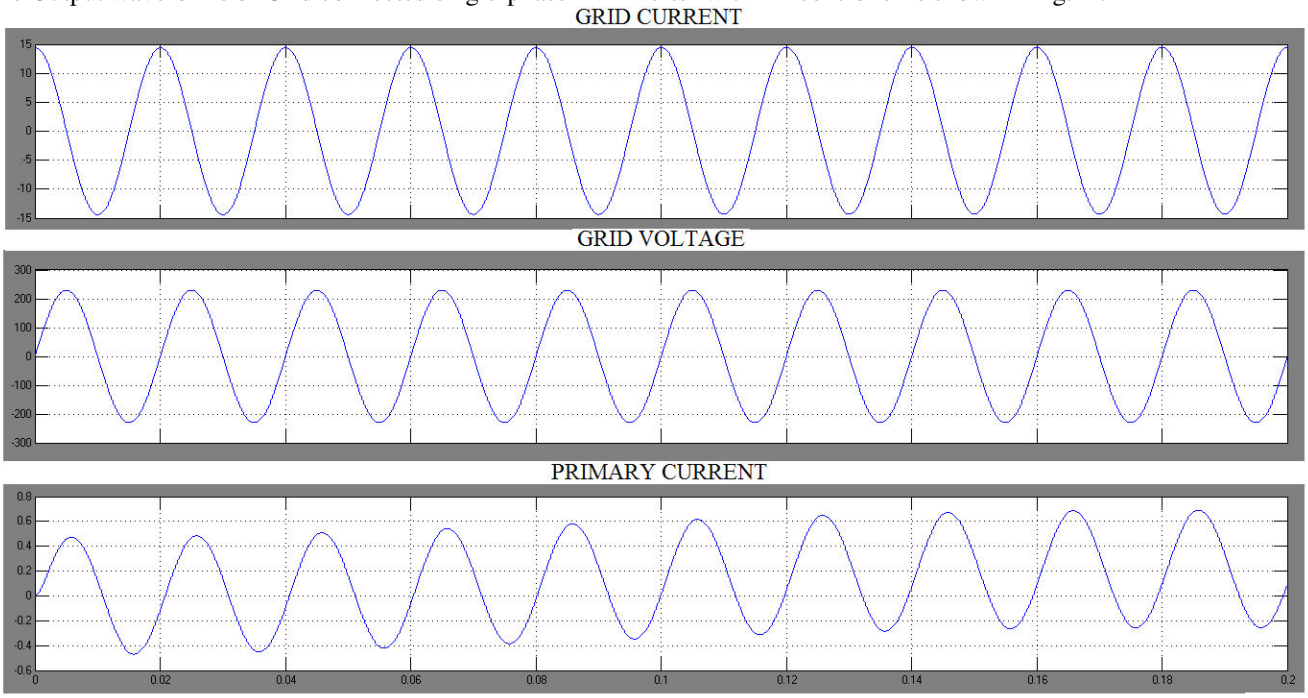

Figure 12: output waveforms of Grid connected single-phase PV inverter with PR controller

From the output waveforms Shown in Fig.12. It is observed that the grid current, grid voltage & primary current are in sinusoidal form. Total harmonic distortion in Grid current of single-phase PV inverter with PR controller. It is observed that the THD in Grid current is 2.90%.

6.5 Simulink results of Grid connected single-phase PV inverter with PRI controller

The Output waveforms of Grid connected single-phase PV inverter with PRI controller is shown in fig.13.

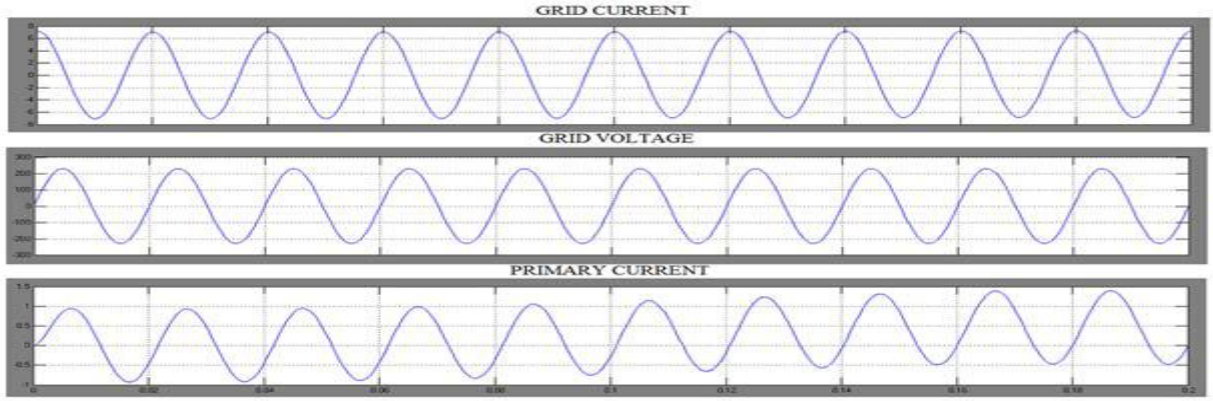

Figure 13: Output waveforms of Grid connected single-phase PV inverter with PRI controller.

From the output waveforms Shown in Fig.13. It is observed that the grid current, grid voltage & primary current are in sinusoidal form. Total harmonic distortion in Primary current of single-phase PV inverter with PRI controller. It is observed that the THD in Grid current is 1.85%.

Table 1: THD Analysis

	Total Harmonic Distortion (THD) (%)		
	Grid current	Grid voltage	Primary current
Before compensation	9.13	0	9.14
PR controller	0.16	0	2.91
PRI controller	0.03	0	1.85

The proposed single-phase PV inverter is simulated using MATLAB/SIMULINK. The corresponding results are showed before compensation, during PR& PRI controllers. Then the THD analyses for the proposed single-phase PV inverter with compensation and without compensation are compared.

7. Conclusion

Modification to the inverter current control for a grid connected single-phase photovoltaic inverter has been proposed in this paper, for ensuring high quality of the current injected into the grid. For the power circuit topology considered, the dominant causes for lower order harmonic injection are identified as the distorted transformer magnetizing current and the dead time of the inverter. It is also shown that the presence of dc offset in control loop results in even harmonics in the injected current for this topology due to the dc biasing of the transformer. A novel solution is proposed to attenuate all the dominant lower order harmonics in the system. The proposed method uses an LMS adaptive filter to estimate a particular harmonic in the grid current that needs to be attenuated. The estimated current is converted into an equivalent voltage reference using a proportional controller and added to the inverter voltage reference. The design of the gain of a proportional controller to have an adequate harmonic compensation has been explained. To avoid dc biasing of the transformer, a novel PRI controller has been proposed and its design has been presented. The PRI controller and the adaptive compensation scheme together improve the quality of the current injected into the grid.

Acknowledgements

This is the time to express my deep sense of gratitude to my college, L.C.I.T College of Engineering and Gujarat Technological University for giving me a great opportunity to take project for my dissertation. I would like to thanks my internal guide Prof. R.H.Patel, HOD of Electrical Department, L.C.I.T.College, Bhandu, Mehsana for his precious help and guidance who always bears and motivate me with technical guidance throughout this semester period. Also I would like to thank to the other faculties of power electronics department. I would also like to thanks Mr.Pankaj Patel Assistant professor of L.C.I.T College showing interest in the project and for giving valuable suggestions in improving this work. Most importantly, I would like to thank my parents and my brother for everything that they have done for me throughout my life and the joy they have brought to me for just having their support. Much of my success has been because of their love and encouragement.

References

[1] R. C´ardenas, C. Juri, R. Pen˜na, P.Wheeler, and J. Clare, "The application of resonant controllers to four leg matrix converters feeding unbalanced or nonlinear loads," *IEEE Trans. Power Electron.*, vol. 27, no. 3, pp. 1120– 1128, Mar. 2012.

[2] S. Jiang, D. Cao, Y. Li, J. Liu, and F. Z. Peng, "Low- THD, fast-transient, and cost-effective synchronous frame repetitive controller for three-phase UPS inverters," *IEEE Trans. Power Electron.*, vol. 27, no. 6, pp. 2994– 3005, Jun. 2012.

[3] J. M. Olm, G. A. Ramos, and R. Costa-Costel´o, "Stability analysis of digital repetitive control systems under time-varying sampling period," *IET Control Theory. Appl.*, vol. 5, no. 1, pp. 29–37, Jan. 2011.

[4] Q. Mei, M. Shan, L. Liu, and J. M. Guerrero, "A novel improved variable step-size incremental-resistance MPPT method for PV systems," *IEEE Trans. Ind. Electron.*, vol. 58, no. 6, pp. 2427–2434, Jun. 2011.

[5] A. K. Abdelsalam, A. M. Massoud, S. Ahmed, and P. N. Enjeti, "High-performance adaptive perturb and observe MPPT technique for photovoltaic-based microgrids," *IEEE Trans. Power Electron.*, vol. 26, no. 4, pp. 1010– 1021, Apr. 2011.

[6] R. Kadri, J.-P. Gaubert, and G. Champenois, "An improved maximum power point tracking for photovoltaic grid-connected inverter based on voltage oriented control," *IEEE Trans. Ind. Electron.*, vol. 58, no. 1, pp. 66–75, Jan. 2011.

[7] D. De and V. Ramanarayanan, "A proportional + multiresonant controller for three-phase four-wire high frequency link inverter," *IEEE Trans. Power Electron.*, vol. 25, no. 4, pp. 899–906, Apr. 2010.

[8]M. Cirrincione, M. Pucci, G. Vitale, and A. Miraoui, "Current harmonic compensation by a single-phase shunt active power filter controlled by adaptive neural filtering," *IEEE Trans. Ind. Electron.*, vol. 56, no. 8, pp. 3128–3143, Aug. 2009.

[9] B. Singh and J. Solanki, "An implementation of an adaptive control algorithm for a three-phase shunt active filter," *IEEE Trans. Ind. Electron.*, vol. 56, no. 8, pp. 2811–2820, Aug. 2009.

[10]J. R. Glover Jr., "Adaptive noise cancelling applied to sinusoidal interferences," IEEE Trans. Acoust., Speech, Signal Process., vol. 25, no. 6, pp. 484–491, Dec. 1977.

[11]J. Allmeling, "A control structure for fast harmonics compensation in active filters," IEEE Trans. Power Electron., vol. 19, no. 2, pp. 508–514, Mar. 2004.

Mitigation of Voltage Sags and Swells by Using FACT Device to Improve Power Quality

Parul D. Oza
M.E.Power Electronics and Electrical Drives,LCIT Collage,Bhandu-384120,India

Abstract
Power Quality is an occurrence manifested as many type of disturbance in voltage current or frequency, sensitive industrial loads that results in failure of end user equipment. So this paper represents the techniques for improve in sag and swell using device like DVR. The Dynamic Voltage Restorer (DVR) is a series compensator which can compensate for power quality problems such as voltage harmonics, voltage unbalance, voltage flickers, voltage sags, and voltage swells. Among all these power quality problems, two are identified as the major concern to the customers namely voltage sag and swell. A control technique based on a proportional integral (PI) controller is implemented. In fact with the aid of Pulse width modulation (PWM) inverter capable of generating accurate high quality voltage waveforms from the power electronic device. Simulation result shown by MATLAB/Simulink.

Keywords: Power Quality; DVR; Voltage sags/swells; PWM.

Nomenclature

A	Area of parallel plates on capacitor (m^2)
C	Capacitor (F)
R	Resistance (ohm)
V	Voltage (volt)
T	*Time (sec)*

1.Introduction

Continuous production throughout the period is ensured only when the final objective is to optimize the production while achieving maximum profits and achieving minimized production cost. The reason for demanding high quality un-interruptible power during production process. As soon as the fault occurs the action of DVR starts. On event of fault which results in voltage sag, the magnitude reduction is accompanied by phase angle shift and the remaining voltage magnitude with respective phase angle shift is provided by the DVR. Employing minimum active voltage injection mode in the DVR with some phase angle shift in the post fault voltage can result in miraculous use of DVR. If active voltage is less prominent in DVR then it can be delivered to the load for maintaining stability.

1.1Power Quality Problems

The IEEE defined power quality disturbances into seven categories based on wave shape:

1. Transients 2.Interruptions 3.Sag / Under voltage 4.Swell / Overvoltage 5.Waveform distortion
6 .Voltage fluctuations 7.Frequency variations.

Among all these power quality problems, two are identified as the major concern to the customers voltage sag and swell.

Voltage Sag**:**

IEEE standard sag can be define as the "A decrease to between 0.1 and 0.9 pu in rms voltage or current at the power frequency for durations of 0.5 cycles to 1 minute." It caused by sudden increase in load such as short circuit or faults, turning on electric heater, motor starting.

Voltage Swell:

Voltage swell can define as the "An increase to between 1.1 pu and 1.8 pu in rms voltage or current at the power frequency durations from 0.5 cycles to 1 minute." It caused by abrupt fall in load with poor voltage and also caused by loose or damage neutral connections.

2. Principle and Operation of Dynamic Voltage Restorer (DVR)

2.1 Principle

A power electronic converter based series compensator that can protect critical loads from all supply side disturbances other than outages is called a dynamic voltage restorer. The restorer is capable of generating or absorbing independently controllable real and reactive power at its AC output terminal. A DVR is a solid state power electronics switching device consisting of either GTO or IGBT, a capacitor bank as an energy storage device and injection transformers. It is connected in series between a distribution system and a load that shown in Figure 1. The basic idea of the DVR is to inject a controlled voltage generated by a forced commuted converter in a series to the bus voltage by means of an injecting transformer. A DC capacitor bank which acts as an energy storage device, provides a regulated dc voltage source.

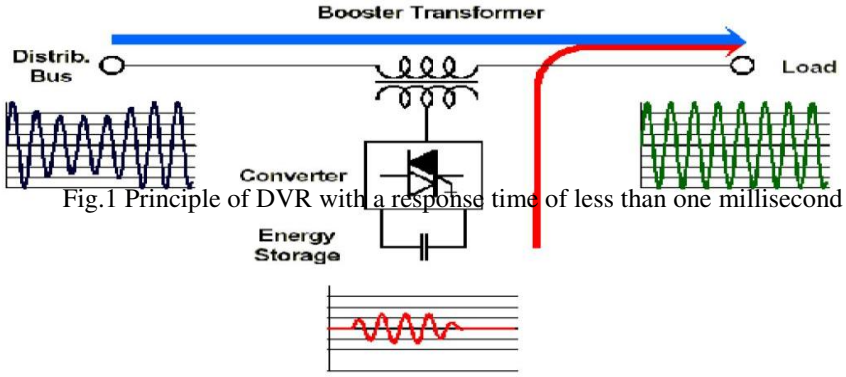

Fig.1 Principle of DVR with a response time of less than one millisecond

Fig.1 Principle of DVR with a response time of less than one millisecond

2.2 Components of DVR

A typical DVR consist of the following major components:

- Voltage Source Inverter (VSI)
- Injection Transformer
- Harmonic Filter
- Energy Storage Unit
- Bypass switch
- Control and Protection System

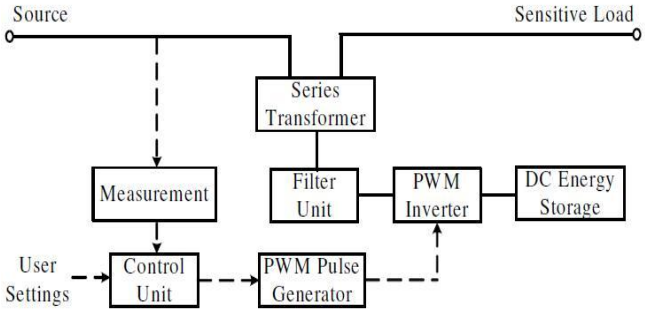

Fig.2 Simplified DVR block

(i) DC Storage Device
It supply necessary energy to VSI during compensation. VSI will convert it into alternating quantity and fed to injection transformer
(ii) Voltage Source Inverter
VSI is power electronics system consist of switching device (IGBT, GTO) which can generate a sinusoidal voltage at any required frequency, magnitude and phase angle.
(iii) Filter Unit
The main task of filter is to keep the harmonic voltage content generated by VSI to the permissible limit (i.e. eliminate high frequency harmonics)

(iv) Voltage injection Transformers

It consist of two side one is high voltage side and low voltage side. The high voltage side is normally connected in series with distribution n/w while low voltage side is connected to DVR it isolate distribution line from DVR system.

(v) Control System

The aim of control system is to maintain constant voltage at point where a sensitive load is connected under disturbances.

The magnitude of load voltage is compared with reference voltage and if any difference is there error signal will be generated. This signal is actuating signal which drives PI controller.

(vi) PWM Generator

The PWM modifies the width of the pulses in a pulse train by using control signal. When the value of control voltage increases, it results wider pulses. The waveform of control voltage for a PWM circuit will determine the waveform of the produced voltage.

3. **DVR Compensation Techniques**

The compensation control technique of the DVR is the mechanism used to track the supply voltage and synchronized that with the pre-sag supply voltage during a voltage sag/swell in the upstream of distribution line.

(i) Pre-sag Compensation

Pre-sag compensation is a method which is generally used for nonlinear loads such as thyristor controlled drives. In nonlinear loads the voltage magnitude as well as he phase angle needs to be compensated.

(ii)In-phase Compensation

This technique of compensation is generally used for active loads. Only compensation for voltage magnitude is required whereas no phase compensation is required. In this particular method the compensated voltage is in phase with the sagged voltage.

(iii)In-phase advanced compensation method

In this method the real power spent by the DVR is decreased by minimizing the power angle between the sag voltage and load current. In case of pre-sag and in-phase compensation method the active power is injected into the system during disturbances. The active power supply is limited stored energy in the DC links and this part is one of the most expensive parts of DVR.

(iv)Energy optimization technique

In this particular control technique the use of real power is minimized (or made equal to zero) by injecting the required voltage by the DVR at a 90° phase angle to the load current.

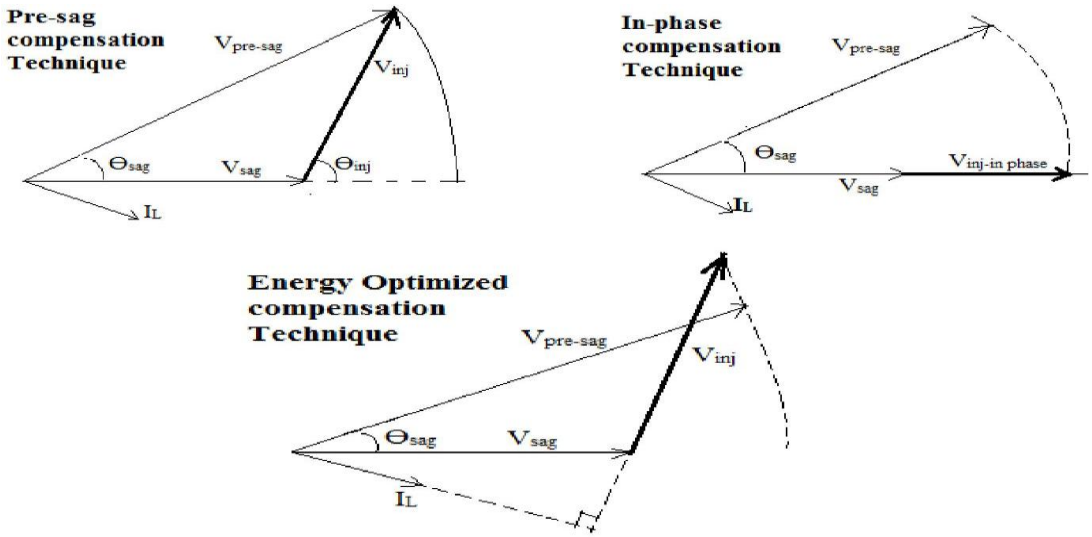

Fig.3 DVR compensation Techniques.

3.1 PI Controller

The DVR control system exerts a voltage angle control as follows: an error signal is obtained by comparing the reference voltage with the rms voltage measured at the load point. The PI controller processes the error signal

and generates the required angle δ to drive the error to zero, for example; the load rms voltage is brought back to the reference voltage.

The controller input is an error signal obtained from the reference voltage and the value rms of the terminal voltage measured. Such error is processed by a PI controller the output is the angle δ, which is provided to the PWM signal generator. It is important to note that in this case, indirectly controlled converter, there is active and reactive power exchange with the network simultaneously: an error signal is obtained by comparing the reference voltage with the rms voltage measured at the load point. The PI controller process the error signal generates the required angle to drive the error to zero, i.e., the load rms voltage is brought back to the reference voltage.

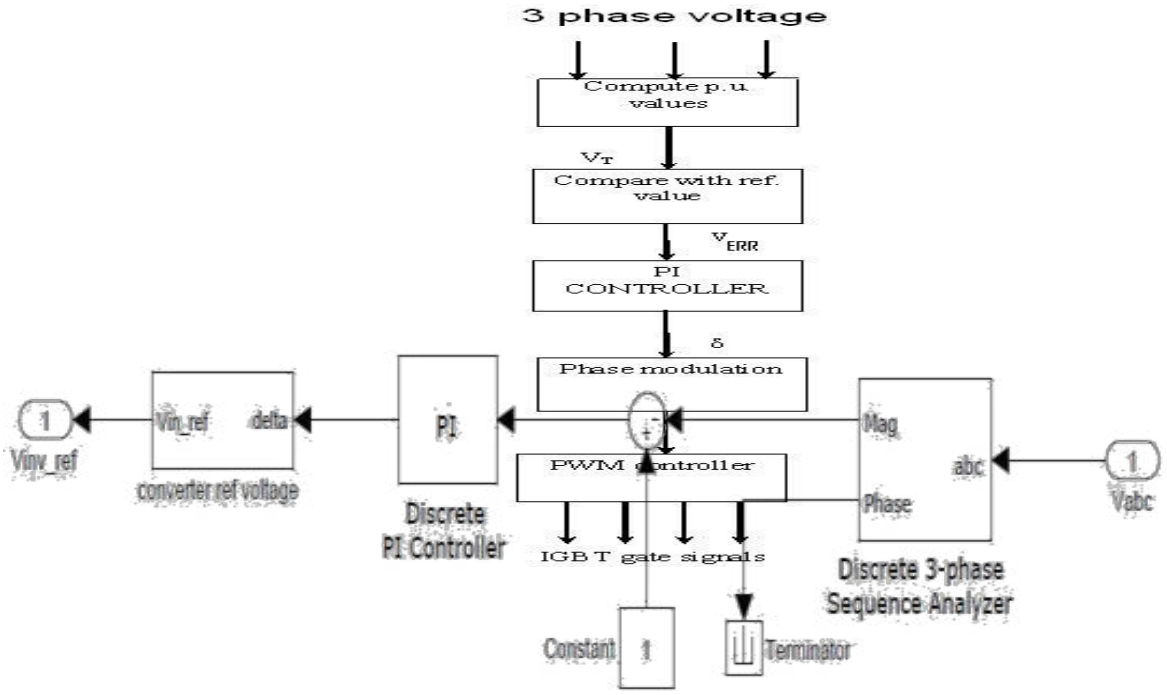

Fig.4 Control algorithm of DVR with PI controller

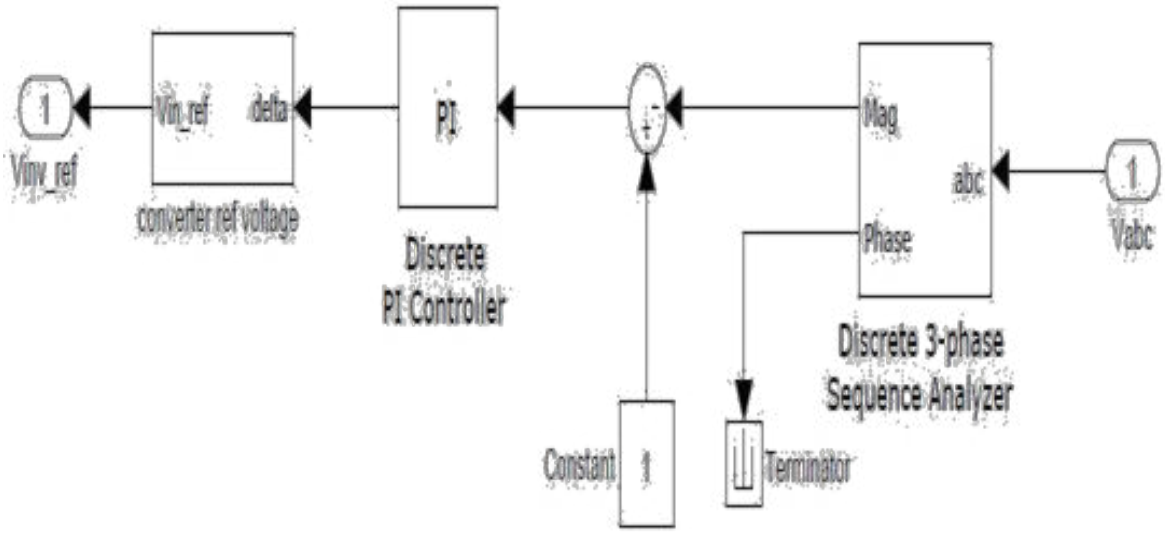

Fig.5 Simulink model of Controller

4. Test System and Simulation Result

DVR is composed by a 13 kV, 50 Hz generation system, feeding two transmission lines through a 3- winding transformer connected in Y/S/S, 13/115/115 kV. Such transmission lines feed two distribution networks through two transformers connected in S/Y, 115/11 kV. To verify the working of DVR for voltage compensation a fault is applied at point X at resistance 0.66 U for time duration of 200 ms. The DVR is simulated to be in operation only for the duration of the fault.

Table 1.System parameter

System device	Parameters /standards
Inverter Specification	IGBT based,3 arms , 6 Pulse, Carrier Frequency =1080 Hz, Sample Time= 5 μs
Transmission Line Parameter	R=0.001 ohms , L=0.005H
PI Controller	Kp=0.5 , Ki=50, Sample time=50 μs

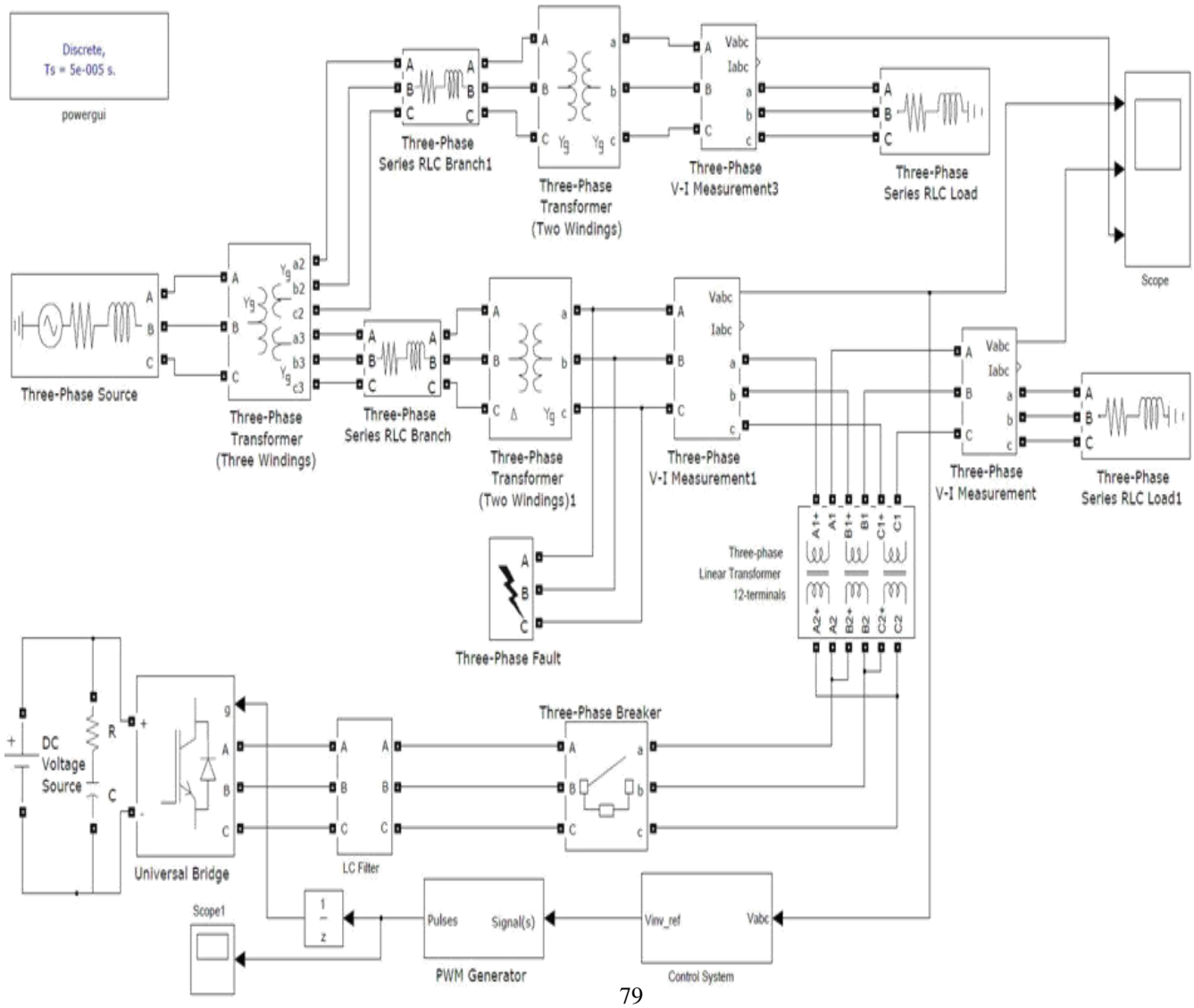

FIGURE5.2 DYNAMIC VOLTAGE RESTORER WITH TEST SYSTEM IMLIMENTED IN MATLAB

4.1 Simulation Results for Sag:
Three phase to ground Fault Sag

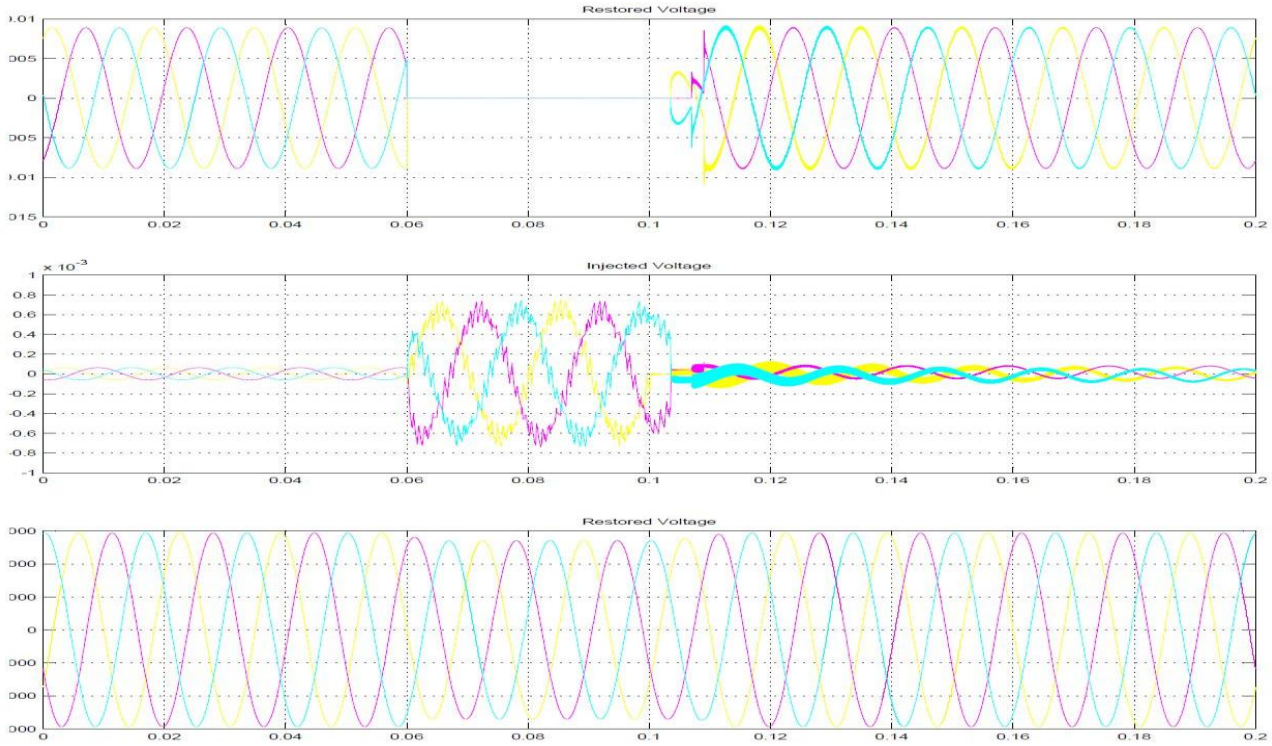

4.2 Simulation Results for Swell
Single Line to ground Swell

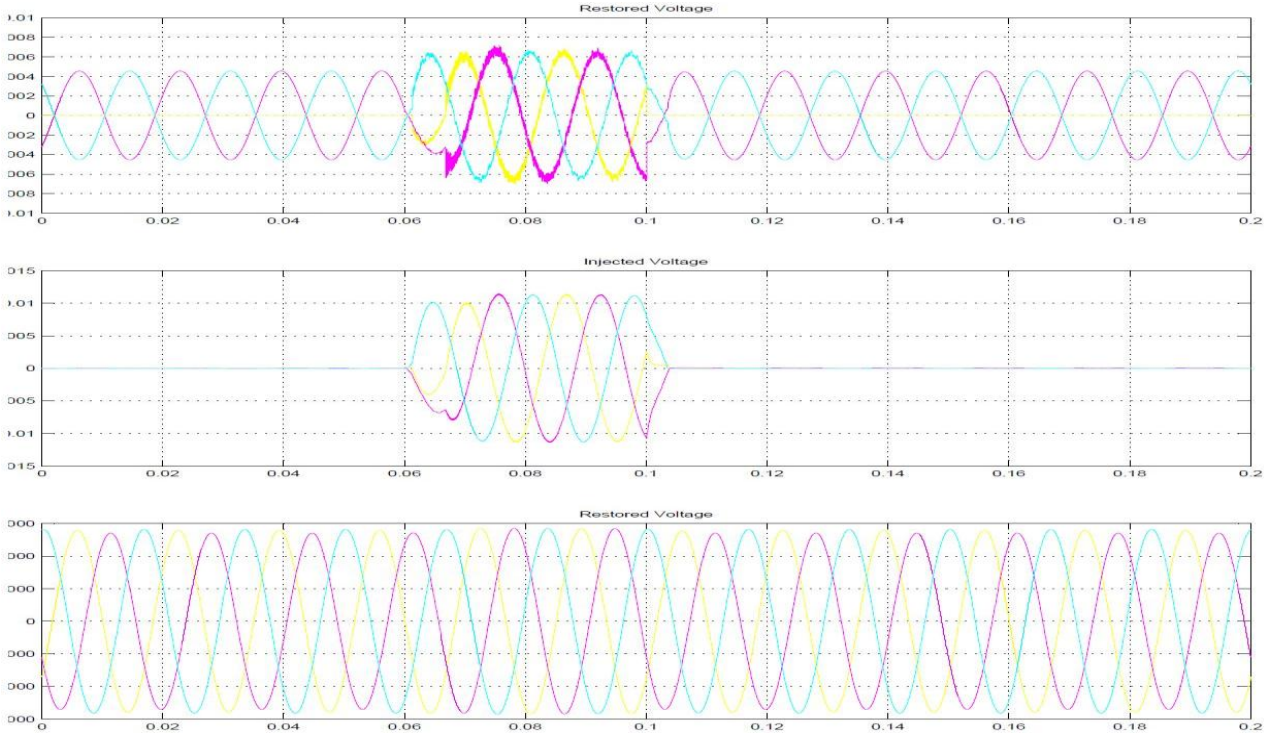

Fig.6 Simulation Result

5. Conclusion

Dynamic voltage restorers (DVR) are used to protect sensitive loads from the effects of voltage sags/swells on the distribution feeder. In all cases it is necessary for the DVR control system to not only detect the start and end of a voltage sag but also to determine the sag depth and any associated phase shift. The DVR, which is placed in series with a sensitive load, must be able to respond quickly to voltage sag if end users of sensitive equipment are to experience no voltage sags. As conclusion, voltage sag/swell is unwanted phenomenon which unavoidable but can be reduced using all techniques, but not limited to the techniques that have been discussed. There is no one mitigation technique that will suitable with every application, and whilst the power supply utilities strive to supply improved power quality, it is up to the applications engineer to minimize power quality problems. It means, power quality problem cannot be eliminated but we can reduce and try to avoid this problem form occur.

References

[1] C. Benachaiba and B. Ferdi, "Power Quality Improvement Using DVR", American Journal of Applied Sciences, vol.6, no.3, 2009, pp. 396-400 .

[2] Joseph Seymour Terry Horsley, "The Seven Types of Power Problems", American Journal of Power Conversion, 2005, pp.1-24

[3] H.P. Tiwari, Sunil Kumar Gupta, "Dynamic Voltage Restorer Based On load Condition", International Journal of Innovation, Management and Technology, vol.1 no.1, April 2010

[4] K.Sandhya, Dr.A.Jaya Laxmi, Dr. M.P.Soni, "Direct and Indirect Control Strategies of Dynamic Voltage Restorer", Proc. of Int. Conf. on Control, Communication and Power Engineering 2010, pp.281-285

[5] Arindam Ghosh and Gerard Ledwich, Senior Member IEEE, "Compensation Of Distribution System Voltage Using DVR", IEEE Transaction On Power Delivery vol.17,no.4, 2002, pp.1030-1036

[6] Rosli Omar, Nasrudin Abd Rahim and Marizan Sulaiman, "New Control Technique Applied in Dynamic Voltage Restorer for Voltage Sag Mitigation", American Journal of Applied Sciences vol.3, 2010, pp.858-864"

[7] H.P. Tiwari and Sunil Kumar Gupta, "DC Energy Storage Schemes for DVR Voltage Sag Mitigation System", International Journal of Computer Theory and Engineering, vol.2 No.3, June 2010, pp.313-318

[8]Saripalli Rajesh, Mahesh K. Mishra and Sridhar K, "Design and Simulation of Dynamic Voltage Restorer (DVR) Using Sinusoidal Pulse Width Modulation (SPWM)", 16th s National Power System Conference, Dec 2010, pp.317-322

Abbreviations

Symbol	Description
AC	Alternating Current
DC	Direct Current
IEEE	Institute of Electrical and Electronics Engineers
FACTS	Flexible AC Transmission Systems
DVR	Dynamic Voltage Restorer
GTO	Gate Turn-Off Thyristor
VSC	Voltage Source Converter
IGBT	Insulated Gate Bipolar Transistors
Hz	Hertz
ms	millisecond
pu	Per unit
PCC	point of common coupling
PWM	Pulse Width Modulation
RMS	root mean square

A review on
Analysis of different type of welding joints used for fabrication of pressure vessel considering design aspects with operating conditions

Priyank Solanki[a],Vijay Parekh[b]
[a]ME(AMS)SVMIT, Bharuch,392001,India
[b]Asist. Professor Mech SVMIT, Bharuch,392001,india

Abstract
Pressure vessels are the containers or pipelines used for storing, receiving or carrying the fluid under pressure. Various type of pressure vessels like horizontal, vertical, spherical are used in industry. In most of case cracks are finding between nozzles and head dish joint of pressure vessels. The failure of vessel in service may cause loss of life and properties and welded joint plays significant role in the failure of pressure vessel. Weld joint are usually main failure part under loading condition. Welding defects are also observed at nozzle joint due to testing of pressure vessel in industry. In this review paper analysis of various parameters such as types of weld grooves & angle will consider for FEA analysis to overcome the defects related to welding joint at nozzle to head joint and improve the strength of weld joint.

Keywords: Pressure vessel, welding joint ,analysis.

Nomenclature

PV	Pressure vessel
UV	U-type & V-type groove
SEM	Scanning electron microscopy
OM	Optical microscopy
DU	Double U- groove
HAZ	Heat affected zone
RS	Residual stress

1. Introduction

Pressure vessels are the containers or pipelines used for storing, receiving or carrying the fluid under pressure. The pressure vessels are designed with great care because the failure of vessel in service may cause loss of life and properties. The material of pressure vessels may be brittle such as cast iron or ductile as plain carbon steel and alloy steel.

The main component of pressure vessel are (1) Shell, (2) Head, (3) Nozzle, (4) Support and the type of pressure vessel A) Horizontal Pressure Vessels, B) Vertical Pressure Vessels, C) Spherical Pressure vessels as shown in Figure 1.1

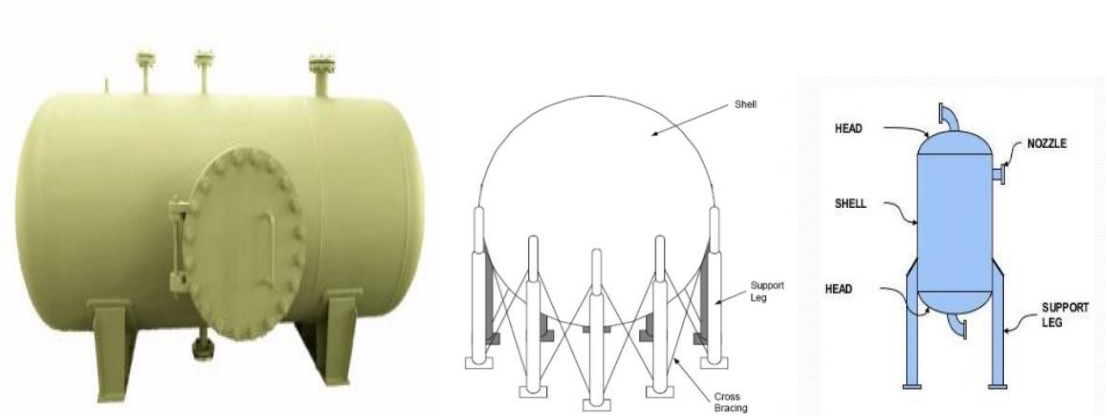

(a) (b) (c)

Figure 1.1- (a) Horizontal PV [1], (b) Vertical PV, (c) Spherical PV [2]

1.1 Types According To Wall Thickness

- Thin Walled Pressure Vessel - inner radius to wall thickness ratio of "10" or more ($r / t \geq 10$)
- Thick Walled Pressure Vessel - inner-radius-to-wall-thickness ratio of "10" or less ($r / t \leq 10$)

1.2 Different Types of grooves & welded joints

The various type of grooves used for fabrication of pressure vessel which is listed as below shown in figure 1.2 and work piece thickness limit per joint type describe in below table1.1

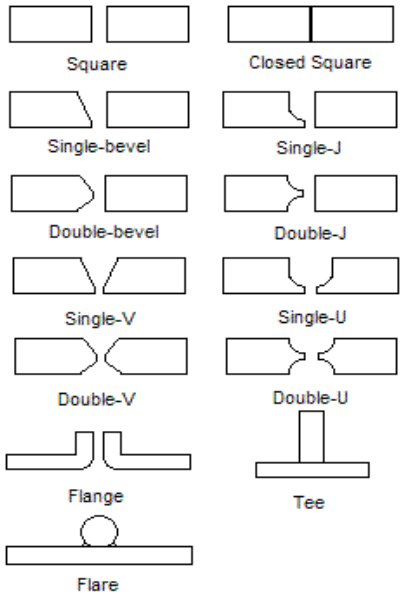

Figure 1.2 Types of grooves symbol [3]

Table 1.1- Work piece Thickness Limit per Joint Type [4]

Work piece Thickness Limit Per Joint Type	
Joint type	**Thickness**
Square joint	Up to 1/4 in (6.35 mm)
Single-bevel joint	3/16–3/8 in (4.76–9.53 mm)
Double-bevel joint	Over 3/8 in (9.53 mm)
Single-V joint	Up to 3/4 in (19.05 mm)
Double-V joint	Over 3/4 in (19.05 mm)
Single-J joint	1/2–3/4 in (12.70–19.05 mm)
Double-J joint	Over 3/4 in (19.05 mm)
Single-U joint	Up to 3/4 in (19.05 mm)
Double-U joint	Over 3/4 in (19.05 mm)
Flange (edge of corner)	Sheet metals less than 12 gauge (0.1046 in or 2.657 mm)
Flare groove	All thickness

1.3 Selection of Material for Pressure Vessel

The pressure vessel withstand with following condition of material.

- High or very low temperatures
- High pressure
- High flow rate
- Sometime corrosive fluid

The selection of material is based on the required mechanical strength other mechanical properties and anti-corrosive properties. In addition fabrication problem commercial availability of material and cost of material will have to be assessed in final selection of material.

1.4 Material Used for Pressure Vessels

Cast Irons, Plain Carbon Steel, Alloy Steels, Aluminium Alloys, Copper And Copper Alloys, Nickel and Nickel Alloy,etc as per application of pressure vessel.

1.5 Welding Techniques

Oxyacetylene welding, Shielded metal arc welding (SMAW), Gas-tungsten arc welding (GTAW), Gas-metal arc welding (GMAW), Flux-core arc welding (FCAW), Plasma arc welding (PAW), Submerged arc welding (SAW), Electro-slag welding (ESW), Electron beam welding (EBW), Laser beam welding (LBW) etc.

1.6 Failures in pressure vessels

Vessels failure can be grouped into four major categories. Failures can also be grouped into type of failures which

describes how the failure occurred
1. Material- improper selection of material, defects in material
2. Design – incorrect design data, inaccurate or in correct design method
3. Fabrication – poor quality control, improper or insufficient fabrication procedure including welding, heat treatment or forming method.
4. Services- change of services condition by the user, in experienced operation or maintenance personnel.

1.7 Types of failures

1) Elastic deformation, 2) Brittle fracture, 3) Stress rupture, 4) Excessive Plastic Deformation, 5) High stain, 6) Stress corrosion, 7) Corrosion fatigue etc.

2. Literature survey

Hessamoddin Moshayedi [5] in 2015 in this paper analysis is done by FE analysis using ABAQUS 6.14 software and studied an internal circumferential crack is generated at the weld line. Residual stresses (RS) can be generated in a component after fabrication process like welding, manufacturing, processing or assembly which is weld by Welding technique manual gas tungsten arc welding process. Axial and hoop stress residual stress distribution is shown in figure 1.3.

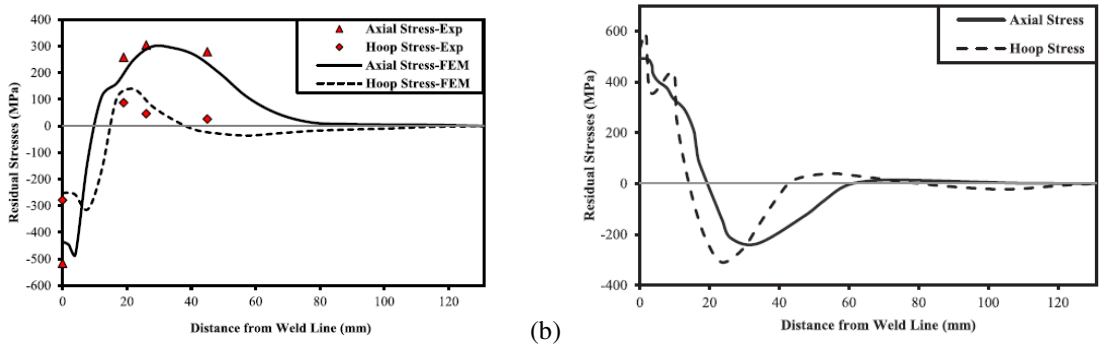

(a) (b)

Figure-1.3 (a) Axial and hoop RS distribution on the outer surface of pipe & (b) Axial and hoop RS distribution on the inner surface of pipe.

Kamal H. Dhandha [6] et al in 2015 in this paper material is steel P91 and it is widely used for high temperature components of power plants. A TIG welding process was applied on P91 steel in which oxide powders CaO, Fe2O3, TiO2, ZnO, MnO2 and CrO3 were used to produce a bead on plate welds.
The weld penetration is increase and the bead width is decrease significantly with the use of the activating fluxes Fe2O3, ZnO, MnO2 and CrO3. There is increase in aspect ratio with the flux ZnO by 320% as compared to conventional TIG welding process. Making of oxide flux is as shown in figure 1.4(a) and graph of results as shown in figure 1.4(b).

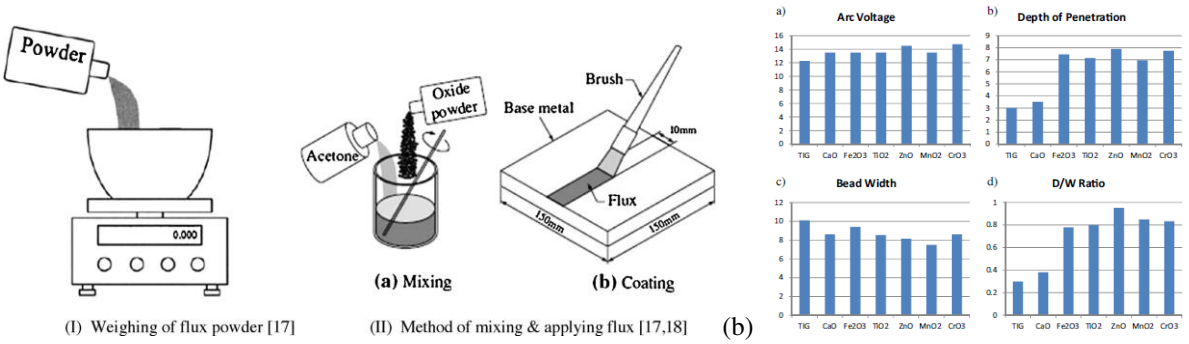

(a) (I) Weighing of flux powder [17] (II) Method of mixing & applying flux [17,18] (b)

Figure-1.4 (a) Application of flux for A-TIG welding process & (b) Relative changes in penetration depths, bead width, voltage and D/W ratio of welds with and without flux

Xiao-Tao Zheng [7] et al in 2015 in this paper observed that butt welded joints are usually the main failure part and for analysis they have made Finite Element Modelling of various circumferential welded joints with UV-groove, DU-groove, X-groove, U-groove, V-groove, and single-side weld and the conclude Result when the thickness of welded pipe is relatively small, then U, V, X groove and single-side weld are used, while UV- and DU-groove are chosen for welded pipe with greater thickness.

Jingqiang Yang [8] et al 2014 in this paper observed that the Failure analyses of weld joint between the nozzle and the head of the reactor which is made of 2205 duplex stainless steel was performed by optical microscopy (OM) and scanning electron microscopy (SEM). Cracks were found in HAZ of the weld. In this work, the failure mechanism of a reactor vessel after 1 year of operation was studied**.** Crack location at nozzle to dish joint as shown in figure 1.5.

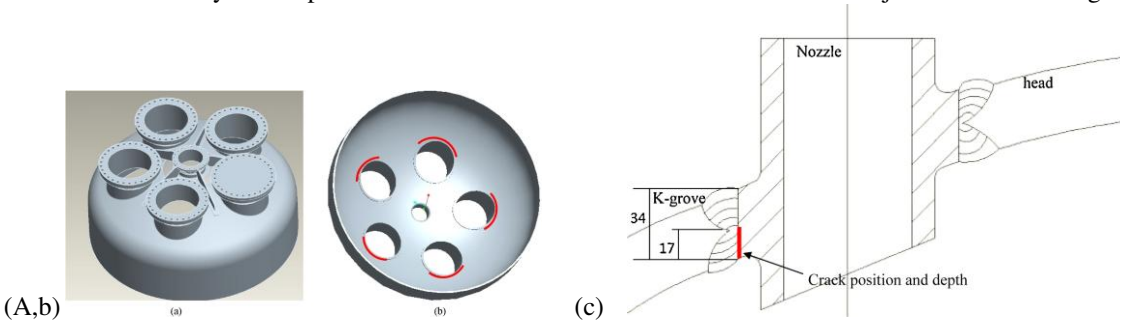

Figure 1.5 - Crack between nozzle and the heat for the reactor with (a) outside and (b) inside [4] (c) crack

The connections between the nozzles and the head are welded by SMAW (shielded metal arc welding) with a K-grove preparation as shown in figure 1.5 (c). The welds are completed in four to five passes. The cracks can be found in all of the five outer nozzles and all are located at the outer ring of the nozzles The cracks are further developed during hydrostatic pressure test due to the embrittlement of the weld joint The welds are going to be repaired by GTAW (gas tungsten arc welding) method, The weld presents very uneven distribution of ferrite/austenite with 80–90% ferrite.

M. Clyde Zondi [9] in 2014 in this paper observed that Residual stresses generate during welding which are affect the fatigue life of pressure vessel. Residual stress generate due to non-uniform heating of the metallic surfaces, which in turn cause plastic straining of the different portions of the weld-piece material, In this study three categories of influential factors as pre-welding conditions, in-process parameters, and post welding conditions are illustrate.

Shugen XuWeiqiang Wang [10] et al 2014 in this paper Layered cylindrical vessels are widely used in process industries. In this paper, the Finite Element Method (FEM) is used to predict the residual stresses in a layered-to-layered joint. Due to the material mismatching between inner stainless steel layer and outer low alloy steel layer, discontinuous stress distributions are presented. The gap between discrete layers has a great effect on the residual stress in HAZ.

Yupiter H.P. Manurung[11] et al 2013 in this paper author investigate the welding sequence effect on induced angular distortion using FEM and experiments. To validate the simulation results, a series of experiments was conducted with contain two different welding sequences using an automated welding process, parent metal is low carbon steel , digital GMAW power source with premixed shielding gas and both-sided clamping technique. Sequence 1 “from inside to outside” and sequence 2 “from outside to inside”. Welding sequence 2 (from outside to inside) shows less angular distortion than welding sequence 1 (from inside to outside).

Duncan Camilleri [12] et al 2013 this study Three different filler materials used to weld Lloyds 2000 grade DH36 mild steel plates (similar to EN 10025 S355J2G3), are investigated. The filler materials include two commercial filler wires; a metal cored (MC) filler wire according to EN758: T46 4 mm 1 and a flux cored (FC) filler wire according to EN758: T42 2 PM 1 H5 together with nickel based filler wire (referred to as LT). The finite element models were applied to butt welding of two 0.5 m*.25 m * 4 mm thick plates. The use of nickel based filler materials promotes the formation of martensite. This results in the development of compressive longitudinal residual stresses at the weld region, so reducing the amount of longitudinal contraction force and consequently reducing the longitudinal bowing.

Wen-chun Jiang [13] et al in 2013 half pipe jacketed pressure vessels are used for cooling and heating process in chemical industries but the leakage welding joint between the jacket and cylinder is a big problem, which is affected by residual stress and deformation. The simulation of weld residual stress by finite element method (FEM) can obtain the stress and deformation distribution in the total structure By using FEM, they observed that changing the heat input, weld passes, groove shape, material properties and geometrical dimensions of the weld structure can decrease the residual stress.

Mostafa Jafarianet[14] al in 2012 in this paper in this study, nine important welding processes were used in the system. They use Methodology of Fuzzy AHP&TOPSIS to determine the result GTAW and PAW are the most appropriate welding process and OFW and SAW are not appropriate for high pressure vessel production. If cost is not consider then EBW and LBW use for welding.

John W. H. Priceet[15] al 2006 In this paper, they present experimental neutron diffraction measurements of weld stresses generated by single and multi-beads on- plate. Result in transverse and normal directions maximum residual stresses of around half of the maximum value of longitudinal stress have been observed.

B. Arivazhagan[16] et al 2015 in this study they welding 2.25Cr-1Mo (P22) steel plate by TIG welding. 12 mm thick double side square butt joint is use for welding. Effect of post weld heat treatment (PWHT) on the impact toughness was studied
An activated flux in the form of paste is applied on the joint of weld area to achieve depth of more penetration up to 300 %.
The weld was found to be free from cracks after welding.

C.R. Das [17] et al 2013 in this study the fatigue failure of fillet weld nozzle joint is studied. Material is AISI 304L stainless steel and weld joint Failed during transportation. In this pressure vessel crack area is near fusion line. SEM (scanning electron microscope) observation of fracture-surface, ratchet, and notches found that shows the fatigue failure.

Han-sang Lee [18] et al 2005 in this paper the cracks in the tube propagates from inner surface of the heat affected zone.
TIG welding technique is used. Formation of course Cr carbide found in the heat affected zone of failed tube. Induced martensite in inner side of heat affected zone.

Nausheen Naz [19] et al 2009 Steel nozzle cracking observed after circumferential welding process. Nozzle –material is C-Cr MoV alloy steel. Butt weld joint used and TIG welding technique used for welding. Cracks on the surface in the area adjacent to weld bead (HAZ). Failure was occurred by the presence of course untempered martensite in heat affected zone due to localize heating. High heat input and low welding speed result in high transformation stresses. Transformation stresses combine with the thermal stresses and the constraint condition to cause intergranular brittle structure

H.M. Shalaby [20] et al 2015 In this paper duplex stainless steel grade 2205 DSS material is used. Failure of duct nozzle occurred due to poor welding practice. Nozzle was subjected to repeated welding thermal cycle. Heat input was relatively high and percentage % of austenite in the weld region above 70%.
Shugen Xu [21] et al 2014 in this paper the material of the liner is austenitic stainless steel 1Cr18Ni9 is used, discontinuous stress distribution occurred due to inter layer gap between two layer of head. Stress concentration occurred because of discontinuous structure. With increased preheating temperature, the peak residual stresses decrease in the structure. The welding heat input cause effect on the residual stresses. The welding joint as shown in figure 1.6 (a) and FEM is shown in figure 1.6(b) and the residual stress generated counters at weld joint are sawn in figure 1.6(c).

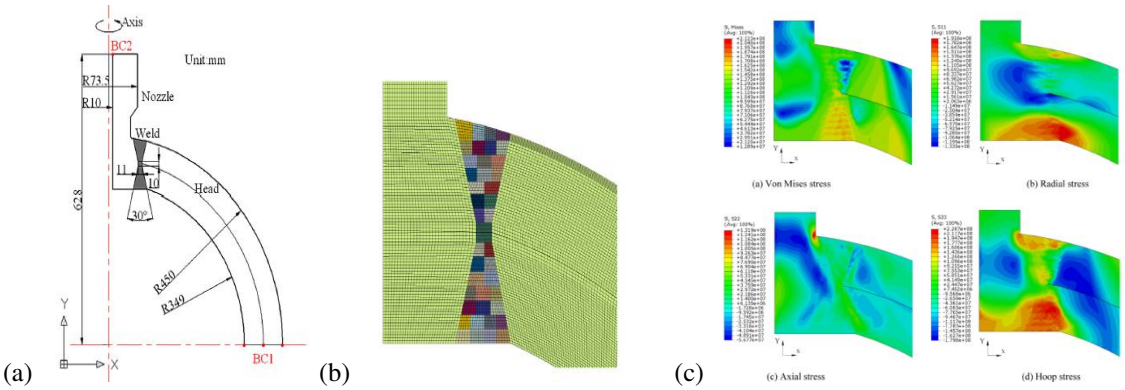

Figure1.6- (a) The geometrical model of the nozzle-to-head welding joint.(b) FEM modelling (c) The residual stress contours[21]

2.1 Finding from Literature

- There are many types of defects in weld joint cause failure of weld joint for e.g. Cracks, porosity, lake of penetration, etc. This defect can cause major problem at weld joint as well as failure of pressure vessel.
- The cracks also develop during hydrostatic pressure test due to internal pressure at nozzle location of pressure vessel.
- In pressure vessel Due to geometric discontinuities, region presents high stress concentration levels and it is where failure is more likely to occur. Due to difficulties in manufacture, these intersections are more suitable to fabrication imperfections, such as lack of weld deposition and/or weld penetration, which consequently cause crack propagation
- The simulation of weld residual stress by finite element method (FEM) can obtain the stress and deformation distribution in the structure and observed that by variation of the heat input, weld passes, groove shape, material properties and geometrical dimensions of the weld structure can decrease the residual stress.
- In many of the article author have done various experiment on various weld joints of pressure vessel and also used different FEA tool for analysis and validation purpose. Some authors have done work on various parameters of weld joints such as groove dimension and shape and observed that parametric variation also affect the residual stress at the weld joint.

Conclusion

- Design of pressure vessel is required great care because the failure of vessel in service may cause loss of life and properties. Failure in pressure vessel is occurred with many ways. Weld related failure play significant role in the design of pressure vessel. So selection of weld techniques & their joints are also important for a safe design. Welding defects are also observed at nozzle joint due to hydrotest testing of pressure vessel in industry.
- Using of flux cored electrode the depth of penetration and temperature is achieved more at weld joint.
- Many authors have done work on weld joint by changing various parameter of weld joint and reduce the amount of residual stress. For analysis FEA tool used to simulate the result of stress and deformation and reduced the amount of residual stress at weld joint location and improve the weld joint strength.

Future work

- In future for analysis of different types of weld joint will done by taking the experimental model of failure at weld joint from industry and make the model using parametric software. FEA tool will have used for analysis weld joint at the failure location and improve the weld joint strength by variation of parameter of weld groove and angle.

Acknowledgements

It is indeed a pleasure for me to express my sincere gratitude to those who have always helped me for this Dissertation work. First of all I am humbly expressing thanks to my respected guide Mr. Vijay r. Parekh for their valuable time and constant help given to me. They have been a pillar of support and inspired me throughout this study, without them this would not have been possible.

I am grateful to the teaching faculties of Mechanical Engineering Department for their valuable Suggestions and instruction regarding my work. I have also received tremendous amount of help from my friend's within and outside the institute.

References

[1] http://3.imimg.com/data3/BJ/VK/GLADMIN-148203/chemical-pressure-vessels-250x250.jpg
[2] http://image.slidesharecdn.com/pressurevessels-130216100425-phpapp02/95/pressure-vessels-9-638.jpg?cb=1361009131
[3https://upload.wikimedia.org/wikipedia/commons/6/63/Butt_Weld_Geometry.png
[4] R.s khurmi machine design, a textbook
[5] HessamoddinMoshayedi, IradjSattari-Far "The effect of welding residual stresses on brittle fracture in an internal surface cracked pipe" International Journal of Pressure Vessels and Piping vol-126-127, 29-36, pp. 2015
[6] Kamal H. Dhandha, Vishvesh J. Badheka, "Effect of activating fluxes on weld bead morphology of P91 steel bead-on-plate welds by flux assisted tungsten inert gas welding process" Journal of Manufacturing Processes vol-17, 48–57, pp. 2015
[7] Xiao-Tao Zheng, Chang-Fei Peng, Jiu-Yang Yu1 "A Unified Shakedown Assessment Method for Butt Welded Joints with Various Weld Groove Shapes"Journal of Pressure Vessel Technology Vol. 137 / 021404, 1to 8, Pp. APRIL 2015
[8] Jingqiang Yang, Qiongqi Wang, Zhongkun Wei, Kaishu Guan "Case study Weld failure analysis of 2205 duplex stainless steel nozzle" Case Studies in Engineering Failure Analysis vol-2,69–75, pp. 2014
[9] M. Clyde Zondi "Factors That Affect Welding-Induced Residual Stress and Distortions in Pressure Vessel Steels and Their Mitigation Techniques: A Review" Journal of Pressure Vessel Technology Vol. 136 / 04080,1-9, pp. AUGUST 2014
[10] Shugen Xu, Weiqiang Wang, Yinglei Chang "Using FEM to predict residual stresses in girth welding joint of layered cylindrical vessels" International Journal of Pressure Vessels and Piping vol-119, 1-7, pp.2014
[11] Yupiter H.P. Manurung, Robert NgendangLidam, M. RidzwanRahim,M. YusofZakaria, M. RidhwanRedza, M. ShaharSulaiman, GhalibTham ,Sunhaji K. Abas "Welding distortion analysis of multipass joint combination with different sequences using 3D FEM and experiment" International Journal of Pressure Vessels and Piping,vol-111-112,89-98, Pp.2013
[12] Duncan Camilleri , Norman mcpherson, Thomas G.F. Gray "The applicability of using low transformation temperature welding wire to minimize unwanted residual stresses and distortions" International Journal of Pressure Vessels and Piping, vol-110, 2-8, pp. 2013
[13] Wen-chun Jiang, Xue-wei Guan "A study of the residual stress and deformation in the welding between half-pipe jacket and shell" Materials and Design, vol-43, 213–219, pp.2013
[14] Mostafa Jafarian , S. EbrahimVahdat "A fuzzy multi-attribute approach to select the welding process at high pressure vessel manufacturing" Journal of Manufacturing Processes vol-14, 250–256, pp.2012
[15] John W. H. Price, Anna M. Pardowska,Raafat Ibrahim "Residual Stresses Evaluation in Welds and Implications for Design for Pressure Vessel Applications" Journal of Pressure Vessel Technology Vol-128 / 643, 638-642, pp. NOVEMBER 2006
[16]B. Arivazhagan∗, M. Vasudevan "Studies on A-TIG welding of 2.25Cr-1Mo (P22) steel" Journal of Manufacturing Processes vol-18,55–59,pp.2015
[17] C.R. Das, A.K. Bhaduri, S.K. Ray "Fatigue failure of a fillet welded nozzle joint" Engineering Failure Analysis vol-10,667–674, pp.2003
[18] Han-sang Lee, Jine-sung Jung, Doo-soo Kim, Keun-bong Yoo "Failure analysis on welded joints of 347H austenitic boiler tubes" Engineering Failure Analysis vol-5,413–422,pp.2015
[19] Nausheen Naz , Fawad Tariq , Rasheed Ahmed Baloch "Failure Analysis of HAZ Cracking in Low C–Cr MoV Steel Weldment" J Fail. Anal and Preven vol-9,370–379, pp.2009
[20] H.M. Shalaby , B. Al-Wakaa, N. Tanoli " Failure of large-scale pilot evaporator duct nozzle" Engineering Failure Analysis vol-57,521–527,pp.2015
[21] Shugen Xu ,Renchao Wei , Weiqiang Wang , Xuedong Chen "Residual stresses in the welding joint of the nozzle to head area of a layered high pressure hydrogen storage tank" international journal of hydrogen energy xxx(2014) 1e10.

A Review on Parametric Optimization of Electric Discharge Machining

Prof. Chintan Barelwala

Assistant Professor, Mechanical Engineering Department,Gandhinagar Institute of Technology, Moti Bhoyan, Dist. Gandhinagar.

Abstract

EDM is an unconventional electro thermal machining process used for manufacturing geometrically complex or hard material parts that are extremely difficult-to-machine by conventional machining process. The EDM process that we know today is a result of various researches carried out over the years. EDM researchers have explored a number of ways to improve the sparking efficiency with various experimental concepts.The Taguchi method has been utilized to determine the optimal EDM conditions in several industrial fields. High cost of non conventional machine tools, compared to conventional machining, has forced us to operate these machines as efficiently as possible in order to reduce production cost and to obtain the required reimbursement. This paper represents review on the parametric optimisation of Electric Discharge machining process.

Keywords: EDM, Polarity, Design of Experiments, Taguchi Method, MRR, EWR.

Nomenclature

T_{on}	spark on-time (μs)
T_{off}	spark off -time(μs)
MRR	material removal rate (mm^3/min)
EWR	electrode wear ratio
RWR	relative wear ratio
SR	surface roughness

1. Introduction

Technologically advanced industries like aeronautics, automobiles, nuclear reactors, missiles, turbines etc., requires materials like high strength temperature resistant alloys which have higher strength, corrosion resistance, toughness, and other diverse properties. With rapid development in the field of materials it has become essential to develop cutting tool materials and processes which can safely and conveniently machine such new materials for sustained productivity, high accuracy and versatility at automation. Consequently, non-traditional techniques of machining are providing effective solutions to the problem imposed by the increasing demand for high strength temperature resistant alloys, the requirement of parts with intricate and compacted shapes and materials so hard as to defy machining by conventional methods.

EDM is one of the most extensively used non-conventional material removal processes. Its unique feature of using thermal energy to machine electrically conductive parts regardless of hardness has been its distinctive advantage in the manufacture of mould, die, automotive, aerospace and surgical components. In addition, EDM does not make direct contact between the electrode and the work piece eliminating mechanical stresses, chatter and vibration problems during machining.The basic principle in EDM is the conversion of electrical energy into thermal energy through a series of discrete electrical discharges occurring between the electrode and work piece immersed in the dielectric fluid.EDM is the machining process of controlled erosion of electrically conductive materials by the rapid and repetitive spark discharge between the workpiece (anode) and the tool (cathode) separated by flooded dielectric fluid through the small gap (about 0.02 to 0.5) mm, and known as spark-gap [12]. Electrical discharge machining is a process that removes metal with good dimensional control from any soft or hard metal. It cannot be used for machining glass, ceramics or other non-conducting materials.

Electrical discharge machining (EDM) is one of the most promising advanced manufacturing processes used in industry for high-precision machining of all types of electrically conductive materials such as metals, metallic alloys, graphite, or even some conductive ceramic materials, irrespective of the hardness. It is widely used in the manufacture of mould, die, automotive, aerospace and surgical components. It is difficult to comprehend, expect and optimize EDM process performance because there are so many dependent and independent variables that have direct or indirect influence on machining efficiency, which makes it complex and difficult to model. To reduce its production cost and to improve product quality, optimization of machining processes are required. However, experimental optimization of any machining process is costly and time consuming due to the complex, coupled and

non-linear nature of the input–output variables of machining processes. Hence, many researchers have concentrated on improvement and optimization of performance measures of EDM process by using different modifications and optimization methods like Taguchi, response surface methodology, artificial neural network, genetic algorithm, grey relational analysis, fuzzy logic, factorial design etc. with variation of different electrical and non-electrical process parameters.

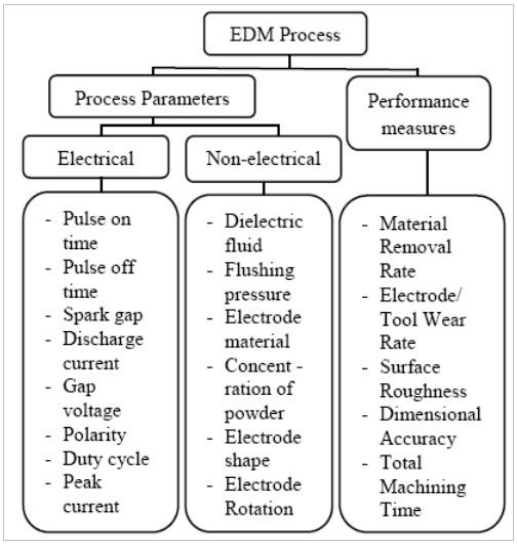

Fig-1: Process parameters and performance measures of EDM

2. Working Principle of EDM:

The machine consists of a power supply, a dielectric system; a control system with a servo-mechanism is to control the rate of feed of the quill where the tool holder is attached. The work piece is clamped on the machine table. Spark is produced between the work piece and tool electrode. The duration of spark is measured in micro second. In the spark area temperature is very high due to which there is partly melting and vaporizing of work piece and tool electrode and results in removal of material in form of craters. The System moves in different axes and the movement is controlled manually or by a computer numerical controlled system. The transistor pulse generator power supply is now commonly employed in EDM as Power supplier [13].

2.1 Details of work piece and tool material

The Work piece and tool electrode is the most critical part in the EDM. Copper is used as the electrode material because of its lower electrical and thermal resistance.

2.2 Selection of electrode materials

Graphite is the most common material because it has fair wear characteristics, is easily machinable and small flush holes can be drilled in electrodes. Copper (Cu) electrode is used as electrode material to machine their product for rough and finish machining. It is commonly used by industries, due to cheaper and produces good surface finish. Copper is highly stable material under sparking conditions and having excellent electrical and thermal conductivity. Copper is generally used for better finishes in the range of 0.5 μm R_a. Copper tungsten and silver tungsten are used for making deep holes under poor flushing conditions, especially in tungsten carbides. It offers high machining rates as well as low electrode wear. Copper graphite is good for cross section electrodes. It has better electrical conductivity than graphite, although the corner wear is higher. Brass ensures stable sparking conditions and is normally used for specialized applications such as drilling of small holes, where the high electrode wear is acceptable. Good electrode materials must be selected because it gives good surface finish, low diameter overcut, and high material removal rate (MRR) and less electrode wear when machining hardened material [14].

2.3 Selection of Dielectric System

1. Generally transformer oil, Kerosene oil is used as dielectric.
2. The dielectric must have high strength.
3. The dielectric should take minimum possible to break down when breakdown voltage is reached.
4. The dielectric should deionizer the gap as soon as spark has occurred.

5. The dielectric should be good cooling agent.
6. The dielectric should have high degree of fluidity. [15]

3. EDM Process Parameters

There are various important parameter of EDM. [2]

3.1Electrical Parameters

(a) **Spark On-time (Pulse Time or T_{on}):** The duration of time (μs) the current is allowed to flow per cycle. Material removal is directly proportional to the amount of energy applied during this on-time. This energy is really controlled by the peak current and the length of the on- time [3]. See Fig. 1.

(b) **Spark Off-time (Pause Time or T_{off}):** The duration of time (μs) between the sparks (that is to say, off-time). This time allows the molten material to solidify and to be wash out of the arc gap. This parameter is to affect the speed and the stability of the cut. Thus, if the off-time is too short, it will cause sparks to be unstable.

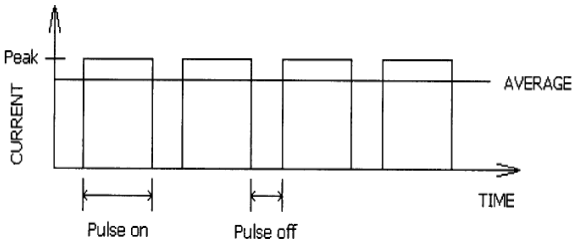

Fig.2. Typical waveform of pulse generator.

(c) **Arc gap (or gap):** The Arc gap is distance between the electrode and work piece during the process of EDM. It may be called as spark gap. Spark gap can be maintained by servo feed system. To obtain good performance and gap stability a suitable gap should be maintained.

(d) **Discharge current (current $I_{p)}$:** Discharge current is directly proportional to the Material removal rate.

(e) **Duty cycle** (t)**:** It is a percentage of the on-time relative to the total cycle time. This parameter is calculated by dividing the on-time by the total cycle time (on-time pulse off- time). It indicates the degree of efficiency of the operation.

$$\text{Duty Cycle} = \frac{T_{On}}{T_{On} + T_{Off}}$$

(f) **Voltage (V):** It is a potential that can be measure by volt it is also effect to the material removal rate and allowed to per cycle. Voltage is given by in this experiment is 50V.

(g) **Diameter of electrode (D):** It is the electrode of Cu-tube there are two different size of diameter 4mm and 6mm in this paper. This tool is used not only as an electrode but also for internal flushing.

(h) **Polarity**: It may be positive or negative connected to tool electrode or work material. Polarity can affect processing speed, finish, wear and stability of the EDM operation. It has been proved that MRR is more when the tool electrodes are connected at positive polarity(+) than at negative terminal(-) .This may be due to transfer of energy during the charging process is more in this condition of machining. When a electrical discharge is generated electrons dispatch from the negative polarity collides with neutral molecules between the work piece and electrode which is responsible for ionization process in EDM. However, ionization is taken because the electron arrives at the positive terminal of the surface.

3.1Non Electrical Parameters

Non-electrical parameters such as the Rotational movement of electrode, flushing of dielectric fluid and aspect ratio (tool shape) together play a significant role in delivering optimal performance measures. Most dielectric media are

hydrocarbon compounds and water. The hydrocarbon compounds are in the form of refined oil; better known as kerosene.

Rotation of Tool Electrode:
It is the rotational effect of cylindrical (pin shaped) or disc shaped electrode tool measured in revolution/minute. The rotational movement of electrode is normal to the work surface and with increasing the speed, a centrifugal force is generated causes more debris to remove faster from the machining zone.

Injection *flushing*:
Flushing removes eroded particles from the gap for efficient cutting and improved surface finish of machined material. Flushing also enables fresh dielectric oil flow into the gap and cools both the electrode and the work piece. Basic characteristics required for dielectric used in EDM are high dielectric strength and quick recovery after breakdown.

Tool Geometry*:*
Tool geometry is concerned with the shape of the tool electrodes. i.e, square, rectangle, cylindrical, circular.etc. The ratio of length /diameter of any shaped feature of material. In case of rotating disk electrode the ratio becomes thickness/diameter.

Tool *Material (Electrode)*:
Engineering materials having higher thermal conductivity and melting point are used as a tool material for EDM process of machining. Copper, graphite, copper-tungsten, silver tungsten, copper graphite and brass are used as a tool material (electrode) in EDM. They all have good wear characteristics, better conductivity, and better sparking conditions for machining. Copper with 5% tellurium, added for better machining properties. Tungsten resist wear better than copper and brass .Brass ensures stable sparking conditions and is normally used for specialized applications such as drilling of small holes where the high electrode wear is acceptable. The factors that affect selection of electrode material include metal removal rate, wear resistance, desired surface finish, cost of electrode material manufacture and material and characteristics of work material to be machined.

4. Planning Phase:

In this phase following things are to be planned for the experiment.
I. Selection of process variables and there levels for EDM.
II. Design of experiment (DOE).
III. Selection of work piece material.

5. Experimentation:

Experiments were conducted according to Taguchi method by using the machining set up. The control parameters like diameter of electrode (D) , discharge current (I_p) and pulse duration (T_{on}) conductivity were varied to conduct different experiments and the weights of the work piece and Tool and dimensional measurements of the cavity are taken for calculation of MRR , EWR. The experiments were conducted under various parameters setting of Discharge Current (I_p), Pulse On-Time (T_{on}), and diameter of the tool. Flow chart of Experiment for MRR, TWR and surface roughness (SR) is shown in Fig 2.

5.1 *Design of Experiment:*

Design of Experiment (DOE) is to find the optimal settings of process parameters in order to identify the most influential factors, and minimize process variability and the effects of uncontrollable factors. The machining process in the EDM depends on various parameters. These parameters are divided into two groups of input and output parameters. The input parameters could be on-line or off-line. To optimize the output parameters, the on-line parameters can be controlled or changed. The off-line parameters can only be adjusted before the start of machining operation. The spark current, pulse on time, circuit voltage, tool polarity, tool material, type of Di-electric and the flushing method are some of the important input parameters that are regulated prior to machining. The input parameters during machining include the pulse off time, gap between tool and work-piece and flushing. The off-line output parameters that constitute the main results of the process include the MRR, surface roughness and tool wear [3].

The design of experiments technique is a very powerful tool, which permits to carry out the modeling and analysis of the influence of process variables on the response variables. Improving the MRR and surface quality are still challenging problem that restrict the expanded application of the technology. Semi-empirical models of MRR for various work piece and tool electrode combinations have been presented by various researchers. The influence of pulse current, pulse time, duty cycle, open circuit voltage and dielectric flushing pressure over the MRR and surface roughness on tool have also been studied.

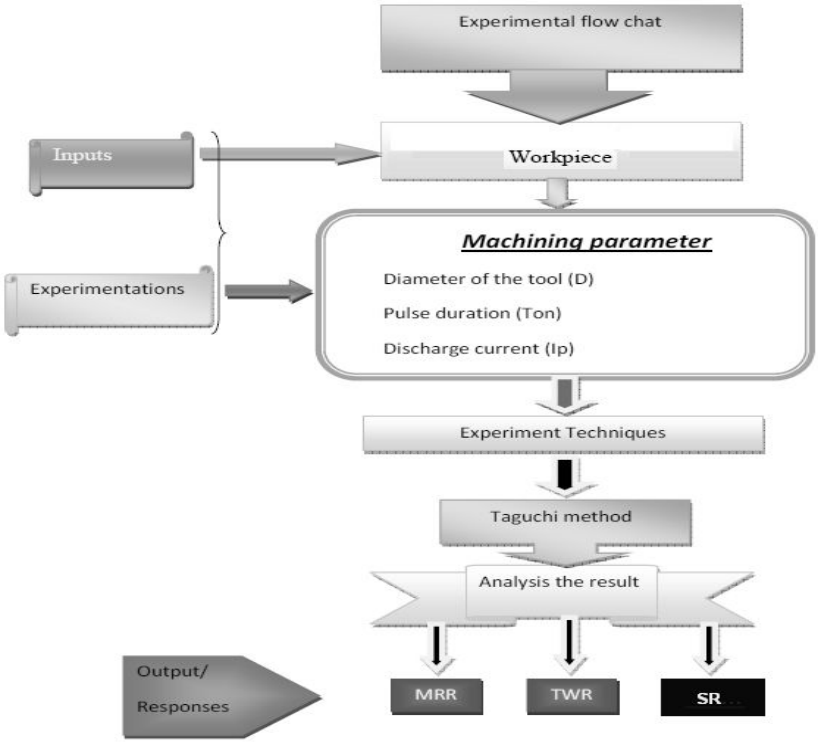

Fig. 3. Flow chart of Experiment.

5.2 *Taguchi Method:*

Dr. Genichi Taguchi is regarded as the foremost proponent of robust parameter design, which is an engineering method for product or process design that focuses on minimizing variation and/or sensitivity to noise. When used properly, Taguchi designs provide a powerful and efficient method for designing products that operate consistently and optimally over a variety of conditions. Taguchi proposed several approaches to experimental designs that are sometimes called "Taguchi Methods." These methods utilize two-, three-, four-, five-, and mixed-level fractional factorial designs. Taguchi refers to experimental design as "off-line quality control" because it is a method of ensuring good performance in the design stage of products or processes. [4]

MINITAB provides both static and dynamic response experiments in a static response experiment; the quality characteristic of interest has a fixed level. The goal of robust experimentation is to find an optimal combination of control factor settings that achieve robustness against (insensitivity to) noise factors. MINITAB calculates response tables and generates main effects and interaction plots for:-

- Signal-to-noise ratios (S/N ratios) vs. the control factors.
- Means (static design) vs. the control factors.

5.3 Signal-to-noise Ratio:

Classical experimental design methods are too complex and not easy to use. Furthermore, a large number of experiments have to be carried out as the number of the process parameters increases. To solve this important task, the Taguchi method uses a special design of orthogonal array to study the entire parameter space with only a small number of experiments. The experimental results are then transformed into a signal-to-noise (S/N) ratio. The S/N ratio can be used to measure the deviation of the performance characteristics from the desired values. The categories

of performance characteristics in the analysis of the S/N ratio depend upon output parameters to be controlled. Generally, there are three categories of quality characteristic in the analysis of the S/N ratio, i.e. smaller-is-better, larger-is-better, and nominal-is better.

Author selected two categories which are as follows.

- The lower-the-better for EWR & ROC.
- The higher-the-better for MRR.

6. Material Removal Rate (MRR) & Electrode Wear Rate (EWR):

Material removal rate denotes the volume of material removed from the work piece in unit time. MRR depends on various properties of the work piece material, including its melting point and latent heat. It is also influenced by the properties of tool electrodes and by geometric factors such as the shape and dimensions of the tool and work piece. For a specific work piece and for a tool with a defined polarity and constant Di-electric, the MRR depends on the spark current, pulse on time and pulse off time. Figure 3 shows material removal rate versus voltage, spark current, pulse on time and pulse off time.

The material MRR is expressed as the ratio of the difference of weight of the work piece before and after machining to the machining time and density of the material. The parameter MRR is selected as response variable, which refers to the machining efficiency of the EDM process and defined as follows:

$$\text{MRR} = \frac{W_i - W_f}{t \times \rho}$$

Where, W_i = Weight of work piece before machining. (gms), W_f = Weight of work piece after machining.(gms), t = Machining time in minutes, ρ = Density of work piece material. The work piece is weighed before and after each experiment using an electric balance to determine the value of MRR. For efficient evolution of the EDM process, the larger MRR is regarded as the best machining performance.

Electrode or tool wear (EWR) is an important factor because if affects dimensional accuracy and the shape produced. Tool wear is related to the melting point of the materials. EWR is affected by the precipitation of carbon from the hydrocarbon dielectric on the electrode surface during sparking. EWR is expressed as the ratio of the difference of weight of the tool before and after machining to the machining time.

$$\text{EWR} = \frac{W_i - W_f}{t}$$

Where, W_i = Weight of work piece before machining.(gms), W_f = Weight of work piece after machining.(gms), t = Machining time in minutes.

7. Major areas of Research in EDM

A large no of papers have been studied on ways of yielding optimal EDM performance like high MRR and low tool wear rate. Modeling and optimization of various electrical and non electrical parameters in EDM could be done to improve precision machining of work materials. Ho and Newman (2003) have classified research areas in EDM machining process as shown in the Fig. 3 [1].

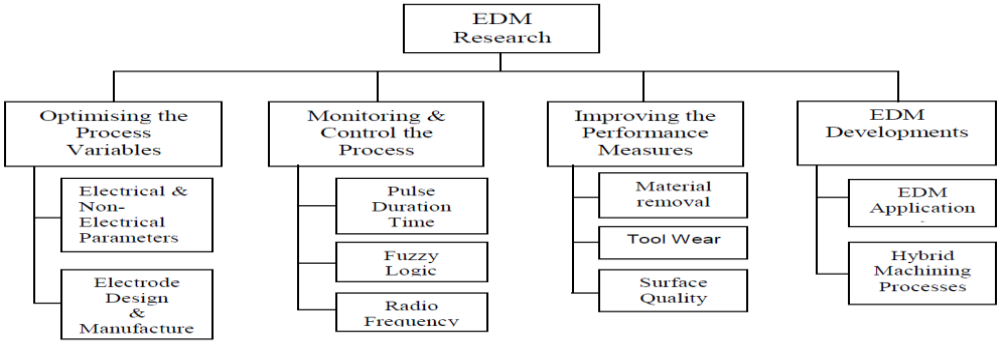

Fig. 4. Classification of major EDM research areas.

The correct selection of manufacturing conditions is one of the most important aspects to take into consideration in the majority of manufacturing processes and, particularly, in processes related to Electrical Discharge Machining (EDM). It is a capable of machining geometrically complex or hard material components, that are precise and difficult-to-machine such as heat treated tool steels, composites, super alloys, ceramics, carbides, heat resistant steels etc. being widely used in die and mold making industries, aerospace, aeronautics and nuclear industries.

In EDM, for optimum machining performance measures, it is an important task to select proper combination of machining parameters. Generally, the machining parameters are selected on the basis of operator's experience or data provided by the EDM manufactures. When such information is used during EDM, the machining performance is not consistent. Data provided by the manufacturers regarding the parameter settings is useful only for most commonly used steels. Such data is not available for special materials like Maraging steels, ceramics, and composites. For these materials, experimental optimization of performance measures is essential. Optimization of EDM process parameters becomes difficult due to more number of machining variables. Slight changes in a single parameter significantly affect the process. Thus, it is essential to understand the influence of various factors on EDM process. Analytical and statistical methods are used to select best combination of process parameters for an optimum machining performance.

Mohd Amri Lajis, H.C.D. Mohd Radzi and A.K.M. Nurul Amin [6] have discussed the feasibility of machining Tungsten Carbide ceramics by EDM with a graphite electrode [6]. Taguchi method has been used to determine the main effects, significant factors and optimum machining condition to the performance of EDM. In this study, all the analysis based on the taguchi method is done by Taguchi DOE software (Qualitek- 4) to determine the main effects of the process parameters, to perform the analysis of variance (ANOVA) and to establish the optimum conditions. Fig. 4 shows the main effects of MRR of each factor (machining voltage V, peak current P, pulse duration A & interval time B) for various level condition. It was observed the MRR increases with pulse duration and slightly increases with peak current. According to Fig. 5, the EWR decreases with the two major parameters, P and B. And also we notice that minimum machining voltage (negative polarity), maximum peak current, minimum pulse duration and maximum interval time may imply a smaller EWR. The results presented that, the peak current of EDM mainly affects the EWR and SR. The pulse duration largely affects the MRR.

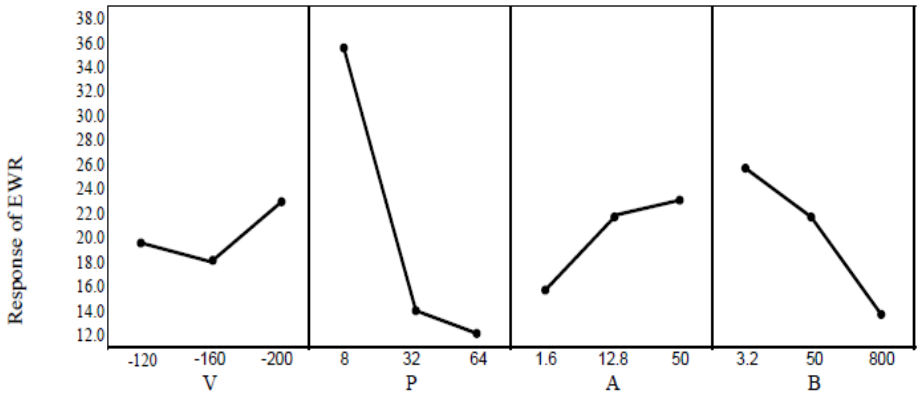

Fig. 5. Main effects of each factor on EWR.

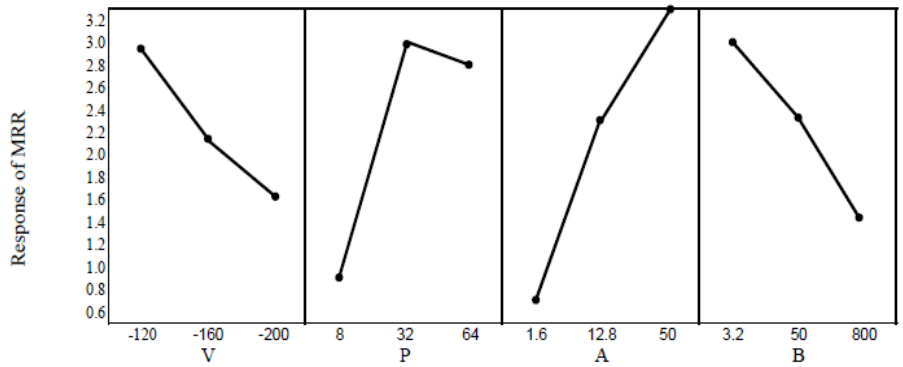

Fig. 6. Main effects of each factor on MRR.

Saeed Daneshmand, Ehsan Farahmand Kahrizi, Mehrdad Mortazavi Ghahi [7] investigated the impacts of the input parameters of the EDM process including the discharge current, pulse on time, pulse off time and voltage on the output machining parameters of NiTi shape memory alloy obtained by using brass tools and De-ionized water by using the Taguchi method. [4] For the design of experiments, the Taguchi's method and theLI8 orthogonal array were employed. The experimental results indicate that the increase of discharge current and voltage causes the pulse energy to increase and as a result, the material removal rate and tool wear increase. With the increase of voltage, relative electrode wear increases and consequently, material removal rate diminishes. With the increase of discharge current and pulse on time, relative electrode wear decreases and as a result, material removal goes up. With the increase of voltage, discharge current and pulse on time, spark energy builds up and causes the surface roughness of NiTi60 SMA to increase. Fig.6 illustrates the impacts of input parameters of the machining process including the discharge current, voltage, pulse on time and pulse off time on tool wear for the NiTi60 shape memory alloy.

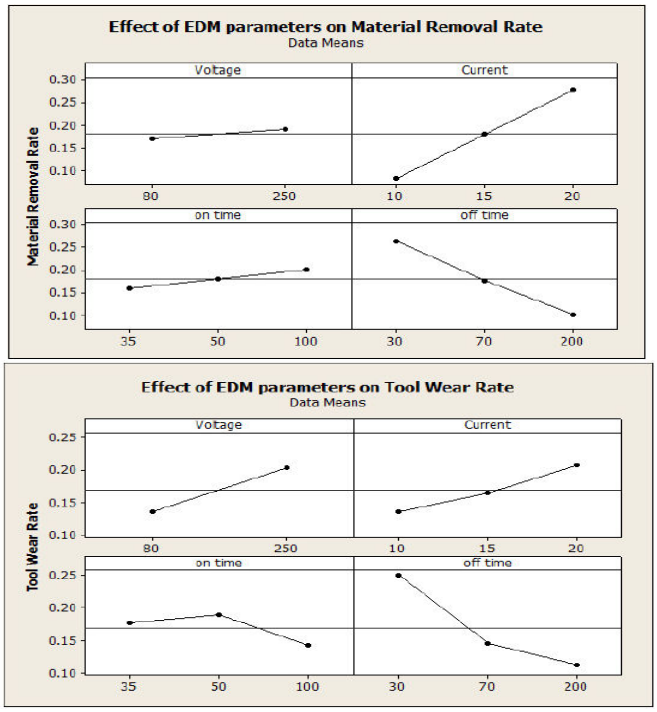

Fig. 7. Variation of MRR & TWR with pulse-on-time, pulse-off-time, discharge current and gap voltage.

Prof. S.R.Nipanikar has used EDM for cutting of D3 Steel material with a copper electrode. He used Taguchi L9 orthogonal matrix experiment and found that the material removal rate (MRR) mainly affected by peak current (Ip). Duty cycle (t) has least effect on it. The electrode wear rate (EWR) is mainly influenced by peak current (Ip). The effect of gap voltage (Vg) is less on EWR and has least effect on it. Peak current (Ip) have the maximum effect on the radial overcut (ROC). The gap voltage (Vg) has least effect on it.

A. M. Nikalje & A. Kumar & K. V. Sai Srinadh [8] investigated the influence of the process parameters and optimization of MDN 300 steel in the die sinking EDM by using Taguchi method. Maraging steel (MDN 300) exhibits high levels of strength and hardness. From ANOVA, discharge current is more significant than pulse on time for MRR and TWR; whereas pulse on time is more significant than discharge current for RWR and SR. Detailed analysis of structural features of machined surface was done by using scanning electron microscope (SEM) to understand the influence of parameters. Surface morphological study indicates that at higher discharge current and longer pulse on duration gives rougher surface characteristics with more craters, globules of debris, and micro cracks than that of lower discharge current and lower pulse on duration.

Amit Joshi & Pradeep Kothiyal [9] have tried to investigate effect of machining parameter such as discharge current, pulse on time, and pulse of time on MRR in EDM while machining OHNS-EN-31 STEEL using Cu tool. A well-designed experimental scheme was used to reduce the total number of experiments. Parts of the experiment

were conducted with the L18 orthogonal array based on the Taguchi method. The results of analysis of variance (ANOVA) indicate that the proposed mathematical model can be adequately describing the performance within the limit of factors being studied. The optimal set of process parameters has also been predicted to maximize the MRR. Theyfound that MRR increases with increase of D.C. MRR first increases and then after getting a peak value it decreases with increase of T_{on}. MRR increases partially and then decreases with increase of T_{off}.

8. Conclusion

After a detailed analysis of the literature, the following conclusions can be drawn.

- Various approaches like powder additives, different dielectric fluid, tool-workpiece rotation, vibration, cryogenic cooling of electrode, different tool material, etc. have been used by different researchers for improvement in EDM process performance.
- It is also found that most of the research work has been carried out on improvement and optimization of same performance measures like MRR, EWR, Surface roughness for different materials, but some performance measures like power consumption, dimensional deviation, hardness, etc. are either not much focused or not focused yet. So, this area is yet to be explored more.
- Optimization of performance measures is essential for effective machining. Taguchi method, used to determine the influence of process parameters and optimization of electrical discharge machining (EDM) performance measures.
- When assigning process tolerances for EDM all aspects of the process, such as type of electrode, type of dielectric and duration of the operation, should be considered. All these activities may give errors, which should be taken into account.

9. Future Scope

Further research on EDM could be done in the following direction:

- The mathematical model can be developed different work piece and electrode materials for EDM processes.
- Responses like roundness, circularity, cylindricity, machining cost etc .are to be considered in further research.
- The standard optimization procedure can be developed and the optimal results are to be validated.
- To remain competitive as a micro-manufacturing technology, EDM process should use computer numerical control. This should make the new strategy attractive to industry.

References

[1] K.H. Ho, S.T. Newman., 2003. “State of the art electrical discharge machining (EDM)”,International Journal of Machine Tools &Manufacture, 43, p.1287–1300.

[2] Anand Pandey,Shankar Singh., 2010. “Current research trends in variants of Electrical Discharge Machining: A review”, International Journal of Engineering Science and Technology, 2 (6), p. 2172-2191.

[3] Mohit Tiwari, Kuwar Mausam, Kamal Sharma, Ravindra Pratap Singh., “Experimental Analysis of Electro-Discharge Machining Parameters for Minimum Tool Wear Rate on Machinability of Carbon Fiber/Epoxy Composites Using Taguchi Method”, International Journal of Engineering Research & Technology, 2(10), p. 3182-3188.

[4] Vikas, Apurba Kumar Roy, Kaushik Kumar., 2013. “Effect and Optimization of Machine Process Parameters on Material Removal Rate in EDM for EN41 Material Using Taguchi”, International Journal of Mechanical Engineering and Computer Applications, 1 (5), 35-39.

[5] Mohd Amri Lajis, H.C.D. Mohd Radzi, A.K.M. Nurul Amin, 2009. The Implementation of Taguchi Method on EDM Process of Tungsten Carbide. European Journal of Scientific Research. 26 (4), p. 609-617.

[6] Saeed Daneshmand, Ehsan Farahmand Kahrizi, Mehrdad Mortazavi Ghahi, 2012. Investigation of EDM Parameters on Surface Roughness and Material Removal Rate of NiTi60 Shape Memory Alloys. Australian Journal of Basic and Applied Sciences, 6(12), p. 218-225.

[7] Prof. S.R.Nipanikar, 2012. Parameter optimization of electro discharge machining of AISI D3 steel material by using taguchi method. Journal of Engineering Research and Studies, 3(3), p. 07-10.

[8] A. M. Nikalje & A. Kumar & K. V. Sai Srinadh. 2013. Influence of parameters and optimization of EDM performance measures on MDN 300 steel using Taguchi method. Int Journal of Advanced Manufacturing & Technology, 69, p. 41–49.

[9] Amit Joshi, Pradeep Kothiyal, 2012. International Journal on Theoretical and Applied Research in Mechanical Engineering, 1 (2), p. 54-59.

[10] Anand Pandey,Shankar Singh, 2010. International Journal of Engineering Science and Technology, 2 (6), p. 2172-2191.

[11] Singaram Lakshmanan, Mahesh Kumar, 2013. Optimization of EDM parameters using Response Surface Methodology for EN31 Tool Steel Machining. International Journal of Engineering Science and Innovative Technology, 2(5), p. 64-71.

[12] R.K.Jain., 2012. Production Technology, Khanna Publishers.

[13] P.C.Sharma., 2007. A Textbook of Production Technology: Manufacturing Processes, S Chand & Co. Ltd.

[14] Hassan Abdel-Gawad El-Hofy., 2007. Fundamentals of Machining Processes: Conventional and Nonconventional Processes, CRC Press, Taylor & Francis Group.

[15] Prof. P.C. Pandey & Prof. C.K. Singh., 2006.Production Engineering Sciences, Standard Publishers Distributors.

A review on Investigate the operational parameters for joining of dissimilar polymer using ultrasonic welding

Shreyas Patel[a],Khushbu Patel[b],Akash Pandey[c]
[a]*ME(AMS)SVMIT, Bharuch,392001,India*
,[b]*Asistant Professor Mech SVMIT, Bharuch,392001,india*
[c]*Assistant Professor Mech M.S University Baroda,390005,India*

Abstract
Ultrasonic plastic welding has received significant attention in the last few years, and has become more reliable and suitable for a wide range of applications. There are number of advantages for ultrasonic plastic welding, including greater efficiency and speed, longer tool life, higher accuracy and no filler or flux needed to be used. Thus the technique can be viewed as being environmental friendly.The main objectives of this study is to investigate and evaluate the effect of different ultrasonic welding parameters (amplitude, pressure, weld time and thickness ratio) on Welding tensile strength of different two thermoplastic (HDPE, PP) materials. Literature review has been done on The effect of Different Parameter and its Effect on The Strength of The joint of Metal Sheet So Trying and investigate about the effect of different parameter on the strength of dissimilar thermoplastic material. Design of conical horn has been done using the COMPUTER AIDED RESONATOR DESIGN software.

Keywords: Ultrasonic, welding joint ,Tensile Strength.

Nomenclature	
HDPE	High density polyethylene
PP	Polypropylene
CARD	Computer aided resonator design

1 Introduction

Ultrasonic plastic welding is the joining or reforming of thermoplastics through the utilize of heat generated from high-frequency mechanical motion. It is accomplished by converting high-frequency electrical energy into high-frequency mechanical motion. That mechanical motion, along with applied force, generates frictional heat at the plastic components' mating surfaces (joint area) so the plastic material getting melt and form a molecular bond between the parts.

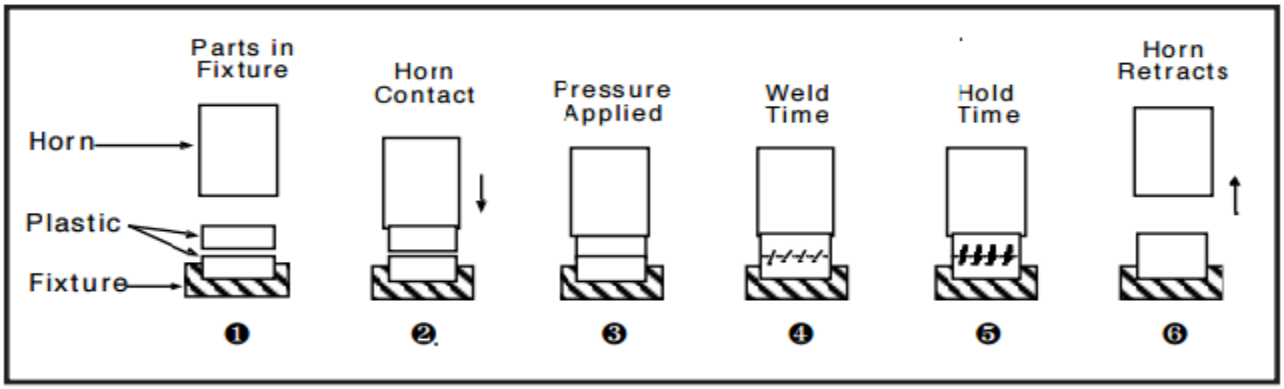

Figure 1.1 Ultrasonic welding, (1) Parts in Fixture, (2) Horn Contact, (3) Pressure Applied , (4) Weld Time, (5) Hold Time, (6) Horn Retracts

1.1Basic Principal

As shown in fig1.1 the basic principle of ultrasonic assembly involves conversion of high-frequency electrical energy to high-frequency mechanical energy in the form of reciprocating vertical motion, which, when applied to a thermoplastic, can generate frictional heat at the plastic/plastic or plastic/metal interface. In ultrasonic welding, this frictional heat melts the plastic, allowing the two surfaces to fuse together; in ultrasonic staking, forming or insertion, the controlled flow of the molten plastic is used to capture or retain another component in place (staking)

or encapsulate a metal insert.

1.2 Near-Field / Far-Field Welding

Near-field welding refers to welding a joint located 1/4 inch(6 mm) or less from the area of horn contact; while far-field welding refers to welding a joint located more that 1/4 inch (6 mm) from the horn contact area. The greater the distance from the point of horn contact to the joint, the more difficult it will be for the vibration to travel through the material, and for the welding process to take place.

1.3 Components

- A press to put the two parts to be assembled under pressure
- A nest or anvil where the parts are placed and allowing the high frequency vibration to be directed to the interfaces
- An ultrasonic stack composed of a converter or piezoelectric transducer, an optional booster and a sonotrode (US: Horn). All three elements of the stack are specifically tuned to resonate at the same exact ultrasonic frequency (Typically 20, 30, 35 or 40 kHz)
- Converter: Converts the electrical signal into a mechanical vibration
- Booster: Modifies the amplitude of the vibration. It is also used in standard systems to clamp the stack in the press.
- Sonotrode: Applies the mechanical vibration to the parts to be welded.
- An electronic ultrasonic generator (US: Power supply) delivering a high power AC signal with frequency matching the resonance frequency of the stack.
- A controller controlling the movement of the press and the delivery of the ultrasonic energy.

1.4 Thermoplastics

When classified by chemical structure, there are two generally recognized classes of plastic materials: Thermosets, having cross-linked molecular chains and Thermoplastics, which are made up of linear molecular chains. There are two types of thermoplastic polymers: Crystalline and Amorphous.

1.4.1 Crystalline Polymers

Crystallinity is indication of amount of crystalline region in polymer with respect to amorphous content. So while selecting polymer for required Application its crystallinity plays foremost role. When polymers extruded through the spinneret, the molecules orient themselves in the direction of the extruded melt.

- Have a relatively sharp melting point.
- Have an ordered arrangement of molecule chains.
- Generally require higher temperatures to flow well when compared to Amorphous.
- Reinforcement with fibers increases the load-bearing capabilities considerably.
- Shrink more than Amorphous, causing a greater tendency for war page.
- Fiber reinforcement significantly decreases war page.
- Usually produce opaque parts due to their molecular structure.

1.4.2 Amorphous Polymers

A parameter of particular interest in synthetic polymer manufacturing is the glass transition temperature (T_g), at which amorphous polymers undergo a transition from a rubbery, viscous liquid, to a brittle, glassy amorphous solid on cooling.

- Have no true melting point and soften gradually.
- Have a random orientation of molecules; chains can lie in any direction.
- Do not flow as easily in a mould as Crystalline Polymers.
- Shrink less than Crystalline Polymers.
- Generally yield transparent, water-clear parts.

1.4.3 The Performance And Cost Illustration

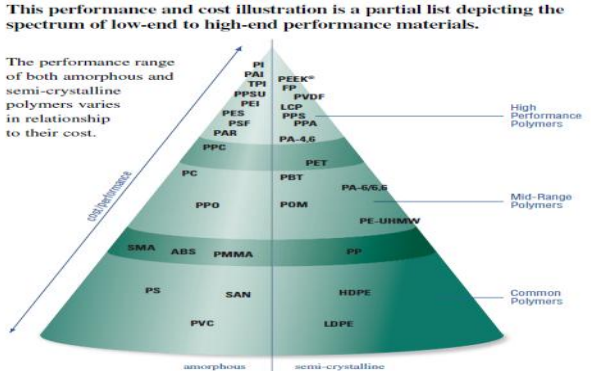

Abbreviation	
ABS	acrylonitrilebutadienestyrene
FP	fluoropolymers
HDPE	high density polyethylene
LCP	liquid crystal polymers
LDPE	low density polyethylene
PA-4,6	polyamide-4,6
PA-6/6,6	polyamide-6/6,6
PAI	**polyamideimide (Torlon®)**
PAR	polyarylate
PBT	polybutylene terephthalate
PC	polycarbonate
PE-UHMW	ultrahigh molecular weight polyethylene
PEEK®	**polyetheretherketone**
PEI	polyetherimide
PES	polyethersulfone
PET	polyethylene terephthalate
PI	**polyimide (Aurum®)**
PMMA	polymethyl methacrylate
POM	polyoxymethylene (also polyacetal)
PP	polypropylene
PPA	polyphthalamide
PPC	polyphthalate carbonate
PPO	polyphenylene oxide
PPS	polyphenylene sulfide
PPSU	polyphenylsulfone
PS	polystyrene
PSF	polysulfone
PVC	polyvinyl chloride
PVDF	polyvinylidene fluoride
SAN	styrene acrylonitrile
SMA	styrene maleic anhydride
TPI	thermoplastic polyimide

Figure 1.2 Performance And Cost Illustration

1.5 HDPE (HIGH DENSITY POLYETHYLENE)

High-density polyethylene (HDPE) or polyethylene high-density (PEHD) is a polyethylene thermoplastic made from petroleum. It is sometimes called "alkathene" or "polythene" when used for pipes. With a high strength-to-density ratio, HDPE is used in the production of plastic bottles, corrosion-resistant piping, geo-membranes, and plastic lumber. Property of hdpe as shown in table 1.5.1

1.5.1 Properties

Table no 1.5.1

Physical Property	Value
Tensile strength	0.20-0.40 N/mm^2
Notched impact strength	No break Kj/m^2
Thermal coefficient of expansion	100-220 x 10^{-6}
Max. Continued Used temp.	65^{0}C (149 ^{0}F)
Melting point	120 ^{0} -180 ^{0}C (320 ^{0}F)
Density	0.93-0.97 g/cm^3

1.6 Polypropylene

Polypropylene (PP), also known as polypropene, is a thermoplastic polymer used in a wide variety of applications including packaging and labelling, textiles (e.g., ropes, thermal underwear and carpets), stationery, plastic parts and reusable containers of various types, laboratory equipment, loudspeakers, automotive components, and polymer banknotes. An addition polymer made from the monomer propylene, it is rugged and unusually resistant to many chemical solvents, bases and acids. Property of pp as shown in table 1.6.1

1.6.1 Properties

Table no 1.6.1

Physical Property	Value
Tensile strength	0.95 – 1.30 N/mm^2
Notched impact strength	3.0-30.0 Kj/m^2
Thermal coefficient of expansion	100-150 x 10^{-6}
Max. Continued Used temp.	80^{0}C (176 ^{0}F)
Melting point	160^{0}C (320 ^{0}F)
Density	0.905 g/cm^3

1.7 Application of ultrasonic in thermoplastic

The applications of ultrasonic welding are extensive and are found in many industries including electrical and

computer, automotive and aerospace, medical, and packaging. Whether two items can be ultrasonically welded is determined by their thickness. If they are too thick this process will not join them. This is the main obstacle in the welding of metals. However, wires, microcircuit connections, sheet metal, foils, ribbons and meshes are often joined using ultrasonic welding. Ultrasonic welding is a very popular technique for bonding thermoplastics. It is fast and easily automated with weld times often below one second and there is no ventilation system required to remove heat or exhaust. This type of welding is often used to build assemblies that are too small, too complex, or too delicate for more common welding techniques.

(1) Extensively used in the appliance industry for assembling, toys, pumps, particulate-filled soap dispensers, and packing. ex. mecasonic uk ltd
(2) Automotive applications include all-plastic automotive bumper, headlight, taillight, instrument panel assemblies, gasoline reservoirs, dash-and-trim components, air conditioning and heater ducts etc.
(3) Manufacturing of the automotive air intake manifold. The manifold is made in two or three injection moulded parts and linear vibration welding is used to assemble the final manifold.
(4) Widely used in making high quality joints in polyethylene (PE) gas distribution pipes.

1.7 Advantages

- Fast, economical and easily automated.
- Mass production, up to 60 parts per minute is possible.
- Increased flexibility and versatility
- Possibility to join large structures.
- Used in health care industries due to clean welds.
- Produce the high strength joints consistently.

1.8 Disadvantages

- Large joints (>250 x 300 mm) cannot be welded in a single operation.
- Specifically designed joints are required.
- Ultrasonic vibrations can damage electric components.
- Tooling costs for fixtures are high.

1.9 CARD (Computer Aided Resonator Design)

Computer Aided Resonator Design (CARD) is software that applies quantitative techniques to the design of ultrasonic resonators (horns, boosters, and transducers) that vibrate in a longitudinal mode. CARD provides assistance in the design of resonators having low-to moderate complexity.

With CARD, alternative resonator designs can be quickly evaluated without machining and testing. The effects of proposed resonator modifications can be easily determined. CARD is especially useful for designing low-stress resonators, resonators with a specified gain, and resonators with a specified node location. CARD automatically tunes the horn to the desired frequency by adjusting the resonator dimensions. The adjustable dimensions include the length, thickness or diameter, and location of a transition radius. In addition, CARD can automatically adjust the gain and minimize the stress.

CARD calculates numerous acoustic parameters, including tuned length, tuned frequency, gain, node location, maximum stress, stored energy, loss, overall quality factor (Q), and weight. When calculating the stress, CARD considers the effect of stress concentrations at radii and slot ends. CARD graphically displays the calculated amplitude, stress, and strain loss distributions at each point along the length of the resonator.

The resonator shape can be graphically displayed to verify its correctness. The resonator can be composed of multiple, user-defined materials. The resonator can have a cavity in the face and can have studs, wrench flats, and spanner wrench holes. CARD allows up to 10 different user-defined materials and ultrasonic equipment configurations. These defaults can be saved to disk. CARD is very easy to learn and use, so that even those with minimum computer experience should have little difficulty. All user input is from menus; there are no commands to memorize. From any menu within CARD, a single key press will change between metric and English units. Extensive hypertext help is available for each menu option. Also included with the help is a glossary of over 300 acoustic terms. (Note: although CARD is very easy to use, the user must have some understanding of resonator design in order to evaluate the computer-generated output.)

Except for flatted-cylindrical horns (above), CARD cannot be used for resonators whose cross-sectional shape changes along the length of the resonator. Thus, for example, if a resonator has a rectangular cross section, then this

cross-sectional shape must continue along the entire resonator length. Although the cross-sectional shape cannot change, the cross sectional dimensions can be adjusted as desired. Note that certain non symmetric entities (e.g., wrench flats and spanner holes) are permitted. CARD cannot be used on bar horns with risers on the back.

2 Literature survey

Anahi et al [1] studied on welding technologies for thermoplastic composites in aerospace applications. Joining plays an important role in manufacturing of composite structures in marine, automotive, and aerospace industry. He examined different welding techniques such as ultrasonic welding, induction welding, microwave welding, resistance welding, hot plate welding, and laser welding, for joining of thermoplastic composite laminates devised for structural aerospace applications. Fusion bonding methods present a huge potential for volume intensive applications in which short processing cycles are necessary. These bonding processes offer additional advantages including reduced surface preparation requirements, reprocessing, recyclability, and improved integrity/ durability. Microwave heating is still under development stage and there are no currently reported industrial applications. One disadvantage of microwave energy only homogeneous material heating is possible with simple geometries.

M. Roopa Rani and R. Rudramoorthy [2] (2012) studied that The tensile strength of joint using the different horn profile, they using the finite element analysis using simulation for the ABS sheet material and aluminium horn material. in this paper Power of USW machine, frequency, material of sheet, field, weld time, hold time, weld pressure, collapse as input parameter and measure the Modelled and experimental temperatures for different horn profiles.

Hoseinlaghab, S. et al (2014) [3] studied the weld quality and creep resistant of samples decreases with increasing tool tilt angle. It means that using a tool with 0 ° tilt angle is recommended, in this HDPE as a material as sheet is used. Work is to study the effects of rotational speed, traverse speed, geometry and tilt angle of the tool on the quality and creep behaviour of friction stir welded HDPE plates. In this paper they use Trial and error method. The weld quality and creep resistant of samples decreases with increasing tool tilt angle. It means that using a tool with 0 ° tilt angle is recommended. Results showed that pins with the cylindrical geometry are preferred in comparison to pins with conical geometry. Also, it was observed that the pin geometry is relatively independent of welding parameters.

Irene Fernandez Villegas & Pablo Vizcaino Rubio (2015) [4] studied carbon-fiber (CF) reinforced polyether-ether ketone (PEEK) with CF/epoxy take as sheet material. And measure the welding surface edge by wary the heating time by FTIR and fractography analysis method. Heating time is input parameter and welding surface parameter is output parameter. They conclude that, in high-temperature welding of thermoplastic and thermoset composites, keeping the heating time well under 1 s is of vital importance to prevent thermal degradation of the thermoset composite. Such short heating times, only offered by ultra-fast welding techniques such as ultrasonic welding, are able to turn a thin thermoplastic coating layer into the most efficient heat shield and hence can provide a solution for the welding of virtually any thermoset/thermoplastic composite material combination.

S.Elangovan et al (2008) [5] studied that In ultrasonic welding, high frequency vibrations are combined with pressure to join two materials together quickly and securely, without producing significant amount of heat. During ultrasonic welding of sheet metal, normal and shear forces act on the parts to be welded and the weld interface. In this study a model for the temperature distribution during welding and stress distribution in the horn and welded joints are presented. With the knowledge of the forces that act at the interface it is possible to control weld strength and avoid sonotrode welding. The presented finite element model is capable of predicting the interface temperature and stress distribution during welding and their influences in the work piece, sonotrode and anvil. The study also included the effect of clamping forces, material thickness and coefficient of friction during heat generation at the weld interface.

D. Stavrov and H.E.N. Bersee (2004) [6] studied an extensive overview of resistance welding of thermoplastic composites. The objective is to provide a deeper insight into the nature of the resistance welding process and a summary of the vast experimental investigative effort put into it over the years. The main focus is set on the parameters that govern the welding process and the principal phenomena that affect the quality of the joint. The standard experimental procedure, the experimental set-up and the main evaluation methods are also looked at in detail. several alternative resistance welding methods that involve non-thermoplastic materials and offer possibilities

for future applications.
Resistance welding has proven to deservedly hold its place in the group of the fusion joining methods with greatest potential. Its numerous advantages with respect to the traditional joining techniques and the other fusion bonding methods make it very attractive for joining composite parts.

Fernandez et al [7] studied the visual and microscope method for analysis the part. They also studied the influence of the shape of the energy director on the performance of the weld. This paper presents an experimental study on the influence of several configurations of energy directors in the quality and the mechanical performance of the weld. In first place, the effect of the direction of the energy director with respect to the load direction was investigated. Secondly, attention was paid to the effect of the size and distribution of multiple energy directors. Influence of the energy director on the strength and the quality of the weld was investigated from two different points of view, the influence of the orientation of the energy director and influence of the multiple energy director.

Rashiqah Rashli et al (2013) [8] studied analysis of different parameters on the strength of welding. In this paper take the weld time, hold time, Frequency, amplitude and check the its effect on strength of weld joint. also describe the energy director effect on joint and function of energy director as the weld pressure, weld time, hold time, amplitude increase the strength is also increase. They conclude that ultrasonic welding has proven to be a suitable technology in joining especially on thermoplastic composites. A number of studies that have been done clearly showed the performance of ultrasonic welding for application in thermoplastic composites.

Negin Amanat et al (2010) [9] studied the Welding methods for joining thermoplastic polymers for the hermetic enclosure of medical devices. In this paper they analyses the thermal, laser, friction welding technique for polymer material. Describe the welding technique for thermoplastic material thermal, friction and electromagnetic technique. The advantages and disadvantages for each of the methods discussed for applications to implantable medical device. Laser welding, where it can be used, is the most suitable technique. It provides almost instantaneous bonding, highly localised heating, and minimal effect on sensitive contents. Ultrasonic or resistance welding could be considered in cases where laser welding is not possible.

K. Palanikumar and J. Paulo Davim (2006) [10] studied a mathematical model has been developed to predict the tool wear on the machining of GFRP composites using regression analysis and analysis of variance (ANOVA) in order to study the main and interaction effects of machining parameters, cutting speed, feed rate, depth of cut and work piece fiber orientation angle. The adequacy of the developed model is verified by using coefficient of determination and residual analysis. This model can be effectively used to predict the tool wear on machining GFRP components within the ranges of variables studied. They using the carbide coated tool which composition is Co 6.0%; composite carbide 8.0%. tool wear increases with increase of cutting speed and vice versa. The higher cutting speed was found to cause a large deformation rate of glass fiber and severe tool wear and hence the cutting speed has been set at low level and is between 75 and 175 m/min. The depth of cut plays only a small role in composite machining process compared to cutting speed and feed rate, but the higher depth of cut cause a deleterious effect on surface quality in GFRP machining and it also leads to more tool wear and hence low limits of depth of cut are chosen for the present study. The increase in feed rate increased the heat generation and hence, tool wear, which resulted in the higher tool wear .The increase in feed rate also increase the chatter and it produces incomplete machining at a faster traverse, which leads to more tool wear.

Jiromaru Tsujino & Tetsugi Ueoka [11] studied the different parameter like Weld time, clamping force, thickness of plate, width, amplitude and measure the strength of the welded joint. Ultrasonic multi-spot welding using two vibration systems of 15 kHz and 27 kHz crossed at a right angle are studied. They conclude that welding plate specimens of aluminium, aluminium alloy, copper and steel plate specimens of 0.5 to 2.0 mm thickness and 100 mm to 200 mm width were successfully welded continuously with almost uniform welding strength.

Farid Haddadi [12] studied on the process parameters weld time, clamping force, thickness, temperature of weld for measuring the strength of welded joint using modelling and structure analyses. They take aluminium and steel for joint. Rectangular shape of 100 mm length and 25 mm width to be welded at 25 mm over lapped position. Conclude that similar aluminium welding was seen to give a 3.0 kN strength with a nugget pullout fracture mode under optimum conditions, but in a considerably shorter welding time compared to dissimilar aluminium to steel joints.

The same maximum weld strength and Fracture mechanism (nugget pullout) of similar aluminium welds was observed when aluminium was welded to un-coated steel.

Mantra Prasad Satpathy et al [13] studied vibration amplitude, weld pressure and weld time this three input parameter for study , they measuring the weld strength of joint for the aluminium and brass sheet of 0.3 mm thickness material using the full factorial, non-linear second order regression model between the responses and predictors. A variety of weld quality levels, such as "under weld", "good weld" and "over weld" have also been defined by performing micro structural analysis. they conclude that Based on its main effects results, the most influencing parameter on the response is the vibration amplitude as it occupies rank 1 followed by weld time and weld pressure. An amplitude of 68 mm, weld pressure of 0.3 Mpa and weld time of 0.8 Sec are the optimum inputs to get excellent weld using this method.

Sheets Hyung-Seop Shin & Michael de Leon[14] studied on parameter of Weld time, amplitude and they measure the Strength of weld, tempeture of weld, fracture pattern for 3 types of horn they take the three different types of horn which have different surface pattern. Then they measure the strength of lap joint. They also measure the strength for different horn surface pattern; they measure the temperature at weld zone for different horn.

M. Roopa Rani et al (2014) [15] studied on design of horn, they using the stainless steel , mild steel ,aluminium , titanium material of horn for ultrasonic welding using finite element analysis method , they measure the weld time , hold time , applied pressure . It is seen that parts welded using a horn made of titanium have the highest strength as compared to parts welded by the other horns. Energy utilization of 95% as compared to 80% by aluminium horn, 70% by mild steel horn and 65% by stainless steel horn. The horn is designed in such a way that it maximizes the amplitude of the sound wave passing through it.

Mr. Bhavik Pandya et al (2014) [16] studied on design of different shaped acoustic horns like conical, stepped and exponential made from EN24 material for ultrasonic welding Then testing the weld tensile strength of HDPE sample with different welding parameter (pressure, Amplitude, thickness) with respect to different hone profile in ultrasonic welding .they are using CARD software. A stepped shape horn produced lower amplitude, since it produced low strength. Tensile strength results show that for ultrasonic plastic welding, conical shaped horn and exponential shaped horn are better than step-cylindrical shape horn. Where manufacturing cost and time is important parameters exponential shape horn is rarely use because of cost of manufacturing & design of horn is more costly compare to other type horn have near to same amplitude and gain Conical horn shape is easy to manufacture and also has almost nearest amplitude as exponential shape horn. Therefore, conical shaped horn is extensively used in industry.

2.1 Summary of Literature Review

1. From the literature review it was found that various works was done on different materials with different process parameters of Ultrasonic welding.
2. The main process parameters that influence the weld strength are weld time, weld pressure, amplitude, frequency, thickness of samples.
3. It also provides the information about the different methods which are used for experimental design**.**
4. Different horn profile and horn material also affect the strength of material.
5. Different horn can be design using the card software.

Conclusion

From literature survey, it was conclude that different parameter weld time, amplitude & pressure is most affecting parameter. Different horn shape is also affect the strength of welding joint, from literature it was found that conical horn is best suitable for joining for thermoplastic material. Horn design can be easily done with the card software. Temperature at the weld zone is also measured with the help of thermocouple.

Acknowledgements

It is indeed a pleasure for me to express my sincere gratitude to those who have always helped me for this literature review presentation work.
First of all I am humbly expressing thanks to my respected guide Mrs. Khushbu patel and Mr. Akash B. Pandey

(Asst. Prof., Dept. of Mechanical Engg., MSU, Baroda) for their valuable time and constant help given to me. They have been a pillar of support and inspired me throughout this study, without them this would not have been possible. I am grateful to the teaching faculties of Mechanical Engineering Department for their valuable Suggestions and instruction regarding my work. I have also received tremendous amount of help from my friend's (sk) within and outside the institute.

4 References

[1] Anahi Pereira Costa, Edson Cocchieri Botelho, Michelle Leali Costa, Nilson Eiji Narita, Jose Ricardo Tarpani (2012) "A Review of Welding Technologies for Thermoplastic Composites in Aerospace Applications" Manag, Sao Jose dos Campos, Vol.4, No 3, pp. 255-265

[2] M. Roopa Rani, R. Rudramoorthy (2012) "Computational modeling and experimental studies of the dynamic performance of ultrasonic horn profiles used in plastic welding" Ultrasonics 53 (2013) 763–772

[3] Sadegh Hoseinlaghab, Seyed Sajad Mirjavadi, M.K. Besharati Givi, M., Azarbarmas (2014) "Influences of welding parameters on the quality and creep properties of friction stir welded polyethylene plates" Materials and Design (2014)

[4] Irene Fernandez Villegas, Pablo Vizcaino Rubio (2015) "On avoiding thermal degradation during welding of high-performance thermoplastic composites to thermoset composites" Composites: Part A 77 (2015) 172–180

[5] S. Elangovan, S. Semeer, K. Prakasan (2008) "Temperature and stress distribution in ultrasonic metal welding An FEA-based study" journal of materials processing technology 2 09 (2009)

[6] D. Stavrov, H.E.N. Bersee (2004) "Resistance welding of thermoplastic composites-an overview" Composites: Part A applied science and manufacturing 36 (2005) 39–54

[7] I. Fernandez, D. Stavrov, H.E.N. Bersee "ultrasonic welding of advanced thermoplastic composites : an investigation on energy directing surfaces" Design and Production of Composites Structures

[8] Rashiqah Rashli, Elmi Abu Bakar, Shahrul Kamaruddin, Abd Rahim Othman (2013) "A Review of Ultrasonic Welding of Thermoplastic Composites" Caspian Journal of Applied Sciences Research, 2(3), pp. 01-16, 2013

[9] Negin Amanata,b, Natalie L. Jamesb, David R. McKenzie (2010) "Welding methods for joining thermoplastic polymers for the hermetic enclosure of medical devices" Medical Engineering & Physics 32 (2010) 690–699

[10] K. Palanikumar a, J. Paulo Davim b (2006) "Mathematical model to predict tool wear on the machining of glass fiber reinforced plastic composites" materials and design 28 (2007)

[11] Jiromaru Tsujino, Tetsugi Ueoka "Ultrasonic multi-spot continuous welding of metal plate specimens using a two-vibration-system welding equipment" Ultrasonics 34 (1996) 229-233

[12] Farid Haddadi (2014) "Rapid intermetallic growth under high strain rate deformation during high power ultrasonic spot welding of aluminium to steel" Materials and Design (2014)

[13] Mantra Prasad Satpathy, Bikash Ranjan Moharana, Shailesh Dewangan, Susanta Kumar Sahoo, (2015) "Modeling and optimization of ultrasonic metal welding on dissimilar sheets using fuzzy based genetic algorithm approach" Engineering Science and Technology, an International Journal (2015).

[14] Hyung-Seop Shin, Michael de Leon (2015) "Parametric study in similar ultrasonic spot welding of A5052-H32alloy sheets" Journal of Materials Processing Technology 224 (2015) 222–232

[15] M. Roopa Rani , K. Prakasan, R. Rudramoorthy (2014)"Studies on thermo-elastic heating of horns used in ultrasonic plastic welding" Ultrasonic 55 (2015) 123–132

[16] Mr. Bhavik Pandya, Mr. Patel Saral, Mr. Patel "Viral effect of horn (sonotrode) profile on weld strength of HDPE plastic weld by using ultrasonic welding" International Journal For Technological Research In Engineering Volume 2.

[17] Sonics & Materials, Inc. Registered by UL to ISO 9001

[18] www.nptel.ac.in/courses/112101005/.../Module_4_Lecture_6_final.pdf

[19] Ultrasonic plastic welding system (roop telsonic ultrasonix limited)

[20] journal- "Minnesota Rubber and QMR Plastics"

[21] http://www.mecasonic.com/

[22] http://www.dukane.com/us/PPL_whatisUPA.htm

[23] http://www.plasticmoulding.ca/

[24] https://en.wikipedia.org/wiki/

[25] Khyati vyas (2013) Thesis on "parametric analysis of composite using ultrasonic welding" merchant engineering college, basna.

Nanomechanical Resonator for Nano-Scale Level of Mass Sensing

Mitesh B Panchal

Associate Professor, Mechanical Engineering Department, Institute of Technology, Nirma University, S G Highway, Ahmedabad – 382 481, India

Abstract

This paper illustrates,the possible use of nano-mechanical resonator as a mass sensor system. The high frequency dynamic behavior of nano-mechanical resonator is analyze considering continuum mechanics based analytical and simulation approaches. The resonant frequency variation based analysis has been performed to analyze the possible mass sensitivity of the nano-mechanical resonator system for the possible mass sensing application. The mass sensitivity of 10^{-26} kg can be achieved using nano-mechanical resonator. The possible mass detection of nano-scale level can be utilized for development of mass based sensor system for detection of gas, bacterium / viruses, etc. The biocompatible materials can be considered for the development of the biosensor systems in the field of biomedicine.

Keywords: Nano-mechanical resonator, resonant frequency, mass-sensitivity, mass-sensor.

Nomenclature	
SWBNNT	Single walled boron nitride nanotube
FEM	Finite element method
NEMS	Nano electro mechanical system

1. Introduction

The growth of nanotechnology enables the development of nanoscale functional devices designed for specific intentions such as nanoscale actuation, sensing, and detection [1-3]. For instance, micro/nano-electro-mechanical system (MEMS/NEMS) devices have allowed the detection of physical quantities such molecular mass [4-7] thermal fluctuation [8,9], coupled resonance [10-12], and biochemical reactions [13]. Among MEMS/NEMS devices, nano-mechanical resonators have been recently played up for their unprecedented dynamic characteristics, as they can easily reach ultra-high frequency (UHF) and/or very high frequency (VHF) dynamic behaviour up to the Giga Hertz (10^9 Hz) regime. The high-frequency dynamic behaviour can be achieved by scaling down the size of the resonator because the resonant frequency is proportional to L^{-2}, where L is the length of a device. This implies that, if the resonator length is decreased by an order of magnitude, then its resonant frequency is increased by two orders of magnitude. Furthermore, the ability of the resonator to detect physical quantities (i.e. mass, force or pressure) is closely associated to its resonant frequency. For sensing mass that is added onto a resonator, the detection sensitivity is given by the relation $\Delta f_n / M = (1/2\ m)\ f_n$, where f_n and m represent the resonant frequency and the effective mass of a device, respectively, while Δf_n and M indicate the resonant frequency shift and the added mass. This relationship suggests that as the frequency of the resonator increases, its ability to sense or detect smaller masses increases, which implies that UHF/VHF resonators are suitable for ultra-sensitive detection, where the eventual limit of a single atom or molecule is within reach.

The splendid performance of nano-mechanical resonators for sensing applications is highly correlated with their dynamic characteristics. It is therefore, essential to characterize and understand the dynamic behaviour of nano-mechanical resonators for the novel design of resonant based sensing toolkits.

1.1 Dynamics of Nano-mechanical Resonators and Required Material

The operational principle underlying micro and nanoresonators is that they can be used to detect minute forces, masses, and biological/chemical species through the resulting changes that are induced in their resonant frequencies. This shows that characterization of the resonant frequency and/or its shift due to mass is essential to elucidate the sensing performance for a resonator. In general, it has been accepted that the resonance behaviour of a MEMS/NEMS device is well described by continuum elasticity theory. For instance, the dynamic behaviour of micro cantilevers has been shown experimentally to be accurately represented by the harmonic, flexural motion that is assumed in classical linear elastic Bernoulli-Euler beam theory. The merit of micromechanical resonators is that miniaturization of their dimensions enhances the mass sensitivity of these sensors. It has been reported that the detectable mass can be as small as several femtograms by using microsized silicon or silicon nitride cantilevers.

Mass sensing based on nanotubes are inertial: Nanotube behave like a spring, which means that it has a

characteristic resonance frequency that is inversely proportional to the square root of its effective mass. For the fixed-free beam geometry of resonator construction (Fig. 1), the fundamental mode resonance frequency of the beam can be estimated as,

$$f = 1.03\sqrt{\frac{E}{\rho}}\frac{t}{l^2} \quad (1)$$

Where, E is Young's modulus of the material, ρ is the mass density, t is the thickness of the beam along the direction of motion, and l is the length of the beam. Materials with a higher Young's modulus and lower mass density are more desirable for the fabrication of ultra-high-frequency nano-mechanical resonator devices. Table 1, lists these important properties for a few commonly used materials for nano-electromechanical systems (NEMS), including silicon, the traditional material for the semiconductor industry, and a few other examples of relatively newer materials under current investigation.

The material properties suggest that CNTs and BNNTs are more suitable material for the nano-mechanical resonators, as they are having higher Young's modulus and lower density compared to other materials. Different from CNTs, which are highly toxic to the human body and depending on their chirality can be semiconductor and conductors, BNNTs of different chirality show good biocompatibility and are always semiconducting with a large band gap.

2. Cantilevered Configuration Of BNNT With Attached Mass At Free-End (tip)

Fig. 2. shows atomic model of cantilevered configuration of single walled BNNT with attached mass M, at the free-end (tip), considering that added mass M, giving a virtual force at the location of the mass so that the deflection under the mass becomes unity. For cantilevered configuration with attached mass at the free-end, the equivalent stiffness of the system can be expressed as,

$$k_{eq} = \frac{3EI}{l^3} \quad (2)$$

The deflection shape under assumed condition of the unity deflection at the location of the attached mass also can be expressed as,

$$W(x) = \frac{x^2(3L-x)}{2l^3} \quad (3)$$

The equivalent mass of the combined system (cantilevered configuration of single walled BNNT + attached mass) can be derived by considering the harmonic motions and kinetic energy of single walled BNNT.

Assuming the harmonic motion $W(x, t) = W(x)\ exp(i\omega t)$, where '$\omega$' is the frequency. The kinetic energy of cantilevered single walled BNNT is obtained as,

$$T = \frac{\omega^2}{2}\int_o^L \rho A W^2(x)dx + \frac{\omega^2}{2}MW^2(L) \quad (4)$$

$$= \rho A\frac{\omega^2}{2}\int_o^L W^2(x)dx + \frac{\omega^2}{2}M(1)^2 \text{ (unit deflection at the location of attached mass M)}$$

$$= \frac{\omega^2}{2}\left(\frac{33}{140}\rho AL + M\right)$$

therefore, equivalent mass,

$$m_{eq} = \frac{33}{140}\rho AL + M \quad (5)$$

Substituting Eq. (2) and Eq. (5) in Eq. (1), the resonant frequency can be obtained as,

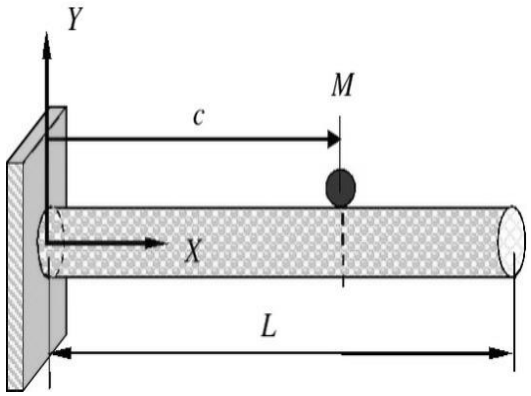

Figure 1. Simulated fixed-free type nanotube as a mass sensor system.

Table 1. Properties of NEMS Materials

Material	Young's Modulus (GPa)	Mass Density (10^3 kg/ m3)
Si	110	2.4
SiC	440	3.2
AlN	345	3.3
Diamond	*1000*	*3.5*
Carbon nanotubes (CNT)	1070	1.13
ZnO nanotubes	200	0.4
Boron nitride Nanotubes (BNNT)	*1200*	*2.18*

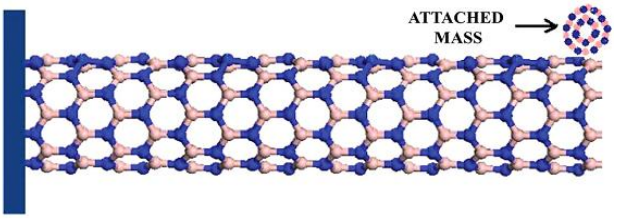

Figure 2. Cantilevered configuration of single walled BNNT based resonant nano-mechanical sensor system with attached mass at the free end.

$$f = \frac{1}{2\pi}\sqrt{\frac{\frac{3EI}{L^3}}{\frac{33}{140}\rho AL + M}} = \frac{1}{2\pi}\sqrt{\frac{140}{11}}\sqrt{\frac{EI}{\rho AL^4}}\sqrt{\frac{1}{1+\frac{M}{\rho AL}\frac{140}{33}}}$$

$$f = \frac{1}{2\pi L^2}\frac{\alpha^2_{cantilevered}\ \beta}{\sqrt{1+\Delta M\mu_{cantilevered}}} \tag{6}$$

where,

$$\alpha^2_{cantileverd} = \sqrt{\frac{140}{11}},\ \beta = \sqrt{\frac{EI}{\rho A}}, \Delta M = \frac{M}{\rho AL} \text{and} \mu_{cantileverd} = \frac{140}{33} \tag{7}$$

2.1 Attached mass and resonant frequency shift relationship

The rational of mass sensing using resonant nano-mechanical sensor is based on the conception that, the resonant frequency is sensitive to the mass of the resonant nano-mechanical sensor, which includes the self-mass of the senor and the mass attached on it. The change of the mass attached on the sensor can cause a shift of the resonant frequency. The key issue of mass sensing is to quantifying the change in the resonant frequency due to added mass.

The resonant frequency of the single walled BNNT with no attached mass can be considered as a baseline data to calculate the resonant frequency shift due to the attached mass on it. The resonant frequencies considered for both the end constraints: cantilevered and bridged, with no attached mass can be expressed by considering the $\Delta M = 0$ in Eq. (6),the general the expression for the resonant frequency (f_0) with no attached mass can be given as

$$f_0 = \frac{1}{2\pi L^2}\alpha^2\beta \tag{8}$$

Therefore the relationship between the resonant frequencies with attached mass *M*, and with no attached mass can be given as,

$$f = \frac{f_{0_n}}{\sqrt{1+\Delta M\mu}} \tag{9}$$

The resonant frequency shift Δf due to attached mass *M*, can be defined as,

$$\Delta f = f_0 - f = f_0 - \frac{f_0}{\sqrt{1+\Delta M\mu}}$$

$$\frac{\Delta f}{f_0} = 1 - \frac{f_0}{\sqrt{1+\Delta M\mu}} \tag{10}$$

Rearrangement of Eq. (3.17) gives expression,

$$\Delta M = \frac{1}{\mu(1-(\Delta f/f_0))^2} - \frac{1}{\mu} \tag{11}$$

This equation relates the change in mass of the sensor with the frequency shift Δf.

Expanding Eq. (11), using Eq. (8)

$$\Delta M = \frac{(\alpha^2\beta/L^2)}{\mu((\alpha^2\beta/L^2)-(2\pi\Delta f))^2} - \frac{1}{\mu} \quad (12)$$

Using Eq. (7), the Eq. (12) can be used to obtain the general relationship, which relates the attached mass and resonant frequency shift as [14-18].

$$M = \frac{\rho AL}{\mu}\frac{(\alpha^2(\beta/L^2))^2}{(\alpha^2(\beta/L^2)-2\pi\Delta f)^2} - \frac{\rho AL}{\mu} \quad (13)$$

This is a general equation to relates the attached mass and resonant frequency shift, the constants appearing in this equation are summarized as,

$\mu_{cantileverd} = 140/33 = 4.243$, and $\alpha^2_{cantileverd} = \sqrt{140/11} = 3.568$,

In continuum model, on application of external load the stresses are distributed and transmitted through continuous wall area of the model. In case of nanotube the same stresses are transmitted through the atoms, as a result the wall thickness 'h' of the continuum model must be smaller than the atom diameter; otherwise the tube (continuum model) equilibrium cannot be maintained. In this sense, calculations which are obtained using continuum model of the BNNT with the wall thickness greater than or equal to the diameter of a boron atom or a nitrogen atom, can give incorrect results. For the continuum mechanics based analytical calculations as well as for the continuum solid modeling for the finite element method (FEM) based simulation approaches, the effective thickness of 0.065 nm, 44% of the average of theoretical diameters of boron atom (~ 0.145 nm) and nitrogen atom (~ 0.150 nm) is taken for the analysis.

3. Continuum Solid Modeling Of BNNT For FEM Simulation

3-dimensional continuum solid FE models of cantilevered and bridged configurations of the single walled BNNTs with attached mass have been developed to perform the resonant frequency based vibrational analysis using ANSYS. The single walled BNNTs are modelled using a 3-D finite element model and the attached mass is model using BOOLEAN operation. BOOLEAN algebra provides a means for combining sets of data, using logical operators as intersect, union, subtract etc. In this analysis, the mass is changed in every iterations and the GLUE Boolean operator is used for modeling to the BNNT, as it allows modifying the solid model construction more easily. GLUE is the Boolean operation, which applies only to cases in which the intersection between entities occurs at a boundary. The entities maintain their individuality i.e. they are not added and become connected at their intersection. SOLID 187 is used for the 3-D modeling of anisotropic solid structures. This element is defined by eight nodes having three degree of freedom at each node (Fig. 3.).

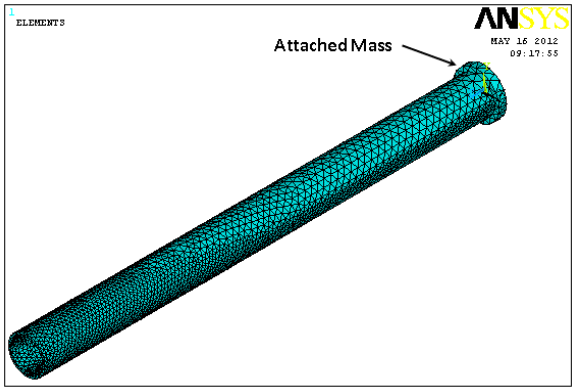

Figure 3. 3-D continuum solid FEM model of cantilevered configuration

4. Results and Discussion

The simulation approaches considering isometric and anisometric properties of BNNTs are validated by comparing the resonant frequency variation analysis for the BNNTs of different diameters 0.8 nm, 1.0 nm and 1.2 nm, of different lengths. The results are summarized in TABLE II, the obtained results using simulation approaches are in good agreements with the analytical results.

After validation of the simulation approaches, the vibrational analysis considering the mode shapes and corresponding frequencies has been analysed. Fig.4. shows the initial first 4 mode shapes of the cantilevered configurations of BNNT.

The mass sensitivity analysis for the cantilevered configurations of BNNT based nano-mechanical resonator has been performed considering the attached mass at the free-end of the nanotube in the range of 10^{-18} kg to 10^{-26} kg. The BNNTs of diameter 1.0 nm and different lengths of 20 nm, 40 nm and 60 nm are considered. The obtained results indicates, that the detectable resonant frequency shift for the magnitude of attached mass of 10^{-26} kg is possible (Fig. 5). Which implies the possible mass detection capabilities of the BNNT based nano-mechanical resonator is 10^{-26} kg.

Table 2. Resonant Frequency Variation of Different BNNT of Different Sizes using Analytical and Simulation Approaches

D, nm	L, nm	Resonant Frequency (Hz)			% error in isometric	% error in anisotropic
		Analytical	Isometric	Anisotropic		
0.8	20	8.68E+09	8.26E+09	8.18E+09	4.86	5.78
	40	2.17E+09	2.06E+09	2.12E+09	5.17	2.55
	60	964954691	8.95E+08	9.46E+08	7.20	1.91
1.0	20	1.103E+10	1.08E+10	1.01E+10	1.66	8.23
	40	2.758E+09	2.66E+09	2.67E+09	3.39	3.25
	60	1.226E+09	1.21E+09	1.20E+09	1.64	2.23
1.2	20	1.338E+10	1.31E+10	1.19E+10	1.82	11.08
	40	3.345E+09	3.30E+09	3.21E+09	1.47	4.09
	60	1.487E+09	1.47E+09	1.45E+09	1.42	2.62

The capability of ultra-high mass sensitivity of BNNT based nano-mechanical resonator can be utilized for the possible detection of gas molecules, biological species, bacterium/viruses etc. The acetone molecules has higher binding energy to the boron, which makes possible detection of acetone gas using BNNT based nano-mechanical resonator systems. The mass of acetone single molecule is considered as 9.64e-27 kg. The resonant frequency analysis has been analysed for the cantilevered configuration of BNNT of diameter 0.4 nm and different lengths of 20 nm, 40nm and 60 nm, having different number of acetone molecules as attached mass at the free-end.

From the Fig. 6, one can observe that as the attached mass in terms of number of acetone molecules increases, the resonant frequency shift increases. The minimum detectable resonant frequency shift due to attached single acetone molecule is possible to estimate the mass-based detection of a single acetone molecule. Also, the results suggest that, by using smaller size of the BNNT based nano-mechanical resonator system, the sensitivity of the overall system can be enhanced for the detection of a single acetone molecule.

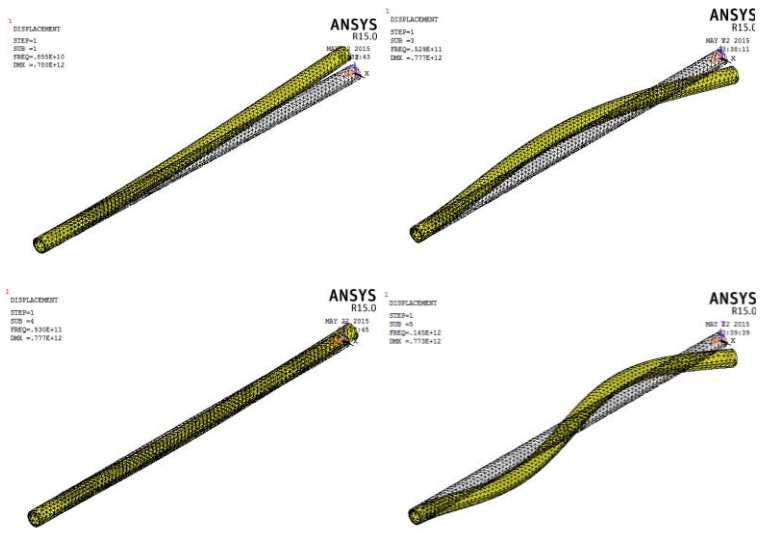

Figure 4. Different vibrational mode shapes of the cantilevered configuration of BNNT.

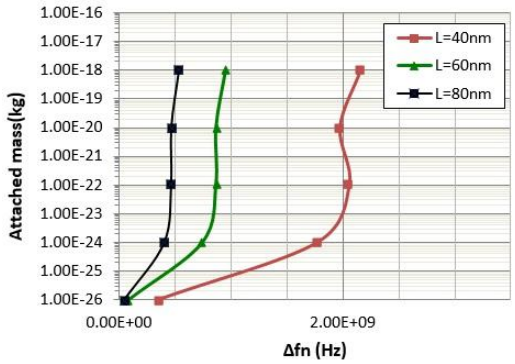

Figure 5. Frequency shift variations against attached mass at the free-end of the cantilevered BNNT based nano-mechanical resonator systems of diameter 1.0 nm and for different lengths 40 nm, 60 nm and 80 nm.

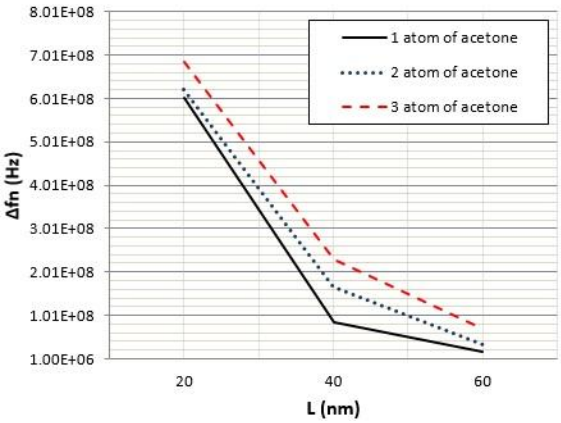

Figure 6. Resonant frequency shift variation for the cantilevered configuration of BNNT having acetone molecules as attached mass at the free-end.

5. Concluding Remarks

The results based on resonant frequency variation analysis confirm the acceptance validation of the presented simulation approaches. The possible mass sensitivity limits of 10^{-26} kg is possible using BNNT based nano-mechanical resonator system. Also, the resonant frequency variation based analysis suggest possible detection of single molecule of acetone using BNNT based nano-mechanical resonant system. The obtained results can be utilized for the realization of the practical application of BNNT based nano-mechanical resonant system in the field of bio medicine as well as for the gas sensor system.

References

[1] Crighead, H. G. 2000. Nanoelectromechanical Systems. Science 290 (5496): 1532-1535.
[2] Roukes M. L. 2001. Nanoelectromechanical systems face of future, Physics World 14: 25-31.
[3] Ekinci K. L. 2005. Electromechanical Transducers at the Nanoscale: Actuation and Sensing of Motion in Nanoelectromechanical Systems (NEMS). Small 1: 786.
[4] Yang Y. T., Callegari C., Feng X. L., Ekinci K. L. and Roukes M. L. 2006. Zeptogram-scale nanomechanical mass sensing. NanoLetters, 6: 583-586.
[5] Li M., Tang H. X. and Roukes M L. 2007. Ultra sensitive NEMS-based cantilevers for sensing, scanned probe and very high-frequency applications. Nature Nanotechnology 2: 114-120.
[6] Jensen K., Kim K. and Zettl A. 2008. An atomic-resolution nanomechanical mass sensor, Nature Nanotechnology 3: 533-537.
[7] Naik A. K., Hanay M. S., Hiebert W. K., Feng X. L. and Roukes M. L. 2009. Towards single-molecule nanomechanical mass spectrometry. Nature Nanotechnology 4: 445-449.
[8] Tamayo J., Calleja M., Ramos D. and Mertens J. 2007. Underlying mechanism of the self-sustained oscillation of a nanomechanical stochastic resonator in liquid. Phys. Rev. B. 76: 180201.
[9] Badzey R. L. and Mohanty P. 2005. Coherent signal amplificationin bistable nanomechanical oscillators

by stochastic resonance. Nature 437: 995.

[10] Shim S. B., Imboden M. and Mohanty P. 2007. Synchronized Oscillation in Coupled Nanomechanical Oscillators. Science 316: 95.

[11] Sato M., Hubbard B. E., Sievers A. J., Ilic B., Czaplewski D. A. and Craighead H. G. 2003. Observation of locked intrinsic localized vibrational modes in a micromechanical oscillator array. Phys. Rev. Lett. 90: 044102.

[12] Kwon T., Eom K., Park J. H., Yoon D. S., Kim T. S. and Lee H. L. 2007. In situ real-time monitoring of biomolecular interactions based on resonating microcantilevers immersed in a viscous fluid. Appl. Phys. Lett. 90: 223903.

[13] Kwon T., Park J., Yang J., Yoon D. S., Na S., Kim C. W., Suh J. S., Huh Y. M., Haam S. and Eom K. 2009. Nanomechanical in situ monitoring of proteolysis of peptide by Cathepsin B. PLoS ONE 4: e6248

[14] Panchal M. B., Upadhyay S. H., and Harsha S. P. 2012a. Mass Detection Using Single Walled Boron Nitride Nanotube As A Nanomechanical Resonator. NANO: Brief Reports and Reviews 7 (4): 1250029 1-11.

[15] Panchal M. B., Upadhyay S. H., and Harsha S. P. 2012b. Vibration Analysis of Single Walled Boron Nitride Nanotube Based Nanoresonators. J. Nanotechnol. Eng. Med. Transactions of the ASME. 3 (3): 031004 1-5.

[16] Panchal M. B., Upadhyay S. H., and Harsha S. P. 2013a. Cantilevered Single Walled Boron Nitride Nanotube Based Nanomechanical Resonators of Zigzag and Armchair Forms. Physica E 50: 73–82.

[17] Panchal M. B. and Upadhyay S. H. 2013b. Vibrational Analysis of Zigzag and Armchair Fixed Free Single Walled Boron Nitride Nanotubes: Atomistic Modeling Approach. Current Nanoscience 9 (2): 254-261.

[18] Panchal M. B. and Upadhyay S. H. 2013c. Effect of Chirality on Resonant Behavior of Single Walled BN Nanotube Based Nanomechanical Resonator. Current Nanoscience 9 (4): 525-531.

A Numerical Procedure for Elastic Solids

Pankaj Jagad
Department of Mechanical Engineering, Institute of Technology, Nirma University, Ahmedabad 380052, India

Abstract
A cell-centered unstructured mesh finite volume procedure is developed for computing displacement and stress fields in an elastic solid. The finite volume discretization is carried out in a structured grid like manner by employing an assumed line-structure in order to evaluate diffusive transport across the cell-faces. The line-structure ensures discretization at the face center in contrast to the traditional methods those involve discretization at the point of intersection of the face with the line joining the cell centers straddling the face. The transformation information between local non-orthogonal curvilinear co-ordinates and global Cartesian co-ordinates is employed for computing Cartesian gradients across the cell-faces. This eliminates the requirement of computing second order gradients at the cell centers as used by conventional methods, which is computationally more cumbersome. The procedure is validated by solving a few benchmark problems.

Keywords: cell-centered; elastic solid; finite volume method; unstructured mesh.

Nomenclature

E	Young's modulus (N/m^2)
f_i	body force in i-direction (N/kg)
x_j	Cartesian coordinate vector
Greek symbols	
δu_i	displacement component in i-direction (m)
δu_j	displacement vector (m)
δ_{ij}	Kronecker delta tensor
λ	Lame's constant (N/m^2)
μ	shear modulus (N/m^2)
ν	Poisson's ratio
ρ	density (kg/m^3)
σ_{ij}	Stress tensor (N/m^2)

1. Introduction

There are two types of approaches employed in general for finite volume discretization. One is vertex-centered procedure in which the computational nodes are located at the vertices of the cells or elements forming the mesh and control volumes are formed surrounding the nodes. Hence the variable values are computed and stored at the vertices. Some vertex-centered methods [1, 2, 3, 4, 5] are based on traditional Finite Element (FE) method employing shape functions to describe the variation of a variable over an element or cell. The other vertex-centered methods [6, 7, 8] do not use shape functions. The second is cell-centered procedure [9, 10, 11, 12, 13, 14, 15] which is based on traditional FV methods those have been applied in context of Computational Fluid Dynamics (CFD). In this procedure the computational nodes are located at the centers of the cells forming the mesh, and cells themselves are used as the control volumes. Hence the variable values are computed and stored at the cell-centers. Depending on the approach employed for domain discretization three types of procedures are found. In structured mesh procedures [9, 11, 16] the cell faces are aligned in the global co-ordinate directions and the neighbouring information for each cell is known a priori. On the other hand, in unstructured mesh procedures [1, 2, 10, 12, 13] all cell faces may not be aligned along the global co-ordinate directions and the neighbouring information for each cell is not known a priory. In curvilinear mesh procedures [17] the governing equations in terms of global co-ordinates are transformed to those in terms of non-orthogonal local curvilinear co-ordinates; then discretization is carried out with respect to the local co-ordinate system. Some studies considered different material behaviours such as elastic [7, 8, 11, 13, 15, 17, 18, 19, 20], thermo-elastic [1, 2, 10, 12, 16], anisotropic thermo-elastic [21], thermo-elasto-plastic [9], elasto-plastic [4, 22, 23], hyper-elastic [24] and viso-plastic [25]. Studies regarding structural dynamics problems have also been reported [6, 7, 8, 18, 26]. A few studies included rotational degree of freedom in the

analysis in addition to the translational degree of freedom and shown higher accuracies with respect to bending type of problems [27]. Staggered grid procedure [16] has also been employed wherein the and displacement components are stored at the vertical and horizontal face centers respectively. Hence the and momentum control volumes are staggered in and directions respectively. The normal and shear stress components stored at the cell centers and the cell vertices respectively . Large strains have also been considered in some procedures [24]. Several studies considered the solid as an incompressible material and included the pressure term in the constitutive relations. These studies are based on displacement - pressure formulation [20, 24] or traditional velocity - pressure formulation [28, 29]. Procedures employed for specific applications such as fracture mechanics [11, 19], crystal growth process [30], metal extrusion and forging [25, 31], welding [22], and casting [3] are also found.

A cell-centered finite volume discretization procedure on unstructured meshes is described in the present study for computing steady state displacement and stress fields in an elastic solid. An assumed line structure is employed to evaluate diffusive transport across the cell-faces in a structured grid like manner. The line-structure ensures that disretization is always at the face center, in accordance of the use of mean value theorem. The formulas for transformation from global Cartesian co-ordinates to local non-orthogonal curvilinear co-ordinates are employed for computing Cartesian gradients of displacement components across the cell-faces. Thus cumbersome procedure of computing second order gradients is eliminated which otherwise would be required if the displacement gradients at a face center is approximated using the Taylor series expansion at the cell centers straddling the face. The benchmark problems considered for validation of the procedure consist of computation of displacement and stress fields in bodies subjected to different load and boundary conditions.

2. Mathematical formulation

For an elastic solid continuity equation is redundant and need not be solved. Also, it is reasonable to assume that for most applications in practice the strains, displacements, velocities and the accelerations are very small. Hence the convective terms are neglected in an elastic solid. Then the governing equations for the transfer of momentum is expressed as

$$-\frac{\partial \sigma_{ij}}{\partial x_j} = \rho f_i, \tag{1}$$

where σ_{ij} is the stress tensor, and f_i is the resultant body force per unit mass in i-direction. Invoking the Hooke's law for an elastic solid for relating the stress tensor with the strain tensor (ε_{ij}), we have

$$\sigma_{ij} = 2\mu\varepsilon_{ij} + \delta_{ij}\lambda\varepsilon_{kk}, \tag{2}$$

where μ is the shear modulus, λ is the Lame's constant, and δ_{ij} is the Kronecker delta. Assuming the material to be homogeneous and isotropic μ and λ are expressed as

$$\mu = \frac{E}{2(1+\nu)} \tag{3}$$

and

$$\lambda = \frac{\nu E}{(1+\nu)(1-2\nu)}, \tag{4}$$

where E is Young's modulus and ν is Poisson's ratio. For small displacements the strain tensor is expressed in terms of displacement gradients as

$$\varepsilon_{ij} = \frac{1}{2}\left(\frac{\partial(\delta u_i)}{\partial x_j} + \frac{\partial(\delta u_j)}{\partial x_i} \right), \tag{5}$$

where δu_j is the displacement vector.

Introducing the constitutive relation (Eq. 2) and the kinematic relation (Eq. 5) into the momentum equations (Eq. 1) we get

$$-\frac{\partial}{\partial x_j}\left[\mu\left(\frac{\partial(\delta u_i)}{\partial x_j} + \frac{\partial(\delta u_j)}{\partial x_i} \right) + \lambda \delta_{ij} \frac{\partial(\delta u_k)}{\partial x_k} \right] = \rho f_i. \tag{6}$$

Equations 6 can be expressed in terms of a general variable ϕ as

$$-\frac{\partial}{\partial x_j}\left[\mu_\phi\left(\frac{\partial \phi}{\partial x_j} \right) \right] = S_\phi, \tag{7}$$

where the diffusion coefficient $\mu_\phi = \mu$, and S_ϕ is the source term. The general variable ϕ stands for the displacement vector. The source term is expressed as

$$S_\phi = \rho f_i + \frac{\partial}{\partial x_j}\left[\mu\left(\frac{\partial(\delta u_j)}{\partial x_i} \right) + \lambda \delta_{ij} \frac{\partial(\delta u_k)}{\partial x_k} \right], \tag{8}$$

The boundary conditions used alongwith Eq. 7 are described below.

2.1 Boundary conditions

There are three types of boundary conditions possible. They are:

(i) Dirichlet boundary condition: The displacement vector is prescribed at the boundary. This is written as

$$\delta u_j(r_j) = \delta u_{j,B},\ r_j \in S, \tag{26}$$

where r_j is the position vector, $\delta u_{j,B}$ is the prescribed displacement vector at the boundary and S is the boundary surface. When the displacement vector is known at the boundaries it is directly substituted into the discretized governing equations.

(ii) Neumann boundary condition: The forces per unit area vector or traction vector is prescribed at the boundary. This can be expressed as

$$t_j(r_j) = t_{j,B},\ r_j \in S, \tag{27}$$

where t_j is the traction vector and $t_{j,B}$ is the prescribed traction vector at the boundary. The boundary on which the traction condition is known is excluded from the discretization process. The traction vector acting on the boundary is used to calculate the force vector acting on the boundary which is then added to the source term.

(iii) The boundary lies on the plane of symmetry of the domain (Symmetry boundary condition), for the transfer of momentum written as

$$\delta u_n = 0, \quad \frac{\partial \delta u_t}{\partial n} = 0, \tag{28}$$

where n is the normal to the symmetry plane. δu_n and δu_t are the displacement components in the normal and tangential directions to the symmetry plane respectively. When symmetry condition is known the displacement vector at the boundary is calculated from the Eq. 28. Then it becomes Dirichlet type of boundary condition.

3. Discretization

Integrating Eq. 7 over an arbitrary control volume (CV) or cell we get

$$\int_{\Delta V}\left[-\frac{\partial}{\partial x_j}\left[\mu_\phi\left(\frac{\partial \phi}{\partial x_j}\right)\right]\right]dV=\int_{\Delta V}\left[S_\phi\right]dV, \tag{9}$$

where ΔV is the volume of the CV .

10.1. Diffusive transport

To express the volume integral of the diffusion term Gauss's theorem is used. The volume integrals are converted to surface integrals to get

$$\int_{\Delta V}\left[\frac{\partial}{\partial x_j}\left[\mu_\phi\left(\frac{\partial \phi}{\partial x_j}\right)\right]\right]dV=\int_{S}\left[\mu_\phi\left(\frac{\partial \phi}{\partial x_j}\right)\right]\cdot dS, \tag{10}$$

where S represents the surface area of the CV . The surface area consists of the CV faces. The surface integrals in Eq. 10 are approximated by summations over the CV faces. The flux through a CV face is assumed as an averaged value over the face passing through the face center, i.e., mean value theorem is used. Therefore we have

$$\int_{\Delta V}\left[\frac{\partial}{\partial x_j}\left[\mu_\phi\left(\frac{\partial \phi}{\partial x_j}\right)\right]\right]dV=\sum_{k=1}^{Nk}\left[\mu_\phi\left(\frac{\partial \phi}{\partial x_j}\right)\right]_{ck} n_{j,ck} A_{fk}, \tag{11}$$

where k on the summation sign represent the k^{th} CV face, Nk is the number of faces enclosing the CV , $n_{j,ck}$ is the unit outward facing normal to the k^{th} face, with subscript ck representing the face center of the k^{th} face. A_{fk} represents the area of the k^{th} face. Equation 11 can be rewritten as

$$\int_{\Delta V}\left[\frac{\partial}{\partial x_j}\left[\mu_\phi\left(\frac{\partial \phi}{\partial x_j}\right)\right]\right]dV=\sum_{k=1}^{Nk}\left[\mu_\phi\left(\frac{\partial \phi}{\partial n}\right)\right]_{ck} A_{fk}, \tag{12}$$

where $\partial(\ )/\partial n$ stands for the normal gradient. Usually the normal gradient is computed as a normal component of the gradient along the line joining the cell centers straddling the face. In general this line may not intersect the face in the face center. Hence this method of computing the normal gradient for a face is not in line with the use of mean value theorem, as the mean value theorem assumes the flux for a face passing through the face center. The error could be significant for real life problems as there is a good chance that a portion of the mesh used to discretize the domain consists of the elements or cells those are skewed. In the present method, for discrete representation of the normal gradient a construction of line structure [32] as shown in Fig. 1 is used. This ensures that the discretization of the diffusive flux for a face is always at the face center. Using Taylor series expansion a second order accurate expression for normal gradient at the face center of the k^{th} face can be written as

$$\left[\frac{\partial \phi}{\partial n}\right]_{ck} = \left[\frac{\phi_{E_2} - \phi_{P_2}}{l_{P_2E_2}}\right]_k \tag{13}$$

with l representing length. Total diffusive transport through the k^{th} face can be written as

$$\left[\mu_\phi\left(\frac{\partial \phi}{\partial n}\right)\right]_{ck} A_{fk} = d_{ck}\left[\phi_{E_2} - \phi_{P_2}\right]_k, \tag{14}$$

where $d_{ck} = \mu_{ck} A_{fk} / l_{P_2E_2}$. In Eq. 14, values of variables at fictitious points P_2 and E_2 and at the face vertices are not known. These unknown values will now be expressed in terms of values at nodes P and E. For that, multi-dimensionally linear variation of ϕ in the neighbourhood of the nodes P and E is assumed. Then the values of ϕ at P_2, for example, are expressed as

$$\phi_{P_2} = \phi_P + \Delta\phi_P \tag{15}$$

or

$$\phi_{P_2} = \phi_P + \left(x_{j,P_2} - x_{j,P}\right)\left(\frac{\partial \phi}{\partial x_j}\right)_P. \tag{16}$$

The gradients of ϕ at the nodes in Eqs. 16 are calculated using the method of least squares. Finally the discretized form of the diffusive transport through the k^{th} face is expressed as

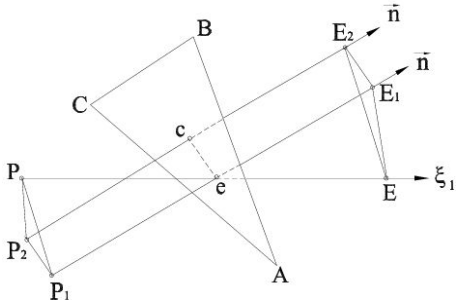

Figure 1: A line structure

$$\left[\mu_\phi\left(\frac{\partial \phi}{\partial n}\right)\right]_{ck} A_{fk} = d_{ck}\left[\phi_E - \phi_P\right]_k - D_k, \tag{17}$$

where

$$D_k = d_{ck}\left[\Delta\phi_E - \Delta\phi_P\right]_k. \tag{18}$$

3.2 .Source term

Expanded form of the volume integral of the source term in Eq. 9 can be written as

$$\int_{\Delta V}(S_\phi)dV = \int_{\Delta V}(\rho f_i)dV +$$

$$\int_{\Delta V}\left[\frac{\partial}{\partial x_j}\left[\mu\left(\frac{\partial(\delta u_j)}{\partial x_i}\right)+\lambda\delta_{ij}\frac{\partial(\delta u_k)}{\partial x_k}\right]\right]dV. \quad (19)$$

The volume integral of the body force is expressed assuming an averaged value of this term stored at the centroid of the CV, i.e., mean value theorem is used. To express the volume integrals of the remaining terms Gauss's theorem is used. The volume integrals are converted to surface integrals to get

$$\int_{\Delta V}(S_\phi)dV = \rho f_i \Delta V +$$

$$\int_{S}\left[\mu\left(\frac{\partial(\delta u_j)}{\partial x_i}\right)+\lambda\delta_{ij}\frac{\partial(\delta u_k)}{\partial x_k}\right]\cdot dS. \quad (20)$$

The surface integrals in Eq. 20 are approximated by summations over the CV faces. The flux through a CV face is assumed as an averaged value over the face passing through the face center. Therefore, we have

$$\int_{\Delta V}(S_\phi)dV = \rho f_i \Delta V +$$

$$\sum_{k=1}^{Nk}\left[\mu\left(\frac{\partial(\delta u_j)}{\partial x_i}\right)+\lambda\delta_{ij}\frac{\partial(\delta u_k)}{\partial x_k}\right]_{ck} n_{j,ck}A_{fk}. \quad (21)$$

Equation 21 can be rewritten as

$$\int_{\Delta V}(S_\phi)dV = \rho f_i \Delta V + \sum_{k=1}^{Nk}\left[\mu\left(\frac{\partial(\delta u_j)}{\partial x_i}\right)n_j\right]_{ck} A_{fk} +$$

$$\sum_{k=1}^{Nk}\left[\lambda\frac{\partial(\delta u_k)}{\partial x_k}n_i\right]_{ck} A_{fk} = S_{\phi,discrete} \quad (\text{say}). \quad (22)$$

Usually, the displacement gradients at the face centers as in the Eq. 22 are calculated by using the Taylor series expansion of the displacement gradients at the cell centers straddling the face and then taking arithmatic mean of the two expanded values. This involves computation of not only the displacement gradients at the cell centers but that of the gradients of displacement gradients at the cell center causing additional computational and storage requirements. This makes a significant difference for real life problems involving a few millions of elements in the computational mesh as the matrix of the gradients of displacement gradients consists of twenty seven elements in 3-dimensions. In present method a direct calculation of the displacement gradients at the face centers is proposed assuming a curvilinear coordinate system for each CV face locally as shown in Fig. 2.

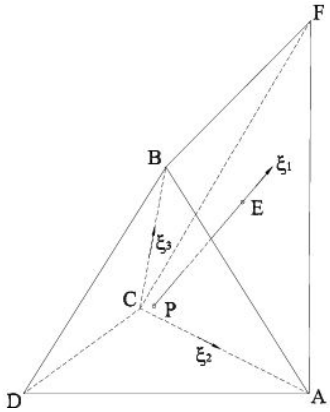

Figure 2: Local curvilinear co-ordinate system

Using Eqs. 17, and 22 discretized form of Eq. 9 can be written as

$$-\sum_{k=1}^{Nk}\left[d_{ck}\left[\phi_E-\phi_P\right]_k-D_k\right]=S_{\phi,discrete}. \tag{23}$$

Equation 23 is rearranged as

$$\sum_{k=1}^{Nk}d_{ck}\phi_P=\sum_{k=1}^{Nk}d_{ck}\phi_{E,k}-\sum_{k=1}^{Nk}D_k+S_{\phi,discrete}. \tag{24}$$

Equation 24 is expressed in the conventional coefficient form as

$$a_P\phi_P=\sum_{k=1}^{Nk}\left[a_E\phi_E\right]_k-\sum_{k=1}^{3}D_k+S_{\phi,discrete}, \tag{25}$$

where $a_{E,k}=d_{ck}$, and $a_P=\sum_{k=1}^{Nk}d_{ck}=\sum_{k=1}^{Nk}a_{E,k}$. Equation 25 represents a set of linear equations with one equation for each cell center.

4. Validation of the procedure

4.1. Flat plate with a circular hole subjected to uniform tension

A case of an infinite flat plate with a small circular hole in its center and subjected to a uniform tension in one direction is considered. The schematic of the problem is shown in Fig. 3. For this problem an analytical solution is available [10, 33]. This is given by

$$\sigma_{xx}=t_x\left[1-\frac{a^2}{r^2}\left(\frac{3}{2}cos2\theta+cos4\theta\right)+\frac{3}{2}\frac{a^4}{r^4}cos4\theta\right],$$

$$\sigma_{yy}=t_x\left[-\frac{a^2}{r^2}\left(\frac{1}{2}cos2\theta-cos4\theta\right)-\frac{3}{2}\frac{a^4}{r^4}cos4\theta\right],$$

$$\sigma_{xy}=t_x\left[-\frac{a^2}{r^2}\left(\frac{1}{2}sin2\theta+sin4\theta\right)+\frac{3}{2}\frac{a^4}{r^4}sin4\theta\right], \tag{29}$$

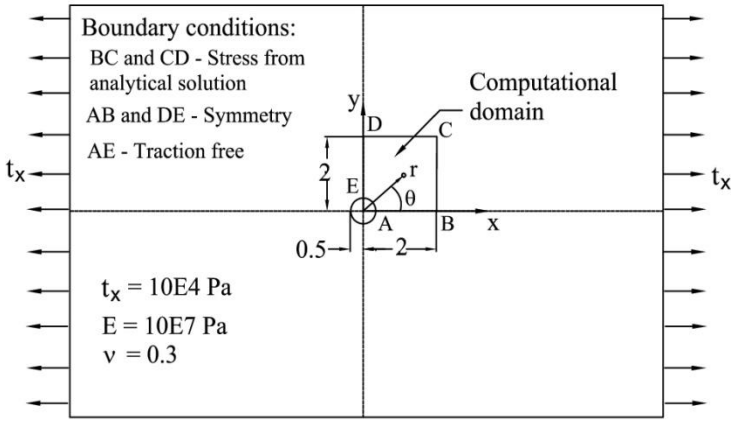

Figure 3: Schematic of the flat plate problem

where a is radius of the hole and $r = \left(x^2 + y^2\right)^{1/2}$ and $\theta = tan^{-1}\left(y/x\right)$ are the usual polar co-ordinates.

The material properties assumed are $E = 10^7$ Pa and $\upsilon = 0.3$. A mesh independent study similar to that in Ref. [10] is performed by employing four systematically refined meshes consisting of triangular elements as shown in Fig. 4. Figure 5 shows the shear stress profile along a circular cross-section $r = 1.25a$ for all four grids as well as the shear stress profile along this section obtained analytically. The mesh consisting of 2520 triangular elements is able to predict accurate solutions. Figure 6 shows the overlapping plots of the contours of stress components in the plate calculated using the present procedure and that obtained using the analytical solutions. Good agreement between the two is seen.

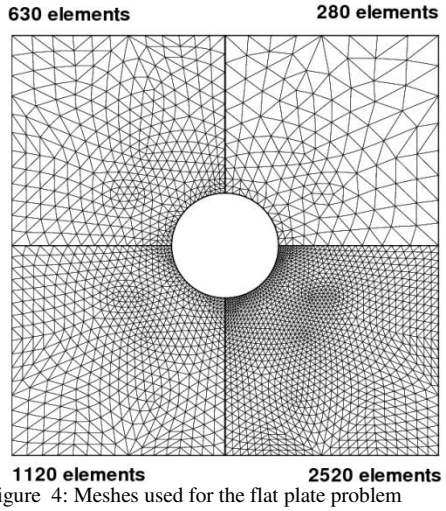

Figure 4: Meshes used for the flat plate problem

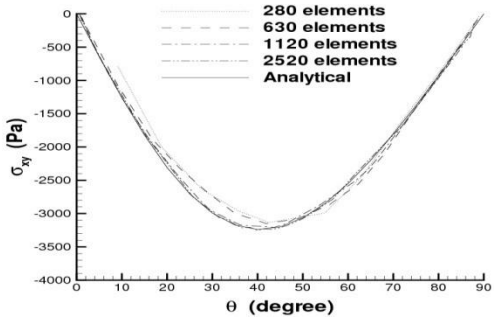

Figure 5: Shear stress profile at a circular cross-section $r = 1.25a$ for the flat plate problem

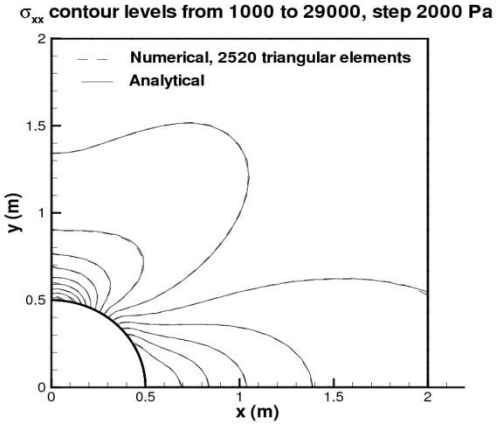

(a) Contours of σ_{xx}

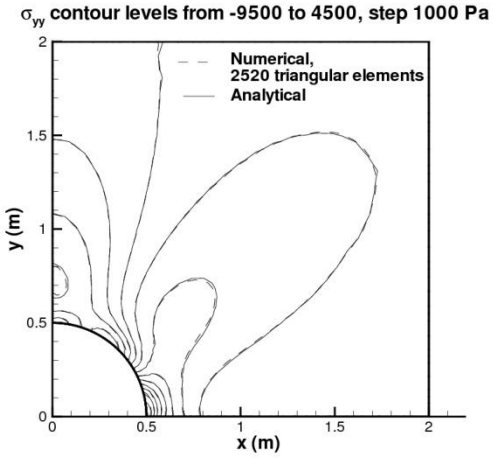

(b) Contours of σ_{yy}

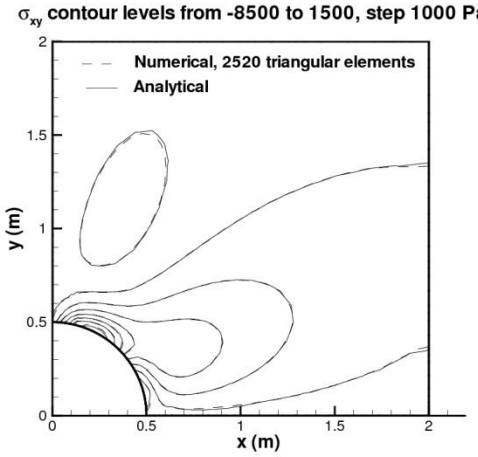

(c) Contours of σ_{xy}

Figure 6: Stress fields for the flat plate problem

10.2. Stretching of a vertical prismatical bar by its own weight

Schematic of the problem as well as the computational mesh is shown in Fig. 7. The analytical solutions [24, 33] are given by

$$\delta u = -\left(\frac{\nu\rho g}{E}\right)xz, \tag{30}$$

$$\delta v = -\left(\frac{\nu\rho g}{E}\right)yz, \tag{31}$$

$$\delta w = \left(\frac{\rho g}{2E}\right)\left(z^2 - l^2\right) + \left(\frac{\nu\rho g}{E}\right)\left(x^2 + y^2\right), \tag{32}$$

$$\sigma_{xx} = \sigma_{yy} = \sigma_{xy} = \sigma_{xz} = \sigma_{yz} = 0 \quad \text{and} \quad \sigma_{zz} = \rho g z. \tag{33}$$

Following material properties are assumed: $E = 2\times10^{11}$ Pa, $\nu = 0.3$ and $\rho = 10000$ kg/m^3. The x and y - displacement profiles at $x = 0.1$ m and $y = -0.1$ m are shown in Fig. 8a. They are found to be linear function of z with zero value at the lower end and the maximum at the upper end of the bar. The profile of z - displacement at $x = 0.1$ m and $y = -0.1$ m is shown in Fig. 8b. The contours of σ_{zz} are shown in Fig. 9. Good agreement is seen with the analytical solutions.

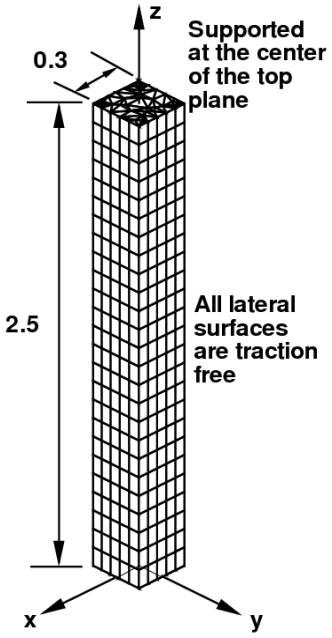

Figure 7: Schematic and mesh for the vertical prismatical bar problem

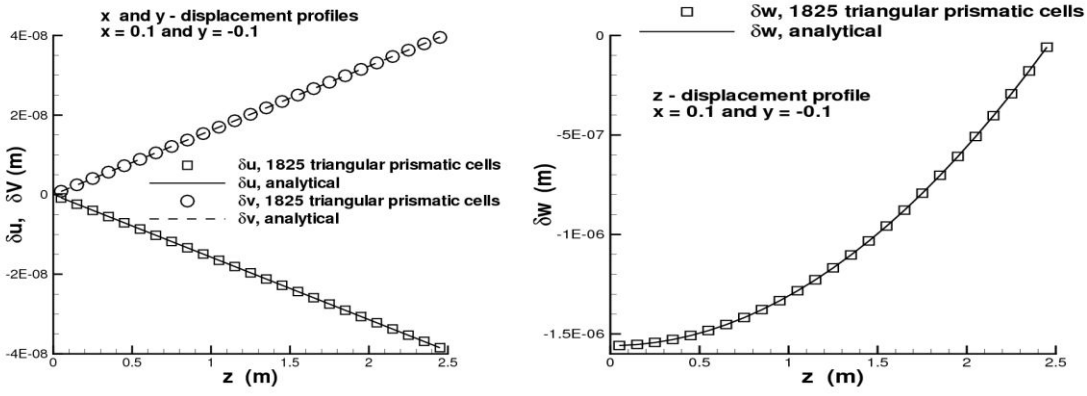

(a) x and y - displacements, $x = 0.1$ m and $y = -0.1$ m (b) z - displacement, $x = 0.1$ m and $y = -0.1$ m

Figure 8: Dispalcement profiles, the vertical prismatical bar problem

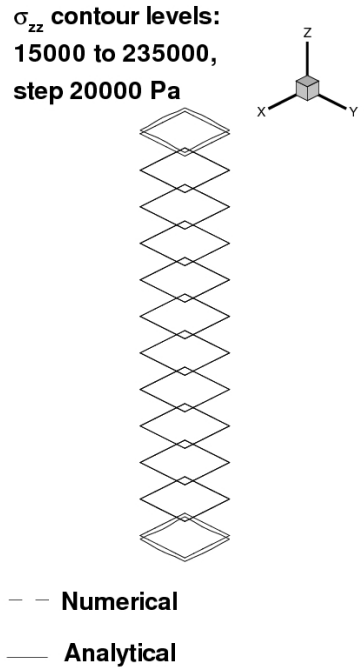

Figure 9: Contours of σ_{zz}, the vertical prismatical bar problem

5. Conclusion

An unstructured mesh finite volume method is presented for solid body stress analysis. The procedure employs an assumed line structure for the discretization of the governing equations. The discretization of the face center gradients is carried out using the relations between the Cartesian coordinates and the curvilinear coordinates. The solutions obtain using the present procedure are compared with the analytical solutions for a few benchmark problems to validate the procedure. Good agreement with the analytical solutions is found.

References

[1] Fryer, Y. D., Bailey, C., Cross, M., Lai, C. H., 1991. A Control Volume Procedure for Solving the Elastic Stress-Strain Equations on an Unstructured Mesh, Appl. Math. Modelling 15, p. 639.

[2] Baily, C., Cross, M., 1995. A Finite Volume Procedure to Solve Elastic Solid Mechanics Problems in Three Dimensions on an Unstructured Mesh, International Journal for Numerical Methods in Engineering 38, p. 1757.

[3] C. Bailey, G.A. Taylor, M. Cross, P. Chow, Discretisation procedures for multi-physics phenomena, Journal of Computational and Applied Mathematics 103 (1999) 3-17.

[4] G. A. Taylor, C. Bailey and M. Cross, Computational Solid Mechanics using a vertex-based Finite Volume Method, in Finite Volumes for Complex Applications II (Problems and Perspectives), Roland Vilsmeier, Fayssal Benkhaldoun, Dieter Hanel, Second International Symposium on Finites Volumes for Complex Applications Problems and Perspectives July 19-22, 1999, Duisburg, Germany, HERMES Science Publications, Paris, 1999, 507-515

[5] E. Onate, M. Cervera and O. C. Zienkiewicz, A finite volume format for structural mechanics, International Journal for Numerical Methods in Engineering, Vol. 37, 181-201, 1994

[6] G.H. Xia, Y. Zhao, J. H. Yeo, X. Lv, A 3D implicit unstructured-grid finite volume method for structural dynamics, Comput Mech (2007) 40:299– 312.

[7] X. Lv, Y. Zhao, X. Y. Huang, G.H. Xia, X.H. Su, A matrix-free implicit unstructured multigrid finite volume method for simulating structural dynamics and fluid– structure interaction, Journal of Computational Physics 225 (2007) 120– 144.

[8] Guohua Xia and Ching-Long Lin, An unstructured finite volume approach for structural dynamics in response to fluid motions, Comput Struct. 2008 April ; 86(7-8): 684– 701.

[9] I. Demirdzic and D. Martinovic, Finite volume method for thermo-elasto-plastic stress analysis, Computer Methods in Applied Mechanics and Engineering 109 (1993) 331-349.
[10] I. Demirdzic , S. Muzaferija, Finite volume method for stress analysis in complex domains, International Journal for Numerical Methods in Engineering, Vol. 37, 3751-3766 (1994).
[11] A. Ivankovic, I. Demirdzic, J. G. Williams and P. S. Leevers, Application of the finite volume method to the analysis of dynamic fracture problems, International Journal of Fracture 66:357-371, 1994.
[12] I. Demirdzic , S. Muzaferija, Numerical method for coupled fluid flow, heat transfer and stress analysis using unstructured moving meshes with cells of arbitrary topology, Comput. Methods Appl. Mech. Engrg. 125 (1995) 235-255.
[13] I. Demirdzic, S. Muzaferija and M. Peric, Benchmark solutions of some structural analysis problems using finite-volume method and multigrid acceleration, International Journal for Numerical Methods in Engineering, 40 (1997), 1893-1908.
[14] I. Demirdzic, S. Muzaferija and M. Pric, Advances in computational heat yransfer, fluid flow, and solid body deformation using finite volume approaches, in Advances in Numerical Heat Transfer, vol. 1, Ed. W. J. Minkowycs and E. M. Sparrow, 1997, 59-96
[15] H. Jasak and H. G. Weller, Application of the finite volume method and unstructured meshes to linear elasticity, International Journal for Numerical Methods in Engineering, 2000; 48:267-287.
[16] J. H. Hattel and P. N. Hansen, A control volume-based finite difference method for solving the equilibrium equations in terms of displacements, Appl. Math. Modelling 1995, Vol. 19, April.
[17] P. J. Oliveira, C. J. Rente, Development and application of a finite volume method for static and transient stress analysis, Proc. NAFEMS World Congress'99 on Effective Engineering Analysis, Vol. 1, pp. 297-309
[18] A. K. Slone, C. Bailey, M. Cross, Dynamic solid mechanics using finite volume methods, Applied Mathematical Modelling 27 (2003) 69– 87.
[19] C. J. Greenshields, G. P. Venizelos and A. Ivankovic, A Fluid-structure model for fast brittle fracture in plastic pipes, Journal of Fluids and Structures (2000) 14, 221}234
[20] I. Bijelonja, I. Demirdzic, S. Muzaferija, A finite volume method for incompressible linear elasticity, Comput. Methods Appl. Mech. Engrg. 195 (2006) 6378– 6390.
[21] J. Fainberg, H. J. Leister, Finite volume multigrid solver for thermo-elastic stress analysis in anisotropic materials, Comput. Methods Appl. Mech. Engrg. 137 (1996) 167-174
[22] G. A. Taylor, M. Hughes, N. Strusevich, K. Pericleous, Finite volume methods applied to the computational modelling of welding phenomena, Applied Mathematical Modelling 26 (2002) 309– 320.
[23] G. A. Taylor, C. Bailey and M. Cross, A vertex-based finite volume method applied to non-linear material problems in computational solid mechanics, Int. J. Numer. Meth. Engng 2003; 56:507– 529.
[24] I. Bijelonja, I. Demirdzic and S. Muzaferija, A finite volume method for large strain analysis of incompressible hyperelastic materials, Int. J. Numer. Meth. Engng 2005; 64:1594– 1609.
[25] H. Basic, I. Demirdzic and S. Muzaferija, Finite volume method for simulation of extrusion processes, Int. J. Numer. Meth. Engng 2005; 62:475– 494.
[26] A.K. Slone, K. Pericleous, C. Bailey, M. Cross, Dynamic fluid– structure interaction using finite volume unstructured mesh procedures, Computers and Structures 80 (2002) 371– 390.
[27] P. Wenke, M.A. Wheel, A finite volume method for solid mechanics incorporating rotational degrees of freedom, Computers and Structures 81(2003) 321– 329.
[28] G. Papadakis, A novel pressure– velocity formulation and solution method for fluid– structure interaction problems, Journal of Computational Physics 227 (2008) 3383– 3404
[29] C. J. Greenshields and H. G. Weller, A unified formulation for continuum mechanics applied to fluid– structure interaction in flexible tubes, Int. J. Numer. Meth. Engng 2005; 64:1575– 1593.
[30] M. Scheafer, I. Teschauer, L. Kadinski, M. Selder, A numerical approach for the solution of coupled fluid– solid and thermal stress problems in crystal growth processes, Computational Materials Science 24 (2002) 409– 419
[31] A. J. Williams, T. N. Croft, M. Cross, Computational modeling of metal extrusion and forging processes, Journal of Materials Processing Technology 125-126 (2002) 53-582.
[32] A. W. Date, Solution of transport equations on unstructured meshes with cell-centered collocated variables. Part I: Discretization, International Journal of Heat and Mass Transfer, 48 (2005), 1117-1127.
[33] S. Timoshenko and J. N. Goodier, Theory of Elasticity, Second Edition, McGraw-Hill Book Company Inc., New York, 1951.

A Review of Solar Stills Augmented with Evacuated Tubes

Winners Parekh[a], NM Bhatt[b]
[a]ME Student,Gandhinagar Institue of Technology, Gandinagar, Gujarat - 382721, India
[b]Director, Gandhinagar Institute of Technology, Gandinagar, Gujarat - 382721, India

Abstract
The productivity of the solar still is determined by the temperature of water in the basin and the glass temperature. Various active methods have been adopted to increase the temperature of the water in the basin, so as to improve the productivity of solar still. Flat plate collectors, concentrating collectors, evacuated glass tubes etc are used for that purpose. This paper reviews various configurations of active solar still which are augmented with evacuated glass tubes to supply external heat to the still.

Keywords: Evacuated Glass Tube, Solar Still, Desalination

1. Introduction

Water is a precious natural gift and is being polluted by human activities, urbanization and industrialization. The ground water is often over exploited to meet the increasing demand of the people. Less than 1% of Earth's water is available for human consumption and more than 1.2 billion people still have no access to safe drinking water. Over 50% of the world population is estimated to be residing in urban areas, and almost 50% of mega cities having population over 10 million are heavily dependent on ground water, especially in the developing countries like India [1].

Most of the rural people still live in absolute poverty and often lack access to clean drinking water. Nearly half of the population is illiterate, not at all aware of the waterborne diseases affecting their health. Nearly 70% of the infectious diseases in India are waterborne. Indian villages are posed with problem of overexploitation of ground water due to increasing dependence on it as other fresh water resources are reducing fast. Various desalination techniques are used to purify the water. Solar distillation is an easy and cost effective method to provide pure drinking water in rural areas without affecting the nature. In general, solar distillation process is carried out both in passive and active modes. Normally passive solar still operates at low temperature and the daily productivity is comparatively low. Whereas, to increase the evaporation rate in an active mode the extra thermal energy is fed into the basin.

The current research in renewable energy indicates a growing interest for solar collectors with evacuated tubes. The evacuated tube solar collectors has more advantages than the flat plate collectors for water heating purposes. In flat plate collectors, sun rays are perpendicular to the collector only at noon and thus a proportion of the sunlight striking the surface of collectors is always likely to be reflected. But in evacuated tube collector, due to its cylindrical shape the sun rays are perpendicular to the surface of the glass for most of the day. Due to vacuum envelope between absorber tube and cover tube, convection losses are eliminated and hence collector efficiency is also higher. [2]

2. Active solar stills

2.1 Solar still with single basin and natural circulation

Singh et al. [3] carried out thermal analysis of a solar still integrated with evacuated tube collector in natural mode. Matlab data processing program was used by the author to determine the various parameters and its unknowns. Natural circulation rate was higher in individual tube when the radiation was at its peak and at high basin temperature. The integration of Evacuated Tube Collector (ETC) with solar still increases the water temperatures as well as yield. The daily yield obtained was 3.8 kg/m^2 for 0.03 m basin water depth. The yield decreased further with increase in water depth. The maximum daily energy and exergy efficiencies were found to be as 33.0% and 2.5% respectively. It was observed that to make the system efficient, the combination between the size of ETC and basin water depth needed adjustment. Smaller size of ETC with 10 number of tubes was preferable compared to a single unit with larger size ETC integrated system.

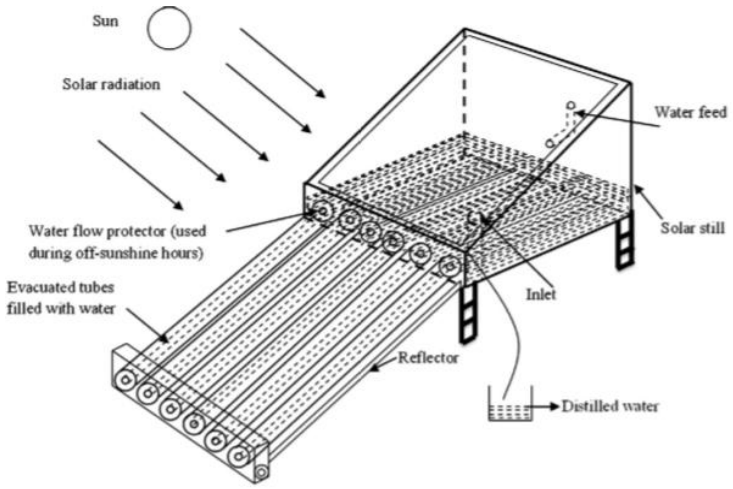

Fig.1. Schematic diagram of solar still integrated with evacuated tube collector [3]

Sampathkumar et al. [4] developed a single slope solar still directly augmented with evacuated tubes to increase the daily productivity by reducing heat losses was developed. Evacuated tubes were directly coupled to the lower side of the single slope solar still with basin area of $1m^2$. Black gravel was used to increase the productivity by means of reducing quantity of water in the basin. Extensive experiments were conducted to explore the performance of solar still in several modes namely still alone, still with black stones, still with evacuated tubes, and still with evacuated tubes and black gravel. Daily productivity was found to be 3910 ml and 4840 ml with evacuated tubes and with evacuated tubes and black gravel respectively. This was found 49.7% higher by introducing the evacuated tubes and 59.48% by coupling evacuated tubes with gravel. Due to simplicity, low cost, less energy losses and high performance, the evacuated tubes were proved to be better option for high temperature distillation when compared to the flat plate collectors. The evacuated tubes were also efficient in the winter season. Annual yield was comparatively more than other active methods like coupling of flat plat collector, parabolic collector etc.

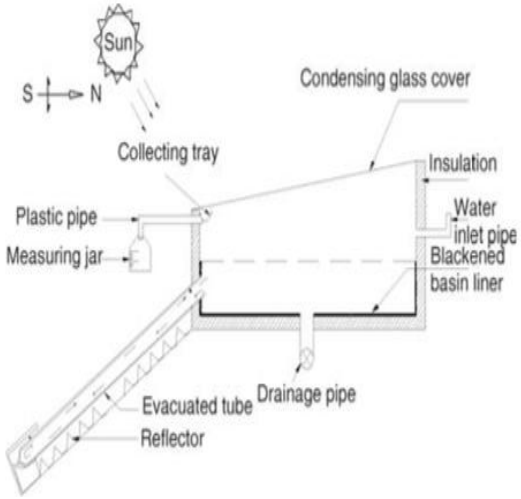

Fig. 2. Schematic diagram of solar still [4]

Fig.3. Pictorial view of solar still augmented with evacuated glass tubes [4]

Patel et al. [5] developed a single basin solar still coupled with evacuated glass tube solar collector for high temperature water feeding in to the basin of solar still. Solar still with basin area of 1 m^2 was tested with different surface coatings/materials. Its performance was varied with black, blue and red dye for brackish water. The results were compared with literature and it was observed that the productivity increased by 30.38% with the presence of black dye in water for solar still containing saline water at 10 mm depth. They concluded that output with black dye was higher compared to other dyes.

Fig.4. Schematic diagram of solar still coupled with evacuated glass tubes [5]

2.2 Solar still with single basin and forced circulation

Kumar et al. [6] developed a solar still augmented with an evacuated tube collector in forced mode was developed. FRP made solar still of 5 mm thickness having thermal conductivity of 0.351 W/m K was considered for analysis. Evacuated tubes 1.4 m long and absorbed diameter 0.044m were mounted over a diffuse reflector with centre-line spacing of 0.07m. Evacuated tubes were inclined at an angle of 45° from horizontal. Water was circulated in the still using pump. The integration of ETC with solar still increased the water temperatures as well yield. The daily yield obtained was 3.47 kg/m^2 for 0.01m basin water depth at 0.006 kg/s mass flow rate.

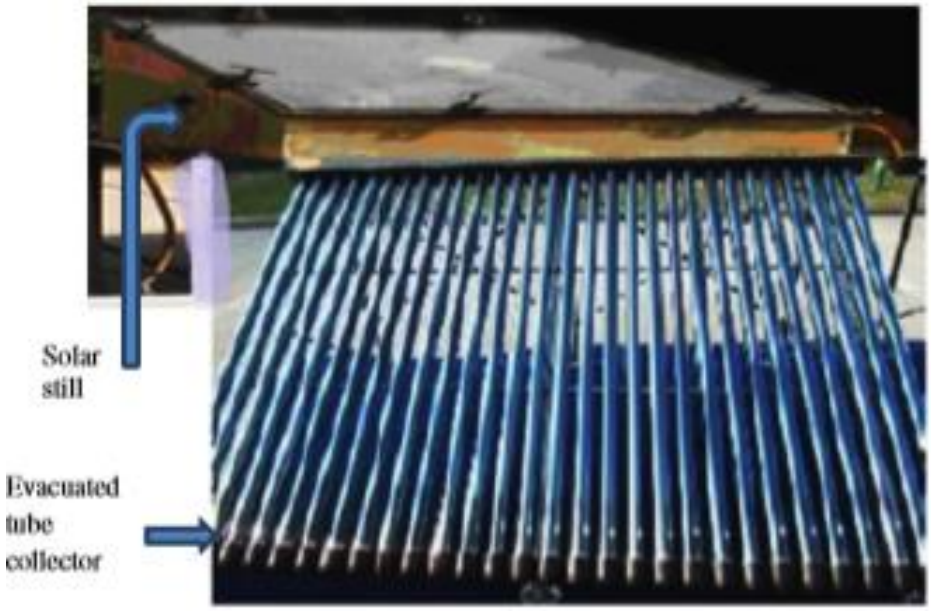

Fig.5. Photograph of evacuated tube integrated solar still in forced mode [6]

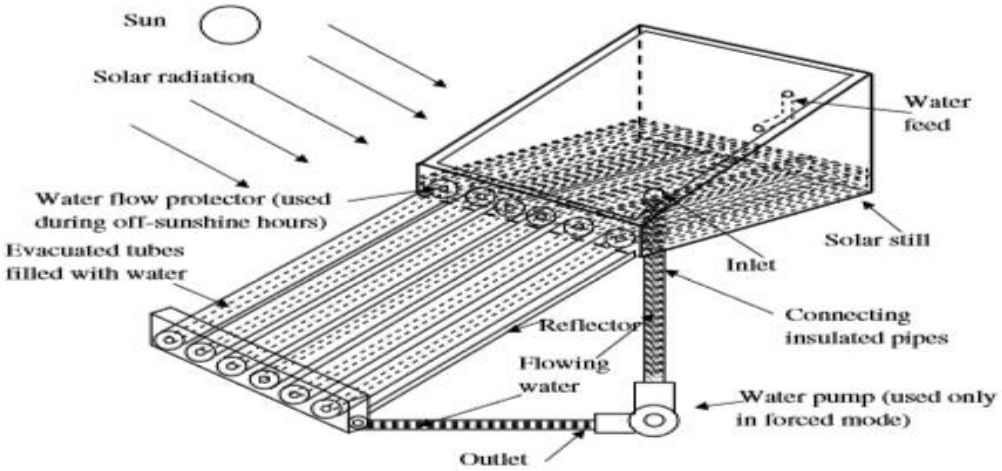

Fig. 6. Schematic diagram of evacuated tube solar still in forced mode [6]

2.3 Solar still with double basin and natural circulation

Patel et al. [7] developed a double basin active solar still coupled with evacuated glass tube solar collector and analysed its performance for high temperature water feeding in to the basin of solar still. The developed solar still with basin area of 1 m^2 was tested with double basin by using glass tray inside the solar still. Heat loss of the upper portion was reduced which gave more output of the pure water. Also the evacuated glass tubes were coupled with solar still to increase the temperature inside the solar still, which was more than 80°C. They concluded that output with double basin is more compared to single basin because of reduction of heat loss from the upper glass. The daily yield of the still was 8.8 kg/day.

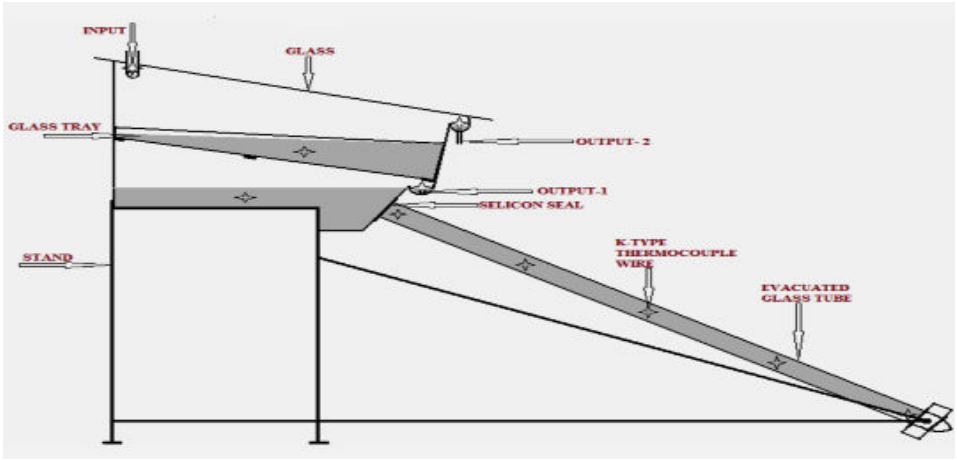

Fig. 7. Schematic diagram of double basin solar still coupled with evacuated glass tubes [7]

Panchal and Shah [8] developed a double basin solar still integrated with vacuum tubes. They introduced an additional basin to the main basin in order to utilize the latent heat of condensation which is usually lost to the environment. Vacuum tubes were also attached to the lower basin which increased the performance of the still. They proposed the use of different sensible energy storage materials like pebbles, black granite gravel and calcium stones to increase the distillate output of the double basin solar still attached with vacuum tubes. On the basis of experimental results they concluded that the distillate output of basin material with calcium stones is greater (74%) compared with that of black granite gravel and pebbles. They also concluded that integration of vacuum tubes with solar still greatly increases the distillate output of the solar still by providing hot water to the lower basin and water depth of 2 cm inside the top basin had significant influence on the thermal performance of the top basin solar still.

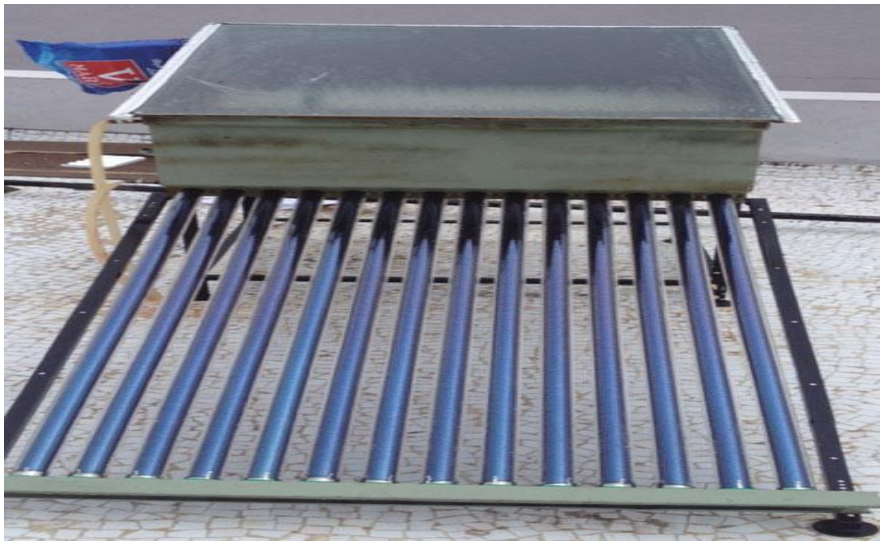

Fig. 8. Experimental setup of double basin solar still with vaccum tubes [8]

2.4 Active solar still coupled with a solar water heater

Shobha et.al. [9] effectively utilized the solar water heater for solar still productivity enhancement which works as a hybrid system. The evacuated tube solar water heater was coupled to a solar still, and the performance study was conducted at various timings with different operating conditions like solar still operated alone and hybrid still operated during daytime with various water depths and various water samples. Both theoretical and experimental analysis were conducted and the results were compared. The water quality results for different water samples for both untreated and treated water were presented. Productivity of solar still increased from 39 to 59% with hybrid unit i.e. when a solar still is coupled to a evacuated tube solar water heater and operated from 8am to 5pm. The efficiency for 1 cm water depth ranged from 43 to 52%, for 1.5 cm it ranged from 39 to 48% and for 2 cm it ranged from 32 to 41% for a hybrid solar still operated during day time. Hence it can be concluded that the efficiency of the still decreases with the increase in water depth. Adding the dissolved salt like $KMnO_4$ to river water increased the efficiency from 46.91 to 48.83% for a water depth of 1 cm.

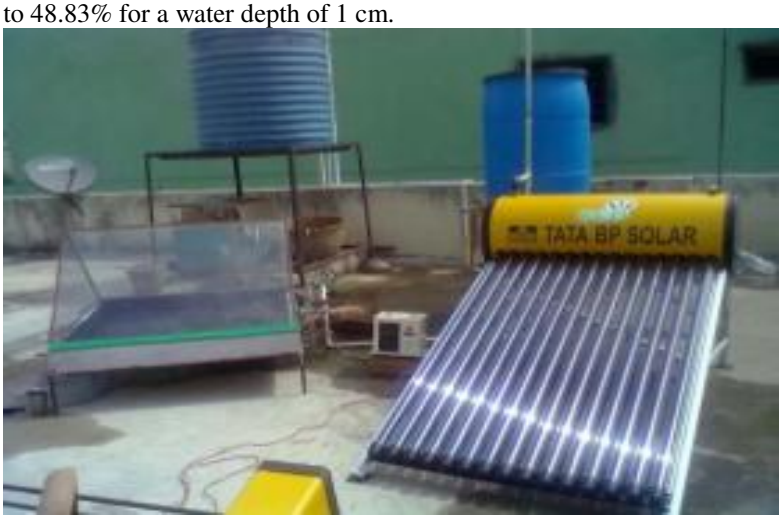

Fig. 9. Experimental setup of solar still coupled with evacuated glass tube [9]

Sampathkumar and Senthilkumar [10] experimented a solar still coupled with an evacuated type solar water heater and performance was conducted at various days at different time intervals. System operated with a hybrid nature and was capable of producing hot water and distilled water based on the situational requirement. The solar collector coupled with the still after the storage tank water temperature reached 60°C increased the yield by 77% compared to

passive solar still. Theoretical analysis was well agreed with the experimental results .The water quality results revealed that, all the samples were well agreed with standard values after distillation. Results revealed that the productivity of the still was doubled when it was coupled for 24 hours. The daily yield of the still was 4.82 kg/m^2.
.

Fig. 10. Photographic view of solar still coupled with solar water heater [10]

Table. 1 shows the comparision of yield for the different types of solar stills augmented with evacuated glass tubes.

Table. 1 Yield comparision of different solar stills

Type of solar still	Daily Yield
Solar still with single basin and natural circulation [3]	3.8 kg/m^2
Solar still with single basin and forced circulation [6]	3.47 kg/m^2
Solar still with double basin and natural circulation [7]	8.8 kg/day
Solar still coupled with a solar water heater [10]	4.82 kg/m^2

3. Conclusions

From above literature following conclusions are drawn.

- The integration of ETC with solar still increases the water temperatures and hence the yield of active solar still.
- Few researchers concluded that the annual yield is maximum when the condensing glass cover inclination is equal to the latitude of the place. However there are other groups of researcher who concluded that the optimum glass cover inclination may be 15 – 20°.
- Output with double basin is more compare to single basin because of reduce the heat loss of the upper glass.
- Solar still with an area of 1m^2 is used as standard design.
- Calcium stones possess good pore holes, which help to store the heat of solar energy as well as saline water at night, thus calcium stones can be better thermal storage material compared to black granite gravel and pebbles to increase the distillate output.
- Solar still augmented with ETC gives better yield in forced mode compared to natural mode.
- The length of solar still, depth of water in basin, inlet water temperature and solar radiation are the major parameters which affects the performance of the still.
- Due to simplicity, low cost, less energy losses and high performance the evacuated tube collector is proved to be better option for higher temperature distillation when compared to other collectors. To make the system efficient the combination between water depth and size of evacuated tube collector needs adjustments.

- Active solar still coupled with evacuated tube collector having 8 to 10 number of tubes is preferable.
- In case of active solar still coupled with evacuated tubes, the saline water directly comes in contact with inner glass tube and cause scale formation which may reduce the heat transfer and efficiency significantly.

References:

11. Journal articles:

[1] Prasad, R. N., Ram Chandra, Tiwari, K.K., 2008. Status of Ground Water Quality of Lalsot Urban Area in Dausa District, Rajasthan, Journal of Nature Environment and Pollution Technology 7, p. 377-384

[2] Desai Nikul, N M Bhatt, Nimesh Gajjar, 2014. A Review on Active Solar Stills, GIT Journal of Engineering and Technology, 7, p.1-7

[3] Ragh Vendra Singh, Shiv Kumar, M.M. Hasan, G.N. Tiwari, 2013. Performance of Solar Still Integrated with Evacuated Tube Collector in Natural Mode, Desalination, 318, p. 25-33

[4] Sampathkumar Karuppusamy, 2012. An Experimental Study on Single Basin Solar Still Augmented With Evacuated Tubes, Thermal Science, 16, p. 573-581

[5] Mitesh I. Patel, P.M. Meena and Sunil Inkia, 2012. Effect of Dye on Distillation of a Single Slope Active Solar Still Coupled With Evacuated Glass Tube Solar collector, International Journal of Engineering Research and Applications, 1, p.456-460

[6] Shiv Kumar, Aseem Dubey, G.N. Tiwari, 2014. A Solar Still Augmented with an Evacuated Tube Collector in Forced Mode, Desalination, 347, p.15-24

[7] Mitesh I. Patel, P.M. Meena and Sunil Inkia, 2011. Experimental Investigation on Single Slope Double Basin Active Solar Still Coupled With Evacuated Glass Tubes, International Journal of Advanced Engineering and Research and Studies, 1, p.4-9

[8] Hitesh N Panchal and P.K. Shah, 2014. Enhancement of Distillate Output of Double Basin Solar Still with Vacuum Tubes, Front. Energy, 8, p. 101-109

[9] Shobha B.S, Vilas Watwe, Rajesh A.M. 2012. Performance Evaluation of a Solar Still Coupled to an Evacuated Tube Collector Type Solar Water Heater, International Journal of Innovations in Engineering and Technology, 1, p.72-84

[10] K. Sampathkumar and P. Senthilkumar, 2012. Utilization of Solar Water Heater in a Single Basin Solar Still – An Experimental Study, Desalination, 297, p. 8-19

A Review of Solar Stills Augmented with Thermal Storage Media

Jigar Rajput[a], Prexa Parikh[b], N M Bhatt[c]

[a]ME Student, L. J. Institute of Engineering & Technology,S.G. Highway Sarkhej,Ahmedabad,Gujarat- 382210,India
[b]Assistant Professor, L. J. Institute of Engineering & Technology,S.G. Highway Sarkhej,Ahmedabad,Gujarat- 382210,India
[c]Director, Gandhinagar Institute of Technology,Khatraj,Gandinagar district,Kalol,Gujarat- 382721,India

Abstract
Solar distillation is both economical and eco-friendly technique to convert impure water into potable water particularly in rural areas. Many active distillation systems have been developed to overcome the problem of lower distillate in passive solar stills. The productivity of the solar still is determined by the temperature of water in the basin and the glass temperature. Different materials such as black cotton, pebbles, rocks, charcoal, rubber, calcium stones, cement, bricks etc. are used in the basin along with water to improve the heat capacity, radiation absorption capacity and enhance the evaporation rate. This paper reviews various solar stills augmented with thermal storage media.

Keywords: Active Solar Still, Desalination, Thermal Storage Media, Heat Capacity

1. Introduction

There is an urgent need of clean, pure drinkable water in many countries. Often water sources are brackish and or contains harmful bacteria and therefore cannot be used for drinking. The ground water is often over exploited to meet the increasing demand of the people. Less than 1% of Earth's water is available for human consumption and more than 1.2 billion people still have no access to safe drinking water. More than 50% of the world population is estimated to be residing in urban areas, and almost 50% of mega cities having population over 10 million are heavily dependent on ground water, especially in the developing countries like India [1].

Only 3% of total water is potable but this amount is also evenly not distributed over the earth. Lack of fresh water is a prime factor in inhibiting regional /economical development. The oceans constitute an inexhaustible source of water but are unfit for human consumption due to their salt content in the range of 3% to 5%. In addition, there are many coastal locations where seawater is abundant but potable water is not available. In recent years desalination of water has been one of the most important technological work undertaken in many countries. Solar distillation is an easy and cost effective method to provide pure drinking water in rural areas without affecting the nature. In general, solar distillation process is carried out both in passive and active modes. Normally passive solar still operates in low temperature and the daily productivity is comparatively low. Whereas, to increase the evaporation rate in an active mode the extra thermal energy is fed into the basin [2].

The current research in renewable energy indicates a growing interest for use of various thermal heat storage media like die, calcium stones, cotton, charcoal, rubber, ink, sponge, black rock, clay pots, cement, bricks, sand and pebbles in order to increase the productivity of the still.

2. Solar stills with thermal storage media

2.1 Passive solar stills

2.1.1 Single slope still using charcoal

Naim and Kawi [3] developed a solar still in which charcoal functioned as a heat absorber medium and as wick. The still presented a 15% improvement in productivity over wick-type stills reported in literature. The still was cheap, simple to construct, and in addition had the advantages of low thermal capacity, lightweight and ease of operation. It was made of plastic outer rectangular body in which salt water was allowed to percolate through a charcoal bed of particles that extended the length of the still, and above which a glass plate was made to cover the still at an optimum distance from the charcoal bed. The still bottom was insulated by a suitable layer of sawdust and the still was mounted on a wooden frame of adjustable inclination. The factors investigated were size and range of charcoal

particles, brine flowrate, and still inclination to the horizontal. They concluded that the maximum yield of the still was 2.12 l/m^2 day for a sunny day in summer. The efficiency of the still was 32.3 %.

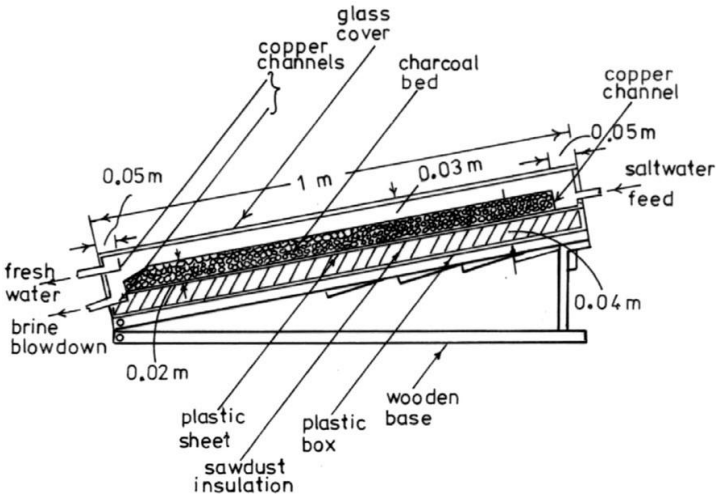

Fig. 1 Schematic diagram of the charcoal solar still [3]

2.1.2 Single slope still using rubber matt, ink and black dye

Different types of absorbing materials like rubber mate and charcoal were used in the basin along with water to improve the absorption and heat capacity and hence the production of solar still [4]. The researchers have also performed experiments by adding black dye in the basin water to improve the absorption of solar radiation by top layer of the water. Fig. 2 compares the effect of different energy absorbing materials placed along with basin water. Results showed that black dye was the best energy absorbing material to increase the still productivity.

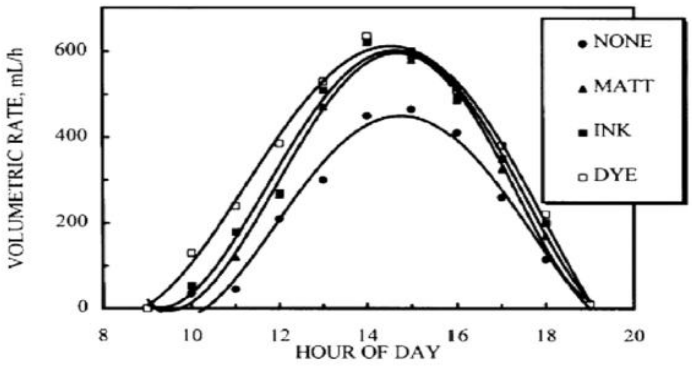

Fig. 2 Water production for various absorption materials [4]

2.1.3 Single slope still using black granite and iron steel

Jadhav [5] developed a single basin solar still and used black granite and iron steel as different basin materials to increase the productivity of the still. The experimental results showed that the productivity of distilled water was enhanced by black granite basin solar still as compared to iron steel basin solar still. The productivity of the granite basin solar still was 3.784 l/m^2 day, whereas the same for iron steel basin still was 2.358 l/m^2 day, which was nearly 38% higher than the iron steel basin still. Basin water temperature in the granite basin still was increased up to 87°C compared to 79°C in iron steel basin still water.

Fig. 3 Photographic view of black granite single basin solar still [5]

Fig. 4 shows that the productivity of both stills was increasing until it reached the maximum during the afternoon, and then decreased. The productivity of the granite basin solar still increased fast after 10 a.m. and reached to maximum at 12 a.m. and became nearly constant up to 2 p.m., and then decreased. Whereas the productivity of iron steel basin still increases linearly and reaches the maximum between 1p.m. to 2 p.m., and then decreased. The productivity rate of granite still was considerably greater than that of iron still between 11 a.m. to 3 p.m. The granite solar still gave more yield than iron steel solar still due to higher water temperature in the still. Higher water temperature of granite solar still attribute to higher absorption of solar radiation and higher heat capacity. An overall result showed that the productivity of granite basin still was 15% higher than that of the conventional still.

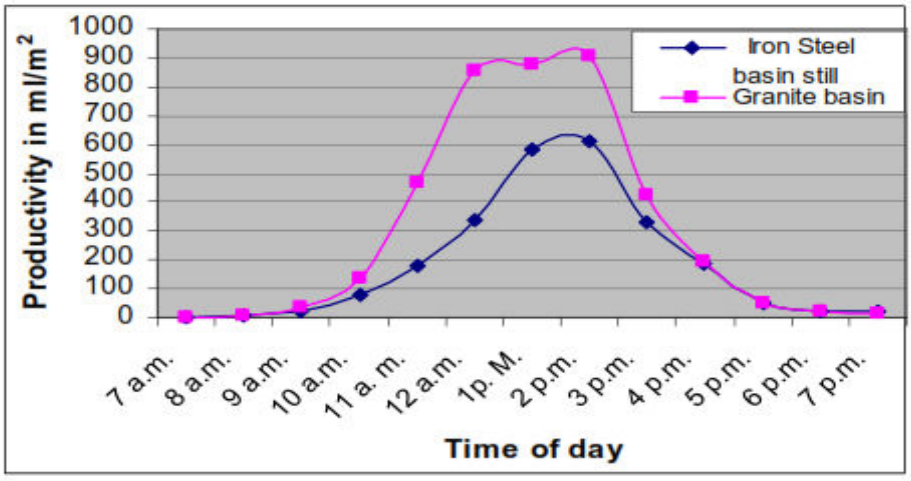

Fig. 4 Time versus productivity for granite and iron steel basin solar still [5]

2.1.4 Double slope single basin still using cotton cloth, sponge sheet, coir mate and light jute

Murugavel and Srithar [6] developed a single basin double slope solar still in which layer of water with wick materials in the basin was used to decrease the volumetric heat capacity of the basin in order to increase the evaporation area and to enhance its productivity as shown in Fig. 5. A basin type double slope solar still with mild steel plate was fabricated and tested with minimum mass of water and different wick materials like light black cotton cloth, sponge sheet, coir mate, waste cotton pieces and light jute cloth in the basin. Still with aluminium rectangular fin arranged in different configurations and covered with different wicks were also tested. They found that the still with light black cotton cloth was the most effective wick material. The still with rectangular aluminium fin covered with black cotton cloth and arranged in length wise direction was more effective.

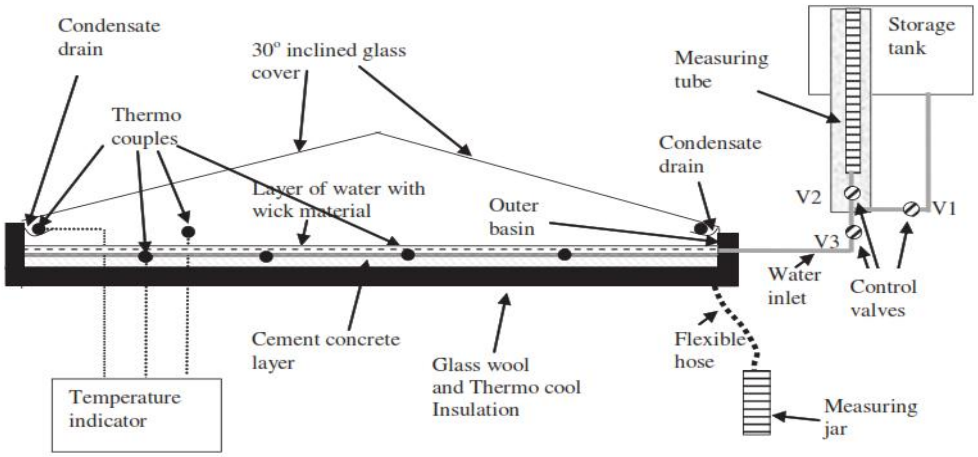

Fig. 5 Single basin double slope solar still [6]

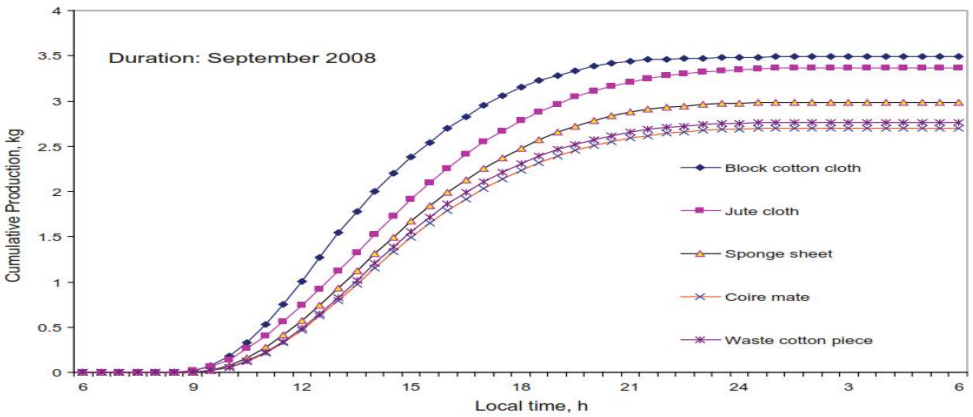

Fig. 6 Variation of cumulative production for different wick materials [6]

Fig. 6 shows the actual cumulative production rate variations of the still for different wick materials in the basin. The production rate variations and the cumulative production was higher throughout the day for the still with black cotton cloth in the basin compared to other materials.

Fig. 7 Variation of total distillate production for various basin materials [6]

Fig. 7 shows the actual total production variations of the still for different wick materials in the basin. The

aluminium rectangular fin covered with cotton cloth and arranged in length wise direction was more effective and gave slightly higher production than the light black cotton cloth. It was also observed that different arrangement of the aluminium fin had insignificant effect on the productivity for particular wick material. This is obvious also as aluminium fin acts thermal storage media only.

2.1.5 Single slope stills using black rock and coated and uncoated metallic sponge

Abdulla et al. [7] conducted experiments by using three different absorbing materials viz. uncoated metallic wiry sponges, coated metallic wiry sponges and black volcanic rocks as heat absorbing materials as shown in Fig.8. Experiments were carried out in three different stills using the above absorbing materials in each still. The fourth still was used as a reference still with no absorbing materials. The top cover of the stills was at an angle inclined to 32° with the horizontal. It was made of glass of 4 mm thickness. Water was poured at a height of 6 cm into all the stills. The volume of the basin with untreated water was 69.3 cm × 69.3 cm × 6.3 cm. All the three stills with absorbing materials gave better productivity than the reference still. The water collection gain in the still with black rock was 60% whereas for coated and uncoated metallic wiry sponges it was around 28% and 43% respectively. Also, there were corrosion problems in the metallic wiry sponges. Hence it was concluded that the black rocks were effective than coated and uncoated metallic wiry sponges.

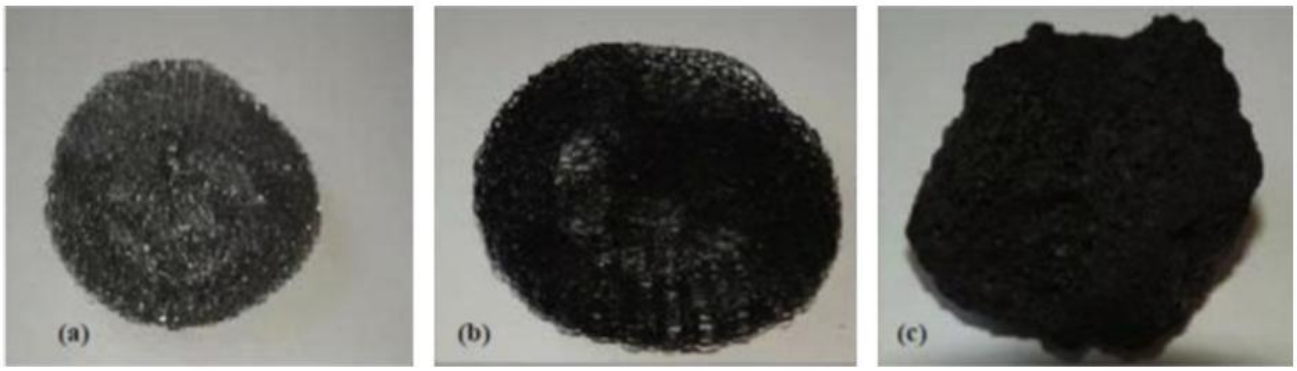

Fig. 8 Absorbing materials used in solar stills (a) uncoated metallic wiry sponge (b) coated metallic wiry sponge (c) black rock [7]

Fig.9 shows the amount of distilled water collected for the four solar stills from 7:00 to 19:00 hrs. Figure shows an increase in the collected water during early hours of the day until it reaches the maximum yield around mid-noon corresponding to the highest solar radiation and then decreases due to sunset. It clearly indicates that three stills that contained the absorbing materials gave much better water collection than the reference still. Also the maximum water collection in the reference still was around 13:00 to 15:00 hrs, whereas the maximum water collection for the other stills was shifted to 15:00 to 17:00 hrs. This was due to the absorbing and releasing of the solar heat from the storage materials.

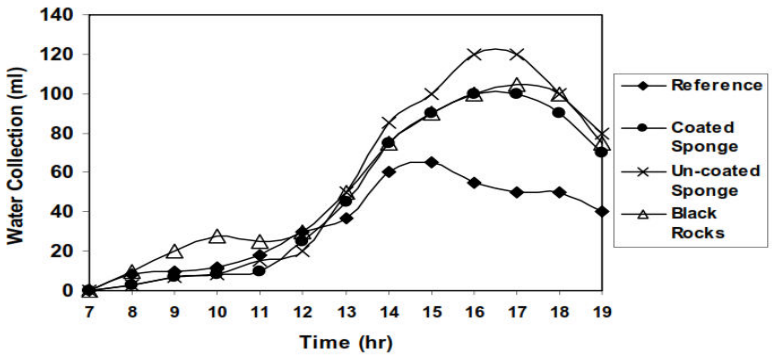

Fig. 9 Collected distilled water for the four solar stills with and without porous materials [7]

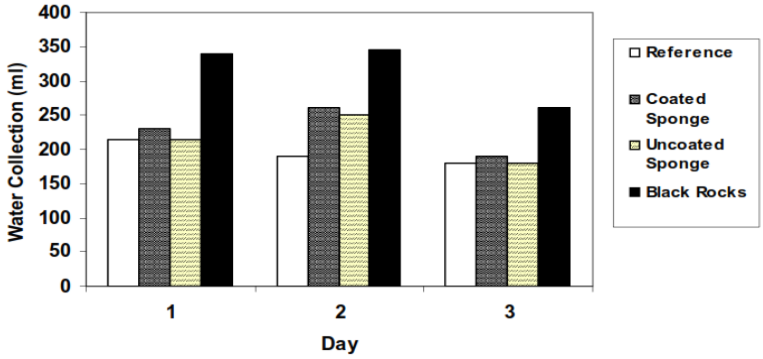

Fig. 10 Overnight water collection for the four solar stills with and without porous materials over three days [7]

Fig.10 shows that black rocks followed by black coated wiry sponge gave the highest water collection overnight. It may be due to capability of the black rocks and coated sponges to absorb and store large amounts of solar radiation and to act as heat storage media for the water in the basin.

2.1.6 Single basin double slope still using quartzite rock, concrete pieces, bricks, stones and iron scraps

Murugavel et al. [8] developed a single basin double slope solar still fabricated with mild steel plate and tested it with a layer of water and different sensible heat storage materials like quartzite rock, red brick pieces, cement concrete pieces, washed stones and iron scraps. Fig. 11 shows the photographic view of different energy storing materials used in the basin and Fig.12 shows the photograph of the still with 1½ in. cement concrete pieces in the basin. The still was also theoretically modelled and theoretical performance was compared with actual performance. They concluded that the theoretical results were deviated more with actual results.

Fig. 13 compares the overall production of the still with different basin materials. Of all basin materials ¾ in. quartzite rock was the most productive material when water depth was 7.5mm. At the same condition the production rate was enhanced by 6.2% compared with the still with layer water of 5mm depth and light cotton cloth as spreading material.

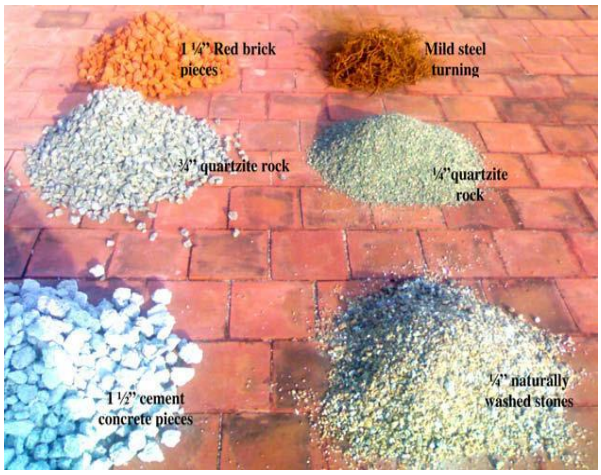

Fig. 11 Photograph of sensible energy storage materials pieces in the basin [8]

Fig. 12 Photograph of the still with 1½ in. cement concrete used in the basin [8]

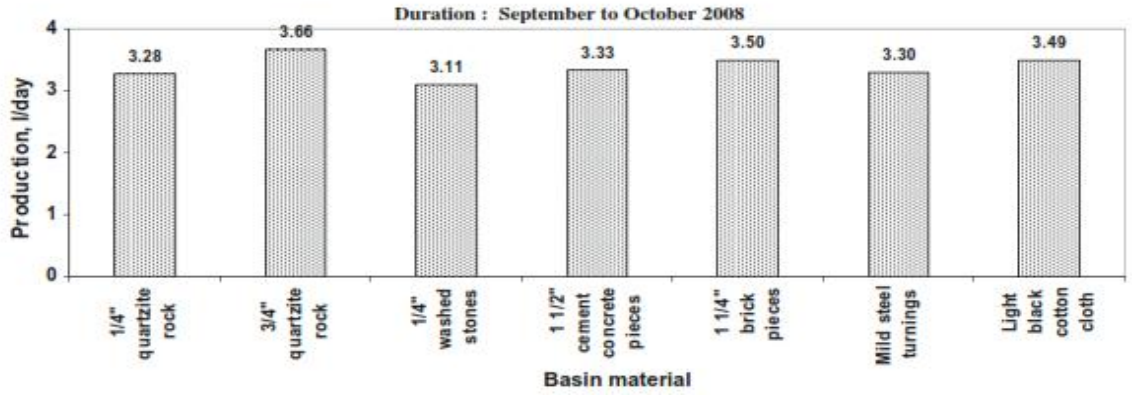

Fig. 13 Overall productions for different materials [8]

2.1.7 Single and double basin double slope stills using cotton, clay pots and mild steel

T. Rajaseenivasan et al. [9] adopted a new approach to enhance the productivity of a solar still by introducing an additional basin in the double slope solar still. As shown in Fig.14, two solar stills, single basin double slope and double basin double slope with the same basin area were fabricated and tested at Kovilpatti, Tamil Nadu, India. The experiments were conducted with various depths of water, different wick materials, porous material and energy storing material. In double basin still, mass of water in upper basin was constant for all experiments. For both stills, water production decreased with increase of water depth.

Performances of the stills were studied for wick materials (black cotton cloth, waste cotton pieces and jute cloth), porous material (clay pot facing up and facing down) and heat storing material (black painted mild steel pieces) in the single basin and lower basin of the double basin still. For double basin still, various wick and other materials were used only in the lower basin.

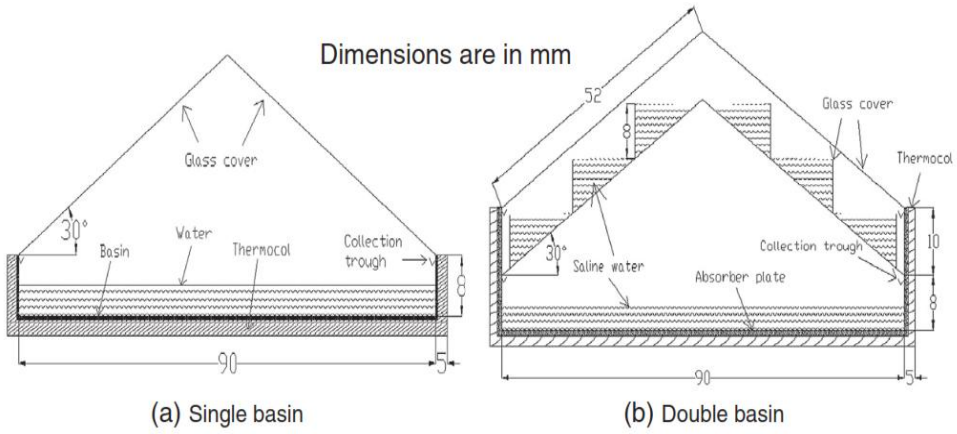

Fig. 14 Schematic diagram of the stills [9]

Along with these materials as shown in Fig.15 water mass equivalent to 2 cm depth was used in both the stills. Basin water heating and cooling rate significantly vary with volumetric heat capacity of the basin. Temperature rise was fast during heating and reverse effect was observed during cooling for the still with cotton cloth which had minimum heat capacity. They noticed that mild steel stored, retained and released heat at higher temperature during the cooling process.

1. Black cotton cloth, 2. Jute cloth, 3.Waste cotton pieces, 4. Clay pot – facing up,
5- Clay pot – facing down, 6. Mild steel pieces

Fig. 15 Photographic view of different wick, porous and heat storage materials used for the study [9]

Fig. 16 shows the cumulative production of the stills for different materials in the basin. Due to higher temperature and diffusion effect, the still with black cotton cloth had higher production during heating period and the cumulative production was higher through the entire day. Due to porous effect, the still with clay pot has higher production at lower temperature. During heating period because of lower basin temperature the production was low but due to release of heat at higher temperature during prolonged cooling period, the cumulative production was higher for still with mild steel pieces. The cumulative production for the mild steel for single basin was 1.94 l/day and for double basin was 3.58 l/day which was highest compared to all other wick and porous materials.

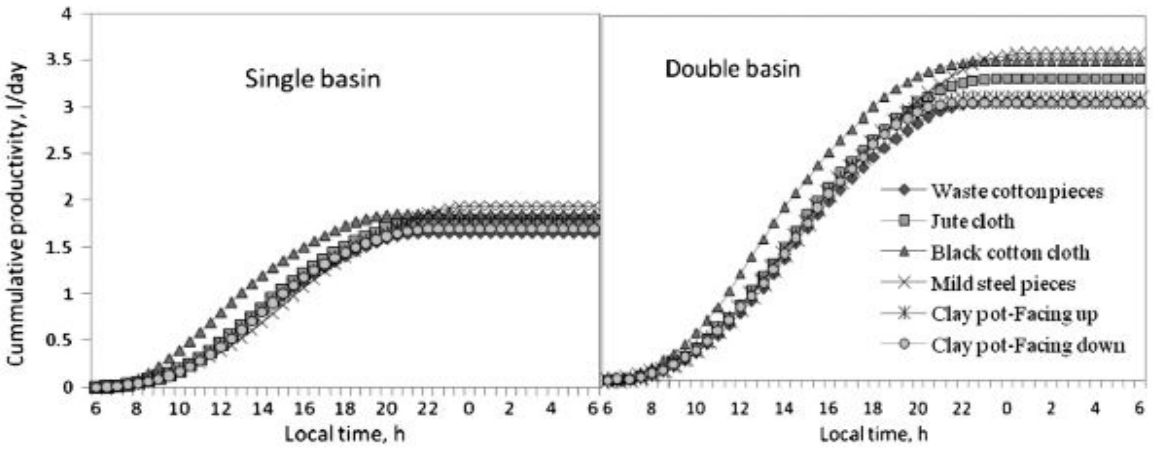

Fig. 16 Variation of cumulative production for different materials [9]

2.2 Active solar stills

2.2.1 Single slope still using different dyes

Mitesh et al. [10] developed a single basin solar still coupled with evacuated glass tube solar collector for high temperature water feeding in to the basin of solar still as shown in Fig.17. Solar still with basin area of 1 m^2 was tested with black, blue and red dyes for brackish water.

Fig. 17 Schematic diagram of solar still coupled with evacuated glass tubes [10]

The results were compared with literature where it was observed that the productivity increased by 30.38% with the presence of black dye in water for solar still containing saline water at 10 mm depth. They concluded that output with black dye was higher compared to other dyes. They also noticed marginally better performance with dye for higher depths.

2.2.2 Single slope still using rocks and pebbles

Alaudeen et al. [11] used a stepped solar still to enhance the productivity of the solar still as shown in Fig. 18. The concept of integrating the stepped solar still along with inclined flat plate collector was introduced. In the stepped type solar still, a conventional basin of 1 m^2 area was placed at the bottom. Another stepped type absorber plate was fixed on the top of the conventional basin. It consisted subsequent trays and inclined flat plate collectors. This ensured an additional exposure area which augmented evaporation rate. Experiments were conducted with various depths in the conventional basin solar still which was tested simultaneously with the experimental set up for comparison. Sensible heat storage mediums such as rocks, pebbles were added to the top basin of stepped trays and bottom of conventional basins to increase the temperature of water in the still. Wicks were placed on the inclined flat plate collector to augment the evaporation rate due to capillarity.

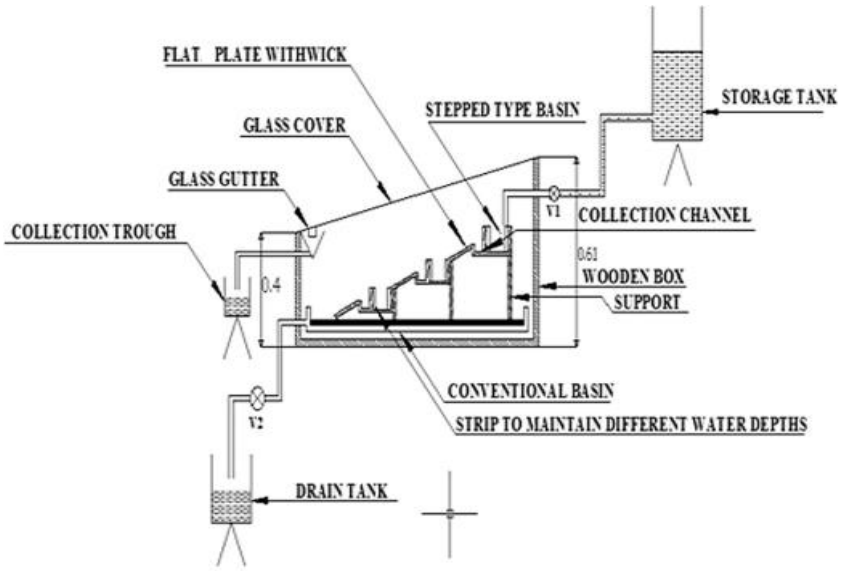

Fig. 18 Sectional view of the stepped type solar still [11]

Fig. 19 shows the daily efficiency for different modifications made in the stepped type basin as well as the conventional basin. It can be observed from the figure that the daily efficiency of the conventional still tested on various days were ranging from 7% to 14% where as in the stepped type basin still it was maximum up to 16%. Also providing high sensible heat by pebbles or rocks in the trays of the stepped solar still,more energy was stored and hence the efficiency was higher.

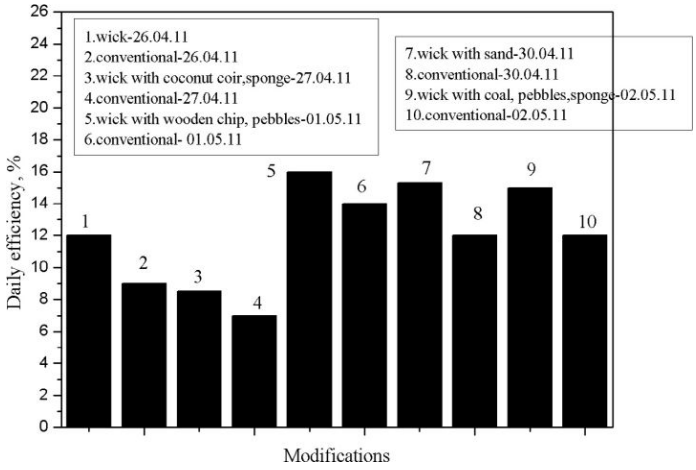

Fig. 19 Effect of modifications on daily efficiency [11]

2.2.3 Single slope still using sand

El-Sebaii et al. [12] developed transient mathematical models for an active single basin solar still with and without a sensible storage material in the basin of the still as shown in Fig. 20. Sand was used as a storage material due to its availability. The flowing water temperature was assumed to vary with time and space coordinates. Analytical expressions were obtained for various temperatures of the still elements as well as for the temperature of sand. The performance of the still with and without storage was investigated by computer simulation using the climatic conditions of Jeddah (lat. 21° 42' N, long. 39° 11' E), Saudi Arabia. Effects of mass flow rate and thickness of the flowing water for different masses of the storage material on the daylight (P_{dl}), overnight (P_{on}), daily productivity (P_d) and efficiency (η_d) of the still were studied. The dependence of daily productivity and efficiency of the still on the thickness and thermal conductivity of the basin liner material was also investigated. They found that daily productivity and efficiency of the still decreased with the increase in mass of the storage material, due to the increased heat capacity of the storage material. Furthermore, that daily productivity and efficiency of the still were found to decrease with increasing thermal conductivity of the basin linear material. On a summer day, daily yield of 4.005 kg/m^{2}day with a daily efficiency of 37.8% was obtained using 10 kg of sand compared to 2.852 kg/m^2 day with a daily efficiency of 27% when the still was used without sand at 0.03 m depth of water in the basin. The annual average of daily productivity of the still with storage was found to be 23.8% higher than that when it is used without storage.

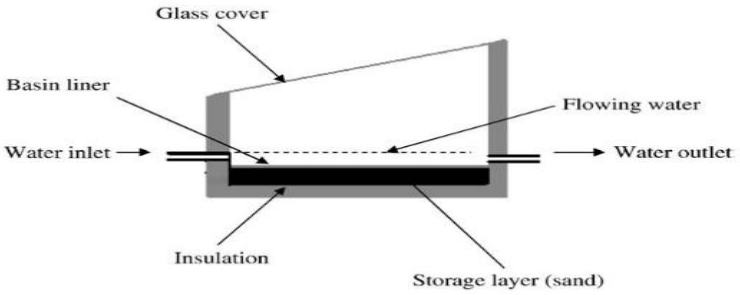

Fig. 20 Schematic diagram of the active single basin solar still with sensible storage material [12]

They concluded that daylight, overnight, daily productivity and efficiency of the still decreases with increasing mass of the storage material (m_{st}) due to the increased heat capacity of the sand, but overnight productivity is less dependent on mass of the storage material.

Fig. 21 shows that a maximum productivity of 0.431 kg/m^{2}h was obtained at 18:00 hrs compared to 0.316 kg/m^{2}h at 13:00 hrs with and without storage respectively. The daily productivity, calculated from the results was 3.908 kg/m^{2}day with a daily efficiency of 36.9% when the still was used with 10 kg of sand. Without sand, the corresponding values of daily productivity and daily efficiency were 2.875 kg/m^{2}day and 27.24%, respectively.

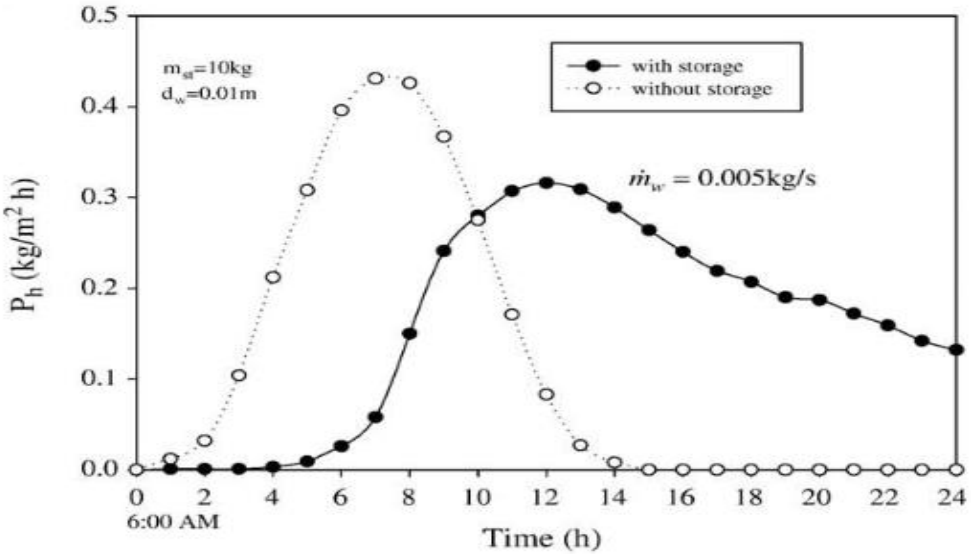

Fig. 21 Hourly variations of productivity of the still without and with sand as a storage material on a summer day [12]

Fig. 22 shows the variations of of hourly productivity with time for different masses of sand. It shows that hourly productivity decreases gradually with the increase in mass of sand. Also at higher values of the mass of sand the curve becomes more flat especially during the night time due to the high storage capacity of the sand itself.

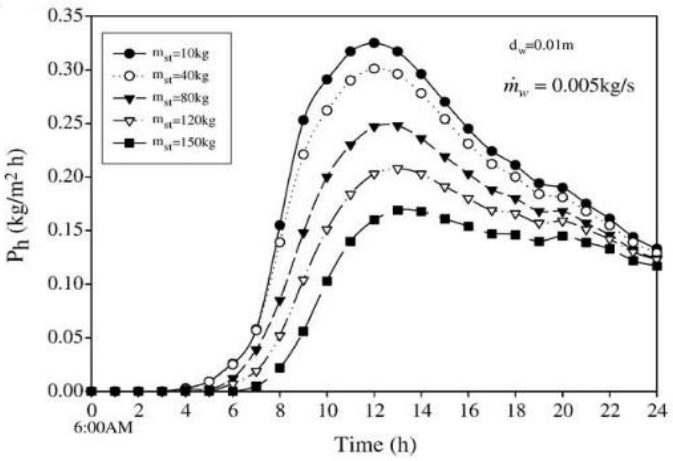

Fig. 22 Variations of hourly productivity of active solar still for different masses of sand on a summer day [12]

3. Conclusions

From above literature study, following conclusions are drawn.

- Charcoal granules can effectively work as thermal storage media as well as wick material. Optimum sized charcoal can give improvement up to 15% in the productivity over other wick-type solar still.
- Dye of various colours and ink have been used in active and passive solar stills to increase the absorption of solar radiation. Due to higher absorptivity, black dye gives better performance over other dye and ink.
- Cotton cloths, sponge sheet, coir mate, light jute have been effective as wick materials which decreases the volumetric heat capacity of water for different types of still. This increase the yield compared to conventional still. Due to higher absorptivity, black cotton cloth has proved to be better compared to other wick materials.
- To store the solar energy during day time and use the same during night hours, black granite, black rock, coated and uncoated wiry sponge, quartzite rocks, cement concrete pieces, brick pieces, mild steel pieces, aluminium fins, sand, rubber mate etc. have been used as thermal storage media in different types of still. It can be concluded form the experiments performed by different researchers that there is optimum mass/heat capacity of thermal storage media which gives maximum yield for given configuration of solar still. For same thermal storage media, optimum mass/heat capacity depends on location and types of solar still.
- Thermal storage materials along with wick materials gives slightly better output. However different arrangements of thermal storage materials as long as they are evenly distributed in the basin, have insignificant effect on distil output of the still.
- Output of the double basin passive and active solar still is higher than that of conventional single basin passive solar still due to use of latent heat of condensation to generate additional distil output and higher absorption of solar radiation respectively.
- For lower solar radiation intensity places shallow basin still is preferable whereas for higher solar radiation intensity deep basin still is preferable.
- Daily cleaning of the basin along with the thermal storage media increases the productivity of the still.

References:

- Journal articles:

[1] Prasad, R. N., Ram Chandra, Tiwari, K.K., 2008. Status of Ground Water Quality of Lalsot Urban Area in Dausa District, Rajasthan, Journal of Nature Environment and Pollution Technology 7, p. 377-384

[2] Shobha B.S, Vilas Watwe, Rajesh A.M., 2012. Performance Evaluation of a Solar Still Coupled to an Evacuated Tube Collector Type Solar Water Heater, International Journal of Innovations in Engineering and Technology, 1, p.72-84

[3] Mona M. Naim, Mervat A. Abd EI Kawi, 2002. Nonconventional Solar Stills with Charcoal Particles as Absorber Medium, Desalination 153, p. 55-64

[4] Bilal A. Akash, Mousa S. Mohsen, Omar Osta and Yaser Elayan, 1998. Experimental Evaluation of a Single-Basin Solar Still Using Different Absorbing Materials, Renewable Energy, 14 p. 307–310.

[5] Jadhav Madhav V., 2011. Performance of Black Granite Solar Still - A Comparative Study, International Journal on Engineering Technology and Sciences Vol 2. p. 161-168.

[6] K. Kalidasa Murugavel, K. Srithar., 2011. Performance Study on Basin Type Double Slope Solar Still with Different Wick Materials and Minimum Mass of Water, Desalination 36, p. 612-620.

[7] Abdullah Salah, Mazen Abu-Khader M, Badran Omar, 2009. Effect of Various Absorbing Materials on the Thermal Performance of Solar Stills, Desalination 242: p. 128–37

[8] K. Kalidasa Murugavel, Kn.S.K. Chockalingam, S. Sivakumar, J. Riaz Ahmed K. Srithar, 2010. Single Basin Solar Still with Minimum Basin Depth and Energy Storing Materials, Applied energy, 87, p. 514-523

[9] T. Rajaseenivasan, T.Elango, K Kalidasa Murugavel, 2013 .Comparative Study of Double Basin and Single Basin Solar Still, Desalination 309, p. 27-31.

[10] Mitesh I. Patel, P.M. Meena and Sunil Inkia, 2012. Effect of Dye on Distillation of a Single Slope Active Solar Still Coupled With Evacuated Glass Tube Solar collector, International Journal of Engineering Research and Applications, 1, p.456-460

[11] A.Alaudeen, K. Johnson, P. Ganasundar, A.Syed Abuthahir, K. Srithar, 2014. Study on Stepped Type Basin in a Solar Still, Desalination 26 p. 176-183.

[12] A.A. EI – Sebaii, S.J. Yaghmour , F.S. Al- Hazmi, Adel S. Faidah, F.M. Al – Marzouki, A.A. Al- Ghamdi, 2009. Active Single Basin Solar Still with a Sensible Storage Media, Desalination 249, p. 699-706.

Hydroforming Process - An Automotive Guide

Parekh V.R.

Assistant Professor, SVMIT-Bharuch,Old National Highway-8,Gujarat-392001,India

Abstract

The Tube Hydroforming (THF) & Sheet hydroforming process are relatively new manufacturing technologies & become most famous in recent years, due to the increasing demands for lightweight parts in various fields, such as bicycle, automotive, aircraft and aerospace industries. Hydroforming enables manufacturing of closed sections with non-uniform cross-sectional areas along the length by using a circular tube as the input material. Sheet hydroforming process is an alternative to drawing process where either punch or die is replaced by hydraulic medium, which generates the pressure and forms the part, while tube hydroforming (THF) is best & most popular unconventional metal forming processes which is widely used to form various tubular components. More focus of this paper on tube hydroforming process, profile & parameters. By this process, tubes are formed into different profile using internal pressure and axial compressive loads simultaneously to force a tubular blank to conform to the internal shape of a given die cavity. The success of a THF process is, however, dependent on a various parameters such as the loading path, lubrication conditions, and material formability & many others. THF offer some other advantages as compared to conventional manufacturing via stamping and welding. THF also offers potential in design of structures with high stiffness & alternatives in the use of lightweight materials and hence can have a great impact in saving energy in the automotive industry. The computer simulation of THF processes using the FEM has proven to be most efficient and useful, as it allows for the virtual testing and comparison of several candidate processes, thus avoiding the use of costly "trial and error" prototype tests.

Keywords: Hydroforming , Automotive Applications, Failure mode, Bulge Test, FEM

1. Introduction

Metal Forming has played central role as societies have developed [1]. Sheet-metal forming processes are technologically among the most important metalworking processes. Products made by these processes include a large variety of shapes and sizes. In general metal forming processes are characteristic in that the metal being processed is plastically deformed in order to shape it into a desired geometry. The material actually gets stronger the more it is deformed plastically. This is called strain hardening or work hardening. As may be expected, strain hardening is a very important factor in metal forming processes. During a metal forming operation it is important to know the force and power that will be needed to accomplish the necessary deformation. The flow stress is the instantaneous value of the force necessary to continue the yielding and flow of the work material at any point during the process. The flow stress value can be used to analyze what is going on at any particular point in the metal forming process. In general there are many manufacturing processes such as rolling, extrusion, forging, bending, tube bending, stamping, shearing, sheet metalworking, pressing, explosive forming, micro forming, hydroforming & many others for different types of metal forming processes the flow stress analysis may be different. The strain rate for any particular manufacturing metal forming process is directly related to the speed at which deformation is occurring. A greater rate of deformation of the work piece would mean a higher strain rate.

In all metal forming process a Tube hydroforming process is one of the best & most popular unconventional metals forming processes which is widely used to form various tubular components. Tube Hydroforming (THF) has been called by many other names such as bulge forming of tubes (BFT's), liquid bulge forming (LBF) and hydraulic pressure forming (HPF) depending on the time and country in which it was used [2]. Establishment of process goes back to 1939 when Grey et al. [3] investigated manufacturing of Seamless copper fittings with T protrusions using a combination of internal pressure and axial load. The investigation was considered as a US patent in the 1940, which gave an indication of the coming period of tube hydroforming. By [4] define the Hydroforming process basically is a technique that uses a fluid either to form or aid in forming a part from ductile metal. By [5] in between 1950 and 1970, researchers in the United States, United Kingdom and Japan developed related patents and application products. After 1970, researchers in Germany studied tube hydroforming and applied it to produce structural parts for automobiles. Since the early 1980's, tube hydroforming has been increasingly used in the automotive and aerospace industries, manufacturing of household appliances, and other applications. THF offers potential alternatives in the use of lightweight materials and hence can have a great impact in saving energy in the automotive industry.[6] In 2000 has summarized a technological review of

hydroforming process from its early years to very recent dates on various topics such as material, tribology, equipment, tooling, and many others. [7] Has discussed the application of bulge forming to manufacturing near net shape components. He has also discussed about that machine & tool design & illustrates how FE simulation is playing an improving role in design of bulge forming process in 2001. [25] In 2002 have analyzed necking & bursting effect in flange & tube hydroforming by considering influence of material & process parameter, which were applied to illustrating for tube and flange hydro-forming, bulging tests and classical stamping with good agreement with experimental knowledge.

In 2006 [8], was conducted an experiment and simulation techniques for investigation the influence of wrinkling behaviour on formability and thickness distribution in tube hydroforming process & found different types of wrinkles in which a useful wrinkle can meet both the stress condition and the geometrical condition during calibrating. Lubricants are usually employed to increase the formability of the work piece so [9], in 2008 have use different lubrication regimes and observed along the different forming zones which vary with the lubricant layer thickness, applied load and sliding velocity. In 2010 the free bulge test for the roll-formed tubular material are carried out by [10], can be concluded that the flow stress of the tubular material should be determined from the actual free bulge test to find the practically valuable forming limit curve for the THF process.

- **T-shape profile**

Since most of the parametric study for hydroforming process have been done many of the researchers by using different symmetrical or unsymmetrical sections such as T-shape, X-shape, Y-shape, Un-Equal T-shape, Bi-Layered. T-section is one which was used by most of the researchers. In 2004 [11] have used of the finite element method in conjunction with adductive network is presented to predict an acceptable product of which the minimum wall thickness and the protrusion height fulfil the industrial demand on the T-shape tube hydroforming process. Similar action for T-shape part or tube using the designed adaptive system in combination with the finite element method is proposed by [12], in 2005 & found efficient way of process control & for the simulations ABAQUS/Explicit is used.

A hydroforming test machine with counter punch was designed and developed by [13] in 2007 & found the effects on branch height of formed product with & without a counter punch. Different process parameters like velocity and pressure profiles, and bucking system characteristics related to the finished product were studied by [14], in 2010 through copper T-shaped tube with FE simulation techniques with used codes such as LS- Dyna and ABAQUS. Single & bi-layered tube hydroforming processes were numerically simulated using the finite element method in this paper by [15] in 2011. It was found that the final bulges heights resulted from the models were in good agreement with the experimental results. So from above of the research review THE FE techniques adopted by most of the researchers in this paper same techniques. For this Finite Element Code HYPER FORM is used for parametric study of hydroforming process.[16] Hydroforming systems, equipment, controls and tooling ,Deformation mechanism and fundamentals of hydroforming ,Materials and their characterization for hydroforming ,Formability analysis for tubular hydroformed parts, Design and modeling of parts, process and tooling in tube hydroforming, Tribological aspects in hydroforming. In general the hydroforming techniques involved Pre-forming: tube rotary draw bending and pre-flattening/crushing in hydroforming, Hydroforming-hydro piercing , end-cutting, and welding, Hydroforming sheet metal forming components, Bending and hydroforming of aluminum and magnesium alloy tubes, Low pressure tube hydroforming ,Comparative analysis of hydroforming techniques.

The Tube Hydroforming (THF) process is a relatively new manufacturing technology, which has been used in the past decade. The major advantage of forming processes is that they avoid the waste of material as happens in machining. Productivity can also be very high compared with machining. Furthermore, THF also offers potential in design of structures with high stiffness THF offer some other advantages as compared to conventional manufacturing via stamping and welding. These advantages include: (a) part consolidation, for example stamped and welded sections to form a box section, can be formed as one single piece from a tubular material using hydroforming, (b) weight reduction through more efficient section design and tailoring of the wall thickness in structural components, (c) improved structural strength and stiffness via optimized section geometry, (d) lower tooling costs due to fewer parts, fewer secondary operations, tighter dimensional tolerances and reduced

distortion due to spring back and reduced scrap, since to trimming of excess material can be completely eliminated in THF (Dohmann and Hartl, 1996).

II. Tube Hydroforming Process (THF)

The tubular blank is firstly placed between the two die halves and then filled with high-pressure liquid through holes in the plungers to remove any air bubbles trapped inside. The tube is then forced to adopt the inner contour of the tool by application of internal pressure (via high pressure liquid) and two axial forces (via plungers) simultaneously.

In many cases, internal pressure can be transmitted via an elastomer (e.g. rubber or polyurethane), or a soft metal (e.g. lead). For limited applications, the tube can be formed by the increasing internal pressure only. This means that the axial plungers do not feed more material into the expansion zone. However forces acting on the tube ends must exceed a certain level to prevent leakage. This limit is known as sealing**.** Steps for THF of T-shape profile is shown in below fig.1. Initial to final positions of T-section easily understand from fig.1.

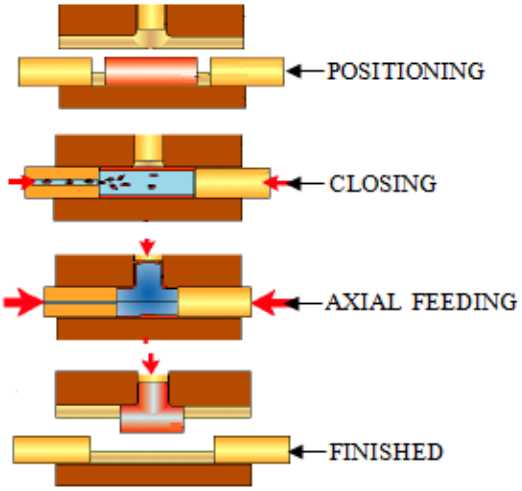

Fig. 1 Hydroforming Sequences for T-Shape

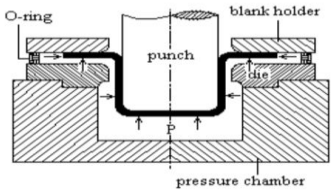

Sheet Hydroforming with Punch (SHF-P)

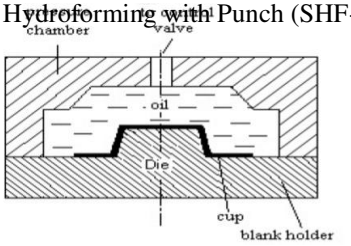

(a) Sheet Hydroforming with Die (SHF-D).

Fig. 2 Sheet hydroforming process

III. Sheet Hydroforming Process (SHF)

Sheet-metal forming processes are technologically among the most important metalworking processes. Products made by these processes include a large variety of shapes and sizes. Typical examples are automobile bodies, aircraft panels, appliance bodies, kitchen utensils and beverage cans. The fluid pressure is very important in this process, because wrinkles will appear if the pressure is not sufficiently high. If the pressure is too high, the blank may be damaged by rupture [27]. The range of the applications of any sheet hydroforming process is limited. Not all the processes can be used for complex industrial parts. In this section, the criteria in selecting a specific process will be explained, such as the high drawing ratio, control of wrinkling, and ease of applying internal pressure.

Sheet hydroforming process is an alternative to drawing process where either punch or die is replaced by hydraulic medium, which generates the pressure and forms the part. Sheet hydroforming is classified into two types Sheet Hydroforming with Punch (SHF-P) and Sheet Hydroforming with Die (SHF-D). In SHF-P as shown in above (Figure 2(a)), the hydraulic fluid is replaced with the die, while in SHF-D (Figure 2(b)), the hydraulic fluid is replaced with the punch. Absence of either punch or die in SHF process reduces the tooling cost [26]. Among the sheet hydroforming processes, hydrodynamic deep drawing assisted by radial pressure (HDDRP) has been used to form complex shapes and has a good drawing ratio [28].

IV. An Automotive Applications of THF

The main application of this method has been found in manufacturing of reflectors, household appliances as well as components in the hygiene, aerospace, automotive and aircraft industries.

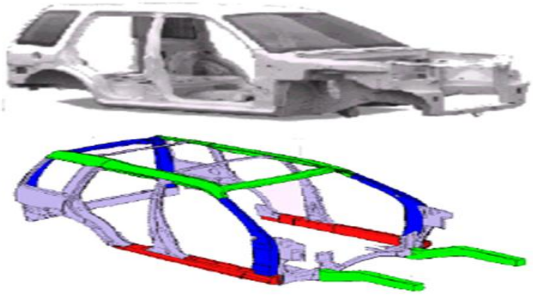

Fig. 3 Example of Hydroform Intensive Body of Land Rover [17]

Apart from various commercial applications a number of studies have been done on the use of hydroformed tubular components in car body. Above fig. 3 an example is shown of a hydroform intensive body, designed by Land Rover in cooperation with Tata Steel and a number of hydroforming companies.

In this body a number of traditional sheet metal components have been replaced by hydroformed tubes by [17], leading to lesser components, weight saving and an excellent crash performance. Likewise, General Motors' (GM) suppliers began using hydroforming to create suspension parts. There was an eventual increase of approximately 20 precent in manufacturing productivity for GM, and the switch to hydroforming may have contributed to the gain. GM continues to use hydroforming in its production methods. In 2006, it became one of the first automakers to use this process to create structural products on vehicles (Pontiac, Chevrolet) for several of its brands.

Other examples of hydroforming in the automobile industry include the making of engine cradles for various, Ford, and Chrysler models. The process has also been used by several European automobile manufacturers, such as Volkswagen, who switched from deep drawing to hydroforming in order to create unibody frames for some of their vehicles. Some of the most common applications of tube hydroforming can be found in the automobile industry. In 2002, the American automobile maker, Chrysler, began incorporating hydroforming to help reduce chassis vibration on its redesigned Dodge Ram. Most common parts manufactured from tube hydroforming process as shown in below fig. 4

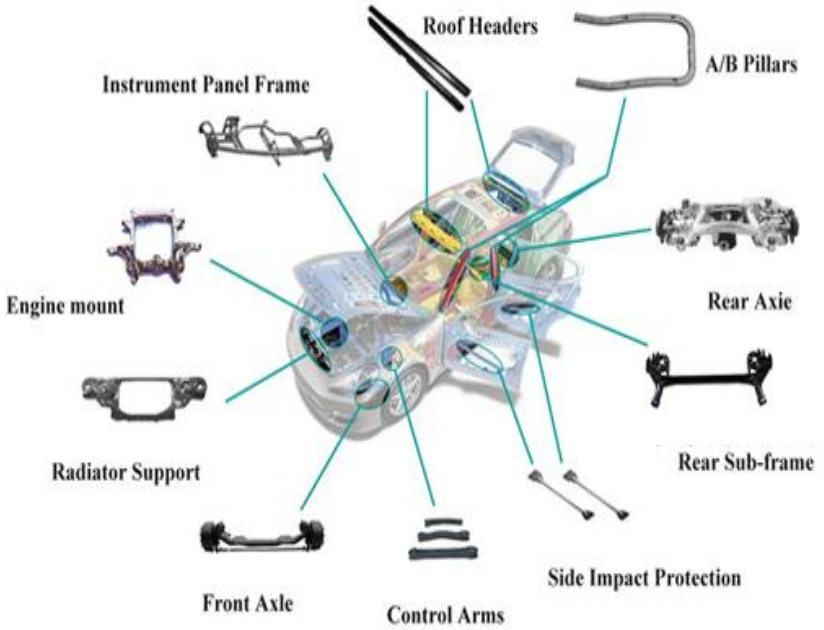

Fig. 4 Examples of the Automotive Parts

One of the leading automotive companies using hydroforming is BMW [21].

Fig. 5 (i) Exhaust system of BMW M3 and (ii) its elements formed by hydroforming as well as (iii) BMW rear axles with hydroformed components. [20]

In the newest models of BMW (e.g. BMW M3) hydroformed exhaust components are used as shown in fig. 5. Energy absorption and component integrity under crash conditions [20]. There exists a considerable interest to reduce vehicle weight through the adoption of lightweight materials, such as aluminium alloys, while maintaining the interaction between tube hydro-forming and behaviour during crash events was studied using lightweight automotive structural members [22].

New technology of tube hydroforming has become so profitable from many points of view, that other car producers have introduced new components into cars, as for example Audi shown in fig. 6.

Fig. 6 .Audi TT Coupe with hydroformed rear axle components [22]

V. Failure of Tube in THF Process

The success of a THF process is, however, dependent on a number of parameters such as the loading path, material formability and lubrication conditions (Aue-U-Lan et al. 2004).

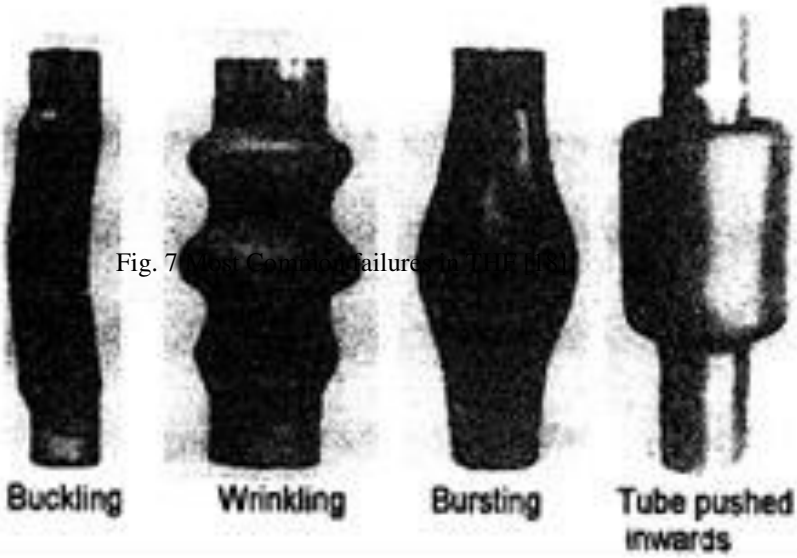

Fig. 7 Most Common failures in THF [18]

A suitable combination of all these variables is vital to avoid part failure. Most failure modes in THF can be classified as wrinkling, buckling, bursting, folding back are shown in fig. 7. These types of failures are caused by either excessive internal pressure or excessive axial end feed during the forming process [18].

(a) Bukling: There is a danger of buckling at the start of the process as a result of excessively high axial force acting on the starting tube. This is a function of the tube parameters. The danger of buckling persists beyond the initial stage of the process and lasts throughout the start-up phase. It is thus necessary to influence the process, through the process control, in such a way that the reduction in free tube length due to upsetting is coupled with a rapid increase in the section modulus of the tube cross-section.

(b) Wrinkling: It is impossible to avoid wrinkling in the intake region of the expansion die; these wrinkles which are symmetrical to the longitudinal axis can be eliminated again by increasing the internal pressure in the final phase of the expansion process.

(c) Bursting: There is a danger of bursting once medium level expansion has been attained ($d_i/d_o > 1.4$) as a result of an excessively high internal pressure. The bursting process is triggered by local constriction of tube wall; the start of construction is a major function of starting wall thickness.

(d) Folding back: The danger of the work piece folding back is conditioned both by the design of die and by the expansion geometry and the tube parameters [24]. Folding back occurs when tubes are expanded in dies where tube wall material is forced into the die from tube holders.

VI. Finite Element Method (FEM)

Although tube hydroforming is a long known technology, the applications of hydroformed tubular components has increased in recent times, because of the more advanced pressing control technology, but also because of the availability of reliable Finite Element Models (FEM), that eliminate the expensive trial and error process in the development of the tools and components. In figure 8 and 9 an example is shown of a state of the art FEM analyses of the complete production process, starting with tube making on a roll forming line (figure 8) followed by pre- bending of the tubes, closing of the tools also pre forming the tube and finally the

hydroforming step (figure 9).

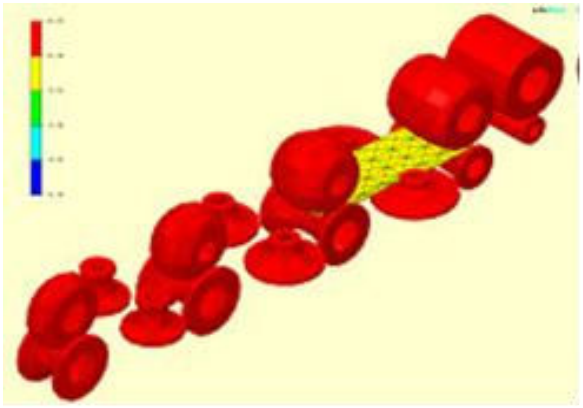

Fig. 8 FEM Calculations of Tube Making Process

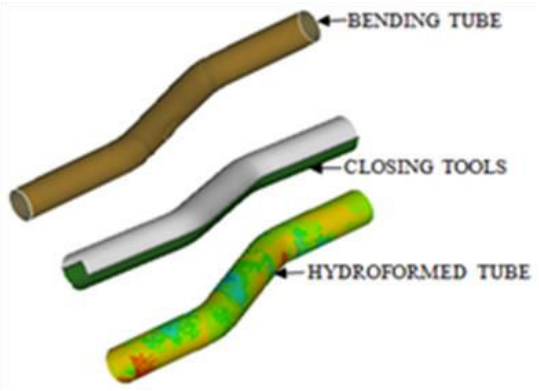

[17] Fig. 9 FEM Hydroformed tube steps

For parametric analysis all kind tests of the of THF process were conducted experimentally and involved significant costs and time. The computer aided simulation of THF processes using the finite element method (FEM) has proven to be efficient and useful [5], as it allows for the virtual testing and comparison of several candidate processes, thus avoiding the use of costly "trial and error" prototype tests. The FEM was a suitable tool for the simulation of forming processes. Finite element code HYPERFORM of HYPER WORKS software adopted. Most common & complex automotive Parts are shown in below fig. 10.

The engine cradle was initially produced from a conventional roll formed and resistance welded tube (ERW). However, the combination of material and process for this application results in two problems are excessive strain hardening introduced by the roll forming process & negative influence on the local mechanical properties due to the heat input of the resistance welding process [17]. Most complex automotive part engine cradle formed with use of various stages bending, preforming & hydroforming as shown in fig. 9.These stages in hydroforming is necessary to eliminates problems create from conventional roll formed & resistance welding process.

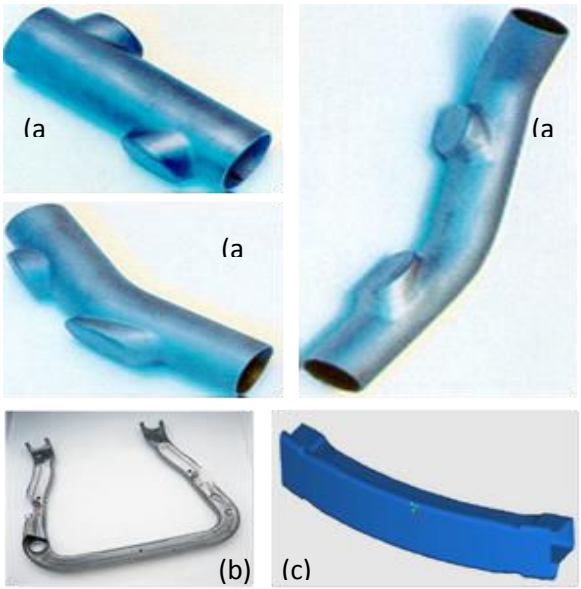

Fig. 10 Complex THF parts with multiple geometrical features (a) exhaust manifolds with protrusions and bends (different spline configurations) [19], and (b) engine cradle: long automotive structural part with bulges and bend (DP600) and (c) bumper system [17].

Formability of material is played a vital role in hydroforming process. So from above research study, found that a bulge formed required in most of automotive parts. In this regard initially the engineering research center for net shape manufacturing (ERC/NSM) at the OHIO state university has developed and implemented the biaxial tube bulge test [23]. This test can be used to determine the formability of various tube materials, including aluminum alloys, stainless steels, carbon steels, and nickel alloys. The hydraulic bulge test is used to test tubes in a biaxial state of stress.

The bulge test consists of the following steps: expand the tube with internal pressure while the ends of the tube are held firmly to prevent axial movement then measure the internal pressure and bulge height continually during expansion after that convert the data into true stress-strain data using analytical equations finally use the least-squares method to fit the data into known and widely used equation forms to obtain a flow stress curve that is easy to use. By using TUBE_STRESS, it is possible to determine the flow stress (true stress versus true strain) of the tubular material accurately in the following forms:

$$s = Ke^n \underline{OR}\ s = K\,(e_0 + e)^n \quad (1)$$

Where: s = true stress, e = true strain, K = strength co-efficient, n = strain-hardening exponent, e_0= pre-strain. Forming limit diagrams (FLDs) are widely used fracture criteria for tube hydroforming. The hydraulic bulge test also can be used for determining the right side of the FLDs. In this paper bulge test conducted with finite element code HYPERFORM is used and found the results for model prescribed in below fig.11.

Fig.11 List of Parameter with Value

SR. No.	Parameters	Value
1	Tube Thickness (t)	1 mm
2	Yield Strength (6y)	145 MPa
3	Strength coefficient	550
4	Strain Hardening (n)	0.3
5	Material	AA6063-T5
6	Initial Pressure	145.14 Psi
7	Final Pressure	1523.97 Psi

VII. Bulge Forming

A simulation set up for bulge model as shown in below fig.12 created with Pro-E. All dimensions of this model taken from the experimental setup of bulge model [13].

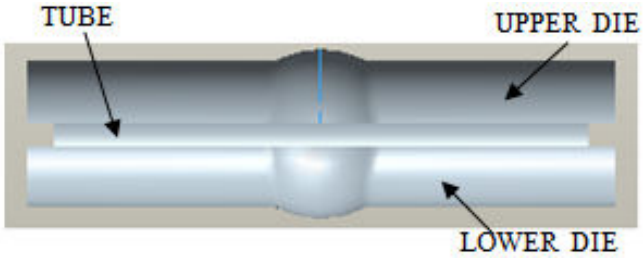

Fig.12 Bulge Model

Fig.13 Initial & Final Stage of bulge formation

A bulge model as IGES format imported to HYPERFORM module of manufacturing solutions. Then organize the imported model. After that meshing the individual parts create a section, defining material, & updated to them through compos tab. A hydro setup tab used to run the process. Due to which two radios file generated as .rad000 & .rad00.Various parameters used for bulge model are tabulated as above. For generating an animation file a RADIOSS SOLVER is used. With time of span total 11 number of file is generated. For analysing the

results a HYPERVIEW module is used. An animation tab is used to animate the process through which we are analysed how to actual process is being done. Initial & final stages of animation are shown in above fig.13. Different results for bulge model are shown in below fig.14.

SR. No.	Parameters	Max. Value	Min. Value
1	Displacement	11.30	0.8918
2	Strain	0.2333	0.03714
3	Stress (N/mm^2)	361.9	67.51
4	% of Thinning	13.68	2.033
5	Thickness (mm)	0.9797	0.8623

Fig.14 Results of Bulge Mode

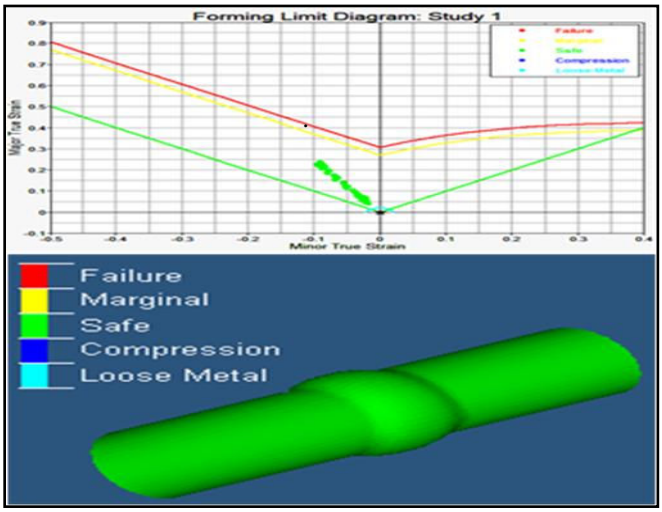

Fig.16 FLC & FLD Curve

A forming limit curve (FLC) & forming limit diagram (FLD) are shown in above fig.14. In spite of the fact that tube deformation can be detected, the determination of the forming severity is not straightforward using circle grid analysis by [5]. A deformed circle is manually or automatically measured at a critical location, and the corresponding surface strains are compared to a forming limit diagram (FLD). The FLD provides information about how much a specific metal can be deformed before necking occurs.

Results & Discussion

Bulge test can plays an important role to determining the formability of various tube materials, including aluminium alloys, stainless steels, carbon steels, and nickel alloys under biaxial deformation conditions at room temperature.

Sr.	Results	Max. Value	Min. Value
1	Displacement	11.30	0.8918
2	Strain	0.2333	0.03714
3	Stress (N/mm^2)	361.9	67.51
4	% of Thinning	13.68	2.033
5	Thickness (mm)	0.9797	0.8623

It is reliable tool for evaluating the "quality" of new incoming materials. Flow stress data obtained from hydraulic bulge test is used for FEM simulation for THF process. In automotive industry quality control of tubes is necessary for reducing scrap/defects in THF & assuring required performance in end use of tubular material. Maximum bulge height is an indication of tube quality & formability for hydroforming. As per defined various parameter for bulge model in above fig. 11, different results are obtained, which is indicated in fig.14 The results of displacement rate higher at bottom side of tube. Value of strain is quite high at middle portion while at same for the stress equal to 361.9 N/mm^2. In case of % of thinning higher the value of it at middle section equal to 13.68% while lowest at both ends equal to 2.033%. As per shown in above fig.6 Forming limit curve (FLC) denotes that up-to these limit tube will be deformed but after that it will be break. From the forming limit diagram (FLD) the different zone results are obtained as loose metal, compression, safe, marginal & failure as indicated as sky blue, blue, green, yellow & red colour respectively. Most of the portion of the tube is indicated with green colour so whole deformation of the tube is under safe zone. Same process carried out for T-section, in which value of % of thinning results up to 90-95% which quite higher with taking the value initial & final pressure limit in between (100- 10000) psi for CRDQ-Steel material so further investigation in these regard will be carried with altering the parameters.

Conclusion

Sheet hydroforming, controlled metal flow during the operation minimizes localized stress concentrations that may cause work piece buckling or wrinkling. Sheet hydroforming is slower than traditional stamping, thus its use is limited to short runs of more highly specialized parts. The Tube hydroforming (THF) is best unconventional metal forming processes which is widely used to form various tubular components. The Tube Hydroforming (THF) process is a relatively new manufacturing technology, which has been adopted by most of automotive industries. Selection of different parameter plays an important role for the success of the any process of the hydroforming. THF offers potential alternatives in the use of lightweight materials and hence can have a great impact in saving energy in the automotive industry. Most famous automotive industries as General Motors, Chevrolet, Land rover, Audi, Walkswagon, BMW & many others are leading user of hydroforming process for many of the automotive parts. Most failure modes in THF can be investigated as wrinkling, buckling, bursting & folding back. Bulge test can be used to determine the formability of various tube materials. The finite element method (FEM) is a powerful tool for rapidly designing both prototype and production components.

References

[1] J. Jeswiet , M. Geiger , U. Engel , M. Kleiner , M. Schikorra , J. Duflou , R. Neugebauer , P. Bariani , S. Bruschi "Review - Metal forming progress since 2000", CIRP Journal of Manufacturing Science and Technology,Vol 1, pp. 2008.

[2] Koc Muammer, Altan Taylan. "An overall review of the tube hydroforming technology", Journal of Material Process Technology, Vol.108, pp. 2001

[3] Grey JE, Devereaux AP, Parker WN. Ing for making wrought metal T's. US Patent; 1939.

[4] http://www.thefabricator.com/article/hydroforming/hydroforming-introduction-to-tube hydroforming.

[5] Honggang An,"Multi objective Optimization of Tube Hydroforming Using Hybrid Global and Local Search", Electronic Theses and Dissertations, University of Windsor Scholarship at UWindsor, T.S. Jan. 2010. F

[6] Muammer Koc, Taylan Altan"An overall review of the tube hydroforming (THF) technology", Journal of Materials Processing Technology, vol.108, pp. Sep 2000.

[7] B.J. Mac Donald, M.S.J Hasmi "near net shape manufacturing of engineering components using bulge forming process: a review", Journal of Materials Processing Technology, vol.120, pp. Sep 2001.

[8] Shijian Yuan , Wenjian Yuan, Xiaosong Wang," Effect Of Wrinkling Behavior On Formability And Thickness Distribution In Tube Hydroforming", Journal Of Materials Processing Technology vol. 177 pp. 2006.

[9] Mariela Luege, Bibiana M. Luccioni," Numerical simulation of the lubricant performance in tube hydroforming", journal of materials processing technology, vol.198, pp. July 2008.

[10] Woo-JinSong, Seong-ChanHeo Tae-WanKu , JeongKim , Beom-SooKang, "Evaluation of effect of flow stress characteristics of tubular material on forming limit in tube hydroforming process", International Journal of Machine Tools & Manufacture, vol. 50 pp. May 2010.

[11] F.C.Lin. "Application of abductive network and FEM to predict an acceptable product on T shape tube hydroforming process", Computers and Structures, vol. 82, p.p.March 2004

[12] A. Aydemir , J.H.P. de Vree , W.A.M. Brekelmans , M.G.D. Geers ,W.H. Sillekens , R.J. Werkhoven " An adaptive simulation approach designed for tube hydroforming processes", Journal of Materials Processing Technology, vol. 159, pp. 2005.

[13] Y.M. Hwang , T.C. Lin, W.C. Chang, " Experiments on T-shape hydroforming with counter punch", Journal of Materials Processing Technology, vol. 192–193, pp. 2007.

[14] J.Crapps, E.B.Marin, M.F.Horstemeyer R.Yassar, P.T.Wang, "Internal state variable plasticity-damage modeling of the copper tee-shaped tube hydroforming process", Journal of Materials Processing Technology, vol. 210 pp. June 2010

[15] Abed Alaswad, K.Y. Benyounis, A.G. Olabi ,"Finite element comparison of single and bi-layered tube Hydroforming processes", Simulation Modeling Practice and Theory, Vol.19, pp. March 2011.

[16] http://www.woodheadpublishing.com/en/book.aspx?bookID=1359.
[17] Nico Langerak, Dinesh Kumar Rout, Rahul Verma, G.Manikandan, Arunansu Haldar", Tata Steel Research Development & Technology", IJmuiden, the Netherlands
[18] F Dohmann Ch. Hart, "Tube hydroforming research and practical application", Journal of Materials Processing Technology, vol. 71 pp.1997.
[19] Suwat Jirathearanat," dissertation advanced methods for finite element simulation for part and process design in tube hydroforming", department of mechanical engineering, the Ohio state university, 2004.
[20] A. Kocańda, h. Sadłowska, "Automotive Component Development By Means Of Hydroforming" Archives of civil and mechanical engineering, vol. III, 2008.
[21] http://nsm.eng.ohiostate.edu/THFModule1/html/ app.lications.html.
[22] http://www.salzgitterhydroforming.de/westsachsen/crimmitschau/salzgitter/de/produkteabgaskomponenten/bsp_kruemmer
[23] http://www.thefabricator.com/article/hydroforming/determining-flow-stress-of-tubes
[24] F. Dohmann, Ch. Hartl, Liquid bulge forming as a flexible production method, J. Mater. Process Technol. 45 (1994).
[25] N.Boudeau, A. Lejeune, J.C. Gelin, "Influence of material and process parameters on the Development of necking and bursting in flange and tube hydroforming", Journal of Materials Processing Technology, vol. 125, pp. Feb 2002.
[26] Hosseinzade M, Mostajeran H, Bakhshi-Jooybari M, Gorji A, Norouzi S, Hossinipour SJ (2009) Novel combined standard hydromechanical sheet hydroforming process, IMechE Journal of Engineering Manufacture, 224: 447-457.
[27] Zhang SH, Danckert J (1998) Development of hydro-mechanical deep drawing. J. Mater. Process. Technol. 83: 14 – 25.
[28] Lang L, Danckert J, Nielsen KB (2004) Investigation into hydrodynamic deep drawing assisted by radial pressure Part I. Experimental observations of the forming process of aluminum alloy. J Mater Process Technol 148:119-131.